Targeting the Epidermal Growth Factor Receptor with DARPins Alone and in Combination with Radiation Therapy

---

Dissertation

zur

Erlangung der naturwissenschaftlichen Doktorwürde

(Dr. sc. nat.)

vorgelegt der

Mathematisch-naturwissenschaftlichen Fakultät

der

Universität Zürich

von

Martina Zimmermann

von

Visperterminen (VS), Schweiz

Promotionskomitee

Prof. Dr. Martin Pruschy (Vorsitz, Leitung der Dissertation)

Prof. Dr. Alessandro A. Sartori

PD Dr. Manuel Stucki

Zürich, 2014

Abstract

The history of radiation therapy for the treatment of cancer began over hundred years ago at the turn of the nineteenth century, and today, still constitutes an important arm of cancer therapy. Advances in tumor imaging techniques and specialized software allow for three-dimensional treatment planning and dose application, and further improved the standard of radiotherapy. With intensity-modulated radiation therapy (IMRT), radiation doses can now be precisely focused on the irregularly shaped tumor area while sparing normal tissue.

It is the goal of radiotherapy to deprive tumor cells of their replicative potential. Ionizing radiation damages cells by the introduction of DNA damage. Ionizing radiation induced DNA double-strand breaks in particular are most toxic for an irradiated cell. Even though cancer cells often exhibit an increased apoptotic threshold, they often also exhibit deficiencies in their DNA repair capacity or in their capability to refrain from cell cycle progression in presence of DNA damage. These factors increase their susceptibility to radiation treatment. Importantly, proliferating cells, such as cancer cells, are more susceptible to DNA damage, based on the increased radiosensitivity of cells residing in late G2 and M phase. Furthermore, the combination of IR with conventional chemotherapy intends to increase DNA damage, to modulate the apoptotic threshold or to synchronize proliferating cells into the sensitive M phase. In recent years, greater understanding of tumor biology also offers the possibility of targeting “cancer-specific” signaling pathways. Pathways considered for targeting include signaling entities related to proliferation and survival or aim for synthetic lethality in combination with the cancer cell’s inherent deficiencies. Today, mainly two classes of molecular targeting agents have been approved for clinical application: monoclonal antibodies that bind and inhibit cell surface receptors or secreted factors, and small molecules that penetrate cells and are designed to interfere with the enzymatic activity of the target protein.

Molecular targeting of cancer cells with regard to radiosensitization is the main topic of this thesis. The first part is dedicated to the inhibition of the epidermal growth factor receptor (EGFR) by a non-immunoglobulin scaffold protein, a designed ankyrin repeat protein (DARPin). The epidermal growth factor receptor signaling cascades are involved in regulation of growth, proliferation, survival and differentiation of mammalian cells. Overexpression of EGFR is often found in cancers of epithelial origin and is associated with a malignant phenotype. EGFR inhibition in combination with radiation therapy has been reported to improve patient outcome, though responses of different tumor entities are heterogeneous and the molecular mechanism is not well understood.

Presently, antibody-based as well as small molecular EGFR inhibitors are in clinical use.

The protein entity we used for EGFR targeting is a designed protein consisting of several assembled ankyrin repeats. The ankyrin motif, two α-helices followed by a β-turn, is adapted from natural ankyrin repeats that are part of protein-protein interaction interfaces. Mechanistically, DARPins can be selected to bind and inhibit extracellular targets similar to antibodies and with even superior affinity.

In this study, we compared efficacy of EGFR inhibition by the DARPin E69_LZ3_E01 with the efficacy of the monoclonal anti-EGFR antibody cetuximab, each agent individually and in combination with ionizing radiation. We determined the effect of EGFR inhibition on cell cycle distribution and proliferation in the vulvar squamous carcinoma cell line A431, a widely used EGFR model cell line. By means of classical and 3D clonogenic assays, we assessed radiosensitization upon EGFR inhibition in A431 cells. Furthermore, and with regard to the *in vivo* application, we investigated the dynamics of EGFR inhibition by DARPin E69_LZ3_E01 and cetuximab, and EGFR reconstitution and cell recovery upon retraction of the inhibitors. Finally, the DARPin E69_LZ3_E01 was tested in a preclinical setting in A431 tumor xenografts in nude mice, as monotherapy and in combination with ionizing radiation, in comparison to cetuximab.

In vitro, inhibition of the EGFR in A431 cells suppressed proliferation, which was also reflected in the accumulation of cells in the G1 phase of the cell cycle. The antiproliferative effect of DARPin E69_LZ3_E01 on A431 cells was more pronounced than for the antibody cetuximab. On the level of EGFR signaling, DARPin E69_LZ3_E01 did not only lead to stronger repression of EGF-stimulated activation of the downstream target Erk, but also to an enhanced downregulation of the EGFR. Upon removal of either inhibitor, cells recovered rapidly within few hours.

In combination with radiation, we could not demonstrate a direct radiosensitization induced by EGFR inhibition in A431 cells *in vitro*. However, combined treatment of A431 tumor xenografts with radiation and cetuximab was superior to either modality alone and resulted in a complete tumor remission in 6 out of 10 animals. In contrast to a dense daily regimen, no tumor growth delay was induced by DARPin E69_LZ3_E01. The pharmacokinetic analysis of DARPin E69_LZ3_E01 revealed that the half-life of the pegylated DARPin, which was used for the *in vivo* experiment, most probably was not sufficient to maintain continuous receptor inhibition.

In the second part of the thesis, radiosensitization by the knockdown of the major vault protein (MVP) was investigated in various human cancer cell lines. MVP is the major component of a big barrel-like protein complex named vault. The precise function of vaults, which are highest expressed in tissues chronically exposed to xenobiotics, is not

well known. Like EGFR, MVP is often overexpressed in cancer cells and correlates with poor patient outcome. Curiously, MVP is not an essential protein, as MVP-deficient mice develop normally. Moreover, no enzymatic activity has been assigned to vaults, but associated proteins, like TEP1, vPARP as well as multiple vRNAs that are localized in the interior of vaults, may have functional roles.

Depletion of MVP by means of siRNA sensitized the lung cancer cell line A549 and the colon cancer cell line HCT116 to irradiation and greatly inhibited their proliferation. The inhibitory effect on proliferation, however, varied greatly among additional cell lines tested. Strikingly, proliferation of p53-proficient cell lines was more strongly affected by MVP silencing than proliferation of p53-deficient cell lines. Unfortunately, the discrepancies among the different phenotypes induced by additional MVP-targeting siRNA sequences and the failure to proof the link between the MVP knockdown and the resulting phenotypes by rescue experiments, led us to conclude that nonspecific effects introduced by the siRNA technique might be the reason for the MVP knockdown phenotype observed.

Consequently and despite in-depth investigations, we could not confirm the previously proposed link between MVP and DNA repair. Nevertheless, independently of the knockdown experiments, we observed that MVP expression was induced by ionizing radiation. An increase in MVP expression levels in response to various other stress stimuli was reported previously. Interestingly, we observed that this irradiation-induced increase of MVP was at least in part regulated in an autocrine manner. This may be the cause for the delayed time point of MVP-induction, we observed. Others demonstrated that MVP was also upregulated in senescent cells to prevent induction of apoptosis. In cancer cells, MVP may be upregulated in response to ionizing radiation or other stress stimuli, to contribute to cell death resistance.

Zusammenfassung

Die Geschichte der klinischen Anwendung von Radiotherapie begann vor mehr als hundert Jahren und bildet auch heute noch eine wichtige Grundlage für die Behandlung von Krebserkrankungen. Grosse technische Fortschritte in Bildgebung und Software ermöglichen eine dreidimensionale Planung des Bestrahlungseingriffs und eine Verbesserung der herkömmlichen Radiotherapie. Zusammen mit modernen Bestrahlungstechniken wie der Intensitätsmodulierten Strahlentherapie (IMRT) wird eine genaue Fokussierung auch auf unregelmässig geformte Tumore gewährleistet, während das umliegende gesunde Gewebe geschont werden kann.

Ziel der Radiotherapie ist es, diejenigen Tumorzellen, die die Fähigkeit haben sich zu teilen, abzutöten oder ihnen die Teilungsfähigkeit zu nehmen. Die Bestrahlung des Tumorgewebes induziert DNA Schäden, wovon Doppelstrangbrüche für die Zelle am schädlichsten sind. Obwohl bei malignanten Zellen der Zelltod oft verspätet ausgelöst wird, ist bei Krebszellen auch häufig die DNA-Reparaturkapazität beeinträchtigt, sowie auch die Möglichkeit in einer Phase des Zellzyklus anzuhalten um die Schäden zu beheben. Zudem sind proliferierende Zellen, wie es Krebszellen sind, strahlenempfindlicher; Zellen, die sich in der späten G2-Phase und in der M-Phase des Zellzyklus befinden, sind anfälliger für Strahlenschäden. Strahlentherapie wird oft mit konventioneller Chemotherapie kombiniert, die die Bestrahlung unterstützt, indem zusätzliche DNA Schäden zugefügt, der programmierte Zelltod gefördert, oder die Zellen in der Strahlen-sensitiven M-Phase synchronisiert werden. Zunehmendes Verständnis der Tumorbiologie eröffnete neue Möglichkeiten tumorspezifische Signalwege zu inhibieren. Zwei Klassen solcher tumorspezifischen Medikamente sind zum heutigen Zeitpunkt in klinischer Anwendung: Monoklonale Antikörper, die Rezeptoren an der Zelloberfläche binden und inhibieren und kleinmolekulare Inhibitoren, die ihre Wirkungen auf die enzymatische Aktivität eines Proteins innerhalb der Zelle entfalten.

Inhalt dieser Doktorarbeit ist das Thema „Tumorspezifische Radiosensibilisierung“. Der erste Teil der Dissertation handelt von der Inhibition des epidermalen Wachstumsrezeptors (EGFR) durch Nicht-Immunoglobulin-verwandte Gerüstproteine, sogenannte DARPins (designed ankyrin repeat proteins). EGFR ist mitverantwortlich für die Regulierung des Zellwachstums und der Proliferation. Der Rezeptor spielt auch eine Rolle für die Erhaltung der Lebensfähigkeit einer Zelle und ist an Differenzierungsprozessen der Zelle beteiligt. EGFR ist in epithelialen Tumoren oft überexprimiert und assoziiert mit aggressiven Krebsarten. Inhibition des Rezeptors in Kombination mit Radiotherapie erzielte gute Ergebnisse und wird in der Klinik eingesetzt, obwohl die molekularen Mechanismen der Wirkung nicht genau ergründet sind. Dabei werden

sowohl anti-EGFR Antikörper wie auch kleinmolekulare Inhibitoren gegen den Rezeptor verwendet.

DARPins, die wir für die Inhibition des EGF-Rezeptors verwendeten, sind Designerproteine, die aus repetitiven Motiven bestehen. Ein einzelnes Motiv besteht aus zwei α-Helices, gefolgt von einer β-Schleife und beruht auf der Struktur natürlich vorkommender „Ankyrin-Repeat“ Motive, die Teil von Proteininteraktionsflächen sind. Ähnlich wie Antikörper, und mit zum Teil noch grösserer Affinität, können DARPins den extrazellulären Teil eines Zielproteins binden und diesen möglicherweise inhibieren. DARPin E69_LZ3_E01 verfügt über zwei solcher EGFR-Bindungsdomänen, die über einen Leucin-Reissverschluss miteinander verbunden sind. Dadurch bilden sich Dimere, die über vier Bindungsdomänen verfügen.

Ziel der Studie war es, die Wirksamkeit von DARPin E69_LZ3_E01 in Bezug auf EGFR-Inhibition und Radiosensibilisierung, mit derjenigen des monoklonalen Antikörpers Cetuximab zu vergleichen. Wir untersuchten den Effekt der EGFR-Inhibition auf die Zellzyklusverteilung der Sarkomazelllinie A431, die häufig für Studien in Bezug auf EGFR verwendet wird. Weiter betrachteten wir die Dynamik der EGFR-Inhibition und die Dynamik der Widerherstellung der ursprünglichen Funktionsfähigkeit der Rezeptoren nach Entfernung der Inhibitoren aus dem Zellkulturmedium. Die klonogene Überlebensrate in Kombination mit Bestrahlung wurde auf klassische Weise in adhärenten Zellen und in 3D-Zellkultur bestimmt und schlussendlich untersuchten wir die kombinierte Behandlung von DARPin E69_LZ3_E01 mit Bestrahlung in einem präklinischen Versuchsaufbau im Nacktmaus-Tumorxenograft-Modell. Zum Vergleich führten wir den gleichen Versuch mit Cetuximab durch.

In der EGFR-überexprimierenden Zellenlinie A431 führte die Inhibition des EGF-Rezeptors in Zellkultur zu einer Verminderung des Wachstums, welche sich auch in der Akkumulation der Zellen in der G1-Phase des Zellzyklus zeigte. DARPin E69_LZ3_E01 zeigte dabei eine stärkere Wirkung als der Antikörper Cetuximab. Zudem war die Wachstumsfaktor-induzierte Phosphorylierung von Erk, einem Folgeprotein der EGFR Signalkaskade, in den Zellen, die mit DARPins behandelt wurden, stärker unterdrückt. Ebenso führte die Behandlung mit DARPins im Vergleich zur Behandlung mit Cetuximab im Allgemeinen zu einer stärkeren Verminderung der Anzahl der EGF-Rezeptoren. Nach Entfernung beider Inhibitoren erholten sich die Zellen jeweils innerhalb weniger Stunden.

Wir konnten keine Radiosensibilisierung durch EGFR-Inhibition in A431 Zellen nachweisen. Im Tierversuch zeigte Cetuximab in Kombination mit Bestrahlung eine synergistische Wirkung und führte bei 6 von 10 Tieren zu einer kompletten Remission der Tumorxenografte. Obwohl DARPin E69_LZ3_E01 täglich initiiert wurde, konnten wir

keine Wirkung in Bezug auf Tumorwachstum feststellen. Eine Untersuchung der Pharmakokinetik zeigte jedoch, dass die pegylierte Form von DARPin E69_LZ3_E01 eine noch immer ungenügende Serumhalbwertszeit aufweist, um eine andauernde Inhibition des Rezeptors zu gewährleisten.

Im zweiten Teil der Dissertation wird das „Major Vault Protein“ (MVP) als mögliches Zielprotein für Radiosensibilisierung in Betracht gezogen. MVP ist der Hauptbestandteil eines fassähnlichen Proteinkomplexes. Die Funktion von MVP, das vor allem in Umwelt exponierten Geweben stark exprimiert wird, ist kaum bekannt. Ähnlich wie bei EGFR, ist eine Überexpression von MVP in Krebszellen mit schlechteren Prognosen für den Patienten assoziiert. Interessanterweise ist MVP kein essentielles Gen und Knockout-Mäuse entwickeln sich normal. Dem Protein MVP, das das Gerüst des Proteinkomplexes bildet, konnte bislang keine enzymatische Funktion zugewiesen werden. Allerdings könnten andere Proteine wie TEP1, vPARP oder auch vRNAs, die alle fester Bestandteil des Komplexes sind, ein solche Funktion haben.

Das Unterdrücken der MVP Expression durch Applikation von siRNA (MVP Knockdown) führte zu einer stark verminderten Zellproliferation und zu einer Radiosensibilisierung der Lungenkrebs Zelllinie A549 und der Darmkrebs Zelllinie HCT116. Der Einfluss auf die Zellproliferation variierte jedoch stark in ihrer Ausprägung in weiteren Zelllinien, die wir untersuchten. Zelllinien mit intaktem p53 Protein waren stärker betroffen, als Zelllinien mit einer p53-Defizienz. Allerdings zeigten sich zwischen den verschiedenen siRNA Sequenzen die wir für den Knockdown von MVP verwendeten grosse Inkonsistenzen. Zudem konnte die Verminderung der Proliferation durch die Expression von siRNA-resistenter MVP-mRNA nicht verhindert werden. Zusätzliche Experimente deuteten ebenfalls darauf hin, dass die Ausprägung des Proliferations-Phänotyps auf unspezifischen Effekten der verwendeten siRNA Sequenzen beruhten könnte.

Wir konnten zwar keine direkte Verbindung zwischen MVP und der DNA Reparaturmaschinerie herstellen, aber konnten feststellen, dass die Expression von MVP in Folge von Bestrahlung erhöht wird. Eine erhöhte Expression von MVP in Folge von verschiedenen anderen Stressfaktoren ist bereits anderweitig beschrieben worden. Interessanterweise stellten wir fest, dass die Induktion von MVP teilweise über sekretierte Faktoren reguliert wird, was auch den späten Zeitpunkt der Aufregulierung erklären könnte. Die MVP Expression ist in seneszenten Zellen erhöht und wirkt der Induktion des programmierten Zelltodes entgegen. Möglicherweise spielt MVP eine ähnliche Rolle in Krebszellen und trägt nach Bestrahlung oder nach Einwirkung anderer Stressfaktoren zur die Resistenz gegenüber dem Zelltod bei.

Content

List of Abbreviations

Ab	Antibody
ABCC1-3	ATP-binding cassette, sub-family C, member 1-3
ADAM	a disintegrin and metalloproteinase
ADCC	antibody-dependent cell-mediated cytotoxicity
ADP	adenosine diphosphate
Ago	argonaute protein
Akt	"Ak" in Akt was a temporary classification name for a mouse bred, the t stands for thymoma
AP-1	activator protein 1
ATM	ataxia telangiectasia mutated
ATP	adenosine triphosphate
ATR	ATM and Rad3-related
Bcl-2	B-cell lymphoma 2
BCRP	breast cancer resistance protein
BER	base excision repair
BRCA1/2	breast cancer gene ½
BrdU	bromodeoxyuridine
BSA	bovine serum albumin
CDDP	cis-diamminedichloroplatinum(II)
Chk1/2	checkpoint homologue kinase 1/2
CHS	chalcone synthase
CKII	and casein kinase II
Co-IP	co-immunoprecipitation
COP1	caspase recruitment domain-containing protein 16
CSC	cancer stem cell
CTC	circulating tumor cell
DAPI	4',6-diamidino-2-phenylindole
DARPin	designed ankyrin repeat protein

DNA	deoxyribonucleic acid
DNA-PK	DNA-dependent protein kinase
DNA-PKcs	DNA-dependent protein kinase catalytic subunit
DMSO	dimethyl sulfoxide
DSB	double-strand break
dTTP	deoxythymidine triphosphate
EGF	epidermal growth factor
EGFR	epidermal growth factor receptor
EGFRvIII	truncated epidermal growth factor receptor
ELISA	enzyme-linked immunosorbent assay
EMT	endothelial mesenchymal transition
EpCAM	epithelial cell adhesion molecule
ErbB	from the Erb-b gene responsible for avian erythroblastosis virus
Erk	extracellular signal-regulated kinases
F(ab)	antigen-binding fragment
FACS	fluorescence activated cell sorting
FDA	U.S. Food and Drug Administration
5-FU	5-Fluorouracil
GABPβ1	GA binding protein β1 subunit
Gy	Gray
H&E	hematoxylin und eosin
HCC	advanced hepatocellular carcinoma
HIF1α	hypoxia-inducible factor 1-alpha
HR	homologous recombination
HRP	horseradish peroxidase
IP	intraperitoneal
IR	ionizing radiation
ITI	human inter-α-trypsin inhibitor
H2AX	histone variant 2AX
HBV	hepatitis B virus

HCV	hepatitis C virus
HDF	human diploid fibroblast
Her2	human epidermal growth factor receptor 2
hOCT	human organic cation transporter
HPV	human papilloma virus
HUVEC	human umbilical vein endothelial cells
ID	injected dose
IFNγ	interferon γ
IGF-1R	insulin-like growth factor 1 receptor
IgG	immunoglobulin G
InlK	internalin like protein
IV	intravenous
JAK	Janus kinase
kDa	kilodalton
keV	kiloelectronvolt
LACI	lipoprotein associated coagulation inhibitor
LDLR-A	low-density lipoprotein receptor class A
LOESS	locally weighted error sum of squares regression
Luc	luciferase
LRP	lung resistance protein
LZ	leucine zipper
mAb	monoclonal antibody
MAPK	mitogen-activated protein kinases
mCRC	metastatic colorectal cancer
MDR	multi drug resistance
MEF	mouse embryonic fibroblast
MET	mesenchymal endothelial transition
MeV	megaelectronvolt
miRNA	microRNA
Mmp-9	metalloproteinase 9

MPP	1-methyl-4-phenylpyridinium
mRNA	messenger ribonucleic acid
MRP1	multidrug resistance- associated protein 1
mTOR	mammalian target of rapamycin
MVP	major vault protein
Myc, c-Myc	the newly discovered gene was similar to myelocytomatosis viral oncogene (v-Myc), thus the cellular gene was called c-Myc
NER	nucleotide excision repair
NK cells	natural killer cells
Nt	nucleotide
NSCLC	non-small cell lung cancer
OER	oxygen enhancement ratio
p53	tumor protein 53 (it runs as a 53-kDa protein on SDS-PAGE)
PBMC	peripheral blood mononuclear cells
PARP1	poly (ADP-ribose) polymerase 1
PBS	phosphate buffer saline
PEG	polyethylene glycol
P-gp	p-glycoprotein
PHD	prolyl hydroxylase (domain)
PI3K	phosphatidylinositol 3-kinase
PI3KK	PI3K-like kinase
PKC	protein kinase C
PTEN	phosphatase and tensin homolog deleted on chromosome 10
pVHL	von Hippel-Lindau tumor suppressor
Ras	stands for ‘Rat sarcoma’, where the protein family was discovered
RdRP	RNA-dependent RNA polymerase
RISC	RNA-induced silencing complex
RNA	ribonucleic acid
RNAi	RNA interference
ROS	reactive oxygen species

RPA	replication protein A
RT	radiotherapy
SCCHN	squamous cell carcinoma of the head and neck
scFv	single chain variable fragments
Ser	serine
SH2/3	Src homology 2/3
shRNA	short or small hairpin RNA
siRNA	short or small interfering RNA
SSB	single-strand break
ssDNA	single stranded DNA
STAT	signal transducer and activator of transcription
TAM	tumor associated macrophage
TBS	tris buffered saline
TEP1	telomerase-associated protein 1
TGF-β	transforming growth factor-β
TGF-α	transforming growth factor-α
Thr	threonine
TIC	tumor initiating cells
TK	tyrosine kinase
TKI	tyrosine kinase inhibitor
TS	thymidylate synthase
Tyr	tyrosine
UV	ultraviolet
VEGF-A	vascular endothelial growth factor A
VH	variable heavy chain domain of a mammalian antibody
VHH	variable heavy chain domain derived from camelid antibodies
VPARP	vault-poly (ADP-ribose) polymerase
vRNA	vault ribonucleic acid
WB	western blot analysis

1 General Introduction

1.1 A Brief Overview on the Prevalence of Cancer

The term “cancer” stands for a multifaceted disease that may arise in virtually any tissue of the human body. Cancer is characterized by uncontrolled growth of cells that do not contribute to or even may impair the functionality of the tissue of origin. Cancer cells may spread to distant sites and compromise multiple organs. Besides cardiovascular diseases, cancer is a major cause of death in developed countries. However, though the number of annual new cases of all cancers combined shows a considerable geographical variation. In 2012, there were an estimated 3.45 million new cases of cancer in Europe. The most common cancers were breast cancer for females, followed by colorectal cancer, prostate cancer in men and in fourth position lung cancer; altogether these four cancer types account for half of the tumor burden. An overview on cancer incidences and mortality divided according to tissue and gender is shown in Figure 1.1.

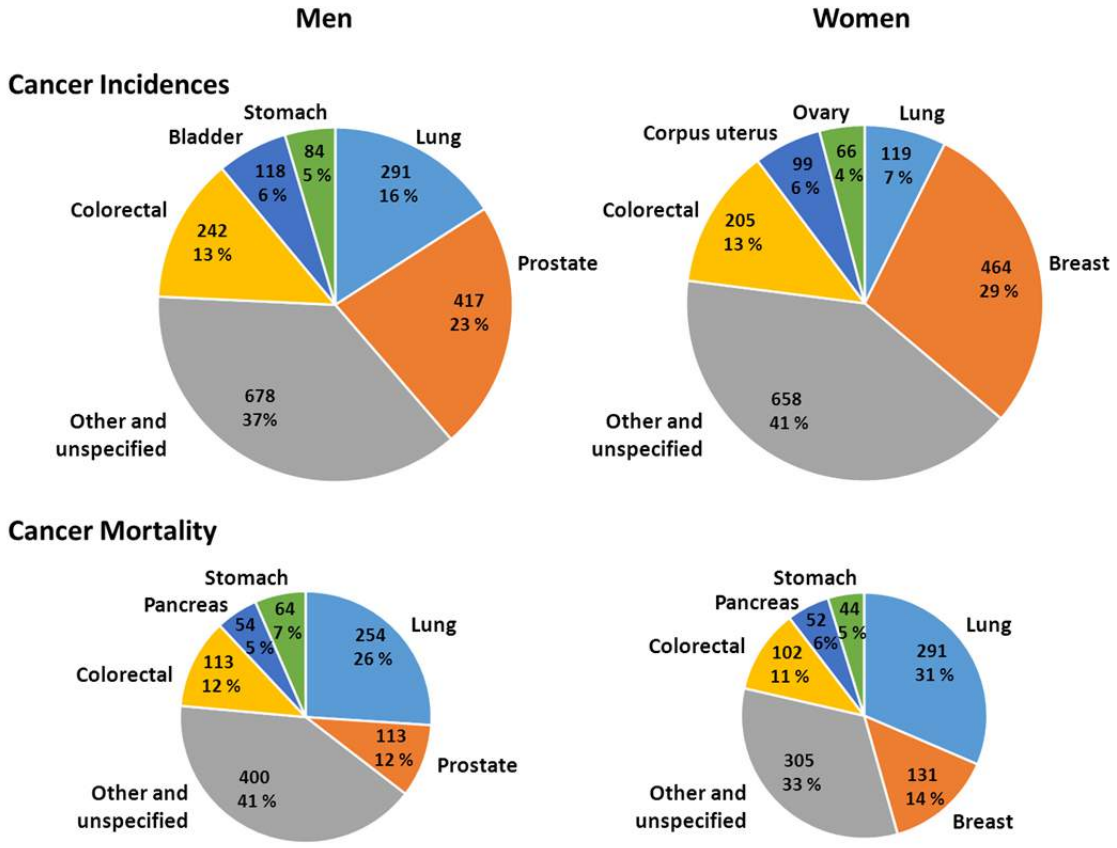

Figure 1.1 Distribution of the expected incidences and deaths for the five most common cancers in Europe 2012. The size of the pie charts reflects the total number of incidences or deaths (adapted from [1]).

1.2 The Development of Cancer and Possible Causes in Brief

Cancer arises from somatic DNA mutations, though the prevalence of a cancer-relevant germ line mutation increases the development of malignant neoplasms [2, 3]. This observation and the fact that the number of cancer incidences increases with age, led to the suggestion that the development of cancer is a multistep process facilitated by the accumulation of mutations [4]. The hypothesis that cellular defects may be inherited by daughter cells and may lead to abnormalities in growth, already had been postulated by Theodor Boveri in the beginning to the 19th century, after he had observed that areas with abnormal growth patterns occasionally emerged from induced multipolar mitosis in a developing *Echinus* embryo (reviewed in [5]). However, not all species seem to be equally prone to develop cancer, and men living in different countries with different habits have differential risks to develop a certain cancer type, independent of the ethnicity. This suggests that genetic factors determine the susceptibility of developing cancer and that customary or environmental factors influence and favor the origination of certain cancer types.

Customary and environmental factors comprise the exposure to hazardous agents, such as ultraviolet (UV) radiation or to chemical substances that directly introduce DNA damage and may lead somatic mutations that have the potential to contribute to malignant transformation of the affected cells. Innate defects in the DNA repair capacity greatly increase the occurrence of mutations and thus the chance of cancer development. Similarly, obtained defects in the DNA repair machinery lead to genomic instability and greatly influence the rate of mutations, whereas under normal circumstances DNA damage is repaired efficiently and the acquisition of mutations is very low. In fact, acquisition of mutations that lead to genomic instability has been proposed to be a prerequisite for tumorigenesis [6].

Chronic inflammation, e.g. induced by exposure to asbestos, has been shown to positively influence the process of cancer formation by modulating enzyme activity in the tumor environment, and the infiltrating immune cells support tumor growth by releasing angiogenic, growth and survival factors [7]. Inflammatory cells such as macrophages produce reactive oxygen species (ROS) that can lead to additional DNA-damage and genetic alterations. Such inflammatory responses have been shown to take place across a wide variety of solid tumors and together with genomic instability are described as "*enabling characteristics*"; characteristics that promote tumorigenesis (see Figure 1.2, section below). Certain habits act on both levels such as smoking, which is associated with a number of cancer types, such as cancer of the lung, the oral cavity, the larynx and the esophagus. Tobacco smoke contains numerous hazardous substances that in combination display increased mutagenic activity and contribute to acute and chronic

inflammatory responses, which increase the risk of cancer development. Explicitly, the number of years of smoking and smoking cessation influence the related cancer death rates [8, 9]. Alcohol consumption, another widespread habit, also influences the risk of cancer development in a dose-dependent manner [10], and in combination with smoking, the observed risk exceeds the multiplicative joint effect determined from either alcohol or smoking alone. [11].

Also viral infections have been associated with cancer formation. The human papilloma virus (HPV) is thought to be the major cause of cervical cancers and hepatitis B (HBV) and hepatitis C (HCV) viral infections may be involved in the formation of liver cancer. Mechanistically, viral gene products may contribute to cell survival to ensure viral replication, and certain viral genomes that integrate into the hosts' genome may lead to deregulated protein expression [12, 13]. Moreover, persisting viral infections contribute to chronic inflammation, indirectly supporting carcinogenesis as described previously [14]. Similarly, the infection with the bacterium *helicobacter pillory* leads to chronic gastritis and is the primary cause of peptic ulcers.

Certain risk factors that contribute to cancer development can be reduced, for example by the banning of known carcinogens, such as asbestos or by refraining from unprotected sunbathing or excessive alcohol consumption and so on. However, other factors cannot be evaded like hereditary predisposition or aging processes that lead to an increased cancer risk. Thus, in developed countries cancer incidences certainly also have increased as a result of the increase in average age.

1.3 Tumor Biology: The Hallmarks of Cancer

Cancer and even tissue-specific cancer is not a single disease, but a collection of diseases. At the beginning of the century, Hanahan and Weinberg suggested that six principles (hallmarks) were inherent to all cancer types and would help to understand how loss or gain of function of certain genes may support disease formation [15]. Over the years, additional hallmark were proposed and incorporated into the theoretical framework (see Figure 1.2). According to theory, cancer development as a multistep process and the hallmarks can be viewed as steps that may take place in various orders. The first steps towards malignancy are probably almost always changes that lead to increased proliferation such as the obtainment of *"self-sustained proliferative capacity"* and the *"capability to evade growth inhibitory signals"*. In normal tissues, proliferation and cell survival is tightly regulated by growth factors whose release and regulation is poorly understood. Cancer cells overcome their dependence on these external signals in various ways, e.g. through autocrine secretion of the necessary growth factors, by increasing the expression of the corresponding receptors or by activating mutations in the downstream

signaling pathways. Homeostasis of cellular proliferation in normal cells is secured by intracellular feedback loops that negatively regulate cell proliferation. However, in the evolving cancer cell the activity of e.g. PTEN, one of the proteins involved in safeguarding, is often quiesced by suppression of expression or by loss-of-function mutations [16]. Furthermore, in pre-malignant cells, the increased activation of proto-oncogenes that leads to aberrant proliferative behavior, normally induces senescence or leads to programmed cell death (apoptosis) of the cell. Thus, the *"evasion of programmed cell death"* is yet another hallmark of cancer and is achieved by loss-of-function mutations of critical regulatory proteins such as the tumor suppressor p53 or by the upregulation of anti-apoptotic proteins like Bcl-2.

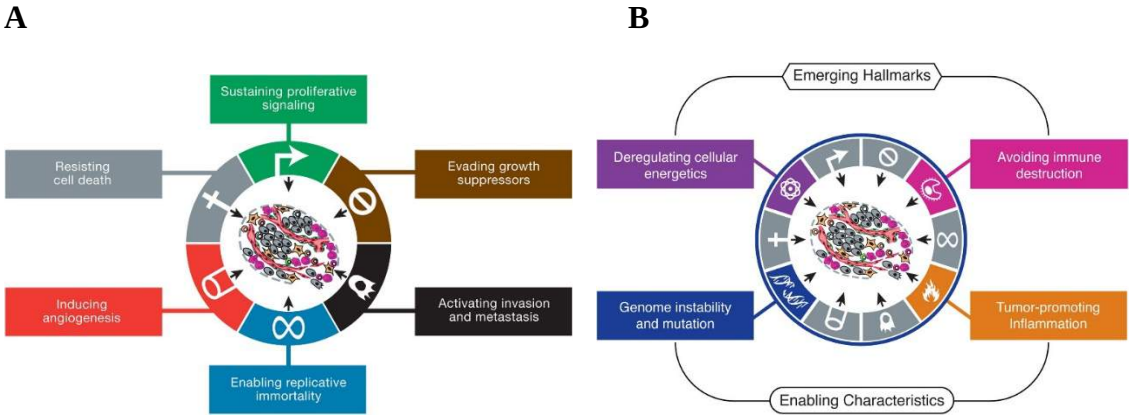

Figure 1.2 Hallmarks of cancer by Hanahan and Weinberg. **(A)** Six traits were found to be common to all types of cancer, and are thought to be indispensable for the development of neoplasms [15]. **(B)** Additional hallmarks have been suggested over the years and were assigned to the category of tumor *"Enabling Characteristics"* or to the category of characteristics that are thought to evolve in order to meet the cancers demands and to ensure its survival *("Emerging Hallmarks")* [6].

In human cells, telomeres shorten at each round of replication. At a critical length, the structure formed by telomeres becomes disrupted, the unprotected DNA ends are recognized by the DNA damage repair machinery, and the cell undergoes senescence. Thus to achieve the trait of *"unlimited replicative potential"* a majority of cancer cells reexpress telomerase, the expression of which is normally only detected in stem cells [17].

Increased proliferation is also connected with replicative stress and increased demands for energy and metabolic resources in order to support cell doubling. Both, replication stress and reactive oxygen species (ROS) from the increased metabolism contribute to mutagenesis and thus promote tumorigenesis. Paradoxically, cancer cells cover their energy need by upregulating the conversion of glucose to lactate even at the presence of oxygen, which is a much less efficient production of ATP than the oxidative phosphorylation taking place in the mitochondria. Increased glycolysis in cancer cells and their dependence on glucose, has been demonstrated by Otto Warburg in 1942, and thus was

named the “Warburg effect” [18]. Aerobic glycolysis as well as other atypical metabolic changes such as increased fatty acid synthesis and increased rates of glutamine metabolism meet the high demand of building blocks for DNA synthesis and cell growth [19].

However, the demand for nutrients and oxygen in continuously growing tumor cell population eventually exceeds the capacity of the existing blood vessels. Thus, the *“induction of angiogenesis”* is considered to be another hallmark of cancer. Though induction of angiogenesis is a physiological process that is triggered in organs that are in the process of growing, upon tissue injury, or in female reproductive organs, angiogenesis in tumors differs and the tightly regulated balance of pro-angiogenic and anti-angiogenic stimuli seems to be tipped towards induction of angiogenesis [20]. Inflammatory responses seem to play a crucial role in tumor angiogenesis [21]. As described above, tumors have been found to arise in sites of chronic inflammation, but inflammatory responses are also induced in tumors that do not originate in such areas. Certain oncogenes, such as *RAS* and *MYC* family members induce a transcriptional program that leads to the secretion of cytokines and chemokines attracting and modulating inflammatory cells involved in tumor progression and angiogenesis [22, 23]. However, the chronic stimulation of angiogenesis results in the formation of unorganized, irregularly shaped and tortuous blood vessels of low functional value. Even though endothelial cells, pericytes and vascular base membrane are present, tumor vasculature seems to be less well organized and the components are loosely associated, leading to increased permeability of the vessels. The leakage of vessels and the absence of functional lymph drainage leads to an increased interstitial pressure in the interior of tumors that may compromise efficient supply of oxygen and nutrients and the removal of waste [24].

It is plausible that the continuous constraint of nutrients and oxygen and the increased mutagenic rate associated with hypoxia might lead to in a more aggressive phenotype capable of forming metastasis [25]. However, several studies indicate that acute hypoxia followed by reoxygenation is a more important determinant of cancer progression and the establishment of distant metastases than chronically reduced perfusion [26–28]. Nevertheless, for a cancer cell to acquire the capacity of *“tissue invasion and metastasis”*, multiple adaptations are required and therefore it is thought to be a late step in malignant transformation. For the achievement of invasive growth, cells need to detach from the basal lamina and neighboring cells and they must be able to degrade and migrate through the extracellular matrix. Depending on the tumor type, spreading of cancer cells may follow different routes. Some cancers only invade neighboring tissues and some form colonies at distant sites in tissue microenvironments that greatly differ from their origin. To achieve the later, cells need to gain the capacity to intravasate into blood or lymphatic vessels, to survive the journey to a distant site, to extravasate, to

adapt to the new microenvironment, and to form a new colony. Obviously, cells may not obtain the capacity to form metastasis at once. Patients can have a numerous circulating cancer cells (CTCs) and not develop metastases; or cells that extravasate may remain dormant for several years.

There is evidence that disseminating carcinoma cells undergo epithelial-mesenchymal transition (EMT) obtaining a more mesenchymal phenotype with even stem-cell-like expression profiles [29]. EMT and the reverse process mesenchymal-epithelial transition (MET) play an important role during embryogenesis in the formation of different types of tissues and organs, and cancer cells may follow this path in their metastatic process. The activation of the TGF-β pathway, which is involved in EMT during embryogenesis, also has been shown to induce EMT in cancer cells *in vitro*. Though TGF-β strongly inhibits growth of epithelial cells, obtained insensitivity to TGF-β-induced growth inhibition may turn the tumor suppressor function of TGF-β into a pro-metastatic function [30]. Some genes, that are induced by TGF-β signaling and have been shown to be involved in EMT, also have been demonstrated to be induced by other factors such as hypoxia and may provide a link between hypoxia and tumor progression [31–33]. However, epithelial-mesenchymal transition has mainly been studied in cell culture. Whether EMT takes place in human neoplasms has been challenged, as cells that have undergone EMT are difficult to distinguish from other stromal cells [34, 35]. Indeed, many breast cancer specimen analyzed in mice and human patients lacked evidence of EMT, but were able to form metastases in the lungs [36]. Thus, although EMT does not seem to be a prerequisite for metastasis, as a naturally occurring cellular migrational process, it is plausible that cancer cells may take this route to disperse.

Certainly, a process as complex as metastasis cannot be fully understood from studies of cell cultures alone, because interaction with the tumor microenvironment most certainly plays a crucial role in this process. The tumor microenvironment consists of fibroblasts and adipocytes as well as infiltrating cells of hematopoietic origin, such as macrophages, neutrophils and mast cells. All of these cell types have been associated with tumor progression, though tumor-associated macrophages (TAMs) have received the greatest attention. The presence of TAMs in the tumor has been correlated with poor patient outcome, but some studies claim the opposite (Reviewed in [37]). Strikingly, poor prognosis related to TAMs also correlates with macrophage growth factors or chemokines expressed and secreted by the tumor cells. Thus, tumor cells may orchestrate TAMs for their use. TAMs have been suggested to facilitate intravasation and primary tumor-stimulated macrophages may be involved in the formation of distant metastases by the induction of matrix metalloproteinase 9 (Mmp-9) and the release of vascular endothelial growth factor (VEGF) [38, 39]. Besides the production of several factors

involved in angiogenesis, macrophages also secrete various growth factors including ligands of the epidermal growth factor receptor family that stimulate tumor growth directly. Although in the early phase of carcinogenesis macrophages of the type M1 are involved in the elimination of tumor cells, in established malignancies M2-polarized macrophages act as suppressors of the adaptive immune system [40]. Tumors infiltrating dendritic cells are kept in an immature state, and as in chronic infections, these dendritic cells are capable of suppressing T-cell activity. Thus, macrophages also play a role in the *"evasion of the immune system"*, described as an emerging hallmark of cancer by Hanahan and Weinberg [6].

Although the big efforts towards a broader understanding of the tumor biology of solid cancers have widened our knowledge, a multitude of questions concerning tumor biology remains unanswered. For example, the composition of tumor tissue provides ample grounds for discussion. There are indications for the existence of cancer stem cells (CSCs), which imply a hierarchical tumor model and on the other side, there is the model of clonal evolution. However, there may not be a clear-cut boundary between the two theories; clonally evolving cancer cells may obtain stem cell like traits, or stem cell derived cancer cells may give rise to progeny that independently expands. So far, mostly immunosuppressed animals served as model system to assess the CSC theory by testing the tumor initiating capacity by engrafting tumor subpopulations. The results of these studies indicate that often only a small subpopulation is capable of tumor formation, which is interpreted as indicative for a stem cell population. However, such studies may underestimate the actual tumorigenicity of the original cell population, as some xenogeneic immune responses cannot be excluded [41]. The finding of valid cancer stem cell markers in solid tumors may be indispensable for shedding light on the heterogeneity and the composition of tumors.

1.4 Cancer Treatment with Focus on Radiotherapy

Treatment of cancer has greatly changed over the last decades. For a long time surgery and radiotherapy were the only effective cancer therapies with the auxiliary support of chemotherapy such as the treatment with cytostatics, or endocrine therapy, which was used for hormone-responsive cancers such as certain breast cancers. The better understanding of tumor biology and the advancement in diagnostics opened the door for therapies aiming at cancer type specific moieties or signaling pathways. Even though for resectable tumors surgery may be the first choice, about 50 % of all cancer patients receive radiotherapy in the course of their illness [42]. Lastly, in combination with molecular targeting, radiotherapy may set new standards.

1.4.1 Ionizing Radiation: Physical Properties and Biological Effects

Photon-based radiotherapy is applied by an external beam or internally by brachytherapy, which involves the introduction of a sealed radioactive source. For irradiation with external beams, X-rays produced by the collision of accelerated electrons with a metal anode, are widely used, as well as γ-rays emitted by a cobalt unit. The latter is increasingly replaced by linear accelerators (X-ray devices). Both, X-rays and γ-rays are electromagnetic waves that differ primarily in their origin. Besides photon therapy, proton beam therapy is applied, which shows a different dose distribution across the

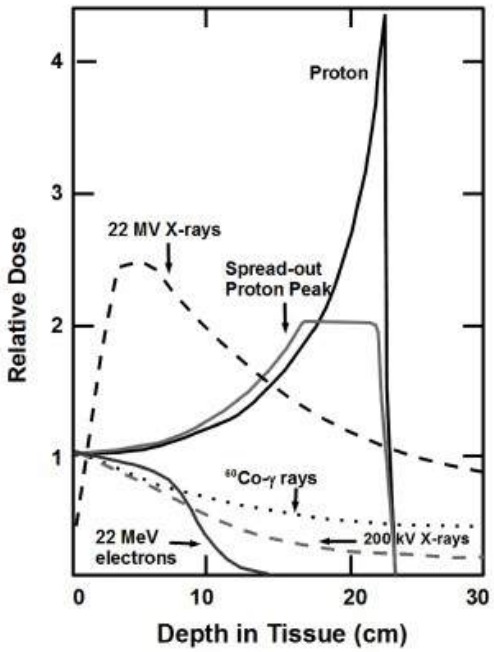

Figure 1.3 Dose distribution profiles of photons, protons and electrons entering biological matter, for 22 MeV X-rays, 200 keV X-rays, ^{60}Cobalt-γ rays, 22 MeV electrons, an unmodulated proton-beam plateau with the Bragg ionization peak, and a spread-out proton Bragg peak used for proton therapy [43].

tissue than the one produced by photons. Protons are particles that enter the tissue and release most of their energy all at once at the so-called “Bragg Peak” (see Figure 1.3, above). The penetration depth of a proton depends on its energy. Electromagnetic waves, on the other hand, propagate through tissue while exponentially losing energy through the interaction with matter. There are different ways of how photons interact with matter, three of which are of interest with regard to radiation therapy: the photo-electric effect, Compton scattering, and pair production (see Figure 1.4). Which effect occurs depends on the energy of the photon and the atomic number of the absorbing material the photon interacts with. Compton scattering is the most frequent incident produced by therapeutic beams. All three events lead to the production of electrons that propagate through the tissue leading to multiple interactions. Photons can directly interact with DNA and damage the genetic material; however, it is thought that their main targets are water molecules due to prevalence of the latter. Ionized water molecules (H_2O^+) are reactive, annex H-atoms or electrons from other molecules and thus introduce damage to chromosomes, proteins and membrane structures of the cell.

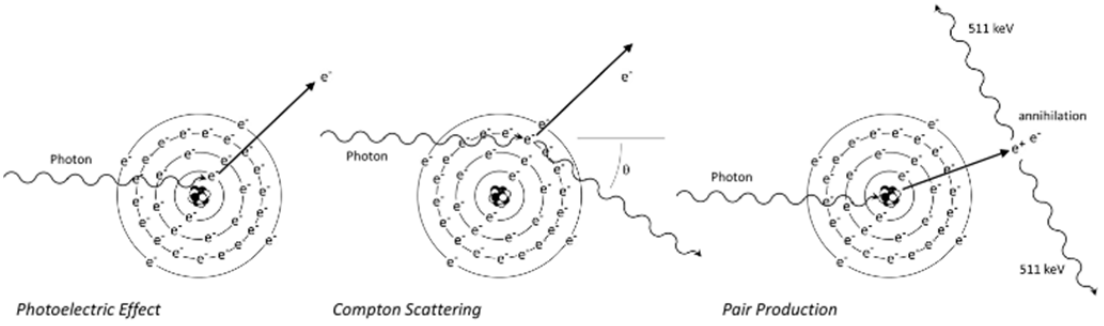

Figure 1.4 The three types of interaction of photons with biological matter, important for radiation therapy. *Photoelectric effect:* photons (10-25 keV) collide with an electron of the inner shell of an atom, whereupon the electron is ejected. The open space is filled by an electron of the outer shell leading to the emission of X-rays. *Compton scattering:* photons interact with loosely bound electrons of the outer shell of an atom. The photon transmits energy to the electron, itself is scattered and undergoes interactions with other atoms. *Pair production:* high-energy photons (>1.02 MeV) that collide with a nucleus lead to the emission of a positron that annihilates with an electron producing two photons, that propagate in opposite directions.

However, it is actually the free electrons, which cause the major part of the damage. They also can damage DNA either directly or indirectly. Electrons do not propagate linearly through the matter as photons do. With a loss of 2 MeV energy per centimeter, their range of action is limited and proportional to their initial energy. Released from the original atom, they cause further ionizations, interact with and excite valence electrons of other atoms, or break chemical bonds. When the energy of an electron has been reduced, it eventually gets trapped, e.g. by a water molecule to form a highly reactive hydroxyl radical, which is capable of introducing DNA single- or double-strand breaks,

or damages DNA bases. In presence of oxygen, different radicals evolve such as oxygen radicals and the relatively long-lived peroxide radical [44]. Furthermore, the DNA radicals emerging from the interaction with such radicals, are thought to become “fixed” upon the reaction with O_2-molecules, which greatly impairs the repair process or even leads to irreparable damage and apoptosis (Reviewed in [45] and [46]). The reduced survival in normoxic versus hypoxic cells is well known and the difference is described as the oxygen enhancement ratio (OER). The rationale behind ionizing radiation as a treatment option is believed to depend mainly on the direct or indirect introduction of lethal DNA damage. However, the role of oxidative damage of proteins and lipids, which may impair the functionality of organelles such as mitochondria, and the oxidative stress induced in general, have received rising interest during the last years [44].

1.4.2 Ionizing Radiation and Cancer Cells vs. Normal Tissue Response

A favorable cancer therapy would only induce damage at the site of the tumor and spare normal tissue, which in the case of photon beams cannot be achieved due to the physical properties of the photons as described above. Even though technical advances now allow a more precise dose application, surrounding healthy tissue still receives a substantial dose. Like cancer therapeutics that interfere with cell division, radiotherapy takes advantage of the fact that cancer cells are fast proliferating cells. Proliferating cells are more radiosensitive than nonproliferating cells, as, for example, radiosensitivity is increased for cells in late G2/M phase [47]. Human cells possess sophisticated DNA repair machineries to eliminate various types of DNA damage, however, the bigger and more complex the damage is the greater is the chance that the cell cannot adequately cope with it. Double-strand breaks (DSBs) are thought to be most toxic to cells. If DSBs remain unrepaired, the cell may undergo apoptosis, or if falsely repaired, chromosomal aberrations can arise that may lead to mitotic catastrophe.

Cancer cells often have corrupted cell cycle checkpoints, which allows them to progress even though there may be unrepaired damage [48]. The G1/S phase checkpoint, which is often deregulated in cancer cells, normally prevents cells from entering the S phase and from starting to replicate their genome in the presence of DNA damage. For instance, in S phase, unrepaired single-strand breaks (SSBs) lead to a collapse of the replication fork and introduce DSBs. Various chemotherapeutics that are combined with ionizing radiation aim to potentiate the damage introduced, to inhibit efficient repair or to arrest cells in the radiosensitive G2/M phase.

Adaptation of the radiation treatment schedule also has been found to contribute to a successful treatment outcome. Standard radiotherapy follows the rule of dose fractionation introduced by Henry Coutard in 1922, who reported impressive results in the

treatment of advanced laryngeal cancers with less side effects on the normal tissue [49]. The success of fractionated treatment relies on the 4 R's of radiotherapy: *Repair* of sublethal damage, *Reassortment* of cells within the cell cycle, *Repopulation* and *Reoxygenation*. Fractionated treatment provides normal tissue with sufficient time to repair sublethal damage and to replace the cells that have undergone cell death. However, different tissues have very different capacities to repair DNA damage and to repopulate damaged tissue. Skin, mucosa and intestinal epithelium are early responding cells and accelerated repopulation is triggered within few weeks after the start of treatment. It is mainly those tissues that are spared by fractionated treatment.

On the level of tumor cell kill, fractionation of the radiation dose offers the possibility to reach cells that were in a more resistant cell cycle phase during the application of a previous dose fraction, which increases the potential to kill all cells. Similarly, hypoxic areas, which are more radioresistant, may become reoxygenated and thus more sensitive to treatment with radiation. However, there is evidence that accelerated treatment, involving higher doses per fraction, but fewer sessions, is actually more efficient than the traditional schedule [50]. In the extreme, a high dose of radiation is delivered in only one or few fractions [51]. This schedule has been shown to be superior to the standard fractionated radiation therapy with respect to the overall survival and local tumor control for inoperable non-small-cell lung cancers [52, 53]. At higher dose fractions, the intrinsic radioresistance of all cancer cells present in the tumor might be overcome.

The aspect of a highly resistant subpopulation has not been considered in the 4 R's of radiotherapy. However, there is *in vivo* and *in vitro* evidence that radiation treatment leads to the selection of more resistant cancer cells, which may result in failure of local tumor control in patients treated with radiotherapy [54–57]. The development of radioresistance may be explained by the heterogeneity of the tumor cell population, leading to the survival and thus to the selection of more resistant phenotypes upon radiation treatment. Pearse et al. obtained several clones with increased radioresistance after irradiation of the parental MDA.MB231 breast cancer cell line with 3-5 fractions of 2-6 Gy per fraction. At doses higher than 6 Gy, even the most resistant cell types appeared to be affected by the damage induced; on the other hand, at doses lower than 2 Gy, most cells were able to cope with the damage introduced. The selected subclones showed a lower apoptotic rate, which may account for at least a part of the increased radioresistance. Moreover, radioresistance did not arise in cell populations from a single clone [54] and not all parental cell lines showed evidence of radioresistant subpopulations [58, 59], indicating that existing heterogeneity may allow for the selection of a resistant subpopulation and rather not lead to the origination of new mutations.

Reduced apoptosis, the capability of activating DNA repair checkpoints or increased capacity to efficiently repair DNA damage, especially lethal double-strand breaks, may contribute to radioresistance of a cell population. This are features common to stem cells, and thus has motivated researchers to focus on determining cancer stem cells (CSCs) or tumor-initiating cells (TICs) [60–62]. In general, regardless whether CSCs, TICs, or just resistant cancer cell subpopulations are present, curative radiation therapy aims to destroy all cells with clonogenic potential. Thus, the combination with compounds that specifically target the intrinsic radioresistance or the inherent weaknesses in such cells has been regarded as having a great potential for increasing the efficacy of radiation therapy.

1.4.3 Conventional Combined Radiotherapy and Chemotherapy

Classical drugs applied in combination with radiotherapy are cytotoxic drugs that target fast replicating cells. 5-fluorouracil (5-FU) acts as antimetabolite and inhibits thymidylate synthase (TS) leading to the depletion of deoxythymidine triphosphate (dTTP), which severely interrupts DNA synthesis and repair. 5-FU metabolites can also be misincorporated directly into DNA, whose repair may lead to a replication fork collapse and lethal DSBs [63]. Similarly, gemcitabine, a cytidine analogue leads to a redistribution of the cells to the S phase due to replication stress [64] and deregulates dNTP pools by depleting dATP [65]. As for the treatment with 5-Fu, this may lead to misincorporation and misrepair of incorrect bases after radiation. Cisplatinum (CDDP) or other platinum derivatives act as DNA crosslinking agents, forming interstrand and intrastrand adducts, which interfere with DNA-replication and mitosis, and also hinder transcriptional activities [66, 67]. Etoposide also interferes with DNA synthesis by forming a complex with topoisomerase II and DNA [68]. Etoposide stabilizes the cleaved DNA intermediate and inhibits further processing, leading to the generation of permanent DNA strand breaks. Paclitaxel and docetaxel on the other hand act on microtubules; they bind and stabilize the microtubule structures and thus interfere with crucial mitotic processes, which leads to an accumulation of proliferating cells in the radiosensitive M phase. A single compound as wells as combinations of the drugs described above can accompany radiotherapy. For example, the combination of docetaxel with cisplatin / 5-FU, followed by chemo-radiotherapy has been investigated in clinical phase II and phase III trials and was found to significantly improve overall survival of patients with locally advanced squamous cell carcinoma of the head and neck [69, 70].

1.4.4 Radiotherapy in Combination with Molecular Targeting

A better understanding of the underlying molecular mechanisms involved in the pathogenesis of cancer revealed the potential of specifically targeting molecular moieties, on which the cancer cell may depend on. Most promising are approaches that make use of cancer specific deficiencies to particularly restrict the recovery of malignant cells after conventional radio- and chemotherapies. Furthermore, various aberrantly activated signaling pathways, necessary for the tumor cell survival, may be inhibited. Even metabolic or microenvironmental differences between tumor cells and normal cells were considered for molecular targeting [71]. However, depending on the type of cancer, different targets might be appropriate. Thus, the use of reliable diagnostic markers is required. Though research on personalized cancer therapy is still at an early stage, some molecular targeting drugs have been already approved for clinical application. Inhibition of the epidermal growth factor receptor (EGFR) by the antibody cetuximab is one example that shows that the determination of the status of the entire pathway and even other connected pathways may be critical for the treatment outcome and must be considered [72].

Up to now, various strategically different molecular targets were investigated for their synergistic effects with ionizing radiation. Bevacizumab a humanized murine monoclonal antibody directed against the vascular endothelial growth factor (VEGF) inhibits the interaction of VEGF-A with the VEGF receptor [73]. Bevacizumab had initially been approved as a single treatment agent to inhibit tumor angiogenesis, but is now considered for the use in combination with radiotherapy in order to counteract IR-induced VEGF expression that was observed to take place in malignant cells. Inhibition of VEGF-A by bevacizumab specifically increased the cytotoxic effects of radiation on endothelial cells [74, 75]. However, even though endothelial cells in tumors may be more instable and fragile, endothelial cells of normal tissue seems to be considerably affected too, which may prove to be an insurmountable obstacle for a combinatorial treatment [76].

On the other hand, VEGF inhibition may actually lead to a normalization of tumor vasculature, which is otherwise destabilized by the excessive VEGF secreted by tumor cells. Normalization of tumor vasculature may improve oxygenation of the tumor tissue, and, thus lead to radiosensitization if given ahead of radiotherapy. NVP-BEZ235, a dual PI3K/mTOR kinase inhibitor, leads indirectly to reduced VEGF secretion and vascular normalization [77]. The PI3K-Akt-mTORC1 pathway is often aberrantly activated in cancer cells and promotes cell growth, proliferation and survival (reviewed in [78]). The administration of NVP-BEZ235, which is already in phase I/II clinical trials, although not in combination with radiotherapy, has been shown to lead to strong radiosensi-

tization of cancer cells and human umbilical vein endothelial cells (HUVECs) *in vitro* [79]. Radiosensitization by NVP-BEZ235 was much stronger than for other PI3K inhibitors, and data obtained by Mukherjee et al. suggest that NVP-BEZ235 also inhibits PI3K-like kinases (PI3KK) other than mTOR, namely ATM and DNA-PKcs, which all have highly homologous catalytic domains [80]. Targeting the DNA repair machinery by the inhibition of ATM or DNA-dependent protein kinase (DNA-PK) to delay or inhibit repair has been shown to successfully sensitize cancer cells or human tumor xenografts before [81–83]. However, DNA-PK is crucial for DSB-repair by non-homologous end joining, which is the repair prominent pathway in the resting G0/G1 phase of the cell cycle and, therefore, is crucial to normal cells. Susceptibility of persons with inherited loss of ATM functionality to DNA damage indicates that normal tissue may be severely affected by ATM inhibition. Thus, NVP-BEZ235 as well as ATM or DNA-PK inhibitors may lead to a sensitization not only of cancer cells, but also of normal tissue and thus may not be feasible for the combination with genotoxic drugs. As for local irradiation, toxicity in the surrounding healthy tissue will have to be carefully analyzed.

The concept of *"synthetic lethality"*, which originates from studies on *Drosophila melanogaster*, has been adapted for molecular targeting of cancer cells with the expectation of reduced normal tissue toxicity and increased treatment efficacy. Synthetic lethality describes the circumstances when two or more mutations in genes lead to cell death, whereas the mutation in each gene alone does not. Cancer cells often show deficiencies in the DNA repair machineries or in cell cycle checkpoints, which contributes to genomic instability and thus cancer progression. On the other hand, such deficiencies can be exploited to generate synthetic lethality. A classical approach is the inhibition of poly(ADP-ribose) polymerase 1 (PARP1), which facilitates base excision repair (BER) and SSB repair. PARP1 inhibition is less toxic to normal than to cancer cells for the following reasons. In cancer cells, unrepaired SSBs may lead to the formation of toxic DSBs if the cell progresses from G1 into S phase due to a defect G1/S checkpoint, which often occurs in cancer cells. The formation of DSBs, renders especially BRCA1- or BRCA2-deficient cancers cells with impaired HR susceptible to PARP1 inhibitors [84, 85]. The initial treatment success of the PFS of the PARP inhibitor olaparib observed in a phase II trial on serous ovarian carcinoma unfortunately did not manifest itself in an increased overall survival. Nevertheless, a phase III trial has been launched this year with olaparib for the treatment of BRCA mutated ovarian cancer[1]. It has been also suggested that PARP inhibitors sensitize cells to treatment with ionizing radiation, by increasing the number of toxic DSBs derived from SSBs [86]. PARP inhibitors specifically sensitize rapidly proliferating cells or cells harboring DNA damage repair

[1] http://clinicaltrials.gov/show/NCT01844986 (downloaded on October 30, 2013)

deficiencies [87] and the radiosensitizing effect has been demonstrated in multiple *in vitro* and in preclinical studies (reviewed in [88]).

The compromised G1/S checkpoint not only renders cancer cells sensitive PARP inhibition, but also to abrogation of the S and the G2/M checkpoint. DNA damage introduced by irradiation may not be repaired before these cells enter premature lethal mitosis. Inhibition of S and G2/M checkpoints can be achieved by Chk1-inhibitors or the combination of Chk1/ATR inhibitors [89, 90]. Interestingly, cancer cell lines with wild type p53 were less prone to undergo mitotic catastrophe than their p53-negative counterparts, even though the G2 checkpoint was equally abrogated [91, 92]. For cancer cells that possess wild type p53, the G1 checkpoint may become sufficiently activated upon the introduction of DNA damage to prevent them from rushing through the entire cell cycle without brake. However, many advanced cancers display aberrant p53 signaling and in those cases, Chk1 inhibitors may provide an option for targeting cell death resistant cancer types, e.g. the aggressive triple negative breast cancer cells as has been demonstrated in preclinical settings [93]. Several Chk1 inhibitors have entered clinical trials and are administered in combination with radiation therapy or DNA damaging agents [94]. Also, the combination of Chk1-inhibitors plus IR with molecular targeting drugs, e.g. with PARP1-inhibitors or with conventional therapeutics such as gemcitabine are under investigation and both show promising results [95–97].

The inhibition of growth factor receptors also has received a great deal of attention with regard to molecular targeting in combination with IR. The first part of the thesis will be dedicated to EGFR inhibition by means of *designed ankyrin repeat proteins* (DARPins) *in vitro* and *in vivo*. Thus, the rationale and consequences of EGFR inhibition will be described in the following sections.

The topic of the second part of the thesis is also dedicated to molecular targeting in combination with ionizing radiation and will be about the major vault protein (MVP) as target for radiosensitization, as well as the analysis of the underlying mechanisms.

2 Targeting the EGFR Receptor by DARPins

2.1 Introduction: Targeting the EGF Receptor

2.1.1 The Epidermal Growth Factor Receptor as Target for Cancer Therapy

The epidermal growth factor receptor (EGFR/ErbB1) is one of the four members of the cell surface receptor tyrosine kinase family ErbB and is expressed in all epidermal, mesenchymal and neuronal tissues. The ErbB receptor tyrosine kinases play an important role in developmental processes and tissue homeostasis [98]. Extracellular signals transmitted by the ErbB receptors are involved in the regulation of cell survival, proliferation and differentiation as well as in angiogenesis, migration and invasion. Deregulation of these important pathways contributes to carcinogenesis. Overexpression of EGFR or deregulation of EGFR signaling is found in many solid tumors. Moreover, increased EGFR signaling correlates to poor patient prognosis, rendering EGFR a promising target for cancer therapy.

2.1.1.1 Activation and Regulation of the EGF Receptor Family

Like the other members of the ErbB family (except for ErbB2), EGFR consists of an extracellular domain for ligand binding, a hydrophilic transmembrane domain and an intracellular domain involved in signal transmission through interaction with other tyrosine kinases and adaptor proteins. No ligand is known to bind to the extracellular domain of ErbB2 (Her2) but it readily dimerizes with other ErbB family members. Dimerization is a crucial step in activation of all ErbB receptor tyrosine kinases. The binding of a ligand to the extracellular domain and the subsequent conformational change allow for the formation of homodimers or the formation of heterodimers with other members of the ErbB family. Pairing of the receptors results in activation of the kinase domain and the phosphorylation of various tyrosine residues in the cytoplasmic receptor domain (for a schematic view of this mechanism, see Figure 2.1). The phosphorylated residues provide docking sites for interaction with the activated EGF receptor. Olayioye et al. suggests that depending on the stimulatory ligand, the composition of the receptor dimer and the signal duration and intensity, the consequential phosphorylation pattern may vary, which leads to a differential recruitment of interaction partners and thus to a diversification of the signaling responses. For example, the adaptor protein Grb2 only interacts with the homodimer of EGFR after stimulation with epidermal growth factor (EGF) but not with the EGFR/ErbB4 dimer activated by neuregulin, whereas Shc, another adaptor protein, interacts with both [99].

So far, more than 13 structurally and functionally closely related ligands of the epidermal growth factor family have been identified [100]. All members of the EGF family are type I transmembrane proteins. With few exceptions, they all localize to the plasma membrane where the extracellular domain, the actual receptor ligand, is shed upon cleavage. This so-called ectodomain shedding is facilitated mostly by metalloproteases belonging to the ADAMs family. The ADAMs are transmembrane proteins with multiple domains, the functions of which are not well known yet, except for the protease function.

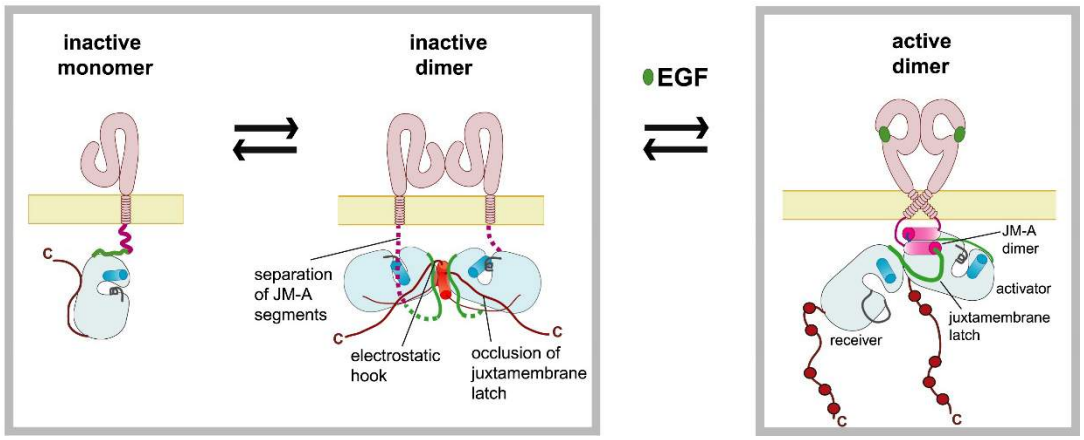

Figure 2.1 Activation of EGFR, image adopted from Jura et al. [101]. Ligand binding leads to a conformational change of the four extracellular protein domains [102], which allows for the formation of asymmetric EGFR dimers. The formation of the helical JM-A dimer and the orientation of the juxtamembrane latches stabilize the dimer and position the kinase domain of one of the EGFR partners (designated as activator) to phosphorylate the receiver. Recent findings imply that electrostatic interactions of the intracellular domains with the membrane are also important for stabilization of the dimer [103].

Activation of the EGF receptor and downstream signaling eventually leads to its endocytosis, which takes place in a clathrin-dependent as well as in a clathrin-independent way. In response to ligand-induced activation, endocytosis of EGFR follows predominantly the clathrin-dependent way [104]. However, at least four redundant pathways through clathrin-coated pits have been reported, involving ubiquitination, interaction with AP-2, C-terminal Lys residues, and Grp2 [105]. Originally, it was assumed that endocytosis primarily stood for the downregulation of EGFR and its downstream signaling. Indeed, aberrantly increased rates of EGFR endocytosis hampers MAPK signaling, which suggests that endocytosis contributes to the regulation of EGFR signaling [106]. However, EGFR activity is not limited to the cytoplasmic membrane, stimulation of certain pathways, such as the Akt/PI3K pathway, may occur to a significant extent from within the cell [107]. Endocytic trafficking is also essential for other functions of EGFR, such as the induction of apoptosis in late endosomes [108], or its proposed func-

tion as co-activator for the transcription of cyclin D1 [109, 110], iNOS [111] and other genes (reviewed in [112]) in the cell nucleus. In the nuclear compartment, EFGR is also thought to be involved in DNA repair through interaction with DNA-PK [113]. Finally, endocytosed EGFR can be recycled to the plasma membrane, which is dependent on which ligand is bound to EGFR [114]. Transforming growth factor alpha (TGFα) preferentially leads to recycling of EGFR, while EGF targets the receptor for degradation [115].

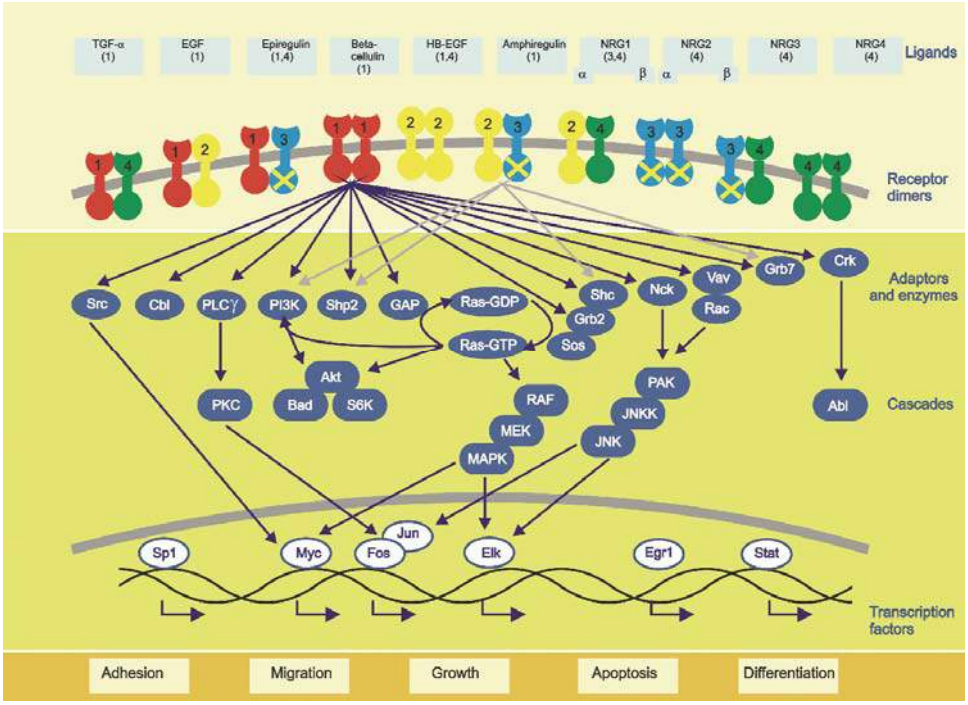

Figure 2.2 The receptor tyrosine kinase family ErbB signaling network adopted from [116]. The complex interplay of the four ErbB family members allows for the regulation of a plethora of signaling pathways, including cell survival, proliferation, migration and differentiation.

2.1.1.2 Signaling of the EGFR Family in Cancer

As mentioned before, EGFR was found to be overexpressed or hyper-activated in many solid cancer types, including cancer of the head and neck, colon, lung, breast, ovary, pancreas, and brain [117–123]. Additionally, other ErbB family members were found to be deregulated in cancer tissue. ErbB3, similarly to EGFR, seems to be overexpressed across various human carcinomas. Although ErbB2 expression has been mainly studied in breast carcinoma, it is expressed in other carcinomas as well. ErB-4 was found to be overexpressed in breast, ovarian and colon cancer albeit with lower frequency than the other ErbB family members are [124–126].

Increased signaling through EGFR was found to be caused by changes on different levels of EGFR regulation. Increased receptor abundance through gene amplification or

decreased degradation, overexpression of receptor ligands, increased shedding of ligands by ADAMs, activating mutations in the tyrosine kinase domain, or truncated, and constitutively active EGFR (EGFRvIII) have all been shown to lead to increased EGFR signaling in cancer.

It is still a matter of debate, however, whether deregulation of the EGFR signaling contributes to malignant cell transformation or whether it is a consequence of the transformation. Different studies demonstrated that overexpression of EGFR in the presence of a sufficient number of growth factors, such as EGF or TGF-α, had the capacity of *in vitro* cell transformation (reviewed in [127]). Moreover, an overexpression of two receptors of the ErbB family has stronger transforming capacity than overexpressing either receptor alone, as demonstrated by ectopic expression of various ErbB receptor pairs in NIH 3T3 cells, which are devoid of ErbB proteins [128]. Except for cells with Her2 expression, stimulatory growth factors were necessary for full transformation. That Her2 can readily dimerize may contribute to its increased potency in cell transformation compared to the other family members.

Further evidence for the role of EGFR in cell transformation was provided by the growth inhibition induced by the downregulation of EGFR in carcinoma cells overexpressing the receptor as well as by inhibition of the stimulating growth factors [129–131]. However, the necessity of the inhibition of several growth factors or both growth receptors, EGFR and ErbB2, at the same time in order to obtain a significant reduction in proliferation, indicates that there is at least a partial redundancy in ErbB signaling. Similarly, in transgenic mouse models, it has been shown that EGFR overexpression alone merely leads to increased proliferation, but not to cellular transformation [132]. Further steps are necessary for a cell to turn into a cancerous cell.

2.1.1.3 EGFR and other ErbB Family Members as Prognostic Marker for Patient Outcome

The prognostic value of EGFR expression and with regard to overall survival and progression free survival has been demonstrated for different cancer types, such as lung, squamous cell carcinoma of the head and neck (SCCHN), breast, and colon [117, 121, 120, 122]. In addition, the expression of ErbB2 has been proposed as independent prognostic factor [133]. However, this is controversial (Reviewed in [134]).

Although heterodimerization of ErbB receptors may play an important role in tumorigenesis, only few studies addressed the prognostic significance of the combined receptor expression. Xia et al. showed that overexpression of all four ErbB family members correlated with decreased overall survival of patients with oral squamous cell carcinoma [135]. Even more predictive significance was obtained by including only the three ErbB

family members EGFR, Her2 and ErbB3, but not ErbB4 [135]. The inclusion of EGFR did not significantly increased the prognostic performance. Abd El-Reim et al. came to a similar conclusion in a study on invasive breast carcinoma, namely that the combinatorial overexpression of Her2/ErbB3 was a strong indication for poor treatment outcome. Furthermore, they observed that even though EGFR and Her2, as independent markers, showed a negative correlation with patient outcome, the combined expression did not. However, triple positive tumors that strongly expressed ErbB4 on top of EGFR and Her2 led to significantly worse overall survival and disease-free survival [136]. Studies on the ErbB family members as prognostic marker for treatment outcome in colorectal cancer were even more contradictory. The investigation of all four family members performed by Lee et al. confirmed earlier findings that EGFR and Her2 alone were not prognostic factors for colorectal cancer patients. Interestingly, they found a strongly biased expression of Her2/ErbB3 in early stage cancers, while in late stages Her2/ErbB4 expression was more prominent. The strong correlation with cancer stages indicates that different ErbB family members may have differential roles in cancer progression [126].

2.1.2 EGFR Targeted Therapy: Current Approaches

The association of EGFR with a more aggressive cancer phenotype and its role in cell proliferation and survival turned EGFR into a target of interest for cancer therapy. Various approaches to counteract EGFR signaling have been developed, whereof inhibition by monoclonal antibodies and tyrosine kinase-specific inhibitors have found their way into clinics.

2.1.2.1 Monoclonal Antibodies

Cetuximab, a chimeric human murine monoclonal anti-EGFR antibody has been approved by the U.S. Food and Drug Administration (FDA) as adjuvant or single therapy in recurrent colorectal cancer and in regionally advanced squamous cell carcinoma of the head and neck (SCCHN)[2]. In a clinical trial (phase III) on SCCHN, cetuximab has been shown to have a survival benefit and an increased 5-year survival in combination with radiation therapy over radiotherapy alone [137, 138]. In colorectal cancer, however, retrospective studies lead to the conclusion that patients with KRAS activating mutations as opposed to patients with wild type KRAS did not profit from EGFR inhibition and that disease progression might even be adversely affected (Reviewed in [139, 140]). In SCCHN, the prevalence of KRAS activating mutations is very low and testing

[2] http://www.cancer.gov/cancertopics/druginfo/fda-cetuximab#Achor-Kras-7612. Updated 07.02.2013

is not routinely performed. In 2006, panitumumab another monoclonal antibody targeting EGFR was approved by the FDA as second line treatment of EGFR-expressing metastatic colorectal cancer with disease progression.[3] Panitumumab is a fully human antibody and is considered safer with regard to infusion reactions that arise in response to the murine sequence of cetuximab [141, 142].

Both antibodies bind to the extracellular portion of the epidermal growth factor, inhibit ligand binding and eventually lead to degradation of the receptor. However, since cetuximab is an antibody of the isotype IgG1 and panitumumab of the isotype IgG2 their mechanism of action in complement activation or in induction of antibody dependent cytotoxic reactions differ [143]. Antibodies of the IgG1 isotype lead to a stronger complement activation than IgG antibodies of the subtype 2 [144, 145]. Both IgG1 and IgG2 antibodies mediate antibody-dependent cell-mediated cytotoxicity (ADCC). Schneider-Merck et al. showed that both panitumumab and zalutumumab (an IgG1 antibody) mediated ADCC with myeloid effector cells *in vitro*, but that only zalutumumab was able to induce ADCC through natural killer cells [146]. Nonetheless, with regard to treatment efficacy, it is too early to draw a conclusion; an ongoing phase III trial compares the efficacy of cetuximab and panitumumab in metastatic colorectal cancer and preliminary results will be published toward the end of the year 2013[4]. Interestingly, tumors that had acquired resistance to treatment with cetuximab through point mutations in the extracellular domain of the EGF receptor showed sensitivity towards panitumumab [147].

However, as mentioned above, not all cancer cells are sensitive to EGFR inhibition in the first place. In metastatic colorectal cancer (mCRC), only 10 to 20 % of the patients respond to therapy with monoclonal antibodies (mAbs) targeting the EGF receptor [148]. For example activation of oncogenic effector proteins downstream of EGFR contribute to treatment resistance. In patients with mCRC, activating mutations in KRAS account for about 35 - 45 % of treatment failure, with additional 10 - 20 % due to activating mutations in BRAF [149]. KRAS mutations and mutations in its downstream target BRAF are mutually exclusive, but are not found in all treatment resistant tumors. EGFR gene amplification is an indicator for treatment response, but on its own is not such a strong predictor as KRAS or BRAF. Likewise, PTEN and PI3K mutational status only have a predictive power in KRAS wild type tumors, whereas wild type PTEN and PI3K status correlates with increased PFS/OS and PFS, respectively. The analysis of ligand expression in correlation with the treatment response to anti-EGFR mAbs was hampered by technical difficulties, though ligand overexpression may be of

[3] http://www.cancer.gov/cancertopics/druginfo/fda-panitumumab Updated 07.03.2013

[4] http://clinicaltrials.gov/show/NCT01001377 Downloaded 09.09.2013

predictive value (reviewed in [150]). Furthermore, the status of other growth factor receptors may critically influence the success of EGFR-inhibition therapy. The insulin growth factor receptor IGFR and c-Met are two such receptors known to confer resistance to EGFR inhibition. However, increased IGFR and c-Met signaling often becomes apparent after or during treatment with EGFR inhibitors and contributes to the evolution of treatment resistance to initially sensitive tumor cells [151, 152]. Secondary treatment resistance will be described in more detail in the discussion (see section 2.5.6).

2.1.2.2 Small Molecular Tyrosine Kinase Inhibitors

The second family of effectors targeting the EGF receptor that is in clinical use comprises the tyrosine kinase inhibitors (TKIs). These small molecular compounds block the ATP binding pocket of the kinase domain, thereby inhibiting autophosphorylation and activation of the receptor, and the induction of downstream signaling cascades. Since the tyrosine domain is the most conserved region among tyrosine kinases, the specificity of a TKI is an issue, but this also offers the chance to target multiple kinases at the same time.

As an advantage over an antibody treatment, TKIs also inhibit EGF receptors harboring activating mutations, which occur predominantly in lung cancers. These mutations are located in proximity of the ATP-binding pocket of the tyrosine kinase domain and consist of small in-frame deletions or point mutations that lead to increased kinase activity [153]. In fact, non-small cell lung cancers (NSCLC) that harbor such mutations and may depend on activated EGFR signaling, and thus show a superior response rate to treatment with TKIs of 70 % as opposed to 10 % for NSCLCs with wild type EGFR (reviewed in [154]).

However, wild type EGFR is by far more common than mutated EGFR. Thus, clinical trials with the EGFR-targeting TKIs gefitinib and erlotinib as first-line or second-line treatment in unselected patients rarely showed superiority in PFS and OS compared to classical chemotherapy; some trials even reported adverse results (reviewed in [155]). The BR.21 study, which led to the approval of erlotinib as a second-line treatment for patients with NSCLC, demonstrated an increased response rate, a PFS of 7.9 months vs. 3.7 months and an OS of 6.7 month vs. 4.7 month as compared to platinum-based therapy [156]. A retrospective study on the BR.21 trial with regard to the mutational status of EGFR and other downstream effectors pointed out that although EGFR activating mutations with KRAS wild type status were strong indicators for treatment response, patients with EGFR gene amplifications may also profit from erlotinib [157]. Nonetheless, recent studies on erlotinib and gefitinib have been mainly performed in an EGFR mutant background and the benefit for patients with wild type EGFR is highly

controversial (reviewed in [158]). Moreover, the mutational status of EGFR alone does not predict the treatment response, as for mAbs therapy the status of the downstream effector kinases or the presence of other members of the tyrosine kinase receptor class also plays a role. Thus, the development of TKIs, inhibiting several tyrosine kinase targets at the same time, aims at a broader range of action to increase tumor control. Lapatinib, a TKI binding to the intracellular domain of both EGFR and Her2, was shown to improve progression free survival for patients with ErbB2-positive, locally advanced or metastatic breast cancer in combination with chemotherapy as compared to chemotherapy alone [159, 160].

However, as for other TKIs, also for multiple tyrosine kinase inhibitors such as lapatinib and sorafenib treatment resistance eventually evolves. Sorafenib binds to and inhibits RAF, VEGFR, PDGFR, stem cell factor receptor (KIT), and fms-like tyrosine kinase 3 (FLT-3) and is approved for advanced hepatocellular carcinoma (HCC). Two independent studies identified EGFR and ErbB3 as possible mediators of treatment resistance [161, 162]. An ongoing phase III trial compares the combination of sorafenib with EGFR-TKI gefitinib to sorafenib alone.[5] However, no additional benefit of the combinatorial treatment has been determined so far.

Development of resistance to TKIs, similarly as for antibodies, may also occur through mutations that reduce interaction with the inhibitor or through activation of downstream effector proteins. As opposed to antibodies, TKIs exert their activity on the intracellular domains of receptors or on cytoplasmic kinases. Due to their hydrophobic characteristics, TKIs depend on cellular uptake mechanisms and are extruded from the cell by efflux transporters. Thus, overexpression of multi drug resistance (MDR) proteins may also confer resistance to TKIs, a conclusion that is not as predictable as it may seem. In the case of lapatinib, exclusion form the cell is facilitated by P-glycoprotein (P-gp) and the breast cancer resistance protein (BCRP). Transport by both transmembrane proteins involves the binding and hydrolysis of ATP. Interestingly, lapatinib does not only bind to the ATP binding pockets of EGFR and Her2 but is also able to inhibit both P-gp and BCRP, albeit with lower efficacy [163]. Likewise, TKIs might also inhibit transporters involved in cellular uptake. Galetti et al. were not able to pin down the transporters of gefitinib and did not observe a difference in intracellular gefitinib concentrations in TKI-resistant or sensitive cell lines. But interestingly enough, gefitinib reduced uptake of 1-methyl-4-phenylpyridinium (MPP), an artificial substrate for organic cation transporters (hOCTs) [164]. hOCTs are involved in the transport of various anticancer drugs such as cisplatin, oxaliplatin, doxorubicin and the TKI imatinib. Therefore, the pharmacodynamics of the combination of TKIs with other drugs has to be carefully evaluated.

[5] http://clinicaltrials.gov/ct2/show/results/NCT00901901?sect=X6015 (downloaded on Oct. 29th 2013)

2.1.3 Alternative Non-Antibody Scaffolds for Molecular Targeting: Designed Ankyrin Repeat Proteins (DARPins)

2.1.3.1 From Antibodies to Alternatives Scaffolds

In the past years, numerous drugs based on monoclonal antibodies have been successfully introduced for a wide range of diseases, including cancer as well as autoimmune and inflammatory diseases. The introduction of the hybridoma technology in 1975 opened up the possibility for the stable production of a selected monoclonal antibody on a large scale [165]. Furthermore, selection methods, such as the still used phage display allow, for efficient selection of suitable antibody candidates [166, 167].

Humanization of rodent antibodies decreases immunogenicity, increases half-life, and allows for possible effector functions. However, antibodies still hold major disadvantages. The application of antibodies is primarily limited to extracellular targets due to their size and properties, which also limit effective tissue penetration. Moreover, antibody production is associated with extremely high costs. Expression of functional antibodies is restricted to eukaryotic expression systems due to their structure, which contains several disulfide bonds and posttranslational modifications such as specific glycosylation not suitable for expression in prokaryotic systems. Often, high amounts of molecules are necessary for treatment and thus stability of antibodies at high concentrations becomes an issue [168]. With regard to the limited tissue permeability of whole antibodies, different steps have been undertaken to reduce their molecular size.

Three general groups of antibody related proteins have successively evolved: antigen-binding fragments (Fabs), single chain variable fragments (scFvs) and “third generation” (3G) molecules comprising a single antigen-binding domain only (see Figure 2.3).

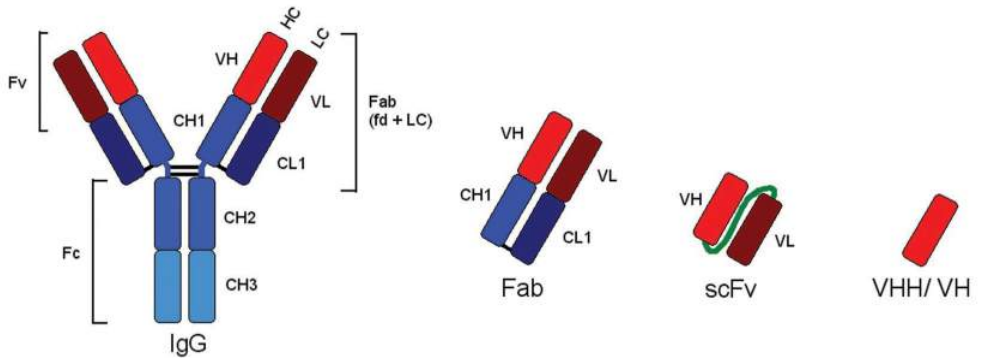

Figure 2.3 Whole IgG antibody molecule consisting of two heavy chains (HC) and two light chains (LC) connected by disulfide bridges (left). Antibody fragments (Fab) single-chain variable fragment (scFv) and single-domain antibodies VHH / VH (heavy chain domain of camelid / of IgG antibody) [169]

However, although these molecules have been shown to penetrate tumor tissue more rapidly, they are also cleared much faster from the blood circulation due to their small size and the absence of Fc-mediated recycling [170]. Yakota et al. investigated the relationship between the molecular size of antibody fragments and tumor uptake of the molecules [171]. With 27.2 % of the injected dose per gram of tissue (ID/g) at 24 hours, IgG showed the highest accumulation in the tumor, followed by $F(ab')_2$, with 19.2 %, Fab′ ,with 3.7 % and scFv, with 1.7 % ID/g. For certain applications, a fast clearance of a drug is favorable: for example, in the field of diagnostics such as tumor imaging, a high tumor to blood ratio is of advantage; or if coupled to a toxic compound or radionuclides, healthy tissue toxicity can be reduced.

Not only immunoglobulin related proteins were taken into consideration for targeting cancer specific proteins. Several non-immunoglobulin-based scaffolds have been studied for suitability, with the aim to develop moieties with improved stability and tissue permeability (Reviewed in [172, 173]. Adequate protein motifs have been adopted from small, soluble and relatively stable proteins as in the case of the Kunitz inhibitors or the lipocalins, or from stably folded extramembrane domains of cell surface receptors in the case of Affibodies, Adnectins or the designed ankyrin repeat proteins.

These protein domains can be divided roughly into two groups, based on the structure of their binding sites. In one category, binding is facilitated by surface-exposed loops, as for the antibody paratope. In the second category, binding is mediated by accessible side chains of secondary structure elements such as α-helices and β-sheets, which assemble into a relatively rigid interface. An overview of several scaffold proteins that are under investigation for therapeutic use is presented in Table 2.1 (see page 28). Designed ankyrin repeat proteins (DARPins) will be described in more detail in the following section.

Table 2.1 Overview on alternative scaffold proteins at various stages of development for targeted therapy [174, 173, 172, 175].

	Scaffold	Binding Motif	Origin and Protein scaffold	Residues/Size	Latest review (*article)	Clinical stage (cancer therapy) Commercialization
Category I	AdNectin	Ig-like: 2-3 loops	based on domain 10 of human fibronectin III (^{10}Fn3): Ig-like β-sandwich	94 aa	(Lipovsek 2011)	phase II adnexus.com
	Anticalin	loop-rich (4 loops)	Lipocalins β-barrel	160-180 aa / 20 kDa	(Gebauer, Skerra 2012)	phase I pieries-ag.com
	Kunitz-domain	single loop (or 2 loops)	Protease inhibitors (LACI-D1 / ITI-D2)	58 aa	(Ranasinghe, McManus 2013)	approved diax.com
	Avimer	oligomeric	(LDLR-A module)$_n$ A-domain in low density lipo-protein receptor: Three disulfides, short α-helical regions	35 aa / 4kDa per unit	(Silverman et al. 2005)	preclinical amgen.com
	Knottins	multiple loops	Toxins of spiders, marine cone snails, scorpions Three disulfides, β-strands	30 aa / 3 kDa	(Moore et al. 2012)	preclinical azurpharma.com elan.com
	Fynomers	2 loops	human SH3 domain of Fyn kinase two anti-parallel β-sheets and two loops	63 aa / 7 kDa	(Grabulovski et al. 2007)* (Schlatter et al. 2012)*	covagen.com in collabo-ration with ROCHE (CH)
	Atrimers	3 binding domains, with 5 loops each	human trivalent plasma protein tetranectin with C-type lectin-binding domains	60 kDa	(Allen et al. 2012)*	preclinical anaphore.com in collab. with Mitsubishi Tanabe Pharma
Category II	Affibody	Rigid secondary structure (RSS) 2 α-helices are involved in binding	Z domain from *Staphilococcus aureus* Protein A three helix bundle	58 aa / 6kDa	(Feldwisch, Tolmachev 2012)	phase II affibody.com
	Ankyrin repeat proteins	Rigid secondary structure	2-4 repeats of α-helices connected a β-sheet	~166 aa / 14 kDa	(Tamaskovic et al. 2012)	preclinical molecularpartners.com allergan.com
	Affilins	RSS, β-sheets with 6 and 8 aas suitable for manipulation	based on human γ-B crystallin or human ubiquitin	176 aa / 20 kDa 76 aa / 10 kDa	(Ebersbach et al. 2007; Mirecka et al. 2009)*	preclinical scilproteins.com
	Armadillo repeat proteins	Rigid secondary structure aa residues of helix 3	Motif present in various proteins, e.g. β-catenin: ~ 6-12 tandem repeats, each comprising three α-helices	~ 42 aa per repeat	(Parmeggiani et al. 2008)* (Varadamsetty et al. 2012)*	structural development

References: [176–179, 175, 180–188]

2.1.3.2 Designed Ankyrin Repeat Proteins and Their Properties

The idea behind the study of ankyrin repeat proteins was to develop a scaffold with superior properties than attributed to antibodies. A prospective scaffold protein should be soluble in body liquids, structurally stable and such that it can be efficiently expressed in a prokaryotic system. Thus, a scaffold protein preferably does not contain disulfide bridges. Moreover, large and rigid interaction interfaces support tighter binding but should also provide for sufficient side-chain variability at positions that do not interfere with the structure and stability of the scaffold protein.

Ankyrin repeat domains fulfill all these requirements; they are built from stacked tandem repeats with a length of approximately 33 amino acid residues each, which assemble into a β-turn followed by two antiparallel α-helices (see Figure 2.4). Repeat motifs, such as the ankyrin repeat, leucine rich repeat, armadillo repeat, and tetratricopeptide repeat are very common in protein-protein interaction interfaces [189].

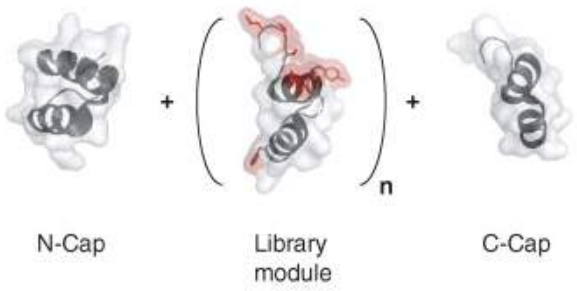

Figure 2.4 Designed ankyrin repeat proteins are composed of two caps (N- and C-) and a varying number of ankyrin repeats composed of a β-turn and two antiparallel α-helices. Seven exposed residues per repeat, displayed as red side chains, make up the variable part and provide for the diversity of the artificial binders. The figure has been adopted from [190].

The ankyrin repeat motif was first discovered in the Notch protein of *Drosophila melanogaster* [191]. The ankyrin repeat domain in the cytoplasmic domain of Notch comprises seven repeats and was shown to be important for Notch signaling [192]. Zweifel et al. determined the structural position of known mutations within the ankyrin domain: Two of the four mutations were located in buried positions and led to the destabilization of the configuration of the domain, whereas the two other were located at the surface and had no substantial effect on protein stability. Nonetheless, both types of mutation similarly impaired Notch signaling, indicating that the surface residues might be involved in the interaction with signaling partners. Similar to the ankyrin repeat domain in Notch, artificial ankyrin repeat proteins are assembled from usually 2 to 4 tandem repeats enclosed by an N-terminal and a C-terminal cap, which both were adapted from mouse GABPβ1. The charged and polar surfaces of the caps enable solubility under neutral pH conditions by hiding the hydrophobic core [193].

Importantly, the capping also supports efficient folding of the designed ankyrin repeat proteins into their native state in bacterial expression systems. Without caps, the proteins have to be refolded from inclusion bodies that form in *Escheria coli*, and additionally, solubility at pH 7 has to be secured by the introduction of positive charges at the C-terminal end [194].

Further improvement in stability of the artificial ankyrin repeat domains was obtained by the introduction of an optimized consensus sequence that is self-compatible and readily assembles into stable repeat stacks if sequentially expressed. Stability of the DARPins increases with the number of repeats. Proteins comprising at least three consensus internal repeats withstand boiling and guanidine hydrochloride degradation [195]. To obtain a reasonably sized collection of different DARPins useful for a target specific selection, amino acid residues suitable for variation and not important for internal stability were determined. The seven eligible residues are located in the β-turns and in the first α-helices of the ankyrin repeats and can be substituted by any amino acid except for proline and glycine, which negatively influence stability. Additionally, cysteine was omitted from the list of possible residues to prevent the formation of unwanted disulfide bonds [193]. The absence of cysteines turned out to be of advantage for the conjugation of functional or structural moieties to the DARPins. After protein expression and purification, a singly introduced cysteine allows for the site-specific crosslinking with a suitable moiety [196].

DARPins with high affinities for a specific target are selected from libraries that consist of ~10^{12} DARPins for ribosome display [197] or ~10^{10} DARPins for phage display [198]. With only few selection cycles, affinities in the nano- and picomolar range can be achieved.

2.1.3.3 Therapeutic Application of DARPins

Designed ankyrin repeat proteins are stable, small proteins and similarly to antibodies they can be selected to bind to a target with high specificity and affinity. Whereas tissue penetration turned out to be a major issue for antibody therapeutics, DARPins have been shown to have superior properties in this regard. For example, DARPin MP0112, developed by the company Molecular Partners[6], binds and inhibits vascular endothelial growth factor (VEGF) for the treatment of wet macular degeneration and diabetic macular edema. Currently two drugs have been approved for treatment of these diseases: ranibizumab, an Fab antibody fragment, and pegaptanib, a pegylated aptamer. Both drugs are applied by intravitreal injections that have to be repeated on a monthly or bi-

[6] http://www.molecularpartners.com/public/index.php?id=105&lang=en (downloaded on Sept. 18th 2013)

monthly basis. DARPin MP0112 successfully passed two clinical phase II trials and seem to be well tolerated after single intravitreal injections with an indication of high efficacy and possibly longer duration of action compared to the present drugs [199]. Importantly, in preclinical studies, DARPin MP0112 was demonstrated to effectively inhibit VEGF and reduce vascular leakage and suture-induced corneal angiogenesis not when administered through intravitreal injections, but also by topical application in the form of eye drops [200]. Topical application would be more convenient for patients and significantly reduce the costs for the treatment.

DARPins also have been considered for tumor targeting and were selected for various tumor cell markers, such as the tyrosine kinase receptors Her2 and EGFR, and the epithelial cell adhesion molecule EpCAM [201–203]. Zahnd et al. determined in a preclinical study in mouse tumor xenografts that for the anti-Her2 DARPin 8 % ID/g localized to the tumor tissue within 24 hours after intravenous injection [204]. This good result and that proteins of the size of a single DARPin domain (14 kDa) were rapidly cleared by glomerular filtration, indicate that DARPins freely extravasate and reach the tumor after systemic application, even though the serum half-life is very short. Accordingly, the affinity of the DARPins toward their target significantly influenced the degree of tumor accumulation.

Several approaches to target tumor cells with DARPins are currently under preclinical investigation: DARPins linked to effector moieties have been used to deliver toxic agents or pro-apoptotic siRNA molecules to tumor cells [205, 206]. Martin-Killias et al. demonstrated a significant growth delay in tumor xenografts in nude mice, which had been treated with the fusion product of a truncated form of *Pseudomonas aeruginosa* exotoxin A and an anti-EpCAM DARPin. Receptor-mediated endocytosis of the DARPin, induced by EpCAM itself, eventually leads to the cellular uptake of the toxin. Other DARPins were selected against the growth factor receptors ErbB2 and EGFR. Recently, a paper about a divalent DARPin targeting ErbB2 and its specific mechanism of action has been published [207]. Whereas the DARPins against the ErbB2 receptor does not induce internalization of the receptor, the tetravalent anti-EGFR DARPin binds the EGF receptor and leads to its degradation [202]. The anti-EGFR DARPin also inhibits ligand-stimulated activation of the receptor, possibly by blocking the ligand binding site.

Though DARPins have a promising potential as drug targeting carriers or can be selected to functionally interfere with their targets, the rapid clearance of the DARPins may be a major issue to be tackled with regard to clinical application.

2.2 Aims of the Study

This study addresses the systemic application of the dimeric tetravalent DARPin E69_LZ3_E01 with inhibitory function on the epidermal growth factor receptor (EGFR). Boersma et al. showed that *in vitro* DARPin E69_LZ3_E01 inhibited EGFR more potently than the clinically approved anti-EGFR antibody cetuximab [202]. Upon stimulation with epidermal growth factor, phosphorylation of Erk, a downstream target of EGFR, was prevented to a higher degree than with the monoclonal antibody cetuximab. Adjuvant treatment with cetuximab on the other hand, has been shown to have a beneficial effect on the overall survival (OS) and the progression free survival (PFS) of patients with solid tumors, especially in combination with radiation therapy [137, 138]. Our main goal is to test the efficacy of the anti-EGFR DARPin in cell culture and against A431 tumor xenografts in nude mice, particularly in combination with radiotherapy and then to compare the results with those of the combined treatment with the monoclonal antibody cetuximab. Furthermore, we will investigate pharmacokinetic properties of the pegylated tetravalent DARPin E69_LZ_E01 after intravenous and intraperitoneal injection. Importantly, the pharmacokinetics and tumor accumulation of a tetravalent DARPin with two 20 kDa PEG extensions has not yet been investigated.

2.3 Material and Methods: Targeting EGFR

2.3.1 Cell Culture and Maintenance

The human vulvar squamous cell carcinoma cell line A431 was purchased at the Leibnitz Institute DMSZ (German Collection of Microorganisms and Cells Cultures, No: ACC-91). The human non-small cell lung cancer cell line A549 was a gift of the laboratory of Dr. Susan Band Horwitz. Both cell lines were maintained in RPMI medium supplemented with 10% (v/v) fetal bovine serum (FBS), 1% (v/v) L-glutamine and 1% (v/v) Penicillin-Streptomycin, at 37°C in 5% carbon dioxide in a humidified incubator.

2.3.2 Irradiation

Irradiation was performed with a Gulmay 200 keV X-ray unit at a dose rate of ~1 Gy/min at room temperature. Dose performance was assessed with help of a Vigilant dosimeter. Determination of the settings and evaluation of the corresponding dose profiles were performed by a radiation physicist.

2.3.3 Reagents and Antibodies

2.3.3.1 DARPins and Application of DARPins in Cell Culture *In Vitro*

All DARPins were kindly provided by Prof. Dr. Andreas Plückthun of the Biochemical Institute of University of Zürich. The DARPins were obtained as aqueous solutions and were stored at -80 °C for long-term storage or at 4 °C for up to four weeks.

DARPins are expressed in E. coli and are purified via specific tags. Further information concerning the cloning of the EGFR-specific DARPin E69_LZ3_E01, or the expression and the purification of DARPins in general, can be found in Boersma et al. and in there indicated references [202].

For *in vitro* administration, the DARPin solutions were diluted in cell culture medium and added in droplets to the medium of the cells, to receive the final concentration.

Table 2.2 List of the DARPins used; both DARPins were also received in the pegylated form.

DARPin	**Target**
E69_LZ3_E01	Extracellular domain of the EGF receptor
Off7_LZ3_Off7	No known target

2.3.3.2 Antibodies and other Reagents

Table 2.3 List of Reagents

Reagents	**Manufacturer**
Agarose A9539	Sigma
Alamar Blue	Biosource Int.
BD Matrigel 354248	BD
Cell culture medium and supplements	Gibco, Invitrogen
Cetuximab (Erbitux)	Merk Serono
EDTA solution 115K8901	Sigma
Dapi Fluoromount-G #0100-20	SouthernBiotech
RNAse A	Qiagen
TMB Substrate Kit #34021	Thermo Scientific
TRITON X-100	Sigma

Table 2.4 List of Antibodies

Antibodies	**Manufacturer**	**Ref. number**
Anti β-Actin Ab from mouse	Sigma	A5441
Anti Akt Ab, from mouse	Cell Signaling	#2920
Anti pAkt Ab (Ser473), from rabbit	Cell Signaling	#4058
Anti EGFR Ab, from rabbit	Cell Signaling	#4267
Anti pEGFR (Tyr1173), from mouse	Millipore	#05-1004
Anti α-GAPDH	Sigma	#9545
Anti p44/42 MAP kinase Ab, from mouse	Cell Signaling	#4696
Anti pErk1/2 (Thr202/Thr204) Ab, from rabbit	Cell Signaling	#4370
Anti RGS-His Ab	Qiagen	34610
Anti-PEG-Biotin (methoxy group) Ab, from rabbit	Epitomics	#2137-1
Anti-Rad51 Ab, from mouse	Santa Cruz	sc-8349
Secondary anti-mouse Ab, from goat, Fluor®488-linked	Mol. Probes®, Invitrogen	A-11001

Secondary anti-mouse Ab, from goat, Fluor®546-linked	Mol. Probes®, Invitrogen	A-11018
Secondary anti-mouse Ab, from sheep, HRP-linked	GE Health Care	NA931V
Secondary anti-rabbit Ab, from donkey, HRP-linked	GE Health Care	NA9340V
Secondary anti-rabbit, from goat, HRP-linked	Sigma-Aldrich	A6154
Secondary anti-rabbit Ab, from goat, Fluor®488-linked	Mol. Probes®, Invitrogen	A-11070
Secondary anti-rabbit Ab, from goat, Fluor®546-linked	Mol. Probes®, Invitrogen	A-11071

2.3.4 Western Immunoblot Analysis

For the assessment of the inhibition of EGFR phosphorylation and signaling, cells were usually plated in medium containing 1 % Serum instead of 10 %. Cells were stimulated with 10-100 ng/ml EGF as indicated for 15 minutes before harvesting.

Cells were washed with cold PBS and lysed immediately with Laemmli buffer (63 nM Trizma base, 2 % SDS, 10 % glycerol and 10 mM DTT freshly added) on ice. The cells were scraped immediately, cooked for 7 min at 96 ºC and stored and -20 °C. Protein concentrations were determined by NanoDrop (Thermo Scientific). Before loading, 1 µl of 2 % Bromophenol blue was added to 100 µl of the thawed protein samples. 50 µg of protein was loaded per lane, separated on 10 % acryl-amid gels by electrophoresis, and transferred to PVDF membranes (Amersham Hybond™-P, GE Healthcare, Cat. No. RPN2106) by a standard wet/tank blotting system from BioRad (100 V for 60 min). The membranes were then blocked in 5 % non-fat milk in TBS buffer for 40 min at room temperature. All primary antibody incubations were performed overnight at 4 ºC, followed by washing and incubation with the secondary antibody coupled to HRP for 60 min at room temperature. The membranes were then washed and incubated with ECL Prime according to the manufacturer. The Western blot signal was detected by a FluorChem Q System (Bucher Biotec), equipped with a CCD camera. For quantification, the software belonging to the FluorChem Q System was used.

2.3.5 Cell Cycle Analysis by BrdU Incorporation and DNA Staining

Before harvesting the cells for analyses, BrdU to a final concentration of 10 µM was added to the cell culture medium. After incubation of 30 min, the cells (ca. 1 million) were trypsinized, washed with PBS and fixed in ice-cold 70 % ethanol overnight at 4 °C. If not stained and analyzed the following day, the cells were stored at -20 °C for up to one week. The cells were washed with 14 ml ice cold PBS once. The following steps were all performed in the 15 ml falcon tube and at room temperature. 0.5 ml 4 M HCl were added to the cells for 10-15 min, for the denaturation of DNA required for the BrdU recognition by the Ab. To neutralize the pH, 14 ml PBS were added and the cells were washed with 14 ml PBS twice more. Neutralization of the pH was verified by a pH test strip. Blocking of nonspecific binding sites was performed by incubation in 2 % BSA in PBS for at least 15 min. For the BrdU detection and DNA staining, the cells were then incubated with 0.5 µg BrdU Ab/100µl/10^6 cells in PBS containing 2.5 mg/ml Propidium Iodide, 10 µl/ml RNAse, 0.2 % BSA and 0.1 % Tween. Depending on the cell number, 50-100 µl staining solution was added and the samples were placed in the dark for 1-1.5 hours. The flasks were tapped from time to time, to disperse the cells. 14 ml PBS was added for washing; and after spinning, cells were resuspended in 250 µl PBS, transferred to a FACS tube and placed on ice until FACS analysis. The FACS analysis was performed with a BD FACSCanto system; and for the evaluation of the data, the software FlowJo version 7.6 was used.

2.3.6 Alamar Blue Assay for Assessment of Cell Proliferation

Cells were seeded in 96-well plates. Alamar Blue was added according to the manufacturer's specification 4 hours prior to measurement of the absorption at 570/670 nm by means of a Tecan GENios plate reader. Alamar Blue contains the weekly fluorescent dye resazurin that becomes irreversibly reduced to the red fluorescent resorufin by mitochondrial metabolic activity. DARPins and cetuximab were added together with the administration of Alamar Blue for the first time line measurement. Cell viability was determined up to 72 or 96 hours after drug treatment at 24-hour intervals. All conditions were measured in triplicates.

2.3.7 Clonogenic Survival Assay

Clonogenicity of cells, which is the ability to form colonies from single cells, was determined by seeding low cell numbers in 10 cm Petri dishes to obtain 50 to 150 colonies. 24 hours after seeding, the cells were submitted to radiation and control cells were sham irradiated. Cells were left to form colonies for 10-14 days, depending on their doubling times. Colonies were fixed with a 3:1 mixture of methanol and acetic acid or

in 70 % ethanol, and DNA was stained with a 0.5 % crystal violet solution. Colonies with more than 50 cells/colony were counted manually with a GALLENKAMP colony counter or automatically by a GelCount™ device (Oxford Optronix). Survival fraction (SF) was determined by calculating the ratio between the number of obtained clones and the initially seeded cells. For normalization, the obtained SF was divided by the plating efficiency PE, which is the ratio of colonies counted for untreated cells to seeded cells. For a single experiment, all conditions were assayed in triplicates.

$$SF = \frac{\#\text{Colonies counted}}{\#\text{Cells seeded}} * \frac{1}{PE}$$

2.3.8 3D Cell Culture and 3D Clonogenic Assay

For 3D cell culture, cells were seeded in medium containing 0.5-0.1 mg matrigel per ml. 3D clonogenic assays were performed in 96-well plates. Before seeding, wells were coated with 50 µl 1 % agarose (sterile). 200 µl of cell suspension already containing the matrigel were added to each well (150 cells per well). Plates were placed into the incubator until the matrigel had solidified (3-4 hours) and 100 µl culture medium was carefully added on top to prevent the matrigel from drying. DARPins and cetuximab were added the following morning and irradiation followed 6 hours after the drug treatment. Colonies were counted by eye with help of a microscope. Survival Fraction was determined as for the classical clonogenic assay (see section 2.3.7).

2.3.9 Immunofluorescence Microscopy of Adherent and 3D Cells

For indirect immunofluorescence detection of EGFR, phospho-EGFR and of DARPins, ~10-20’000 cells/well were plated in 24-well plates on cover slips. The cells were fixed with 4 % Formalin solution in PBS. Cells were permeabilized in 0.2 % Triton X-100 (25 mM HEPES [pH7.4], 50 mM NaCl2, 3 mM MgCl2, 300 mM sucrose, just before use Triton X-100 and 0.1 M EDTA in solution was added) for 5 min on ice, washed with PBS and incubated with 0.3 M Glycine to quench autofluorescence of formaldehyde. Cells were blocked with 3 % BSA in PBS for 20 minutes. Then, the cover slips were incubated with the primary antibodies (dilution indicated on the data sheets) in 3 % BSA in a humid chamber for 1 hour. Cover slips were washed 3x with PBS containing 0.3 % BSA, incubated with the appropriate fluorescently labeled secondary antibody for 30-60 minutes in the dark and washed repeatedly with PBS. For the mounting of the cover slips onto Microscopy slides, mounting medium containing DAPI for counterstaining the DNA was used. Slides were stored at 4 °C.

For the staining of cells grown in matrigel, 100’000 cells/well were seeded in 24-well plates in 1 ml medium containing 0.5 mg matrigel. Before harvesting, the upper part of the matrigel that did not contain cells was removed and discarded; the remaining matrigel with cells was pipetted into a 15 ml falcon tube containing ice-cold PBS and left on ice for 5 minutes. After spinning, cells were incubated with 3x trypsin for 3 min, and then formalin solution was added directly, without spinning, at a final concentration of 4 % for a period of 10 minutes, followed by washing with PBS. Permeabilization was performed using the same buffer as for the adherent cells. Cells were carefully resuspended in permeabilization buffer and incubated for 5 minutes on ice. Before spinning, the permeabilization buffer was diluted with PBS. All further steps were performed as for the adherent cells, but in 15 ml falcon tubes and liquids were exchanged by spinning and removing the supernatant. After the final spinning, the entire supernatant was carefully removed and cells were collected in 8 µl mounting medium containing Dapi, the mounting medium was transferred to onto a microscopy slide and covered by a cover slip.

Fluorescence images were obtained by a LEICA DM6000B fluorescence microscope equipped with a DFC350FX camera or a confocal microscope CLSM Leica SP5.

2.3.10 Mouse Strain and Animal Care

Procedures concerning animals were in accordance with the regulations of the veterinary authority of Zurich and with the ARVO Statement for care and use of animals in research. The protocols were approved by the Swiss Cantonal Veterinary Authorities (Permit number 154/2011). Animals used in the studies were 4 weeks old female nu/nu mice obtained from CharlesRiver Laboratories, Germany.

2.3.11 Preparation and Injection of Tumor Cells

A431 cells of low passage were thawed and cultured for 10 days. For injection into mice, cells of 80 % confluency were harvested by trypsinization. The cells were centrifuged (for 3 min at 500 rpm) and washed with cold, sterile PBS three times. Thereafter the pellet was resuspended in cold PBS to a final concentration of 33 Mio cells/ml and kept on ice. The time from harvesting the cells until injection did not exceed two hours. For the injection of the tumor cells, the mice were anaesthetized with isoflurane. 150 µl cell suspension (5 million cells) were injected subcutaneously on the middle hind back of the nude mice by means of a 26G needle.

2.3.12 Assessment of Tumor Size

Tumor size was assessed by caliper measurement of the two longest perpendicular axes of the tumor and was calculated according to the formula below, whereas length (l) is the longer and width (w) is the shorter axis. Smallest measuring unit was 0.1 mm.

$$Tumor\ size = \frac{1}{2} * l * w^2$$

2.3.13 Application of DARPins and Cetuximab, and Tumor Irradiation

For *in vivo* application, pegylated DARPins were used. 20 kDa PEG-chains were attached to the c-terminal DARPin domain at a single cysteine present in the DARPin E69_LZ3_E01. The pegylated DARPins were prepared by the Biochemical Institute according to the procedure published by Seely and Richey [208].

The administration of DARPins was performed by intravenous via tail vein or intraperitoneal injection according to the schedule on page 62. The treatment lasted 13 days, at a daily dose of 30 mg/kg of body weight.

The three injections of cetuximab were administered intraperitonealy at an interval of five days at a dose of 50 mg/kg of body weight.

For the application of the intravenous injections, the animals were strained in an appropriate device and the tail was warmed to dilate the veins. All injections were performed with standard insulin syringes.

For irradiation, the mice were strained in lead cages with openings on the hind back for the tumor to be displayed. The lead cages were placed in a plexiglass “hotel” with filter-covered air holes and a capacity of six mice. For the treatment of the mice, the same irradiation device was used as for the irradiation of cultured cells. Dosimetry was performed by a radiation physicist.

2.3.14 Histology

Subcutaneous tumors were harvested and fixed immediately in 4 % PBS buffered formalin solution, protected from the light at room temperature. Within one week, the tumors embedded in the paraffin. The stainings were performed in collaboration with Prof. Dr. med. Holger Moch by the Institute of Medical Pathology USZ.

Images were obtained by bright-field microscopy using a LEICA DM6000B microscope equipped with a DFC290 camera.

2.3.15 Collection and Preparation of Serum Samples

For the collection of the blood samples, the animals were strained in a shortened and perforated falcon tube. The saphenous vein was punctured and a few drops of blood (50 µl) were collected in Bd Microtainers (#365950). After coagulation of the blood, the serum was separated by spinning (at 6000 rpm for 5min) and stored at -80 °C.

2.3.16 Sandwich ELISA of the DARPin E69_LZ3_E01 in Serum

All washing steps were performed with 0.2 % BSA, 0.1 % Tween in 1xPBS unless stated otherwise. After each step, the plate was tapped on paper towels to get rid of remaining fluid. For the ELISA Maxisorp NUNC-Immunoplates were coated with RGS-His antibody (1:5000 stock dilution) overnight at 4 °C, washed twice and incubated in wash buffer for 1 hour at room temperature to block nonspecific binding. The plates were washed with 0.1 % Tween in 1x PBS 2 times and the plate was incubated with the diluted serum samples for 1 hour on the shaker, followed by three washing steps. Anti-DARPin antibody (Rabbit Serum, 1:1000 stock dilution in wash buffer) was added for DARPin detection. The secondary anti-Rabbit HRP conjugated antibody (1:1000 stock dilution) was added after 4 washing steps and incubated for 1 hour, followed by another four washing steps. Detection with TMP substrate was performed according to the manufacturer and absorbance at 450 nm was determined by an Ultra Microplate Recorder (Bio-Tech Instruments Inc.).

2.3.17 Statistical Analyses of the *In Vivo* Data

Statistical analyses were performed with Graphpad Prism Software Version 5 and R. The tumor growth curves were approximated with a Locally Weighted Error Sum of Squares regression (LOESS, span 0.5) in R. For the Kaplan Meier curve, the time point were the tumor reached 3x initial tumor size was also determined in R and statistical tests were performed in both R and Graphpad

2.4 Results

The nonimmunoglobulin scaffold protein DARPin E69_LZ3_E01 binds and inhibits the epidermal growth factor receptor (EGFR) even stronger than the clinically approved antibody cetuximab. The mechanism of EGFR inhibition by DARPin E69_LZ3_E01 (see section 2.4.1) is similar to the manner by which cetuximab inhibits the receptor. However, differences exist on the level of EGFR downregulation and inhibition of the downstream signaling, which already were described by Boersma et al [202]. We investigated DARPin E69_LZ3_E01 with regard to *in vivo* application, such as the dynamics of EGFR inhibition, and finally, we tested the *in vivo* efficacy in a xenograft tumor model in nude mice.

2.4.1 Structure of DARPin E69_LZ3_E01 and Proposed Mechanism of EGFR Inhibition

The structure of DARPin E69_LZ3_E01 includes two DARPin domains connected by a leucine zipper motif, which facilitates dimerization of the bivalent DARPin proteins (see Figure 2.5A). Both DARPin domains contain three internal ankyrin repeats and were selected by phage display against the extracellular part of the epidermal growth factor receptor [197]. Each of the two domains recognizes a different epitope [202]. Domain E01 recognizes the EGF binding site in the domain III of EGFR. This binding motif partially overlaps with the binding site of the mAb cetuximab. The binding site of E69 could be located to EGFR domain I.

A **B**

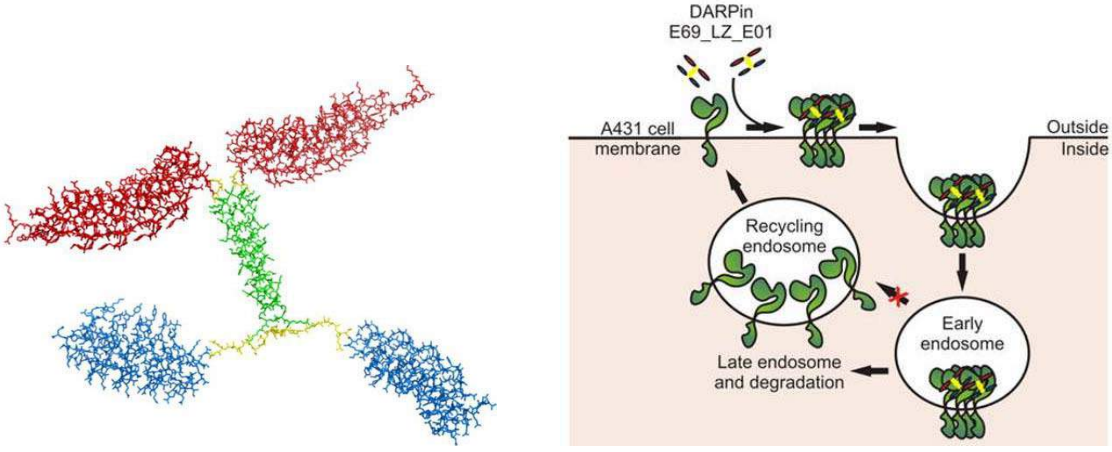

Figure 2.5 Structure of the DARPin E69_LZ3_E01 used in this study. **(A)** Dimerized structure of the DARPin E69_LZ3_E01 represented as stick model: domain E69 (red) and domain E01 (blue), leucine zipper (green) and linkers (yellow). **(B)** Suggested mechanism of action: Binding of the EGF receptor by DARPin E69_LZ3_E01 leads to endocytosis of the receptor/DARPin complex. Original images were adopted from [202].

DARPin E69_LZ3_E01 labeled with the fluorescence label Alexa was shown to internalize upon binding. Moreover, as opposed to EGFR bound by monovalent DARPin domains E01 or E69, EGFR bound by the tetravalent DARPins does not recycle to the plasma membrane, but instead is degraded (Figure 2.5B).

Throughout the section results, the denomination “DARPins” will refer to the specific DARPin E69_LZ3_E01. The control DARPin used for the *in vivo* study resembles the DARPin E69_LZ3_E01 in structure but the domains E69 and E01 were replaced by an non-binding domain called Off7.

2.4.2 DARPins Downregulate EGFR and Inhibit Downstream Signaling

To test the potency of DARPin E69_LZ3_E01 to inhibit EGFR in our A431 cell system in comparison to the potency reported by Boersma et al. [202], we applied DARPins as well as the mAb cetuximab in cell culture and investigated EGFR phosphorylation at Tyr1173 and EGFR signaling upon receptor stimulation. Our results were in good agreement with the previously published data. Inhibition of phosphorylation of EGFR was achieved by both, DARPins and cetuximab, but only DARPins led to a decrease in the expression level of the receptor (see Figure 2.6). Moreover, DARPins led to a stronger decrease of EGF-induced phosphorylation of the downstream target Erk at Thr202/Tyr204 and to a lower extent also to a decrease of the phosphorylation of Akt at Ser473. This indicates that the degradation of EGFR is important for the reduction of the downstream signaling.

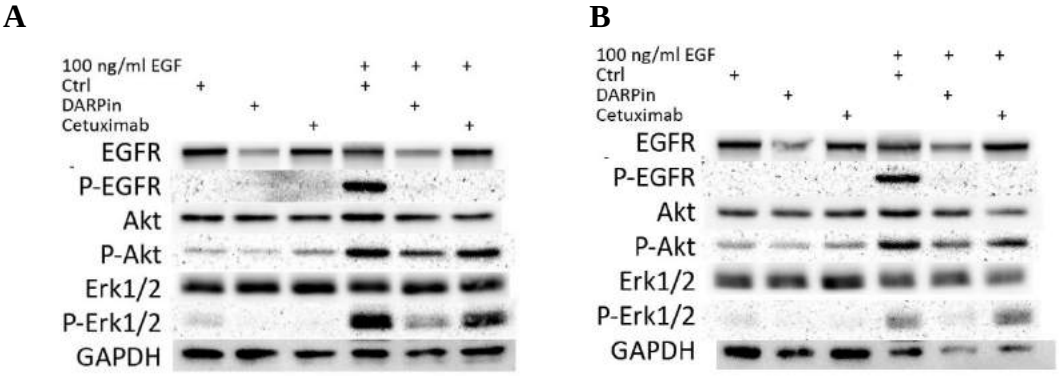

Figure 2.6 Application of cetuximab or DARPin E69_LZ3_E01 inhibited EGF-dependent activation of the EGF receptor. A431 cells were incubated for 24 hours with DARPins (at a final concentration of 100 nM) or with cetuximab at equimolar concentration in medium containing **(A)** 1 % Serum or **(B)** 10 % Serum. EGF was added for 15 min prior to harvesting at the indicated concentration.

The experiment was performed by culturing the cells in medium containing 1 % serum to exclude the possible influence of serum-derived growth factors. The same experiment

was also repeated with cells growing in medium containing 10 % serum, which, in regard to the *in vivo* experiments, may better reflect physiological conditions. However, both setups gave almost the same results. Overall, the results from the Western blot analyses suggest that, *in vitro,* DARPins are the more potent inhibitors of EGFR downstream signaling than cetuximab.

2.4.3 DARPins Induced Phosphorylation of the EGF Receptor and Activation of Downstream Signaling.

Unexpectedly, we observed phosphorylation of the EGF receptor at Tyr1173 in A431 cells 24 hours after treatment with DARPins. The phosphorylated EGFR, which we discovered by indirect immunofluorescence staining of EGFR and phospho-EGFR, was mainly located at the cell-cell interfaces (see Figure 2.7A). We suspected that the clustering of EGFR by the tetravalent DARPin might induce autophosphorylation of EGFR by juxtapositioned kinase domains. Cetuximab also led to an accumulation of EGFR at the contacting plasma membrane between cells, but phosphorylation of the receptor at Tyr1173 was not observed at this time point.

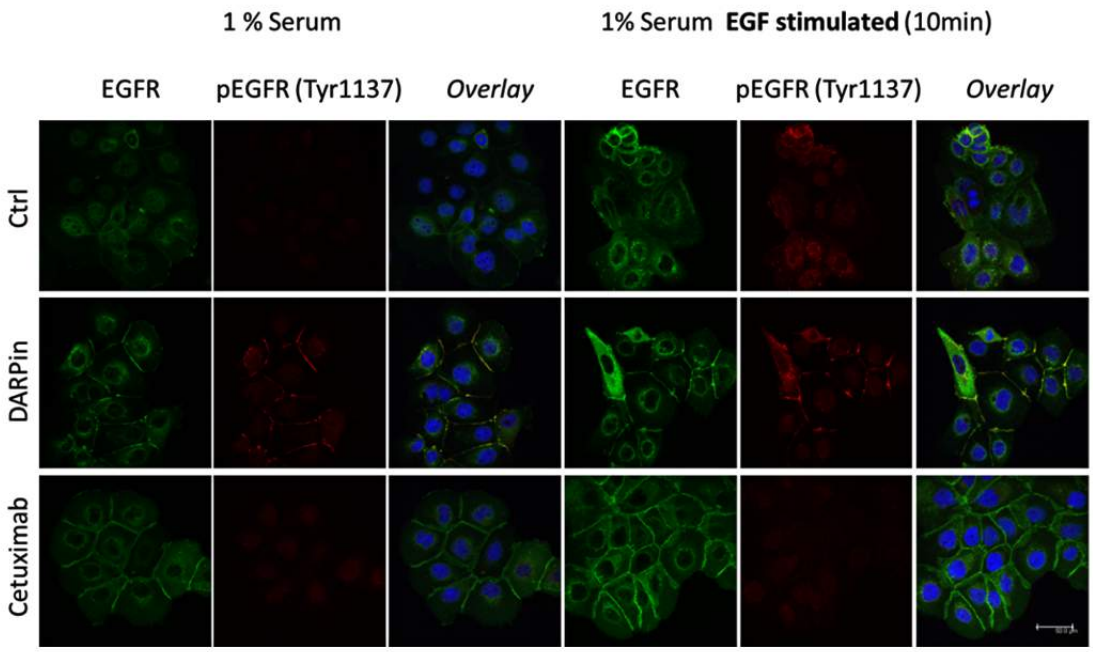

Figure 2.7 The application of DARPins lead to phosphorylation of the EGF receptor. For indirect immunofluorescence A431, cells were fixed 24 hours after treatment with DARPins or cetuximab. Cells were assayed for EGFR expression (green) and the presence of phospho-EGFR (red). Counterstaining for the DNA was performed with Dapi (blue). In the panels on the right side, the cells were additionally stimulated with 100 ng/ml EGF for 10 minutes before fixation.

In the previous Western blot analysis of A431 cells under DARPin-treatment, we were not aware of such a DARPin-induced phosphorylation. We anticipated that the DAR-

Pin-induced phospho-EGFR levels might be higher at early time points, due to the initial high level of EGFR. The results in Figure 2.8A revealed that DARPin-induced phosphorylation of EGFR is detectable by Western blot as well, although the level of phospho-EGFR was significantly lower in the DARPin-treated cells, than in the cells stimulated with EGF. Importantly, DARPin-induced phosphorylation of EGFR also activated the downstream signaling, indicated by phosphorylation of Erk at early time points. At the 24-hour time point, however, Erk phosphorylation was decreased even below the levels observed in untreated control cells. In the non-small cell lung cancer cell line A549 (see Figure 2.8B), we could not detect phosphorylation of the EGF receptor at Tyr1173 in general, not even in EGF-stimulated cells. Nevertheless, we detected increased phosphorylation of Erk upon treatment with DARPins, which indicated that also in A549 cells EGFR is activated by the DARPin-treatment. Whether A549 cells have a mutation in Tyr1173 is not known and remains to be elucidated.

We also noticed that in A431 cells the EGF-stimulated EGFR was not degraded. The strong binding of EGF normally targets the receptor for degradation [114]. In A549 cells, EGFR was strongly downregulated in presence of abundant EGF (100 ng/ml). Probably, in A431 cells, the continuous EGFR signaling in response to EGF stimulation is linked to the growth arrest we observed in EGF-treated A431 cells (see Figure 2.11). EGF-induced growth arrest was described by others before [209]. On the other hand, in EGF-stimulated A549 cells, no difference in proliferation compared to untreated cells was observed (see Figure 2.20).

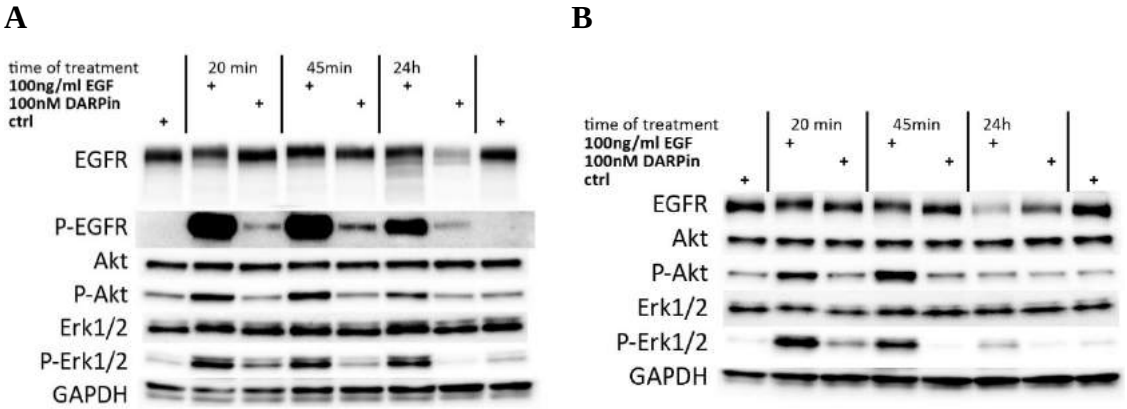

Figure 2.8 The application of DARPins lead to stimulation of the EGF receptor and induced downstream signaling. A431 cells **(A)** and A549 cells **(B)** were treated with EGF or DARPins at the indicated concentrations and were harvested at early time points of 20 and 40 minutes after administration and after 24 hours. Untreated cell were used as control. Lysates were assayed by Western blot analysis for phosphor-EGFR and for phosphorylated downstream targets.

Detection of phospho-EGFR appeared unequally stronger by immunofluorescence microscopy than by Western blotting, which obviously is due to technical reasons.

Clustered objects emit a stronger immunofluorescence signal than individual objects with regard to the background signal. Most importantly, immunofluorescence microscopy provides information about the localization of the phosphorylated EGFR. Thus, in A431 cells, induction of EGFR phosphorylation after DARPin-treatment was followed at 10-minute intervals by immunocytochemistry. Phospho-EGFR was determined as early as 10 minutes and the highest levels were observed at 30 minutes after DARPin-treatment (see Figure 2.9A). Phospho-EGFR was mainly localized at the plasma membrane. Only at the 30-minute time point, there were indications that phospho-EGFR might enter endosomes. Moreover, like at the 24-hour time point the plasma membrane staining was confined to cell-cell interfaces, which indicated that endocytosis in this region might be slower or impaired.

A

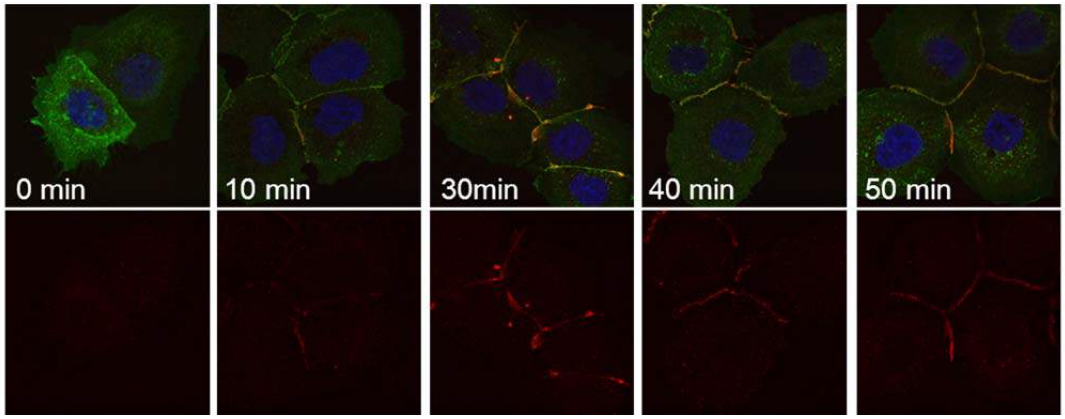

B

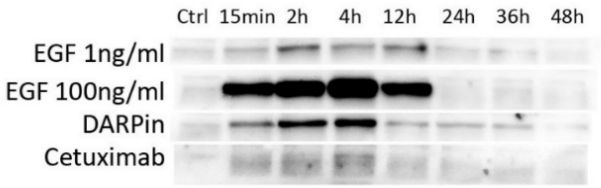

Figure 2.9 DARPin and cetuximab induced phosphorylation of the EGF receptor at early time points. **(A)** A431 cells were treated with 100 nM DARPin, fixed at the indicated time points and stained for EGFR (green) and phospho-EGFR (red) by indirect immunofluorescence. **(B)** Time line of EGFR phosphorylation in A431 cells treated with 100nM DARPin or cetuximab, or EGF at concentrations indicated above. The analysis was performed by Western blotting.

In comparison to the EGF-induced phosphorylation, stimulation by DARPins was lower and of shorter duration (see Figure 2.9B, above). However, the concentration of 100 ng/ml EGF, we had adopted from literature, might even exceed EGF levels in tumors with high EGF expression. Additionally, we observed that also cetuximab was capable of inducing EGFR phosphorylation, but to an extent that was significantly lower than

the phosphorylation induced by DARPins. This difference might reflect the difference in their potency to cluster and downregulate EGFR.

2.4.4 DARPin-Induced Endocytosis of the EGF Receptor is Independent of Its Phosphorylation Status at Tyr1173.

Our results demonstrated that downregulation of the EGF receptor in A431 cells was more pronounced in response to DARPin-treatment than to cetuximab. To test whether treatment-induced phosphorylation of the EGF receptor plays a role in the endocytosis and subsequent degradation of EGFR, phosphorylation was prevented by the dual EGFR/Her2 tyrosine kinase inhibitors AEE778 or PKI-166 prior to the treatment with DARPins. Both inhibitors act on the intracellular kinase EGFR domain and thus should not interfere with the binding of DARPins to the extracellular domain. A431 cells were pretreated with the tyrosine kinase inhibitors, and along with untreated cells, they were incubated for 24 hours with or without DARPins. The kinase inhibitors alone did not lead to a significant change in the EGFR level as determined by Western blot analysis (see Figure 2.10A). More importantly, inhibition of EGFR phosphorylation did not prevent its downregulation upon the treatment with DARPins. Thus, we concluded that phosphorylation or at least phosphorylation at Tyr1173 was not essential in the process of EGFR endocytosis.

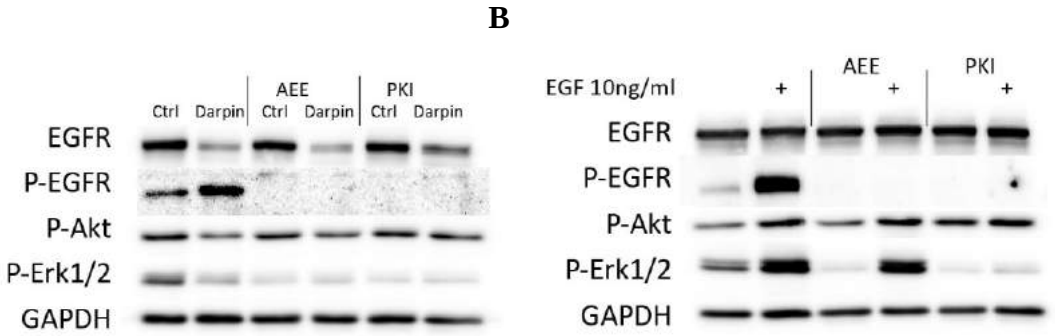

Figure 2.10 Phosphorylation of the EGFR was not necessary for endocytosis of the receptor. **(A)** A431 cells were treated with 1 µMol AEE778 or 4 µMol PKI-166 1 h prior to treatment with 100 nM DARPins. Cells were harvested 24 h after treatment and assayed for the EGFR level and its phosphorylation status, as well as for the downstream targets. **(B)** A431 cells were treated with AEE778 and PKI-166 as above. Persistence of EGFR inhibition by the tyrosine kinase inhibitors for the duration of 24 hours was assayed by EGF stimulation added 15 minutes prior to harvesting.

Curiously, in the Western blot analyses that was performed to validate that the tyrosine kinase inhibitors displayed their inhibitory activity for the entire duration of the 24-hour DARPin-treatment (see Figure 2.10B, above), we observed that EGF stimulation of AEE778-treated cells lead to Erk phosphorylation. Phosphorylation of Erk was of equal

degree as in the control cells, even though EGFR-phosphorylation at Tyr1173 was inhibited. In the PKI-166-treated cells, the downstream signaling was inhibited at the 24-hour time point. Thus, PKI-166 might be better suited for this experiment.

2.4.5 The Antiproliferative Effect of DARPins Is Stronger than that Observed for the Antibody Cetuximab

In vitro, administration of cetuximab or DARPins led to a decrease in cell proliferation in A431 cells (see Figure 2.11A). Even though DARPins always showed a stronger reduction on the level of cell proliferation than cetuximab, the effect of EGFR inhibition on proliferation in adherent A431 cells was not significant and an increase in concentration of the inhibitors did not further decrease cell viability.

Surprisingly, the antiproliferative effect was more pronounced in 3D cell culture, wherein cells were grown embedded in matrigel (see Figure 2.11B). However, quantification of proliferation in 3D, i.e. the determination of the clone size, is not straightforward and was performed only at a qualitative level. Nonetheless, the numbers of clones formed after DARPin-treatment were significantly reduced, compared to the colony numbers of cetuximab-treated or control cells (see also Figure 2.19C, page 55).

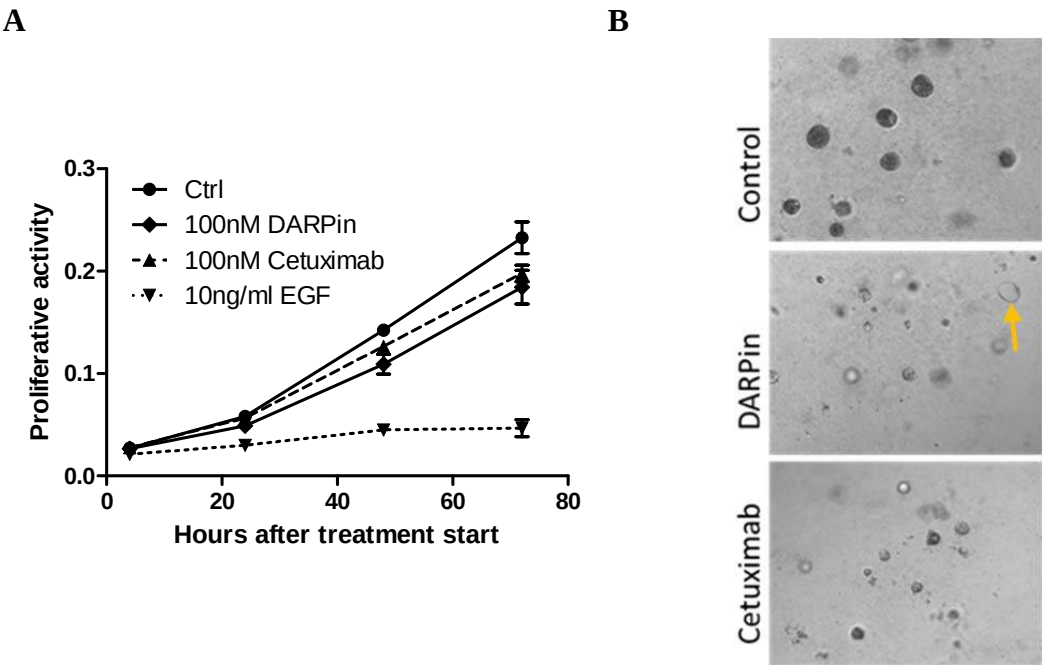

Figure 2.11 EGFR inhibition by DARPins and cetuximab lead to reduced proliferative activity in A431 cells. **(A)** In adherent cell culture, DARPins were only insignificantly more potent than cetuximab. Continuous stimulation by EGF lead to the strongest inhibition of proliferation. Data depicts the mean of three independent experiments; error bars represent the SEM. **(B)** The effect of cetuximab or DARPins on cell proliferation was more pronounced in 3D-cell culture than in 2D cell culture. The arrow indicates a putative senescent cell.

The reduction in cell number was not a result of programmed cell death (apoptosis) in A431 cells. The amount of PARP cleavage upon administration of DARPins or cetuximab was assessed by Western blot analysis, but no cleavage of PARP was observed (data not shown). On the other hand, inhibition of the EGF receptor lead to inhibition of cell cycle progression as was indicated by the shift in cell cycle distribution from the S phase towards G0/G1 phase (see Figure 2.12).

However, reduced cell cycle progression does not explain reduced colony formation of DARPin-treated cells in 3D cell culture. PARP cleavage was only determined in adherent A431 cells and might display a different result in 3D cell culture. Otherwise, the strong inhibition of EGFR by DARPin-treatment also may induce senescence. In the 3D culture of DARPin-treated cells, we observed the occurrence of big, bubble-like cells (see yellow arrow in Figure 2.11B, above), that might resemble senescent cells.

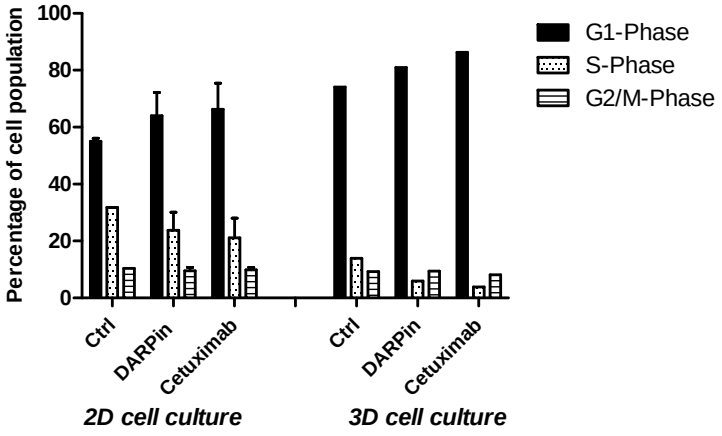

Figure 2.12 A431 cells treated with either EGFR inhibitor displayed an increased G1 phase population and reduced S phase population. Relative reduction of S phase population was stronger in 3D-cell culture (single experiment) than in 2D-cell culture (three combined experiments; error bars represents standard deviation).

Interestingly, proliferation of A431 cells was most strongly reduced by continuous by EGF stimulation (see Figure 2.11A). Konger et al. suggested that EGF at nanomolar concentrations lead to a terminal differentiation in A431 cells [210], even though it was not clear whether differentiation per se is a consequence of growth arrest or vice versa [211, 212]. Only at picomolar concentration, EGF was shown to stimulate proliferation in A431 cells [210]. However, in our study, we investigated whether inhibition of the EGF receptor by cetuximab or DARPins counteracted EGF-induced growth arrest. Pretreatment with cetuximab or DARPins, as well as application of the EGFR inhibitors after EGF stimulation (10 ng/ml), led to a rescue of the EGF-induced growth arrest (see Figure 2.13). This effect was also observed at a higher EGF concentration (50 ng/ml ~ 80 nM), which is almost equimolar to the concentration of the EGFR inhibitors applied

(data not shown). Interestingly, the difference between the application of EGFR inhibitors before or after EGF stimulation was small, indicating that EGFR is very efficiently inhibited by both DARPins and cetuximab.

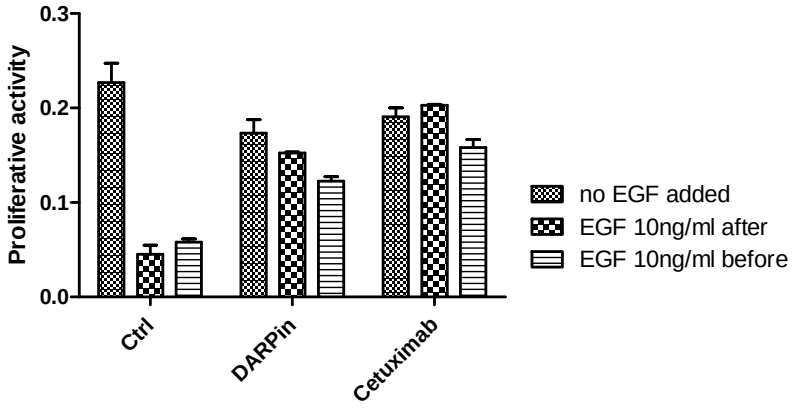

Figure 2.13 EGF-induced growth arrest was rescued by inhibition of EGFR through the binding of cetuximab or DARPins. A431 cells were treated with EGF 4 h before or after treatment with cetuximab or DARPins (100 nM final concentration each). Proliferation was determined 72 h after treatment start by Alamar Blue assay. Data shows mean of two independent experiments; error bars represent standard deviation.

2.4.6 EGFR Expression in 3D Cell Culture upon Treatment with DARPins or Cetuximab

To evaluate the obvious differences in the EGFR pattern of 3D versus 2D cell culture upon DARPin- or cetuximab treatment, we attempted to stain cells derived from 3D cell culture for EGFR and phospho-EGFR. For the immunocytochemical staining, cells have to be partially liberated from the matrigel, which could be achieved by incubation in ice cold PBS for 10 minutes, prior to trypsinization and fixation. This procedure greatly impaired the detection of phospho-EGFR. However, the EGFR staining pattern in 3D control cells was similar to that of adherent control cells. DARPins led to a reduction of EGFR, whereas cetuximab did not, which was easily detectable despite the fact that EGFR expression levels varied greatly among different cells (see Figure 2.9A for 2D and Figure 2.14 for 3D cell culture). Cetuximab-treated cells strongly clustered and remained attached to each other even after trypsinization and thus revealed that all cells within a single clone showed the similar EGFR staining intensity. Cetuximab generally did not lead to a downregulation of EGFR and thus we conclude that the EGFR expression level is inherited by daughter cells. However, we did not investigate whether in control cells EGFR expression also passed to daughter cells and whether cells were capable of switching from low- to high-level EGFR expression over time and vice versa.

Also in 2D cell culture, FACS analyses of cetuximab-treated cells revealed a substantial number of cell duplets, but the cell clustering was more pronounced in 3D cell culture.

The cell clusters could not be resolved by trypsinization. However, it was possible to separate the cells by incubation in EDTA-Glycine buffer (pH 2), which indicates that the antibody cetuximab might be directly responsible for the clustering of the cells. Immunofluorescence microscopy of EGFR 24 hours after application of cetuximab appeared to be strongest at cell-cell interfaces (see Figure 2.9), but was absent at free edges. Possibly, intercellular crosslinking of EGFR by cetuximab inhibited endocytosis and degradation of the receptor. Cells treated with the tetravalent DARPin displayed a similar cell-cell interface staining as well, but to a lower extent. DARPins, however, are supposedly digested by trypsin, and the clustering of cells could not anymore be observed after cell trypsinization. Furthermore, structural properties, such as the size of the antibody may account for the stronger intercellular crosslinking and consequently reduced downregulation of EGFR.

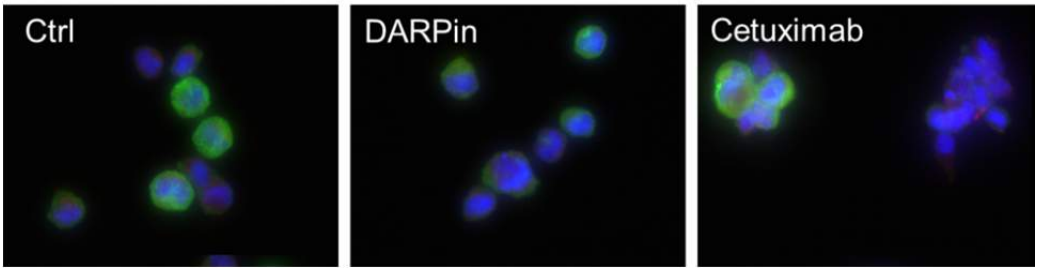

Figure 2.14 EGFR expression in 3D cell culture after treatment with DARPins or cetuximab. A431 cells were seeded as single cells in matrigel. 24 hours after seeding, DARPins or cetuximab was administered at a final concentration of 100 nM. Cells were harvested 48 hours thereafter and stained for the EGF-receptor (green). Nuclei were counter stained with DAPI.

2.4.7 Continuous EGFR Inhibition Does Induce Permanent Changes

With regard to *in vivo* experiments, we investigated whether the continuous treatment with DARPins induced permanent changes in proliferation, EGFR expression and downstream signaling. A431 cells were kept under the influence of DARPins for a period of three weeks, which corresponded to the planned *in vivo* treatment time. Thereafter, the cells were released into fresh medium and their recovery and response to EGFR inhibition by DARPins and cetuximab was assessed. In the control cells that were merely released into fresh medium, the EGFR protein level and its signaling capacity was fully restored at the time point of harvesting (Figure 2.15A).

Moreover, the proliferative activity that was reduced under the prolonged treatment with DARPins recovered within hours (see control cells in Figure 2.15B). There was no significant growth delay observed in comparison to the proliferation of untreated A431 cells in Figure 2.11A. Equally, the anti-proliferative effect of EGF was restored at the time point of EGF-administration, approximately 20 h after the release into fresh medi-

um. Thus, we conclude that during a period of three weeks, DARPins did not lead to the selection of a DARPin-resistant phenotype. However, for the manifestation of newly originated mutations a longer treatment period would be necessary.

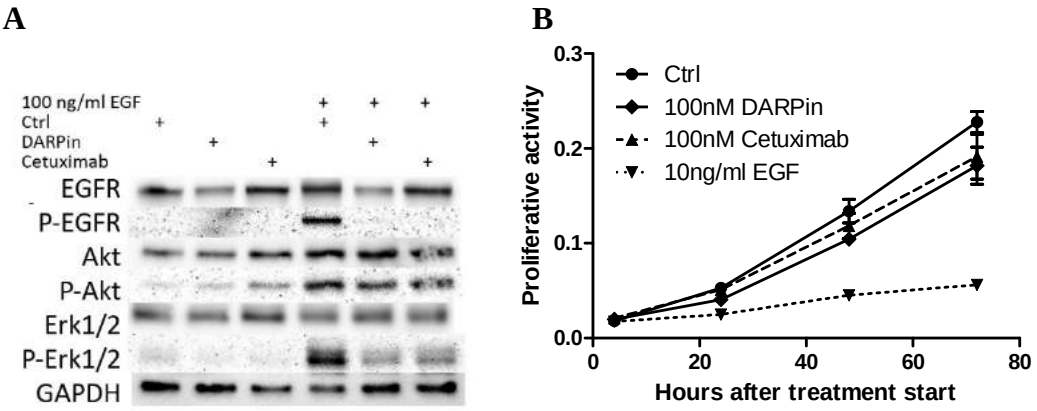

Figure 2.15 Continuous treatment with DARPins for three weeks does not induce a selective process in A431 cells. After the three weeks incubation, the cells were then released into fresh DARPin-free medium. The following day DARPins or cetuximab were administered and **(A)** EGFR expression and signaling with and without EGF stimulation was assayed 24 hours thereafter by Western blot analysis. **(B)** Proliferation was assessed with Alamar Blue at the indicated time points. Ctrl refers to cells released into fresh medium with no drugs added later. Data depicts the mean of two independent experiments; error bars represent the SEM.

2.4.8 The Dynamics of EGFR Inhibition by DARPins and Cetuximab *In Vitro*

To optimize a combined treatment modality of ionizing radiation with a radiosensitizing agent, it is important to investigate the dynamics of the effect introduced by the agent. Thus, we followed the dynamics of EGFR inhibition by DARPins or cetuximab in A431 cells. We examined the EGF receptor abundance and its Tyr1173-phosphorylation status upon EGF stimulation, as well as the downstream signaling by Western blot (see Figure 2.16). Already one hour after treatment with DARPins and cetuximab, respectively, phosphorylation of the EGFR-receptor was inhibited and could not be induced by EGF stimulation. For the DARPin-treated cells, a minimal band of DARPin-induced EGFR phosphorylation was visible. The EGFR receptor itself was gradually reduced in the DARPin-treated cells. Intriguingly, also in the cells treated with cetuximab, EGFR was reduced over time. In the previous experiments, EGFR levels had remained unchanged for cetuximab-treated A431 cells. A possible explanation may be that in this experiment, cells were seeded at a lower density, which lead to a reduced intercellular cross-linking by cetuximab, and thus allowed for increased endocytosis of the receptor-antibody complex.

In contrast to the EGFR-phosphorylation, phosphorylation of Erk was only significantly reduced 4 hours after administration of DARPins and 8 hours after the application of

cetuximab. Hence, phosphorylation of Tyr1173 may not be a precise indicator for the EGF receptor status. The gradual decrease of phospho-Erk correlated better with the dynamics of the downregulation of the EGFR level. In addition, also in cetuximab-treated cells phospho-Erk levels were strongly reduced, which we could not observe in the previous experiments. This indicates that in order to reduce downstream signaling, inhibitors binding to the extracellular domain of EGFR might need to induce endocytosis and degradation of the receptor. Likewise, for Akt, we cannot explain why in the DARPin-treated cells, we did not observe a similar reduction in phospho-Akt as above (see Figure 2.6); a repetition of the experiment may show the reliability of the results concerning phospho-Akt. Furthermore, additional investigations are required to assess the correlation of cellular density and endocytosis of EGFR in response to cetuximab.

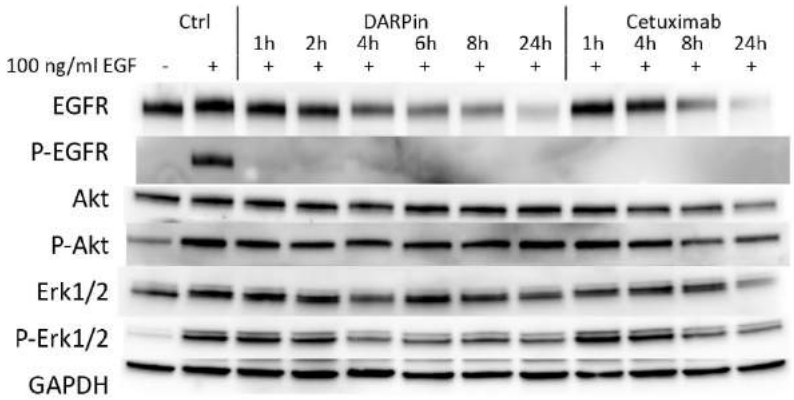

Figure 2.16 Time line of EGFR Inhibition by DARPins or cetuximab. Inhibition of phosphorylation of the EGF receptor by DARPins or cetuximab takes place already at an early time point. A431 cells were treated DARPin or cetuximab, both at a final concentration of 100 nM. Samples for Western blot analysis were harvested at the indicated time points after treatment start. Cells stimulated with EGF were incubated with 100 ng/ml EGF for 15 min before harvesting. Lysates were analyzed for the expression level and the phosphorylation status of EGFR, and phosphorylation of the downstream targets Akt and Erk.

Equally, if not more important than downregulation of the receptor, is the process of the recovery of the EGFR status after withdrawal of the drug, which indicates the duration of the treatment effect. On the other hand, the treatment effect is also dependent on the half-life of the drug. In contrast to cetuximab, the half-lives of DARPins are much shorter and may reach from 10 minutes to 12 hours as published in Zahnd et al. and in reference to information received from the Biochemical Institute, University Zurich [204]. With regard to the shorter half-life, the recovery time of the receptor might be crucial with regard to treatment efficacy.

To assess EGFR recovery, A431 cells that had been treated for 24 hours with DARPins or cetuximab were washed with PBS and released into fresh medium. As early as two

hours after the release, phosphorylation of EGFR at Tyr1173 could be observed by Western blot analysis (see Figure 2.17A, B).

A

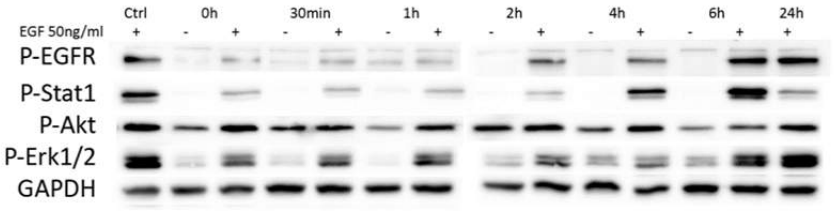

B

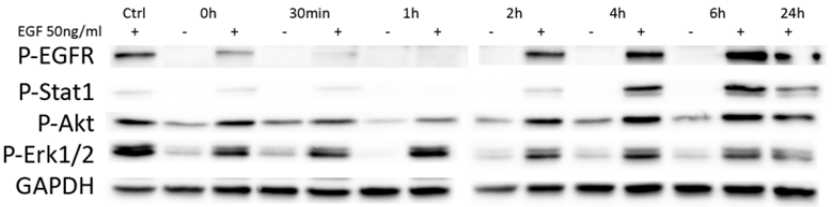

Figure 2.17 Recovery of EGF receptor levels and signaling after withdrawal of DARPins or cetuximab. A431 cells were treated with **(A)** 100 nM DARPins or **(B)** 100 nM cetuximab for 24 h and then released into fresh medium. Recovery of EGFR signaling was assayed by EGF stimulation for 15 min at the indicated time points after drug withdrawal. Samples were collected and subjected to Western blot analysis of the phosphorylation status of the receptor itself and the phosphorylation of the downstream targets STAT1, Erk and Akt.

As a downstream signaling moiety, we included signal transducer and activator of transcription 1 (Stat1) that is involved in growth factor dependent signaling [213]. EGF-stimulated phosphorylation of Stat1 at Tyr701 was strongly suppressed by EGFR inhibition. Phosphorylation returned by 4 hours and reached control or even elevated levels by 6 hours after drug release. As in the previous experiment (see Figure 2.16), phosphorylation of Akt was not substantially suppressed by EGFR inhibition and thus did not contribute to the readout of the experiment. Consistently, EGF-stimulated phospho-Erk was reduced upon application of DARPins or cetuximab and returned to basal level within 6 hours of drug withdrawal. The fast recovery of STAT1 and Erk phosphorylation upon EGFR stimulation indicate a fast reconstitution of the EGFR status after elimination of the EGFR inhibitors from the cell culture medium.

2.4.9 EGFR Inhibition by DARPins or Cetuximab Does Not Lead to Radiosensitization in A431 cells *In Vitro*

The combination of cetuximab with radiotherapy in comparison to radiotherapy alone results in improved locoregional tumor control and overall survival in patients with squamous cell carcinoma of the head and neck (SCCHN) [137, 138]. The proposed mechanism of action by which cetuximab supports radiotherapy, and the degree of

radiosensitization are controversial. An overview of proposed mechanisms is presented in the discussion (see section 2.5.7). Some of the mechanisms of radiosensitization rely on the cell's own repair capacity and on EGFR signaling, which contributes to cell survival signaling. These aspects may be assessed *in vitro*, whereas indirect effects on the level of the tumor microenvironment, such as stabilization of the endothelial cells upon IR-treatment by increased VEGF section, are more complicated to investigate in cell culture. Thus, we mainly inspected direct effects on the level of the cancer cell. We investigated cell proliferation and the clonogenic capacity of A431 cells with regard to the combined treatment of EGFR-inhibition with IR and compared it to the effects of radiation treatment alone.

On the level of the proliferation in response to the treatment with DARPins or cetuximab in combination with IR, we were not able to detect a synergistic effect (see Figure 2.18). However, the results indicate, that there might be an additive effect of EGFR inhibition to radiotherapy. Like in unirradiated cells, the difference in proliferative activity between cetuximab- and DARPin-treated cells was preserved in irradiated cells, but did not increase, as might be the case for a synergistic effect.

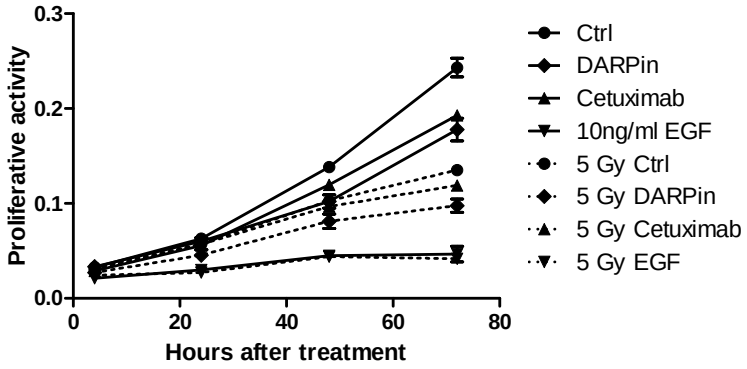

Figure 2.18 Inhibition of EGFR does not sensitize A431 cells to IR. Cells were seeded in 96-well plates; the following day, cells were treated with DARPin or cetuximab at a final concentration of 100 nM each, or with 10 ng/ml EGF. 4 hours thereafter, the cells were irradiated with 5 Gy or sham irradiated and proliferation was followed by Alamar Blue assay at the indicated time points after drug treatment.

A classical experiment to investigate radiosensitization by a drug on the level of the cancer cell is the comparison of the clonogenicity of cells with and without treatment in combination with IR. The clonogenic potential of a cell *in vivo* contributes to tumor growth, thus, a reduction of clonogenicity *in vitro* is an indication of a possibly greater treatment effect *in vivo*. However, by means of the classical clonogenic assay we were not able to determine a direct effect of the inhibition of EGFR by DARPins or cetuximab on radiosensitivity (see Figure 2.19A). The clonogenicity of A431 cells by EGFR inhibition with DARPins or cetuximab alone was reduced by about 40 – 50 %, but as

mentioned, no synergistic effect in combination with IR was observed. In accordance with the results from the proliferation assays, the colonies that formed under treatment with DARPins or cetuximab were of smaller diameter.

Interestingly, in a study that was performed with cells growing in spheres in matrigel, it was shown that EGFR inhibition by cetuximab had a radiosensitizing effect [214]. Eke et al. performed the classical clonogenic assay with adherent cells as well, but could barely determine radiosensitization by cetuximab. The reason behind this observation was proposed to be due to differential protein expression and differential signaling in cells grown in spheres and in contact with matrigel. Eke et al. compared the expression and signaling pattern from cells grown in 2D and in 3D to homogenates from tumor xenografts of the same cells and found that the results from 3D conditions better resemble the *in vivo* pattern. However, this was least applicable for A431 cells, out of the three SCC cell lines that were tested by Eke et al. In the 3D clonogenic experiments performed by us, we did not observe significant radiosensitization, but the number of spheres formed under the treatment with DARPins was by far more reduced than under cetuximab treatment (see Figure 2.19B).

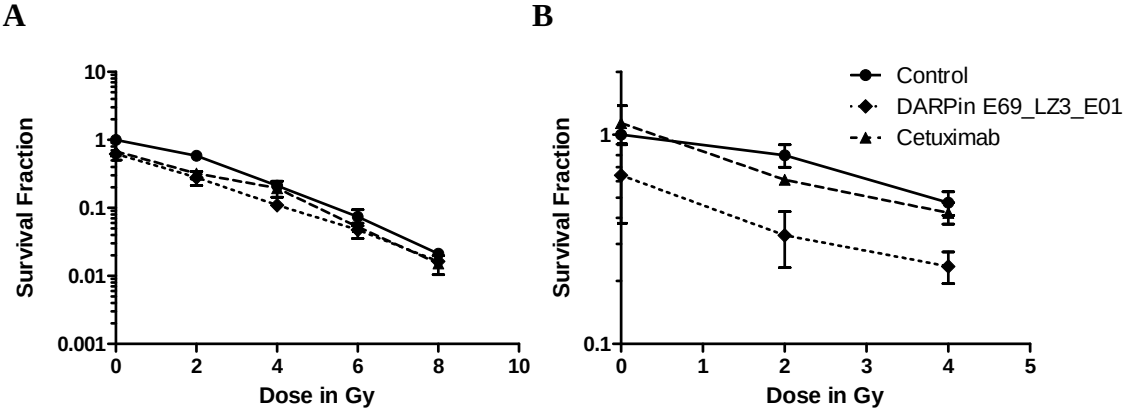

Figure 2.19 Application of anti-EGFR DARPins does not lead to radiosensitization *in vitro*. **(A)** For the classical clonogenic assay, A431 cells were plated in cell culture dishes and treated with DARPins or cetuximab the following day as for the proliferation assay; irradiation at different dose points were performed 6 hours after EGFR inhibition. Data depicts two independent experiments combined, with the error bars representing the SEM. **(B)** For the 3D-clonogenic assay, A431 cells were treated with DARPin or cetuximab as above, but grown in matrigel in 96-well plates. Data represents a single experiment, error bars show standard deviation of five wells counted per condition.

Nevertheless, as mentioned before, both, DARPins and cetuximab strongly inhibited proliferation in 3D (see Figure 2.11B for microscopy image). Moreover, in 3D cell culture the clonogenicity of A431 cells treated with DARPins alone was markedly reduced. This strong reduction in clonogenicity, though not synergistic in our hands, nonetheless

may contribute to the success of radiation therapy by additionally reducing the clonogenic potential of cancer cells.

2.4.10 A549 Are Not Sensitive to EGFR Inhibition or EGF Stimulation *In Vitro*

The non-small cell lung cancer cell line A549 expresses EGFR, but at the same time harbors an activating RAS-mutation, which may render them insensitive to EGFR inhibition. A549 cells have been investigated in the past with regard to EGFR inhibition in combination with IR. Radiosensitization upon EGFR inhibition was observed by Dittmann et al. [215], yet others claimed that the Ras-mutant cell line was insensitive to EGFR inhibitors such as cetuximab [216, 217].

In our hands, A549 proofed to be insensitive to cetuximab. We did not observe inhibition on the level of proliferation, nor did we observe radiosensitization at a concentration of 100 nM cetuximab (see Figure 2.20A, B). Equally insensitive was their response to DARPins, even though, Western blot analysis had previously revealed, that down-regulation of EGFR takes place upon treatment with DARPins (see Figure 2.7B). In A549 cells, EGFR inhibition does not lead to an accumulation of the cells in the G1/S phase as observed for the A431 cells. This may be due to the activating mutation in Ras downstream of EGFR. The activated Ras in A549 cells stimulates the Ras-Raf-Mek-Erk pathway regardless of the EGFR status, which we confirmed by Western blot analysis (data not shown).

Thus, we concluded that EGFR inhibitors might not be an option for cancer cells that harbor activating mutations in Ras.

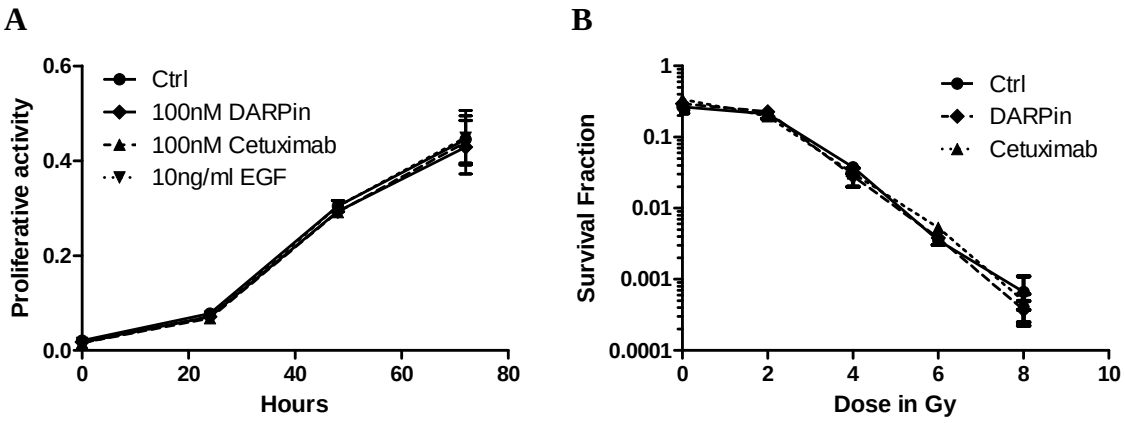

Figure 2.20 A549 cells are insensitive to EGFR inhibition by DARPins or cetuximab **(A)** Proliferation assay: A549 cells were seeded in a 96-well plate. Proliferation was measured by Alamar Blue measurement every 24 hours up to 72 hours after the indicated treatment. **(B)** Clonogenicity of A549 cells was determined in control cells or under treatment with 100 nM DARPins or cetuximab at the indicated in dose points.

2.4.11 Characterization of Pegylated DARPins with Prolonged Half-Life for *In Vivo* Application

For the *in vivo* application, we decided to use pegylated DARPins, which have a prolonged half-life. DARPins on their own are relatively small proteins that may be eliminated rapidly from blood circulation. DARPin monomers administered to mice by intravenous injection were eliminated within minutes, proposedly via the kidneys [204]. On the other hand, whole IgG antibodies, such as cetuximab, have a long serum half-life, which makes them favorable for therapeutic purposes.

DARPin E69_LZ3_E01 is a tetravalent binder consisting of two DARPin constructs dimerized by means of a leucine zipper, and thus has a markedly increased size compared to the single DARPin domains. Yet, the half-life of DARPin E69_LZ3_E01 was surmised not to be sufficiently long, because proteins of the size of 84 kDa may still be eliminated through glomerular filtration. Therefore, for the *in vivo* application, we decided to use a pegylated version of DARPin E69_LZ3_E01 that carried a PEG20 chain on each DARPin monomer.

Pegylation increases the molecular weight, but on the other hand, it may negatively influence the binding affinity of the DARPin domains, which we wanted to investigate. We previously observed that the DARPin E69_LZ3_E01 was capable of rescuing EGF-induced growth arrest in A431 cells (see Figure 2.13, page 49). However, the same experimental set-up performed with the pegylated version of the DARPin E69_LZ3_E01 only led to a partial rescue of proliferation (see Figure 2.21A). This indicates that the binding affinity probably was reduced by the pegylation, which may affect *in vivo* efficacy of the anti-EGFR DARPin. As expected, the nonspecific pegylated Off7_LZ3_ Off7 DARPin used as control in the *in vivo* setting showed no effect with regard to the rescue. A431 cells treated with the control DARPin proliferated at a rate comparable to cells treated with EGF only.

Whereas the affinity may affect tumor localization of the DARPin E69_LZ3_E01, it may also alter the efficacy of DARPins to inhibit EGFR. Thus, we compared the effect of the original and the pegylated DARPin E69_LZ3_E01 on cell cycle distribution. The cell cycle distribution determined 24 hours after treatment with the pegylated version of DARPin E69_LZ3_E01 showed a slightly reduced accumulation of cells in the G1/S phase compared to the original DARPin E69_LZ3_E01 (see Figure 2.21B). However, the accumulation of A431 cells in the S/G1 phase, as well as growth inhibition are effects of low magnitude and, thus, differences are difficult to discern.

Differences in the binding properties of the pegylated DARPin could be assessed by quantification of the DARPins bound to the cell surface of A431 cells. Unfortunately, this is not as straight forward as it may appear at first sight and need to be performed

with radiolabelled DARPins. Labeling of DARPins by indirect immunofluorescence cannot be quantitatively compared, because the binding of the primary antibody to the DARPins may be influenced by pegylation as well. Figure 2.22A depicts A431 cells treated for 30 minutes with pegylated control DARPin Off7_LZ3_ Off7, or pegylated or unpegylated DARPin E69_LZ3_E01. Samples were stained with anti-PEG antibodies and anti-RGS-His antibodies to visualize the bound DARPins. Even though the RGS-His staining for the cells treated with the unpegylated DARPin was much stronger, we could not relate staining intensity to binding efficacy due to the reason mentioned above.

A

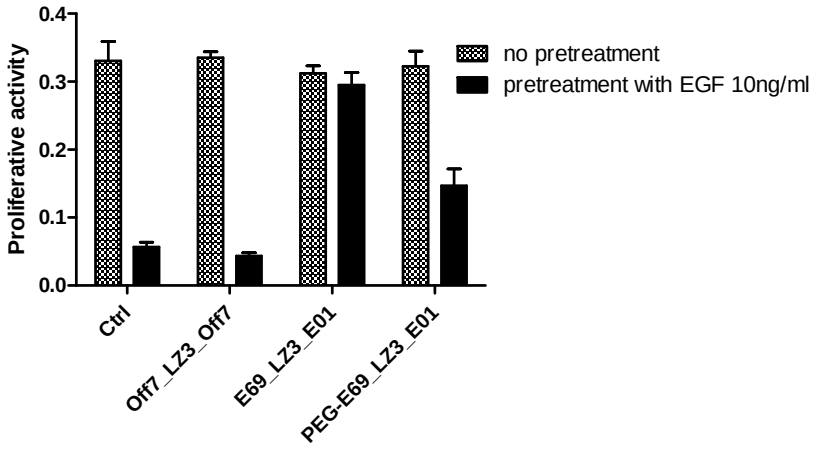

B

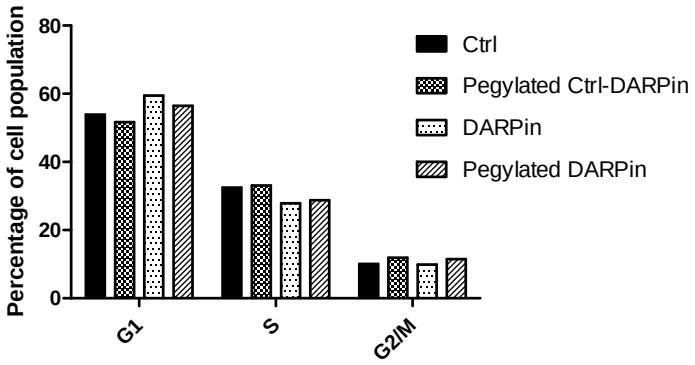

Figure 2.21 Characterization of pegylated DARPins. **(A)** A431 cells were treated with EGF (10 ng/ml) or medium only, followed by administration of the DARPins at a final concentration of 100 nM 4 hours thereafter. Proliferation was determined by Alamar Blue assay. The data shows the mean proliferative activity 72 hours after treatment (triplicates, error bars depict standard deviation). **(B)** A431 cells were treated for 24 hours with the respective DARPins. Cells were fixed and cell cycle was determined by FACS analysis, by means of BrdU incorporation and DNA content (single experiment).

Nonetheless, immunofluorescence labeling of the DARPins in a time line experiment, may be useful to compare the kinetics of EGFR endocytosis and degradation. Since the staining for the pegylated DARPin was stronger with the anti-PEG antibody, this anti-

body was used for visualization of the pegylated DARPin. For detection of the unpegylated DARPin, the RGS-His antibody was used. Endocytosis was readily induced by the unpegylated as well as the pegylated DARPin E69_LZ3_E01, as shown at the 30-minute time point (see Figure 2.22B). At the 18-hour time point, there were less stained intracellular vesicles in the cells treated with the pegylated DARPins. However, a counterstaining for the EGFR levels would have been essentially informative about the EGFR downregulation at the 24-hour time point. Indirectly the reduced levels of DARPins bound in both cases at this time point indicate an efficient downregulation by the original as well as the pegylated DARPin.

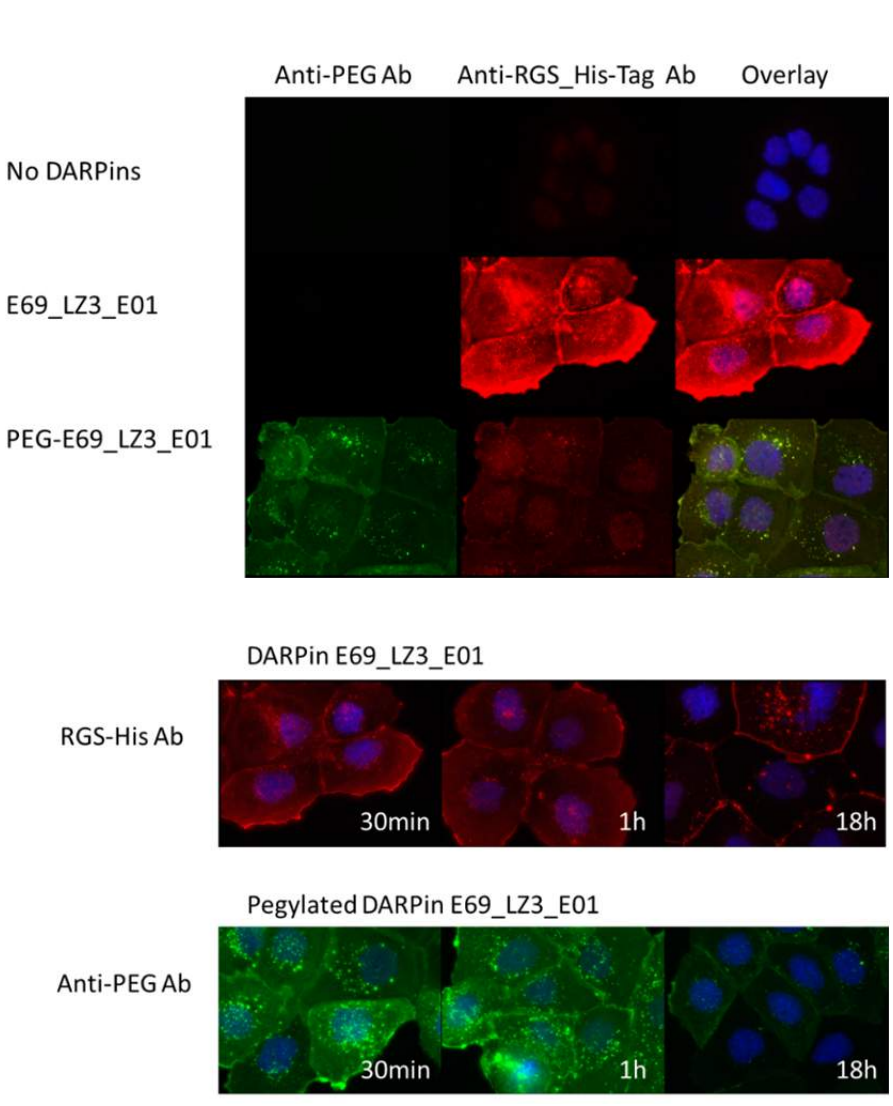

Figure 2.22 Immunofluorescent labeling of DARPins bound to the EGFR receptor *in vitro*. **(A)** A431 cells were treated with the respective DARPins for 30 minutes and stained with anti-PEG antibody and anti-RGS-His antibody. Images were taken with the same microscopy settings. **(B)** Time line of the binding of the EGF-receptor and its endocytosis facilitated by DARPins: E69_LZ3_E01 (top, stained with anti-RGS-His antibody) and pegylated E69_LZ3_E01 (bottom, detected by anti-PEG antibody).

2.4.12 Combined Treatment of A431 Tumor Xenografts with the Pegylated DARPin E69_LZ3_E01 and IR

For characterization of the anti-EGFR DARPin E69_LZ3_E01 *in vivo*, we planned to determine pharmacokinetics of the pegylated DARPin and to analyze histological sections stained for EGFR abundance and its phosphorylation status, for the phosphorylation of the downstream targets Erk1/2 and Akt and for the PEG-DARPins itself. Finally, the efficacy of the treatment with anti-EGFR DARPin E69_LZ3_E01 was determined in A431 tumor xenografts in nude mice.

2.4.12.1 Pharmacokinetics of the anti-EGFR DARPin E69_LZ3_E01

As previously described, the DARPin E69_LZ3_E01 consists of two separate DARPin domains linked by a leucine zipper, which facilitates dimerization of two E69_LZ3_E01 molecules. The tetravalent binder comprises a mass of 84 kDa, to which two 20 kDa linear PEG-chains are attached to. Pegylated DARPins at a dose of 30 mg/kg of body weight were administered intravenously (IV) or intraperitonealy (IP) and blood samples were drawn at the saphenous veins at the indicated time points. The serum half-life of the pegylated DARPin was determined by means of enzyme-linked immunoassay (ELISA) and comprised approximately 20 minutes (see Figure 2.23A, B).

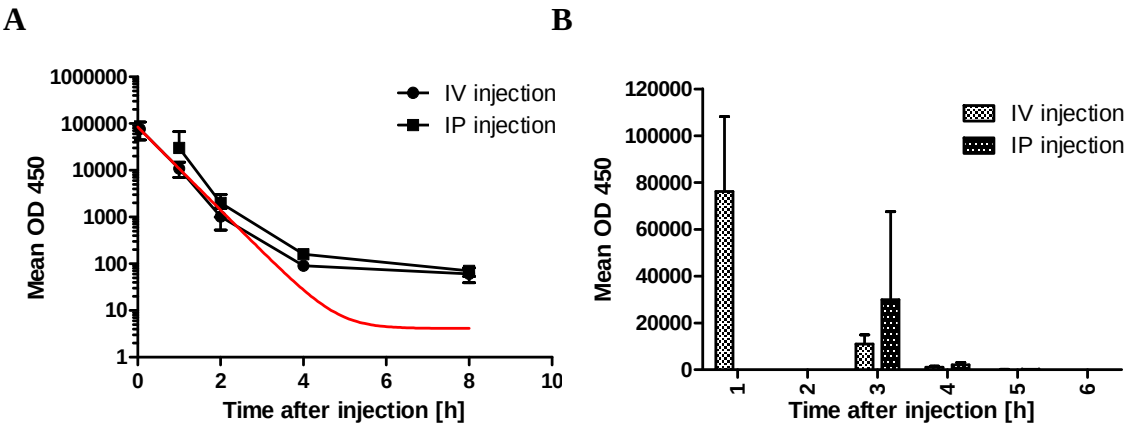

Figure 2.23 Elimination of pegylated DARPin E69_LZ3_E01 from blood serum after IV or IP injection. Both graphs depict the mean DARPin levels at the indicated time points after injection (n=5, error bars depict standard deviation). **(A)** The serum half-life of 20 min was determined by nonlinear regression (R square = 0.8346). **(B)** Data shown with linear scale.

In comparison, a bivalent unpegylated DARPin of 30 kDa exhibited a plasma half-life time of less than 3 minutes [204]. Nonetheless, the half-life of the pegylated DARPins was still much shorter than the half-life of cetuximab, which amounted to 40 hours in nude mice [218]. This implies the necessity for repeated applications of the DARPins. Since the number of injections that can be given intravenously is limited, we tested blood serum levels of pegylated DARPins after intraperitoneal injection as well. The

mean serum level of DARPins determined by ELISA one hour after drug administration was slightly higher compared to the drug serum level after IV injection, possibly due to the delay of the drug in reaching the blood circulation. Nevertheless, variation within the five mice treated intraperitonealy was substantially larger, at the 1-hour time point, than within the animals treated intravenously. This large variation compromises the control over the amount of drug reaching circulation and therefore reaching the tumor.

2.4.12.2 Immunohistological Analysis Does Not Shed Light onto the Functionality of the Pegylated DARPin E69_LZ3_E01

Even though pegylated DARPins show slower elimination from the blood, their bulkiness lead to slower tumor localization [204]. Therefore we harvested tumor xenografts treated with pegylated DARPin E69_LZ3_E01 for histological analyses, first to determine DARPin localization and secondly, to observe if the treatment would lead to changes in EGFR expression or phosphorylation. The treatment consisted of two injections at a 12-hour interval, and tumors were harvested 6 hours and 24 hours after the second treatment. Unfortunately, the anti-PEG antibody that we successfully used for immunocytochemistry (see Figure 2.22, page59) did not detect any pegylated DARPins within the formalin-fixed tumor tissue. From these results, we cannot conclude that the pegylated DARPins reached the tumor. We did not know at that time that the duration of the half-life of the PEG-DARPins would only be 20 minutes, otherwise a 15-minute time point might have served as positive control.

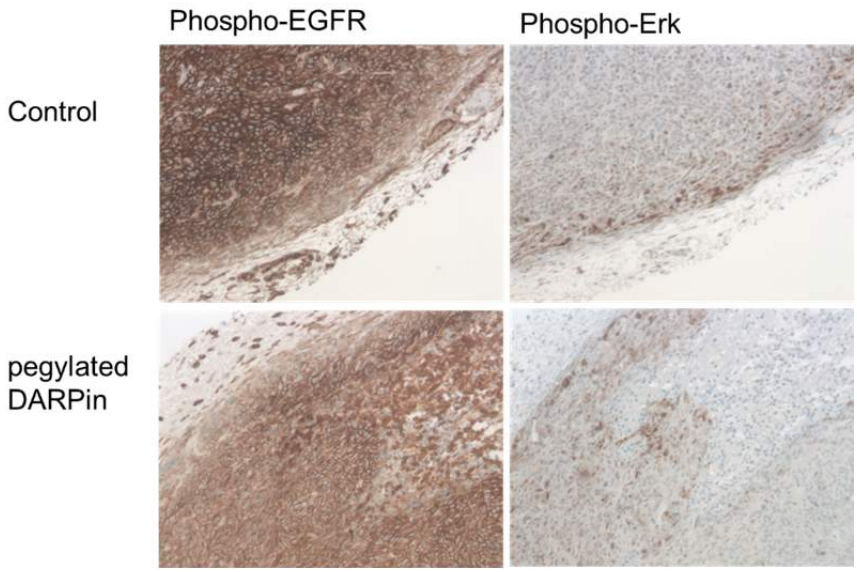

Figure 2.24 Immunohistological analyses of tumor xenografts harvested 6 hours after the second treatment with the pegylated DARPin E69_LZ3_E01.

Moreover, the staining for the EGFR itself was very strong and did not change remarkably in comparison to control tumors. Also in the histological sections derived from tumors treated with cetuximab, no changes in receptor expression could be determined (data not shown). Interestingly, phosphorylation of Erk, a downstream target of EGFR signaling, was strongest in areas were phosphorylation of EGFR was comparably low (see Figure 2.24, above). This rendered the evaluation of EGFR inhibition and its effect on downstream signaling impossible to be evaluated. Overall, histological analyses did not provide clear evidence for the *in vivo* application of the pegylated DARPin E69_LZ3_E01 or the mAb cetuximab. Nevertheless, the latter was shown to have a strong inhibitory effect on tumor growth (see section below).

2.4.12.3 Efficacy of the Pegylated DARPin E69_LZ3_E01 Compared to Cetuximab in A431 Tumor Xenografts in Nude Mice

To assess the efficacy of PEG-DARPins in comparison to cetuximab with regard to tumor growth inhibition and radiosensitization *in vivo*, A431 tumor xenografts were established subcutaneously on the hind back of nude mice. The mice were randomly divided into six treatment groups. Two groups were treated with PEG-DARPin E69_LZ3_E01, one as monotherapy and the second in combination with ionizing radiation. The two control groups were treated accordingly, but instead of the anti-EGFR DARPin, a pegylated nonspecific DARPin (PEG- Off7_LZ3_ Off7) was administered. Two additional groups were treated with cetuximab alone and in combination with IR, respectively.

Due to the rather fast pharmacokinetics, DARPins were administered daily, for 13 days, at a dose of 30 mg/kg of body weight, which is equal to 230 nmol/kg. Cetuximab injections were administered every fifth day at a dose of 50 mg/kg of body weight corresponding to 330 nmol/kg. Drugs were applied intravenously or intraperitonealy as stated in the table (see Table 2.5). Animals treated in combination with IR were given three fractions of 8 Gy with a five-day interval in between the irradiation fractions, one day after application of cetuximab or approximately 4 hours after DARPin-treatment.

Table 2.5 Treatment Schedule for A431 tumor xenografts in nude mice.

	Day 1	Day 2	Day 3	Day 4	Day 5	Day 6	Day 7	Day 8	Day 9	Day 10	Day 11	Day 12	Day 13
Control-DARPin	IV	IV/IR	IV	IP	IP	IV	IV/IR	IV	IP	IP	IV	IV/IR	IV
Control-DARPin & IR	IV	IV	IV	IP	IP	IV	IV	IV	IP	IP	IV	IV	IV
DARPin	IV	IV	IV	IP	IP	IV	IV	IV	IP	IP	IV	IV	IV
DARPin & IR	IV	IV/IR	IV	IP	IP	IV	IV/IR	IV	IP	IP	IV	IV/IR	IV
Cetuximab	IP					IP					IP		
Cetuximab & IR	IP	IR				IP	IR				IP	IR	

IV = intravenous injection; IP = intraperitoneal injection; IR = application of ionizing radiation

Treatment with the pegylated DARPin E69_LZ3_E01 did not reduce tumor growth at the dosage and schedule applied in comparison to the control treatment group. The mean of the tumor growth curves of both groups were congruent (see Figure 2.25). In combination with ionizing radiation, the tumors treated with pegylated DARPin E69_LZ3_E01 regrew even slightly faster (see Figure 2.25 and Figure 2.26), which might be explained by the variance.

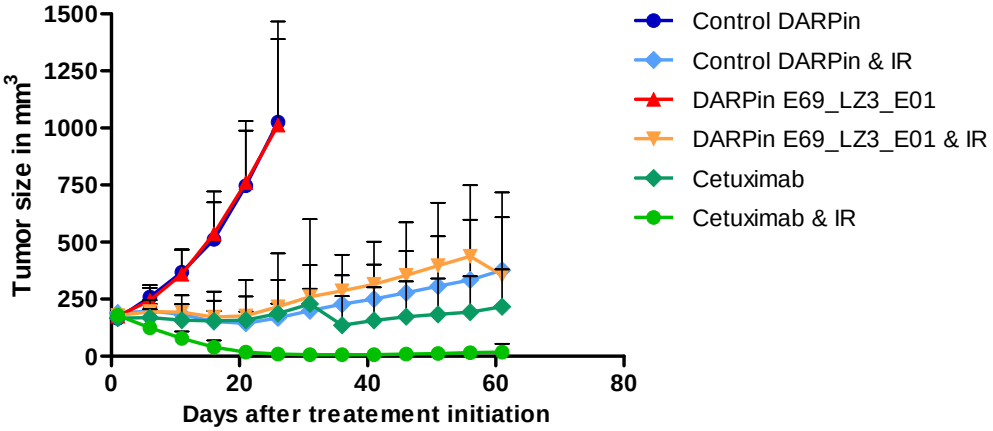

Figure 2.25 DARPin E69_LZ3_E01 does not influence tumor growth as monotherapy or in combination with ionizing radiation. **(A)** Tumor growth curves of A431 tumor xenografts. Mean tumor size and standard deviation at the indicated time after treatment start (n = 10, for all, except for Control DARPin n=14).

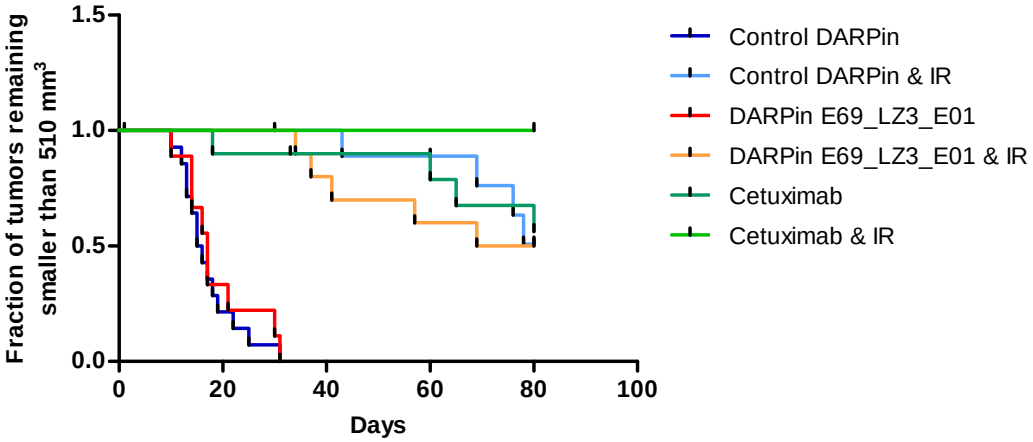

Figure 2.26 Kaplan Meier analysis: Time to reach 3 times the tumor size at treatment initiation. Overall survival was not significantly different between the group “Control DARPin & IR” and the group “DARPin & IR” (p = 0.63 by log-rank test).Cetuximab in combination with IR showed a significant difference from the control or the DARPin-treated group that were irradiated (p = 0.14, p = 0.11 by log-rank test)

The distribution of the tumor sizes, grouped according to treatment, at day 26 (for all treatment groups) and day 51 (for irradiated and cetuximab-treated tumors) confirmed that there was no difference between the control and the anti-EGFR DARPin (see Figure 2.27). Thus, we assume that the half-life of the PEG-DARPins indeed was too short to induce tumor growth delay. For the continuous downregulation of EGFR, a longer half-life is necessary to achieve a steady state of the administered DARPins in the serum.

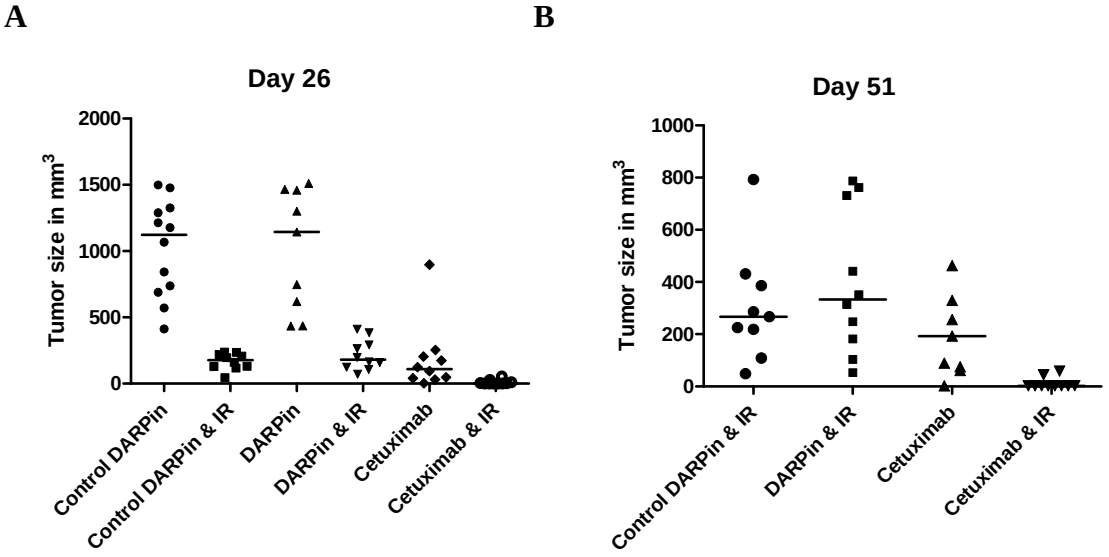

Figure 2.27 Distribution of tumor size on day 26 (A) and day 51 (B) after treatment start. Data is represented as scatter blot with the median indicated. On day 51, one animal had been sacrificed in the "Control-DARPin & IR" group due to necrosis of the tumor. This animal was not considered for calculating the median. The one tumor of the cetuximab group that already had reached 1500mm^3 was considered.

Surprisingly, cetuximab monotherapy was more efficient than ionizing radiation alone. Moreover, growth suppression *in vivo* was far more efficient than in classical cell culture *in vitro* and better resembles the antiproliferative effect observed in 3D cell culture. Partially, the anti-tumor effect of cetuximab in the preclinical settings might also have been due to complement-dependent cytotoxicity or indirect inhibitory effects on the endothelial cells and thus tumor angiogenesis.

Interestingly, one tumor, or one animal (considering a possible immune reaction) did not respond to cetuximab at all. Moreover, one tumor treated with cetuximab initially responded very well with tumor regression, but then started to regrow at an accelerated pace (see Figure 2.28, treatment group cetuximab). This might represent the selection of a more aggressive phenotype. Of the mice treated with the combined treatment of cetuximab and IR, all tumors regressed to a non-measurable size, and 6 out of 10 showed a total regression with no signs of tumor or even scars remaining. Two of the

four tumors that had not fully regressed after the three cycles of combined treatment, started to regrow within the 75 days after termination of the treatment. The two other tumors were barely visible and resembled fibrous scar tissue. To sum up the combined treatment of cetuximab and IR was very effective, which might have been due to EGFR inhibition as well as the antibody properties of cetuximab, contributing to a synergistic treatment response.

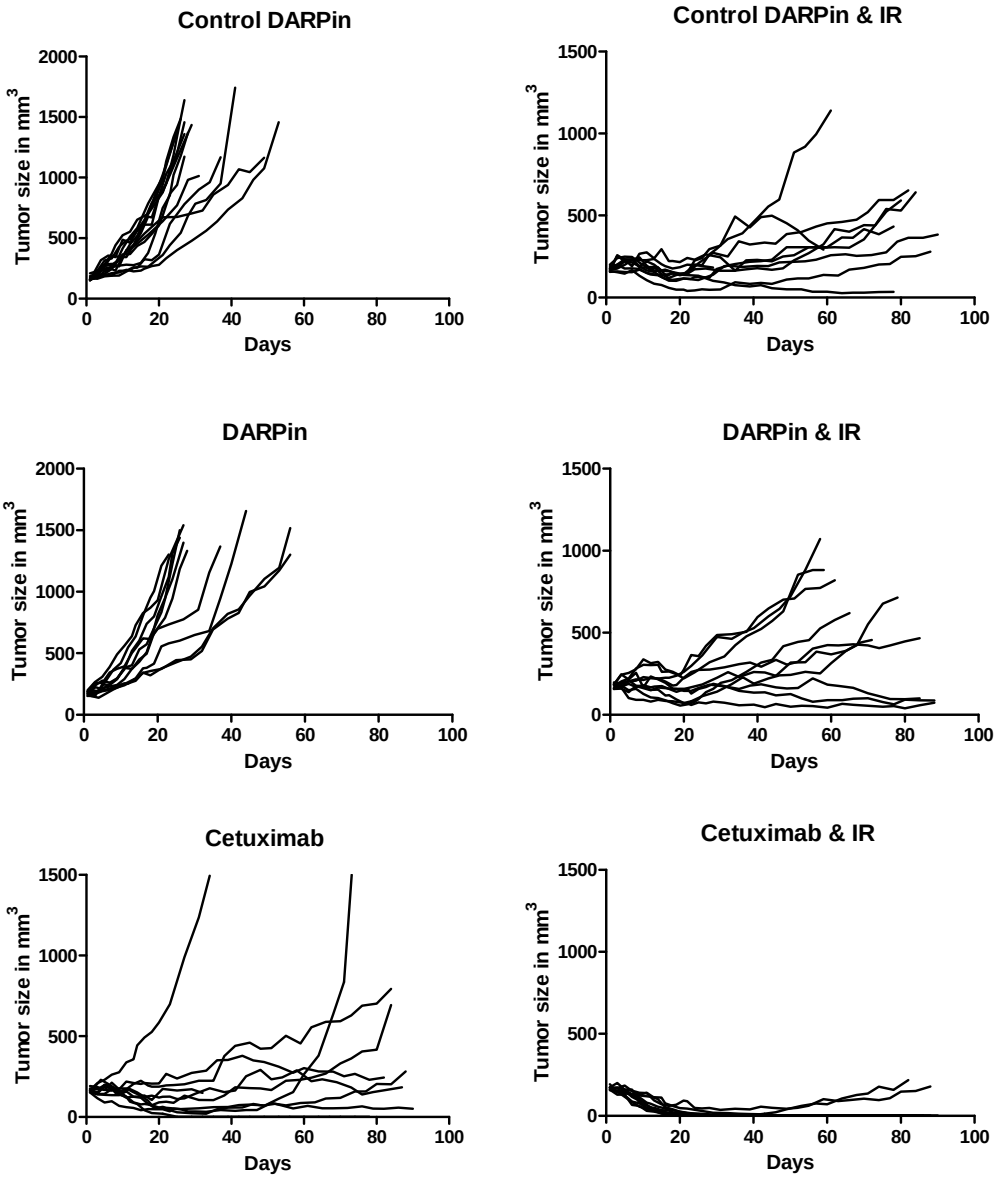

Figure 2.28 Tumor growth curves of individual mice shown separated according to the treatment groups. All groups contain 10 animals, except for the control DARPin group (n = 14). Treatment was initiated at day 1 and was completed at day 13, for treatment schedule see page 62.

2.5 Discussion

The goal of this study was to determine the efficacy of the DARPin E69_LZ3_E01 on epidermal growth factor receptor (EGFR) inhibition in tumor xenografts in nude mice. This designed ankyrin repeat protein (DARPin) was previously shown to efficiently inhibit EGFR *in vitro*. It does so with greater potency than the monoclonal antibody cetuximab. Cetuximab is in clinical use and displays beneficial effects in combination with radiation therapy. We confirmed the inhibitory property of DARPin E69_LZ3_E01 *in vitro*, performed additional studies to determine its potential as radiosensitizer and finally tested its efficacy in a preclinical setting on tumor xenografts in nude mice, in combination with ionizing radiation. All results were compared to those obtained with the mAb cetuximab.

2.5.1 Inhibition of EGFR by DARPins or Cetuximab Does Not Fully Inhibit EGF-Induced Stimulation of the MAPK- and PI3K/Akt-Pathways

With regard to *in vitro* efficacy, inhibition of EGFR by DARPin E69_LZ3_E01 abrogated EGF-induced autophosphorylation of the receptor at Tyr1173 in the same way as cetuximab. DARPins even inhibited EGFR downstream signaling to a higher extent than cetuximab. EGF primarily acts through EGFR homodimers or EGFR/ErbB2 heterodimers, thus we expected a stronger inhibition of Akt and Erk1/2 phosphorylation in response to EGF stimulation in cetuximab- or DARPin-treated cells. However, also in DARPin-treated A431 cells, we still observed an increase of phosphorylated Erk1/2 and phosphorylated Akt after stimulation with EGF.

Notably, the reduction of EGF-stimulated phosphorylation of Erk1/2 correlated with the downregulation of EGFR, which both were strongly reduced in DARPin-treated cells. On the other hand, EGFR downregulation and reduced Erk phosphorylation were in general far less prominent in cetuximab-treated cells. The relationship between EGFR level and Erk phosphorylation became even more apparent, when cells were seeded at low density. Under these conditions, cetuximab was able to induce receptor endocytosis and down-regulation and displayed reduced Erk phosphorylation upon EGF stimulation as well. However, if the EGF receptors are not endocytosed and, though inhibited, remain at the plasma membrane, stimulation with EGF at a concentration as high as 100 ng/ml may overcome the inhibitory effect of the cetuximab or DARPins by competitive binding of the EGFR [219]. The so activated receptors might have been overly few to be detected by Western blot analysis. Moreover, we determined the level of activated EGFR by looking at only one single phosphorylation site; therefore, we might not have acquired the full picture on the extent of EGFR inhibition and activation,

respectively. Interestingly, Berger et al. observed complete inhibition of EGFR phosphorylation at Tyr1068 with the same concentration of cetuximab and were also puzzled to find phosphorylation of Erk to be induced upon stimulation with EGF [220]. They reached the same conclusion that an EGF concentration of 60 ng/ml might overcome EGFR inhibition by cetuximab and that the few activated EGF receptors may sufficiently induce phosphorylation of Erk. Furthermore, in response to strong activation of the EGFR downstream signaling, several feedback loops ensure a controlled negative regulation of the EGFR signaling [221, 222]. Such feedback loops act on multiple levels of the signaling cascade, including EGFR itself [223]. By means of computer-based simulation of the EGFR signaling, it was shown that at very low EGF concentration, signal amplification from MEK to Erk was several fold increased in comparison to stimulation with higher EGF concentrations [224].

For the EGF-stimulated activation of Akt in DARPin and cetuximab treated A431 cells, we did not observe a possible link between Akt phosphorylation and EGFR abundance. Phosphorylation of Akt, in comparison to phosphorylation of Erk, was less strongly reduced in EGF-stimulated cells in response to DARPins, and the results obtained were inconsistent across different experiments. However, inhibition of Akt might be even more important than inhibition of Erk in the context of radiosensitization (see below, section 2.5.7.1). Thus, it would be crucial to understand the mechanism of EGF-stimulated Akt phosphorylation in presence of inhibited EGFR activation.

A feedback loop emanating from Erk may provide an explanation for the minor reduction of Akt phosphorylation in response to EGFR inhibition. For example, EGF stimulation of cells treated with Erk inhibitor resulted in increased activation of the PI3K/Akt pathway as determined by phosphorylation of Akt at Ser473 [225, 226]. The underlying mechanism of this hyperactivation of the PI3K/Akt pathway is not well understood. Turke et al. suggested that inhibition of Erk reduced an inhibitory threonine phosphorylation in the conserved juxtamembrane domain of ErbB3, which then resulted in increased ErbB3 activity and thus increased downstream Akt phosphorylation [227]. Even though the status of Erk-inhibited cells may not exactly represent the status of EGFR-inhibited cells, it is conceivable, that inhibition of EGFR signaling and thus reducing the connected inhibitory feedback signals may increase signaling through other family members of the ErbB family.

2.5.2 Efficacy of DARPin E69_LZ3_E01 and Cetuximab Is Stronger in Cells Grown in Spheres than in Conventional Cell Culture

Most probably, due to the inability of cetuximab and DARPins to completely inhibit EGFR-mediated Erk activation, cetuximab and DARPins per se did not impose major

stress on adherent cells in culture. DARPins were more potent in the downregulation of the EGFR and in the inhibition of the EGFR downstream signaling and induced a slightly stronger growth inhibition than cetuximab. But overall, both treatment modalities, cetuximab and the anti-EGFR DARPin E69_LZ3_E01 induced a minor growth delay *in vitro*. Our results on cetuximab confirmed earlier data published by Kimura et al. [228].

Interestingly, growth inhibition was far more pronounced when cells were grown in 3D, in matrigel. While in 3D, treatment of A431 cells with either cetuximab or DARPins manifested in the formation of much smaller spheres, DARPin-treatment also reduced clonogenicity by about 40 percent. For the cetuximab-treated cells, the sphere number remained the same and only a size reduction was observed. However, it was difficult to discern by microscopy alone whether all spheres counted, met the colony size of 50 cells, that was defined as evidence for the clonogenic potential of a cell. Further analyses, such as staining for cell nuclei would allow for the quantification of cell numbers per sphere. Unfortunately, conventional staining methods cannot simply be applied to spheres and need to be established first. Another drawback of 3D cell culturing is that the drugs applied cannot be easily washed away. Thus, it is difficult to differentiate between the influence of the drug on clonogenicity and the influence of the drug on the proliferative activity of the cells. We did not remove cetuximab and DARPins in the classic clonogenic assay either, but there cell proliferation was not as strongly affected that it interfered with the evaluation of the colonies.

Cell cycle analysis by BrdU incorporation revealed that A431 cells cycle slower in matrigel, with 14 % of the cell population being in S phase as opposed to 30% in adherent cell culture. The S phase analysis of DARPin- and cetuximab-treated cells also corroborated the findings of increased growth inhibition in 3D cell culture: S phase population treated with cetuximab or DARPins in 2D was reduced by approximately 40% and 50%, respectively; in 3D cell culture, reduction comprised 57% and 72%, respectively. However, 3D experiments were only performed once and a more in-depth analysis will be required to verify these results.

2.5.3 Intracellular Crosslinking and Induction of Autophosphorylation, Unwanted Side Effects?

As a result of these 3D cell culture experiments, we realized that the application of the mAb cetuximab led to a strong intercellular crosslinking. Cetuximab-treated A431 cells harvested for FACS analyses or for immunofluorescence staining could not be separated merely by trypsinization, which we attributed to the antibody. Brown et al. reported that 45-60% of the serum IgG withstand digestion with trypsin in Tris-buffer at pH 8 for 8 hours, at a trypsin to substrate concentration of 1:23 [229]. Moreover, biotechnology

and life science companies such as Thermo Scientific list the method of trypsin-digest for the fragmentation of IgM antibodies but not for IgG antibodies, which indicates, that IgGs are not efficiently fragmented by trypsin. By incubation in glycine-HCl buffer at pH 2.5, which is often used for the dissociation of antibody-antigen complexes, we achieved the detachment of the cells. Thus, we assumed that aggregation of A431 cells treated with cetuximab was facilitated by antibody interaction.

In 2D cell culture, the effect of intercellular crosslinking by cetuximab was noted during FACS analysis. A substantial number of duplets or bigger cell aggregates were detectable in FACS samples that were treated with cetuximab, but not in control samples or DARPin-treated samples. Moreover, intercellular crosslinking by cetuximab seemed to impair endocytosis of the EGF receptor. Cetuximab-treated A431 cells displayed a strong EGFR staining at cell-cell interfaces, which was not present at free edges of the cell membrane where cells are not in contact with other cells. This may also explain the discrepancy in the extent of cetuximab-induced EGFR downregulation that we observed between different experiments. We hypothesize that reducing cell density and thus reducing intercellular crosslinking, may allow for a stronger downregulation of the EGFR. However, in solid tumors cells do not grow separated from each other. *In vitro* results should therefore be carefully revised with regard to effects obtained through EGFR downregulation (see below).

Theoretically, the tetravalent DARPin E69_LZ3_E01 could also bind EGF receptors located on two neighboring cells. However, DARPin-treated cells readily separated upon harvesting. On the other hand, trypsin may cleave DARPins and disguise the effect of intercellular crosslinking. Membranes at cell-cell interfaces of cells treated for 24 hours with DARPins also displayed an increased EGFR staining, which indicates that intercellular crosslinking may take place as well. However, the staining in DARPin-treated cells was less intense than in cetuximab-treated cells, correlating with the stronger downregulation of the EGFR by DARPins. More importantly, the binding of the EGFR by DARPin E69_LZ3_E01 resulted in phosphorylation of the receptor at Tyr1173. We hypothesize that the clustering of the EGFR by the tetravalent DARPin enables autophosphorylation. DARPin-induced phosphorylation reached its peak within the first hour of treatment and was then reduced over time, probably due to the internalization of the DARPin/EGFR-complexes. At the 24-hour time point after treatment with DARPins, phosphorylated EGFR still could be detected, but was exclusively localized at cell-cell interfaces. Possibly, phosphorylation was maintained through intercellularly linked receptors that could not be turned off by endocytosis.

Phosphorylation of the EGFR itself did not seem to be necessary for endocytosis and degradation, as previously demonstrated by others [230]. However, DARPin-induced

phosphorylation of the EGFR led to a short-term activation of the downstream signaling, determined by the increase in Erk phosphorylation.

Treatment with cetuximab also resulted in phosphorylation of the EGFR at Tyr1173, however to a much lower extent. Similar observations have been reported before. For instance, Mandic et al. observed increased EGFR phosphorylation also at Tyr1173, whereas Li et al reported a similar effect on the amino acid residue Tyr845 [231, 232]. Both studies were performed on squamous cell carcinoma cells of the head and neck. Raben et al. tested phosphorylation at Tyr1068, another important site in several non-small cell lung cancer cell lines with the same result [233]. Although cetuximab prevents internalization of EGFR to a greater extent than DARPins, the positioning of the receptor kinase domains of receptors clustered by DARPins must favor kinase activation to a higher degree than the clustering by cetuximab.

At this stage, we are not capable to discern the impact of the treatment-induced phosphorylation, which is considerably stronger for DARPins than for cetuximab, on cell proliferation or treatment efficacy.

2.5.4 Pharmacokinetics of DARPins in Comparison to the Pharmacokinetics of Therapeutic Antibodies

Our study demonstrates that DARPin E69_LZ3_E01 is highly efficient in EGFR inhibition and EGFR downregulation *in vitro*. However, its rapid clearance hampers systemic application. While pegylation of the DARPin monomers prolonged serum half-life to a yet insufficient 20 minutes, at the same time pegylation may reduce the binding capacity of the DARPin domains through steric hindrance. Practically all studies on pegylation of antibody fragments (Fab) reported such a loss of antigen binding affinity (reviewed in [234]), which may also be the case for DARPins that are of similar or even smaller size. We did not assess binding affinity directly, however, the reduced capacity of the pegylated DARPin to rescue EGF-induced growth inhibition in A431 cells indicates that binding affinity for EGFR and thereby receptor inhibition was altered by the pegylation status.

Further investigations on the pharmacokinetics and biodistribution of the pegylated DARPin E69_LZ3_E01 are required to understand how the drug distributes in the body, how it reaches its target, and how it is eliminated from the system. *In vivo*, a drug such as DARPin E69_LZ3_E01 that relies on sustained inhibition of the target to be effective is useless if eliminated overly rapidly from the system. As described above, the DARPin E69_LZ3_E01 forms dimers, resulting in a protein with four DARPin domains. However, a previous study on tumor targeting with DARPins demonstrated that the increase in size and affinity by additional DARPin domains did not lead to better tumor localization

[204]. Data obtained by Zahnd et al. suggests that the size of a divalent DARPin of approximately 30 kDa does not prevent the fast elimination of the drug by glomerular filtration. Unfortunately, the increase in size by a second DARPin domain probably reduced vascular extravasation and diffusion and led to an overall lower tumor uptake compared to a DARPin consisting of a single domain. Likewise and probably for the same reason, tumor accumulation of DARPins conjugated to polyethylene glycol (PEG) chains was slowed down, which was compensated though by an increased serum half-life. As a consequence, tumor localization of the DARPins was not greatly improved by pegylation [204]. Unfortunately, we were not able to detect the pegylated DARPin E69_LZ3_E01 in the histological sections of tumor xenografts harvested 6 hours after the second of 2 consequential treatments. Our pharmacokinetic analysis revealed that the pegylated DARPin was cleared from the blood within 2 hours. Thus, tumor-bound DARPins eventually must have been degraded. Experiments with e.g. radioactively labelled DARPins, as performed by Zahnd et al., could shed light on the amount of the pegylated DARPin E69_LZ3_E01 reaching the tumor.

As good as DARPin E69_LZ3_E01 performed in cell culture, the biggest obstacle for a successful application *in vivo* is a stable supply of DARPins to the tumor site. This would be required for a continuous inhibition of the EGFR. As opposed to DARPins, antibodies of the IgG1 isotype such as cetuximab display a long serum half-life, which is not only determined by the difference in size. Depending on the dose administered, saturation of the elimination pathways for antibodies leads to a serum half-life of more than 100 hours [235]. IgG antibodies are mainly eliminated through cellular uptake and consequential degradation [236]. Most therapeutic antibodies can be eliminated by non-specific interaction of the Fc region with Fc-receptors, which are expressed on virtually all cells.

Cellular uptake does not always lead to the degradation of the antibody; IgGs bound by FcRn receptors may be recycled and released into extracellular fluids. This process does not only significantly increase the serum half-life of IgGs, but also facilitates trans-membrane transport of the hydrophilic macromolecules [237, 238]. The role of cells expressing Fcγ receptors in the clearance of IgG antibodies, such phagocytotic cells or other cells of the immune system, is still unknown [239]. Clearance of monoclonal therapeutic antibodies often display a nonlinear clearance due to saturation of the target-mediated clearance pathways, which depend in the case of cetuximab on the abundance, distribution, internalization and turnover of the EGFR [239].

As it is the case for large-sized DARPins, accumulation at the tumor site is much slower for the large size 152-kDa mAb cetuximab than for small molecules. Lee and Tannok demonstrated in tumor xenografts that cetuximab and trastuzumab distributed in a time

and dose dependent manner [240]. After intravenous injection of cetuximab, the antibody was mostly found in the surrounding cell layers of the tumor vasculature at the early time points. The antibody concentration decreased with increasing distance from the blood vessel. 24 hours after application, the staining for cetuximab showed a more homogenous distribution. Interestingly, the antibodies did not reach hypoxic tumor areas. After injections with low antibody concentrations, the staining remained perivascular even after 24 hours, indicating that cetuximab is captured by target sites and only tumor saturating concentrations lead to a relatively uniform pattern with time. Again, these findings suggest that a long half-life of a macromolecular drug or its constant supply is essential for the treatment of solid tumors. For the treatment with the pegylated DARPin E69_LZ3_E01, our daily administration was clearly insufficient, taking the rapid clearance of the drug and the rapid reconstitution of the EGFR signaling into account.

2.5.5 Effect of Cetuximab Monotherapy on A431 Tumor Xenografts

The tumor growth delay induced by the cetuximab monotherapy, was equal if not even stronger than the delay caused by irradiation with three fractions of 8 Gy. The growth inhibitory effect of cetuximab we observed was stronger in 3D than in 2D and interestingly, results from 3D cell culture experiments better predicted the in vivo tumor growth response to cetuximab than the effect observed in adherent 2D cell culture. However, the mode of action of cetuximab on solid tumor growth is still debated.

We compared the outcome of our study on A431 tumor xenografts to similar studies, which were also performed on tumor xenografts derived from the same cell line, and also in nude mice. From these studies, we adopted the treatment schedule for the monotreatment with cetuximab. To increase the effect introduced by the combined treatment modality, we decided to apply three cycles of irradiation, combined with cetuximab or with DARPins. Due to the limited amount of DARPins at our disposal, the initially planned 7-day cycles of daily DARPin administration (30 mg/kg body weight) were shortened to cycles of five days. Cetuximab was administered once per cycle on the day prior to irradiation, or accordingly, 3 times every five days without irradiation, at a dose of 50 mg/kg of body weight, which corresponds to about 1.2 mg per mouse. In the earlier preclinical studies on combined treatment of A431 tumor xenografts, cetuximab was administered once prior to radiotherapy and then every three days or twice per week for 3, or 8 doses of 1 mg mAb cetuximab per mouse, respectively [241, 242]. Interestingly, in the study of Milas et al., A431 tumor xenografts treated with 3 x 1 mg cetuximab, the antibody alone did not lead to a significant growth delay. On the other hand, in the study we performed and in the study of Saleh et al., a clear growth delay was already

induced by the monotherapy with cetuximab. Even though the cetuximab regimen administered by Saleh et al. was longer than the treatment applied by Milas et al., the duration of the treatment probably does not account for the difference in the tumor response between the two studies. In our study, all tumors strongly responded already prior to the second injection, except for one specific cetuximab-insensitive tumor (see below).

Tumor size plays an essential role in the responsiveness of A431 tumor xenografts to the treatment with cetuximab [243, 244]. Fan et al. showed that tumors of a size of 150 mm^3 at the start of the treatment, responded with complete growth inhibition for the period of treatment (1 mg/mouse twice a week for 30 days). In tumors with an initial size of 200 mm^3, only a growth delay could be induced. Cetuximab treatment in tumors of the size above 400 mm^3 did not lead to any absolute growth delay in comparison to the control group. Clinical significance of a drug that only shows an effect in small tumor xenografts and none in well-established tumor xenografts is likely to be questionable. On the other hand, Saleh et al. reported sensitivity of A431 tumor xenografts as big as 400 mm^3 at treatment start. Thus, we conclude that additional factors other than size determine tumor response to cetuximab.

The mouse strains used by all three studies were athymic nude mice, but they were obtained from different breeders. Unless it is because of the acquisition of genomic or epigenetic changes in the A431 cell line over time, tumor-host cell interactions or tumor-host immune interactions may be at least partially responsible for the varying treatment response of A431 tumor xenografts to cetuximab. Notably, Milas et al. used 3 to 4 month old nude mice, while in our study as well as in Saleh's study much younger mice (4 and 6-8 weeks old) were used. Moreover, Milas et al. injected tumor cells intramuscularly, while in the other studies described above as well as in ours, the experiments were performed on subcutaneous tumor xenografts. But then again, tumor localization can also not be the only reason of the differential growth response observed, as a follow up study by Milas et al. was performed in subcutaneously injected tumor cells, affirming the minor growth delay previously observed in intramuscular tumor xenografts.

Reproduction of the various conditions in a single lab would be very laborious, but may reveal the factors influencing the efficacy of cetuximab. Eventually though, the potency of cetuximab will have to be evaluated in human patients. Nude mice lack mature T-cells and thus are used as model for human tumor xenografts, which otherwise would be rejected by the animal's immune system. However, the aspect of T-cell dependent ADCC cannot be studied in this host model. Additionally, NK cells are highly activated in nude mice [245], which also may yield misleading results. Nonetheless, the tumor

xenografts model with tumor growth delay as a readout still represent a good tool to study potential tumor responses to new treatment modalities.

2.5.6 Acquired Resistance to the EGFR-Inhibitor Cetuximab

Intriguingly, one of the ten A431 tumor xenografts treated with cetuximab was not sensitive to cetuximab. This tumor grew as fast as the control tumors, not even showing an initial response. This might be simply related to incorrect application of cetuximab in this specific mouse. However, that the intraperitoneal injection failed three times in the same mouse is rather unlikely. Nonetheless, we did not monitor blood levels of cetuximab after injection and therefore, this possibility cannot be completely disregarded. Another explanation for the nonresponsiveness of this tumor may be clonal expansion of an insensitive cell at an early stage of tumor xenograft formation. A431 tumor xenografts required up to five weeks to grow to the treatment size of 170 mm^3, with a long initial phase with no visible growth. During this initial phase, a cell might have gained a proliferative advantage by an activating mutation downstream of the EGFR or a mutation in a redundant pathway leading to growth advantage and insensitivity to EGFR-inhibition.

Yet a third hypothetical explanation may concern the immune response. Even though nude mice do not have a fully functional immune system, they still possess components of the innate immune system, capable of interacting with the Fc region of an antibody, such as macrophages, natural killer (NK) cells or the complement system. Trastuzumab (Herceptin) an antibody specific to Her2 has been shown to work partially if not predominantly through antibody-dependent cellular cytotoxicity (ADCC) [246, 247]. Rituzimab, the first therapeutic antibody approved by the U.S. Food and Drug Association (FDA), targeting the pan-B cell marker CD 20, induces its antitumor effect through ADCC as well as through activation of the complement system [248]. Cetuximab, of the same isotype (IgG1), was selected for clinical trials because it did not exhibit complement-dependent cytotoxicity (CDC) or trigger inflammatory responses, in contrast to another EGFR-targeting antibody of the IgG2a isotype [249, 250]. Moreover, cetuximab was initially thought not to trigger ADCC either. However, more recently published studies demonstrate that nevertheless, cetuximab-mediated ADCC contributes to its antitumoral mode of action [228, 251]. If ADCC was a major determinant of the *in vivo* effect of cetuximab, the nonresponsiveness of the single mouse might have been associated to a defective NK activity. However, in our study we did not perform additional in-depth studies on the mechanism of action of cetuximab and no experiment were performed to assess ADCC.

Interestingly, a second tumor xenograft, which initially responded with strong tumor regression, started to regrow after treatment completion at an accelerated pace, its growth rate even surpassed that of the control tumors. In this case, clonal selection of a more aggressive phenotype under treatment pressure may have occurred. Treatment-acquired resistance in cancer cells that do not harbor any of the compensatory mutations, such as activating K-Ras or EGFR kinase domain mutations, has been described previously [252]. In some cases, treatment resistance to cetuximab may be overcome by trastuzumab, an inhibitory anti-ErbB2 antibody, and likewise resistance to trastuzumab can be overcome by cetuximab [253]. Supporting the hypothesis that other members of the ErbB family may be involved in acquired resistance to cetuximab, Yonesaka et al. showed that several of the selected cetuximab-resistant HCC827 and GEO cell clones had acquired ErbB2 amplifications. Cetuximab did not substantially reduce Erk1/2 phosphorylation in these clones, unless the ErbB2 kinase inhibitor lapatinib was additionally administered, which restored cetuximab sensitivity [254]. Moreover, Yonesaka et al. identified a cetuximab-resistant A431 cell clone, which had not acquired increased expression of any member of the growth factor receptor family, but overexpressed heregulin at a 2.5 fold increased level. Depending on the isotype, heregulin binds to ErbB3 and ErbB4, or ErbB4 only. A431 cells express ErbB3, but not ErbB4. ErbB2 in turn functions as co-receptor for ErbB3 or ErbB4. These receptor heterodimers are activated by the binding of heregulin and may have a partially redundant function to EGFR. Furthermore, Yonesaka et al. demonstrated that administration of exogenous heregulin to otherwise cetuximab-sensitive cell lines led to a dose dependent increase in cetuximab-resistance and Erk1/2 phosphorylation.

Acquired resistance to the treatment with cetuximab may also occur through the acquisition of new mutations. In an *in vitro* selection process, such a point mutation occurred in the in the EGFR ectodomain (S492R), which then interfered with the binding of cetuximab, and thus conferred treatment resistance [147].

In a similar experimental setup, the expression of members of the Ras family proteins was observed to be substantially increased in resistant clones in comparison to the one in the parental cell line [255]. Ras proteins are not only members of growth factor signaling cascades but their activity also leads to an increased release of various growth factors, that stimulate more growth factor receptors than only EGFR (see section 2.5.7.1).

2.5.7 Combined Treatment of EGFR Inhibition with Cetuximab and Ionizing Radiation

Cetuximab in combination with ionizing radiation substantially increases tumor growth delay or tumor control in preclinical settings [256, 241, 257, 258]. In a clinical phase III trial on squamous carcinoma of the head and neck, the combined treatment modality of cetuximab with radiotherapy resulted in an increased 5-year survival in comparison to radiotherapy alone [137, 138]. In our preclinical study on A431 derived tumor xenografts, we also observed that the treatment response to the combined treatment with IR and cetuximab was superior to radiotherapy alone. However, we could not determine from our data, whether the application of cetuximab elicited a synergistic effect on tumor growth in combination with ionizing radiation. As discussed before, cetuximab alone already led to a significant tumor growth delay, which had not been observed in all of the previously performed preclinical studies (see above).

The reason for the beneficial treatment response when combining irradiation with cetuximab has not yet been fully elucidated. Likewise, no predictive marker for treatment indication could be identified so far. Different mechanisms have been proposed on how EGFR inhibition may contribute to radiosensitization. These include impaired DNA repair, reduced repopulation, and increased apoptosis, enhanced oxygenation in fractioned radiotherapy, and reduced angiogenesis.

2.5.7.1 Radiosensitization through Inhibition of EGFR Downstream Signaling

For clinical use, EGFR inhibition by cetuximab has been approved by the U.S. Food and Drug Association (FDA) for local combination with radiation therapy for the treatment of locally or regionally advanced squamous cell carcinoma of the head and neck (SCCHN). In epithelial-derived solid tumors such as SCCHN, EGFR expression is often upregulated, which has been shown to correlate with poor prognosis for the treatment with radiation [117, 259]. Liang et al. demonstrated increased radioresistance due to ectopically expressed EGF [260]. Moreover, radiation treatment led to ligand-independent autophosphorylation of the EGFR and activation of downstream signaling, which was proposed to lead to accelerated proliferation and enhanced cell survival [261–263]. Furthermore, a second, delayed phase of EGFR stimulation has been attributed to the release of TGFα or amphiregulin in a dose-dependent manner by ionizing radiation [264, 265].

EGFR signaling through the PI3K/Akt pathway increases cell survival after the exposure of cells to DNA damaging agents or IR. Thus, inhibition of either EGFR or the PI3K/Akt pathway leads to radiosensitization [266–268]. The EGFR downstream target Ras has also been linked to resistance to IR, although this radioresistance may not be

directly mediated by the activation of the Ras/MAPK/Erk signaling, but rather by also activating the PI3K/Akt pathway [267]. Cells with activating Ras-mutations show a substantially higher secretion of growth factors after irradiation than cells with wild type Ras [269, 270]. Activation of Akt in response to IR has been shown to depend on these secreted growth factors rather than on a direct stimulation by Ras signaling [271]. This implies that in combination with radiation, EGFR inhibition might have a radiosensitizing effect by inhibiting EGFR stimulation and subsequent Akt activation upon radiation-induced growth factor secretion.

In clinical trials, activating mutations in *KRAS* were determined to be an adverse prognostic marker for treatment of colorectal cancer with cetuximab [272–275]. On the other hand, the prognostic significance of the *KRAS* mutation status for the combination of cetuximab with radiochemotherapy is controversial. Some clinical studies observed a statistical significance for the K-ras status as predictive marker [276, 277]; whereas others report that in combination with radiochemotherapy, the prognostic significance was lost [278–280].

Caron et al. also demonstrated that the radioresistance conferred by activating mutations in *KRAS* or *HRAS* was mediated via the increased secretion of growth factors and the consequential stimulation of growth factor receptor signaling [281], which may provide a rationale for the use of cetuximab. However, the growth factors they found to be of importance, included heregulin, which, as mentioned above, was also suggested to mediate cetuximab-resistance via ErbB3/HER2 signaling in cancer cells [254]. Furthermore, in the *KRAS* mutated cell line A549, the siRNA knockdown of EGFR alone was also not sufficient to sensitize the cells to radiation. In contrast, the elimination of the mutated *KRAS* significantly reduced clonogenicity of A549 cells treated with IR [282]. Moreover, selected, cetuximab-resistant clones, which showed increased activity of Ras family proteins, not only displayed reduced sensitivity to radiation alone, but also were insensitive to EGFR-inhibition by cetuximab in the combined treatment with IR [255]. These findings corroborate that other ErbB family members compensate for the inhibited EGFR signaling.

Accordingly, we did not observe radiosensitization by cetuximab in the *KRAS* mutant cell line A549. In our hands, though, cetuximab did not sensitize the *KRAS* wild type cell line A431 either. Not even DARPins, which led to a much stronger inhibition of the EGFR than cetuximab and a strong reduction of clonogenicity in 3D cell culture, sensitized A431 cells with respect to ionizing radiation.

Former studies on radiosensitization by cetuximab *in vitro* are controversial, and no clear correlation to activating mutations downstream of the EGFR could be identified [283]. Mansoor et al. also did not observe any radiosensitization by cetuximab in the

squamous carcinoma cell line A431 *in vitro*, which reflects well our own results [242]. On the other hand, Dittmann et al. reported radiosensitization upon EGFR inhibition in the non-small cell lung cancer cell line A549 [215], which we could not confirm in our experiments.

Probably, accumulation of cetuximab-sensitive cells in the less radiosensitive G1 phase of the cell cycle may compensate for reduced EGFR signaling. Moreover, in A431 cells Akt phosphorylation at Ser473 was only moderately reduced. This might be sufficient to preserve cell viability after a radiation insult. As mentioned above, the PI3K/Akt pathway seems to play an important role in radioresistance and in response to other DNA damaging agents (reviewed in [284]).

2.5.7.2 Inhibition of EGFR May Lead to Impaired DNA Damage Repair

As mentioned above, stimulation of proliferation and survival pathways are only one aspect of how EGFR modulates cellular and tumor radiosensitivity. Other studies suggest that EGFR is also directly involved in the DNA damage repair process by facilitating nuclear import of DNA-dependent protein kinase (DNA-PK). DNA-PK is a key player in non-homologous end joining, which is a major DNA double-strand break repair pathway in mammalian cells [285, 286]. Huang et al. and Dittmann et al. observed that the cellular application of the mAb C225 (cetuximab) reduced the baseline levels of nuclear EGFR and nuclear DNA-PK, and inhibited their nuclear translocation in response to ionizing radiation [256, 215]. Similar results have been obtained by cellular application of the small molecular EGFR inhibitor gefitinib, which led to time- and dose-dependent relocalization of DNA-PKcs from the nucleus to the cytosol [287]. Interestingly, EGFR inhibition with the mAb C225 or gefitinib induced the molecular interaction of EGFR with DNA-PK. The amount of EGFR/DNA-PK complex formation that followed EGFR inhibition by cetuximab surpassed the amount of complex formation induced by ionizing radiation [215]. Similar results with regard to complex formation were observed upon EGFR inhibition by gefitinib that were compared to cells treated with DNA damaging agents such as etoposide and cisplatin [287]. However, EGFR/DNA-PK complex formation and DNA-PK redistribution is cell line dependent, e.g. the breast cancer cell line MDA-453 did not display any change in complex assembly upon treatment with gefitinib. It would be interesting to assess clonogenic survival of the various cell lines investigated in response to the combined treatment of gefitinib or cetuximab with ionizing radiation, along with additional mechanistic experiments, in order to determine the relevance of nuclear EGFR for radioresistance.

Shin et al. investigated treatment with cetuximab alone or in combination with IR, both *in vitro* and *in vivo* on tumor xenografts. In accordance with our own results, a stronger susceptibility to both treatment modalities was observed in the *in vivo* models than in classic *in vitro* cell culture [283]. Thus, EGFR inhibition may have additional effects on the level of the tumor microenvironment that outweigh the effect of direct cellular radiosensitization.

2.5.7.3 Radiosensitization through the Influence of EGFR Inhibition on VEGF Secretion and Tumor Vasculature

Tumor hypoxia and blood vessel formation (angiogenesis) are at constant interplay in a growing, proliferating tumor. In hypoxic cancer cells, the release of pro-angiogenic factors is triggered, which in turn stimulates endothelial cell proliferation and thus the formation of new blood vessels [288, 289]. There is increasing evidence that EGFR signaling in tumor cells plays a prominent role in increased secretion of pro-angiogenic factors (reviewed in [290]).

Already in 1993, it was discovered that blocking the vascular endothelial growth factor (VEGF) suppressed tumor growth *in vivo* [291]. Similarly, Perotte et al. showed that inhibition of EGFR by cetuximab down-regulated transcription and translation of angiogenic factors such as VEGF in tumor xenografts, along with reduced neovascularization [292]. Downregulation of VEGF and a twofold reduction of micro vessel density (MVD) has also been observed in cetuximab-treated A431 tumor xenografts [293].

Problematically, irradiation increases secretion of VEGF, which correlates with enhanced radioresistance [294, 295]. Interestingly, tumor xenografts, established from sublethally pre-irradiated A431 cells, showed a markedly higher MVD than control tumors. Concurrent treatment with cetuximab partially decreased the MVD of these tumors [263]. Cetuximab also decreased VEGF secretion in established SCCHN tumor xenografts treated with the anti-EGFR antibody alone or in combination with ionizing radiation [256]. Similar to the Pueyo study, a reduction in MVD could only be observed in response to the combined treatment modality and not in response to either treatment alone. These findings suggest that irradiation increases secretion of pro-angiogenic factors, which contribute, as part of the stress response, to the stabilization of tumor vasculature damaged by the irradiation insult.

Garcia-Barros et al. proposed that the tumor response to radiotherapy is mainly regulated by endothelial cell apoptosis [296]. In this study, tumor xenografts established in acid sphingomyelinase (ASMase) knockout mice, with very radioresistant endothelial cells, were refractory to single high doses of ionizing radiation. On the other hand, tumor xenografts established in ASMase wild type mice were much more sensitive.

However, the role of tumor vasculature in tumor radiosensitivity cannot be conclusively derived from the comparison of these two mouse models. Tumor development in ASMase-deficient mice was significantly slowed down. Additional endpoints such as tumor control and not only tumor growth delay will have to be addressed, in particular when the treatment response of tumors with different growth rates is compared.

Paradoxically, in some studies angiogenesis-inhibiting agents not only reduced the formation of new blood vessels but also led to a normalization of the vasculature, which resulted in increased tumor oxygenation [297–299]. Tumor vasculature often holds an increased number of vessels compared to normal tissue. However, tumor blood vessels are often tortuous, physically abnormal and functionally insufficient. The resulting inconsistent blood flow leads to an insufficient supply of oxygen and to acute or chronic hypoxia. It is generally accepted that hypoxic tumors or hypoxic tumor areas are more radioresistant. *In vitro*, it has been shown that clonogenic survival was increased in cells irradiated under hypoxic conditions [300–303, 46, 304]. Furthermore, clinical studies on tumor oxygenation and treatment response to radiotherapy indicate that hypoxia is an adverse prognostic factor for the patient outcome [305, 306]. Based on the current state of knowledge, it is proposed that the presence of oxygen leads to “fixation” of the DNA damage. Absence of oxygen therefore may protect hypoxic cells from obtaining more complex DNA lesions. Lee et al. investigated whether downregulation of VEGF increases radiosensitivity through enhanced oxygenation. He could show that treatment with anti-VEGF antibody led to enhanced oxygenation in tumor xenografts. However, these tumor cells were still sensitized to ionizing radiation even when the tumor blood supply was transiently blocked by clamping for the time of treatment [297]. These results suggest that tumor vascular normalization, including enhanced oxygenation, is not the only explanation for tumor radiosensitization upon downregulation of VEGF. Stabilization of tumor vasculature by VEGF may be equally, if not more important, in conferring radioresistance.

2.5.8 Conclusion

The role of EGFR signaling in radiation response is not fully understood yet. Results derived from independently performed preclinical studies are often contradictory, even when the same cell lines were used and experiments were performed under similar conditions. Furthermore, it is important to keep in mind that even tumor xenografts in nude mice are simplified models and may not encompass the complex tumor biology as a whole. Orthotopic and spontaneous tumor models represent more advanced systems, but at the same time, they are laborious in handling and expensive. Likewise, tumor control

and not tumor growth delay might represent the better endpoint, especially for these more advanced tumor models.

EGFR is a key player involved in diverse regulatory pathways, such as proliferation, cell survival, angiogenesis, and DNA repair. The complexity of the pathways affected by the inhibition of the EGFR receptor renders it difficult to assess the consequences of blocking the receptor. Moreover, cancer cells often show deregulation in one or several pathways downstream of the EGFR or rely on signaling through other family members of the ErbB tyrosine receptor family, which further complicates analysis. Eventually, examination of treatment responses in human patients, in combination with specific molecular testing is indispensable for shedding light on the heterogeneity of treatment responses to EGFR inhibitors.

3 MVP and Ionizing Radiation

3.1 Introduction

3.1.1 Vaults: An Overview of Structure and Composition

Vaults are large ribonucleoprotein particles with a hollow barrel-like structure [307] and a mass of 13 MD. Vault particles are found in many eukaryotic species from protozoans and slime molds to fish, amphibians, avians and mammals [308]. In mammals, they are composed of three proteins: the major vault protein (104 kDa), the vault poly (adenosine diphosphate-ribose) polymerase also known as VPARP (193 kDa), and telomerase-associated protein-1 TEP1 (240 kDa) [309–311]. Besides proteins, several small untranslated RNAs (vRNAs) have been found to associate with vaults. The major vault protein, as its name implies, constitutes the major part of the vault particle and accounts for more than 70% of the total mass of the complex. The molecular architecture of the rat liver vault complex was elucidated at high resolution using cryoelectron microscopy [312]. A vault consists of two dimers of half-vaults, which align at their waists to form together a barrel-like structure with the overall dimensions of 40 x 40 x 67 nm^3.

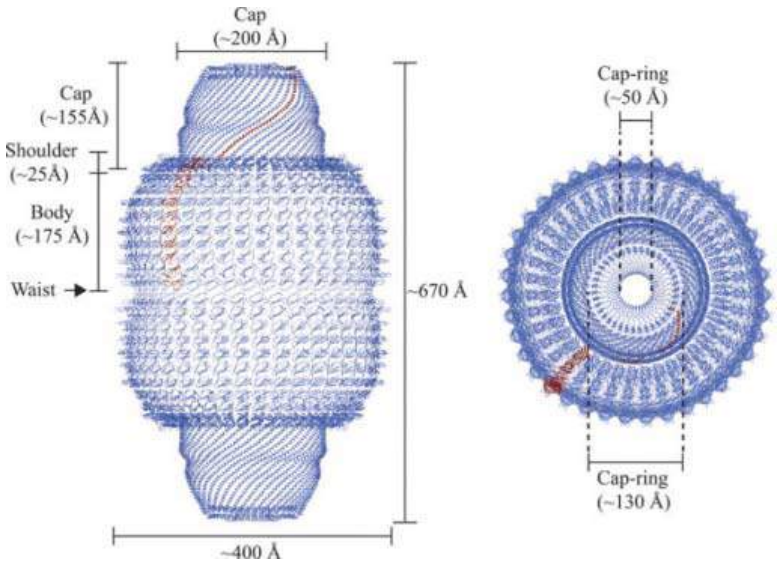

Figure 3.1 Side and top view of the vault structure. One of the 78 major vault proteins constituting the barrel is shown in maroon.

Each half-vault comprises 39 identical major vault proteins (MVP), the major self-assembling structural component (Figure 3.1). Other studies suggest a slightly bigger structure including 48 major proteins per half-vault [313]. Interestingly, vaults can open, the two halves can dissociate at their waists at acidic pH [314], and half vaults can be exchanged to form new vaults in live cells [315–317]. Based on these features and on

its large interior volume, which may encapsulate hundreds of proteins, recent interest in recombinant vaults derives from nanoparticle research trying to exploit vaults as drug delivery system.

The two minor vault proteins VPARP and TEP1 are not part of the shell-like structure and probably reside at the top center of the caps or within the vaults, as determined by cryoelectron microscopy difference mapping with recombinant proteins [318]. VPARP contains a catalytic site related to PARP1 and presumably ribosylates substrates, to which MVP and VPARP itself may belong to [310, 319]. TEP1 has been shown to interact with vRNAs, to be important for their stability and their localization in vaults [320]. Molecular composition of the vault has been roughly estimated as 78-96 MVPs, eight VPARPs, two TEP1s, and at least six copies of vRNA [321].

3.1.2 MVP the Major Component of Vaults

The lung resistance protein (LRP), which was later found to be the human homolog of MVP [309], originally was discovered in a multidrug resistant lung cancer cell line [322]. However, MVP expression is also present in normal tissue and varies among different cell types. Vaults are most numerous in macrophages [323, 324] and epithelial cells with secretory and excretory functions, as well as cells chronically exposed to xenobiotics such as bronchial cells and cells lining the intestine [322]. Most of the vaults are located in the cytoplasm, although a small fraction of these particles apparently has been found to localize at or near the nuclear membrane and possibly to associate with the nuclear pore complex [325].

The human gene encoding MVP has been located in chromosome 16 (16p11.2), approximately 27 cM proximal to the gene location of the multidrug resistance protein-1 (MRP1, also designated as ABCC1) [326]. However, although both ABCC1 and MVP map to the short arm of chromosome 16, they are rarely co-amplified and are normally not located within the same amplicon and can be switched on separately [326, 327]. Analysis of the human MVP gene revealed a TATA-less promoter, which also lacks other core-promoter elements. On the other hand, several putative transcription factor binding sites were recognized, including an inverted CCAAT box, a p53-binding site, and a GC box element [328]. An *in silico* analysis identified a putative STAT-binding site that strongly resembles an interferon-γ-activated site element (GAS), which preferentially binds to STAT1 homodimers [329]. Disruption of the STAT-binding site reduces basal MVP promoter activity, suggesting a role of JAK/STAT signals in the activation of MVP expression [330].

Comparison of the human MVP sequence to the murine MVP sequence revealed an identity of over 90 % [331]. Both the high degree of evolutionary conservation and the complex structure of vault particles, as well as its broad distribution in tissues, suggest an important function in cellular processes [308]. Although vaults have been proposed to play a role in drug resistance, nucleocytoplasmic transport, and regulation of signaling, a definitive function for MVP or vaults has yet to be assigned. Intriguingly MVP knockout mice did not display phenotypes supporting the above-mentioned roles of MVP that had been observed *in vitro* [332]. In fact, MVP-deficient mice develop normally without signs of deteriorating health. Even though the major component of the vault particle is absent in MVP knockout mice, and vault particles are no longer detected, the remaining components TEP1, VPARP, and vRNA might still interact and fulfill a functional role.

3.1.3 Interaction Partners and Putative Functions of Vaults

The detailed knowledge of the structure of MVP and vaults stands in contrast to the poor understanding of their endogenous function. Several observations, though, indicate that MVP may be directly involved in major cytoplasmic signal transduction cascades.

Interestingly, MVP contains various phosphorylation sites that are conserved among different species [333]. MVP is phosphorylated by protein kinase C (PKC) and casein kinase II (CKII) *in vitro*, but itself has no kinase activity [334]. Stimulation of cells with epidermal growth factor (EGF) induces phosphorylation of the tyrosine residues of MVP [335]. The phosphorylated MVP complexes with the SH2-domain-containing tyrosine phosphatase Shp-2. Shp-2 is important for activation of the downstream Ras-Raf-Mek-Erk cascade upon EGF stimulation [336]. MVP also interacts with the kinase Erk, presumably to fine-tune the activity of the Erk-downstream target Elk-1. Furthermore, the findings of another study indicate that EGF-induced tyrosine-phosphorylation also facilitates the interaction of MVP with the SH2-domain of Src-kinase in stomach cancer tissue and healthy stomach tissue. *In vitro*, Src-kinase triggered further phosphorylation of MVP and MVP, on the other hand, suppressed Src activity and reduced EGF-dependent Erk activation [337]. Likewise, MVP binds to the tumor suppressor phosphatase and tensin homolog deleted on chromosome 10 (PTEN); a significant quantity of endogenous PTEN associated with vault particles in HeLa cells, which may implicate that MVP interferes with the tumor suppressor function of PTEN, mediating increased drug resistance [338]. However, MVP-PTEN-interaction might be relevant only for the nuclear import of PTEN, thereby regulating the nuclear function of PTEN [339], see below). Eventually, identification of the specific growth factor-regulated MVP phosphorylation sites and the interaction partners of MVP in response to growth

factor stimulation is required to reveal how MVP/vaults are involved in these signal transduction cascades.

Similarly, a co-immunoprecipitation approach revealed the interaction between MVP and the photomorphogenic 1 ubiquitin ligase (COP1). Yi et al. suggest that MVP affects the capacity of COP1 to interact with the transcription factor Jun in a yet unknown manner. In unstressed cells, cytoplasmic MVP/vaults were shown to bind to and modify COP1, presumably via the other vault components. Following shuttling into the nucleus, COP1 binds to c-Jun with high affinity and suppresses the transcriptional activity of Jun by targeting it for degradation. UV-induced phosphorylation of MVP led to a simultaneous release of bound COP1 and turned off nuclear shuttling, thus permitting Jun to exert activation of the activator protein 1 (AP-1) transcription [340]. Jun, as a member of the AP-1 transcription factor dimer, plays a crucial role in regulation of cell proliferation of various cell types and was linked to neoplastic transformation (reviewed in [341]).

Negative regulation of downstream signaling has been identified also on the level of the hypoxia-inducible factor-1α (HIF-1α). Even though expression of both HIF-1α and MVP increase under hypoxia, the stability of HIF-1α protein was enhanced to higher extents in MVP-depleted cells. Direct complex formation of vaults with HIF-1α, PHDs and pVHL was demonstrated and suggests that MVP/vault might act as scaffold protein for ubiquitination and degradation of HIF1α [342], thereby affecting hypoxia-regulated expression of HIF-1α -dependent genes.

As mentioned above, the generation of MVP knockout mice did not reveal any indication for an essential role of MVP and vaults during embryogenesis. Under normal environmental conditions, there are also no signs of deregulated cellular processes in tissues of adult mice. Furthermore, both embryonic stem cells and bone marrow cells derived from MVP knockout mice display a similar sensitivity towards classic cytostatic agents as their wild type counterpart cells, and *in vivo*, normal tissue toxicity towards doxorubicin remains unchanged in the MVP-deficient mice. Interestingly, though unexpected, MVP and vaults may play a role in the innate immune response and contribute to the uptake and clearance of lung pathogens such as *Pseudomonas aeruginosa* via lipid rafts in lung epithelial cells. Internalization of total bacterial load is 55 % lower in MVP knockout mice, leading to an approximately three-fold increase in mortality [343]. On the other hand, *L. monocytogenes* the bacterium causing lysteriosis, seems to make use of MVP/vaults in order to evade intracellular autophagy. *L. monocytogenes* expresses the surface receptor InlK, a member of the internalin family, which interacts with MVP and thus seems to be protected from recognition by the autophagy machinery in macrophages and in HeLa cells [344]. However, Dortet et al. did not observe that MVP

was involved in the internalization process of *L. monocytogenes*, as in the case of *Pseudomonas aeruginosa*. On the other hand, recently, it has been shown that MVP is involved in cell physiological internalization processes as well. In macrophages, MVP is involved in the ligand-stimulated internalization process of class A scavenger receptors (SR-A). Stimulation of SR-A activates TNF-α synthesis and secretion, leading to autocrine induction of apoptosis in macrophages, which is reduced in MVP-depleted macrophages [345]. The authors suggest that patients with inflammation driven atherosclerosis may benefit from a reduced cytokine release by inhibition of the MVP/SR-A interaction. TNF-α antagonists have been introduced with great success for the treatment of various inflammatory diseases and are currently also in phase I and II clinical trials, in patients with advanced cancer [346].

MVP expression is enhanced by interferon γ through the JAK/STAT pathway providing further evidence that MVP is involved inflammatory processes [330]. Moreover, various other observations indicate that MVP participates in immunological responses as well (Reviewed in [347]). *In vitro*, human dendritic cell maturation was accompanied by a strong upregulation of vault expression, and inhibition of MVP by an antibody mixture impaired expression of maturation markers in monocyte derived dendritic cells [348]. However, despite these findings, no differences in dendritic cell migration and antigen presentation and T-cell responses were observed in the MVP knockout mouse model [349], which may possibly be due to interspecies differences.

Other vault components like vRNAs are hypothesized to be play a role in immune responses too. In response to infection with the Epstein-Barr virus a strong induction of “vault”-RNA expression has been reported [350, 351], which led to the suggestion that they might be involved in antiviral defense.

Finally, the hollow structure, the rapid movements, the distinct subcellular localization (as for example at the nuclear membrane), and the *in vitro* and clinical correlations with drug resistance in several types of human cancers led to the hypothesis that vaults might represent rather promiscuous transport vehicles [352–354].

3.1.4 Drug Resistance: the Best Known Role of MVP

Several proteins have been linked to multidrug resistance (MDR), such as the ABC-drug transporter p-Glycoprotein (P-gp, also designated as ABCB1), members of the multidrug resistant protein family (ABCC1, ABCC2, and ABCC3), the human breast cancer resistance protein (BCRP) and the lung-resistance protein (LRP) [330, 355, 356]. The LRP was initially discovered due to its high expression level in a multidrug-resistant but ABCB1-negative lung cancer cell line [322] and has been identified in

1995 to be the human major vault protein [309]. Thereby, a first link between the MDR and vaults was established. Since then, MVP/vaults have been investigated in numerous studies as predictive marker in various cancer types with regard to treatment response and patient outcome (see section 3.1.6).

MVP has been detected in 78 % of 61 human cancer cell lines, and its expression levels correlate with resistance against a variety of MDR-related but also MDR-unrelated drugs, indicating that the mechanism by which MVP confers drug resistance is different from classical MDR proteins [357, 358]. Moreover, upregulation of MVP was determined in multiple human cancer cell lines upon treatment with anticancer agents, including anthracyclins, etoposide and cisplatin, further supporting a putative link between treatment sensitivity and cellular stress adaptation to cytotoxic agent [322, 359–364]. Overexpression of MVP was also frequently observed at the early steps of resistance selection [365–368]. Multiple preclinical studies corroborated the link between MDR and the MVP expression level in cancer cells, despite some contradictory studies [369] and the fact that the MVP knockout mouse model did not show enhanced hypersensitivity to cytostatics [332]. Even though in MVP-deficient mice an increase of P-gp, MRP1 (ABCC1), and BCRP activity was not observed, unknown mechanisms of MDR may be responsible for the lack of consequences of MVP knockdown with regard to drug sensitivity. In a yet unknown manner, cancer cells may be more sensitive to disruption of functional MVP than normal cells. To investigate the role of vaults in cancer cells with regard to MDR, changes in drug sensitivity were assessed upon ectopic expression of MVP. Siva et al. reported that expression of the major vault protein, which was accompanied by a concomitant upregulation of TEP1 and VPARP, did not confer drug resistance in the human ovarian carcinoma cell line A2780 [370]. On the other hand, Hu et al. found that the ectopic expression of MVP in the gastric cell line GC7901 induced resistance to vincristine and adriamycin [371]. In the same study, a daughter cell line of GC7901 with a selected MDR phenotype was transfected with siRNA against MVP, which led to an increased drug sensitivity. In SW620 colon cancer cells, MVP expression along with expression of MRP and P-gp could be induced by sodium-butyrate, which resulted in increased resistance to several cytotoxic drugs. Interestingly, inhibition of MVP by two MVP-specific ribozymes abolished the sodium-butyrate-induced MDR phenotype [364, 372]. Mechanistically, Kitazono et al. observed a nuclear exclusion and increased accumulation of DNA-damaging agents in the cytoplasm of sodium-butyrate-treated cells. Similar observations had been made before in multi-drug resistant cell lines and was determined to be P-gp independent [373]. However not all drugs to which sodium-butyrate confers resistance to, unfold their activity in the cell nucleus, indicating that increased nuclear efflux as observed for doxorubicin may not be the only function of vaults in drug resistance. Vaults may also

mediate MDR by the transport of drugs away from their subcellular targets, e.g. by the sequestration into exocytotic vesicles, a mechanism that was previously shown to mediate drug resistance [374]. Hervelsen et al. observed not only reduced sequestration of doxorubicin in UMUC-3 bladder tumor cells upon MVP knockdown, but also noted a disarrangement of the lysosomal compartments [375].

Interestingly, human vRNAs produce several small RNAs (svRNAs) by mechanisms different from those in the canonical microRNA (miRNA) pathway. One of the svRNAs downregulates CYP3A4, a key enzyme in drug metabolism, disclosing a new link between vaults and drug resistance [376]. With regard to cancer, the relevance of these findings yet needs to be clarified. CYP3A4 is predominantly expressed in liver tissue, where MVP expression is low. Moreover, CYP3A4 is also expressed in cancer tissue, where in contrast, it was shown to correlate with reduced overall survival [377].

3.1.5 A Novel Role for MVP: Implications in Radiotherapy

In recent years, MVP and vaults have not only been linked to drug-resistance, but also to DNA-damage response and DNA-damage-repair. MVP transcription and protein level is increased in response to various DNA-damaging agents, including ionizing radiation (IR) [378]. Interestingly, VPARP- and to lesser extent TEP-1-deficient mice have an increased incidence of carcinogen-induced colon tumors [379]. These findings indicate that vaults may be involved in maintaining genomic stability and thus may play a role in DNA repair processes.

As described in the “General introduction”, the high cytotoxicity of IR is mainly based on the induction of DNA double-strand breaks (DSB) via the generation of reactive oxygen species. DSBs can be repaired by the two major DSB repair pathways: the homologous recombination (HR) and the non-homologous end joining (NHEJ). The fact that error-free repair by HR depends on the presence of an intact sister chromatid restricts this pathway to the S and G2 phase of the cell cycle. This is in contrast to error-prone repair by NHEJ, which can function throughout the cell cycle and therefore is thought to be the predominant DSB repair pathway in mammalian cells. Tumors typically show an increased S and G2 phase cell population. Thus, HR represents the more interesting target to specifically sensitize tumor cells to DNA damaging agents, leading to an enhanced therapeutic window.

MVP and vaults have been linked to both DSB-repair pathways. With regard to NHEJ, an inverse correlation between high MVP and low Ku70/80 expression levels as well as low pro-apoptotic Bax protein levels was identified in a cohort of 160 patients with localized cervix carcinoma [380]. Ku70 and Ku80 are key proteins in NHEJ, and also

play a regulatory role in apoptosis through the interaction with Bax/Bcl-2 [381, 382]. Newly synthesized Bax is inhibited from inducing apoptosis in two ways: Ubiquitination labels Bax for proteasomal degradation and secondly, Ku70 has been shown by Amsel et al. to sequester Bax away from the mitochondria. Interestingly, Ku70 was shown to bind and either directly deubiquitinate Bax or to mediate deubiquitination of bound Bax. Thus, the binding of Bax by Ku70 prevents Bax from being degraded, but also from promoting cell death. In response to apoptotic stimuli, Ku70 releases Bax, which then acts as mediator of apoptosis [381]. Low expression levels of Ku70 might therefore result in low expression levels of Bax, which indeed has been observed in the study performed by Lloret et al. [380]. In this study, high MVP expression levels were associated with low Ku70/80 protein levels (see above), and additionally correlated with upregulated Bcl-2, altered p53 expression, and increased proliferation. Despite the lack of mechanistic insights, these data suggest that if overexpression of MVP is the cause of reduced Ku70 expression, MVP and vaults might promote carcinogenesis by suppression of NHEJ and apoptosis, leading to increased genomic instability. Eventually, molecular dissection of the key signal transduction cascades that lead to reduced NHEJ-activity in MVP-overexpressing cells will elucidate the association between MVP/vaults, NHEJ and a deregulated apoptotic threshold. A relationship between decreased apoptosis and upregulated MVP-expression has also been described by another study. Ryu et al. observed that cellular MVP levels increased with age, both *in vitro* and *in vivo*. This age-related upregulation of MVP increased apoptotic resistance of senescent human diploid fibroblasts by interfering with c-Jun-mediated repression of Bcl-2 [383]. Thus, MVP was suggested to play a role in regulating cellular signaling and survival, and might be considered as therapeutic target for modulating apoptosis resistance of cancer cells [384].

A novel link between the intracellular level of MVP and homologous recombination (HR) has been considered based on yet unpublished data from our own laboratory. We observed that MVP-depleted tumor cells were more radiosensitive than their wild type cognate cells, possibly due to direct interference with homologous recombination. In comparison to control cells, Rad51-foci were strongly reduced in irradiated, MVP-depleted cells and thus vaults might play a role in the coordination of HR complex formation at the site of DSBs, or they might be involved in the maintenance of Rad51 protein levels. MVP mediates nuclear import of PTEN and regulates its nuclear function [338, 385]. Supporting the hypothesis that MVP may interfere with DNA repair via regulation of PTEN nuclear transport, Shen at al. showed that PTEN was necessary and sufficient for the induction of Rad51 expression levels and DSB-repair [386]. However, PTEN is associated with the function as tumor suppressor and is often lost in tumor cells. The loss of PTEN may actually contribute to tumor progression through the

deregulation of the cell cycle regulator kinase 1 (CHK1) and coherent loss of the G2/M cell cycle checkpoint, leading to increased genetic instability [387]. Interestingly, loss of PTEN in tumor cells with the concomitant reduction in homologous recombination and the deregulated G2/M checkpoint can be exploited by the combination with inhibition of PARP, creating a situation of synthetic lethality [388, 389]. Since MVP and vaults might be involved in nuclear import of PTEN and homologous recombination, it will be of interest to determine whether the MVP expression level may also affect genomic instability and sensitivity to PARP-inhibition.

Despite the fact that we have so far only limited insights into the mechanisms how MVP and vaults interact with the two DNA double-strand break repair machineries, there are indications that MVP and vaults may co-regulate correct DNA repair of spontaneous and treatment-induced double-strand breaks. Due to the barrel-like structure, vaults may act as carriers, not only for toxic agents, but also for the coordinated intracellular transport of DNA repair-related proteins and thereby act as scaffold proteins or shuttling vectors. Otherwise, the vault-associated proteins VPARP or TEP-1 may play a so far not identified role in DNA repair, they may display as part of intact vaults only.

As indicated above, *in vitro* studies revealed that gene expression levels of MDR-related proteins such as P-gp and MVP increased after fractionated irradiation [390]. Furthermore, it is well known that radiation treatment can induce resistance to various cytotoxic drugs [391], although the molecular mechanisms are not fully understood. Bottke et al. observed that the radiation-induced upregulation of MDR-related proteins correlated with increased resistance to cisplatin, doxorubicin and bendamustine [390]. These findings suggest that MVP may not only play a role in radio-resistance by supporting HR, but may also confer radiation-induced chemoresistance.

3.1.6 MVP and Tumor Malignancies: Vaults as a Predictive / Prognostic Marker

Numerous studies were performed to evaluate the expression status of MVP in human malignancies as a predictive and prognostic marker with regard to chemotherapy response and patient prognosis. However, these studies mainly focused on hematological malignancies and the lack of clear guidelines for analyses of prognostic markers hamper the validity of such studies. The results are influenced by factors such as the MVP detection assay performed, the number of patients included, or the type of statistical analysis performed (univariate vs. multivariate analysis). The quality of MVP as a prognostic or predictive marker in this type of malignancy is still questionable, and standardized detection methods are needed. Nevertheless, a direct association between MVP expression and therapy resistance and prognosis in patients suffering from acute myeloid leukemia was identified [392–395]. An inverse correlation between MVP

expression and patient prognosis, therapy response, and survival rate has been reported in acute lymphoblastic leukemia patients [396–398] and similar results have been described for adult T-cell leukemia [399, 400] and multiple myeloma [392, 401, 402].

On the other hand, relatively few studies have addressed the role of MVP in solid tumors, with overall contradictory findings (see Table 3.1). For example, MVP was evaluated as prognostic marker in ovarian carcinoma, resulting in positive [403, 404] and negative [405, 406] associations reported. Results regarding breast cancer [407, 408], non-small cell lung cancer [409, 410], or different types of sarcomas are inconclusive [411, 412]. On the other hand, MVP has been established as a reliable marker for the response to chemotherapy in bladder cancer patients [413], in melanoma [414] and for determining the aggressive phenotype of testicular germ-cell tumors [415] and glioblastoma [416]. Most likely, concomitant operation of several drug resistance mechanisms may be necessary to cause the phenotype of MDR [362]. Izquierdo et al. refer to the frequent occurrence of co-expression of MVP and MRP1, which associates with increased drug resistance levels in MDR-selected tumor cells [357].

Table 3.1 Overview on clinical studies investigating the association between MVP and therapy response and survival.

Author	Patients (n)	Tumor	Response	DFS	OS
Izquierdo et al., 1995 [327]	57	Ovarian cancer	Yes	Yes	Yes
Schadendorf et al., 1995 [414]	71	Melanoma	Yes		
Ramani et al.,1995 [418]	21	Neuroblastoma			No
Dingemans et al., 1996 [419]	36	NSCLC	No		No
Linn et al., 1997 [420]	70	Breast cancer	No		
Uozaki et al., 1997 [421]	60	Osteosarcoma	Yes		Yes
Arts et al., 1999 [405]	115	Ovarian cancer	No	No	No
Pohl et al., 1999 [422]	99	Breast cancer	No	No	No
Volm et al., 2000 [423]	87	NSCLC	Yes		No
Goff et al., 2001 [424]	29	Ovarian cancer	No		
Pohl et al., 2001 [425]	68	Colorrecto	No		
Diestra et al., 2003 [413]	83	Bladder cancer	Yes		
Harada et al., 2003 [426]	57	NSCLC	Yes		
Silva et al., 2007 [417]	78	SCCHN	Yes		Yes

DFS, disease-free survival; OS, overall survival; NXCLC, non-small cell lung cancer; SCCHN, squamous cell carcinoma of the head and neck.

With regard to a putative role of MVP in radiation resistance, MVP expression negatively associates with local disease free survival and cancer-specific survival in a series of patients suffering from squamous cell carcinoma of the oropharynx, who received primary radiotherapy with curative intent (in univariate and multivariate analyses) [417]. In this study, elevated MVP expression also seems to be associated with a radioresistant subset of patients, proposing MVP as a novel useful predictive marker associated with Radiation Therapy [417]. The link between MVP and radioresistance and the underlying mechanisms are not well defined today, but the above-cited role of MVP in DNA repair and in regulation of the apoptotic threshold may be part of it. The complexity of MVP as a predictive and/or prognostic marker is also illustrated by a study on cervical cancer patients who received combined radiochemotherapy [427]. In a subcohort of the patients with clinical complete response, increased MVP and IGF-1R expression were observed to strongly associated with reduced long-term local control. High MVP expression correlates with high IGF-1R expression, and together are associated with chemo-and radioresistance in localized cervical carcinoma and oral cavity squamous cell carcinoma [428, 429]. Probably, both proteins are required to confer chemoradioresistance, and cervical carcinoma patients with low levels of MVP and IGF-1R expression had excellent survival rates [427]. However, this result may not be definitive since the number of patients included in this study was rather low, with 23 patients in the low MVP/IGF-1R and 27 patient in the high MVP/IGF-1R group. It is still unclear how and if MVP and IGF-1R expression is interconnected. In the previously study mentioned study on cervical carcinomas, a strong correlation suggests an interdependency, whereas in the study on oral cavity squamous cell carcinomas, correlation between MVP and IGF-1R was less strong and their predictive power was restricted to cancers of stage III and IV.

As illustrated by these studies and the studies mentioned in the previous sections, we are still far away to have identified a mechanistic link between MVP expression level and treatment response. It is still a matter of debate to which extent vaults are involved in chemo- and radioresistance. It will be important to study the regulatory mechanism for high MVP expression in cancer cells and to evaluate in more detail whether and how cancer cells depend on MVP expression for treatment resistance.

3.2 Background and Aim of the Study

3.2.1 Background of the Study

As mentioned in section 3.1.5, previous experiments performed in our group indicated a novel link between MVP and radiosensitization by interfering with homologous recombination [430].

A dose-dependent increase of MVP was observed upon irradiation in the non-small cell lung carcinoma cell line A549 and in the human colon cancer cell line HCT116. Depletion of MVP lead to radiosensitization in both cell lines. However, this effect was lost in HCT116 with a p53-negative or PTEN-negative background.

Interestingly, formation of Rad51-foci were strongly reduced upon depletion of MVP, whereas RPA-foci formation did not seem to be affected. Preliminary data indicated that MVP might interact with the BRCA2/Rad51 complex. These findings suggest that MVP may be involved in homologous recombination by either direct interaction with HR-proteins or via PTEN-dependent Rad51 transcription. The link of MVP to the nuclear transport of PTEN would explain the absence of radiosensitization in PTEN-negative cells.

3.2.2 Aim of the Study

In this continuative study, we aimed to corroborate the findings above and to further elucidate the precise role of MVP in homologous recombination and Rad51-foci formation, respectively. It was planned to extend the investigation of the role of MVP in DNA repair and radiosensitization to normal cells, and finally to correlate MVP expression in tumor biopsies of squamous cell carcinoma of the head and neck with treatment outcome concerning radiotherapy.

To address the role of MVP in HR we planned to determine the HR-capacity in MVP-depleted cells [431] and to assess the interaction of BRCA2 with MVP by immunoprecipitation of BRCA2 and vice versa. Further, we planned to dissect the kinetics of DNA repair and specifically of HR in MVP-depleted cells by immunofluorescence staining of γH2AX as indicator for DNA damage, and RPA- and Rad51-foci formation as readout for homologous recombination. The study was to be extended to various cancer cell lines with regard to their genetic background, e.g. PTEN-and p53-status. However, the unexpected MVP knockdown phenotype we were confronted with took us by surprise and indicated the necessity for validation of the siRNA approach.

3.3 Material and Methods

3.3.1 Index of Methods Described in the First Part of the Thesis

3.3.2 Cell Culture and Maintenance

All cells were kept at 37°C in 5% carbon dioxide in a humidified incubator.

Cell Line	Description	Culture Conditions
A549 (ATCC No CCL-185) Gift from S. B. Horwitz	Non-small cell lung cancer cell	RPMI medium supplemented with 10% (v/v) fetal bovine serum (FBS), 1% (v/v) L-glutamine and 1% (v/v) Penicillin-Streptomycin (P/S)
SW480 (ATCC No CCL-228)	Human colon carcinoma cells	
SW620 (from the same patient as SW480) (ATCC No CCL-227)	Human colon carcinoma cells from lymph node metastasis	
CAPAN-1 Obtained from Cell Line Service, Eppenheim, DE	Human pancreatic ductal adenocarcinoma, derived from liver metastasis	
BxPC-3 H. Friess, Munich, DE	Human pancreatic ductal adenocarcinoma	
MDA-MB-231 Received from P. Rhode-mann, DE	Human breast carcinoma cell line	
MEF MVP wt MEF MVP-/- gift of E. Wiemer, Rotterdam, NL	Mouse embryonic fibro-blasts derived from MVP wild type and knockout mice	

Cell Line	Description	Culture Conditions
HCT116 (ATCC No CCL-247) Gift from Bert Vogelstein	Human colon carcinoma cells	McCoy medium supplemented with 10% (v/v) FBS and 1% (v/v) P/S
HCT116 V163 PTEN-/- HCT116 V166 PTEN+/+	HCT116 PTEN knock out cell line mother cell line of V163	
U2OS Kindly provided by A. Sartori	Human osteosarcoma cell line	DMEM medium supplemented with 10% (v/v) FBS, 1% (v/v) L-glutamine, 1 mM Sodium Pyruvate, and 1% (v/v) P/S
MEF p53+/+ MEF p53-/- [432]	E1A/Ras transformed mouse embryonic fibro-blasts	

3.3.3 Reagents, Antibodies and siRNA sequences

Reagents	Manufacturer
Agarose A9539	Sigma
Alamar Blue	Biosource Int.
Caspase Inhibitor IV #219011	Calbiochem
Cell culture medium and supplements, if not stated otherwise	Gibco, Invitrogen
EDTA solution E7889	Sigma
ECL Prime WB Detection Reagent RPN2232	GE Healthcare
GelRed™ Nucleic Acid Gel Stain #4100	Biotium
Lipofectamine 2000	Invitrogen
Lipofectamine RNAi MAX	Invitrogen
Caspase Inhibitor Z-VAD-FMK #G7231	Promega
ProLong® Gold	Invitrogen
Triton X-100	Sigma

Antibodies	Manufacturer	Ref. number
Anti β-Actin Ab from mouse	Sigma	A5441
Anti BRCA2 Ab, from mouse	Calbiochem	OP05
Anti BRCA2 Ab, from rabbit, Agarose-immobilized	Novus Biologicals	NB600-417
Anti DYKDDDDK Tag Ab, Fluor®488-linked, from rabbit	Cell Signaling	#5407
Anti pH2AX (Ser139) Ab, FITC labeled, from mouse	Millipore	#05-636
Anti MVP, from rabbit	Sigma	HPA002321
Anti MVP, from mouse	Labvision	MS664PABX
Anti p53 (Ser15) Ab, from rabbit	Cell Signaling	#9284
Anti PARP p85 Fragment Ab, from rabbit	Promega	G734A
Anti-Rad51 Ab, from mouse	Santa Cruz	sc-8349

For secondary Antibodies, see page 34.

siRNA	Sequence	
siMVP#1	GCACCUACAUGCUGACCCA	unknown
siMVP#2	ATCATTCGCACTGCTGTCTT	[375]
siMVP#3	GGGGAAGAAUGGCUGGUCA	[433] siMVP-586
siMVPmurine	CGUGUGAUUGGAAGCACCUAC	siMVP#1 adapted
siMVP_A	CUGACCCAGGACGAAGUCCUG	Ambion
siMVP_B	GAGAGAAGCGAGCCCGCGUGG	Ambion
siMVP_C	UCGCAAGGAACUUUUGGAGCU	Ambion
siLuc	CGTACGCGGAATACTTCGA	Dharmacon
Scramble_A	GAACACCCGACGCGGAGUCUU	derived from siMVP_A
Scramble_B	GGCAUGCUGAUACCGAGUUAU	derived from siMVP_B
sip53	siGenome SMART pool	Dharmacon

3.3.4 Transfection of Cells with siRNA

All cells were transfected according to the reverse transfection protocol for the Lipofectamine® RNAiMAX Transfection Reagent (Invitrogen). Lipofectamine (30 µl) in Optimem to a total of 1 ml was incubated for 5 minutes and siRNA (3.75 µl of 40 µM stock solution) was diluted in 1 ml Optimem. Lipofectamine and siRNA mixture were combined, incubated for another 15 minutes and then transferred to a 10 cm dish. Meanwhile cell suspension of a concentration of 50'000 cells/ml was prepared in antibiotics-free cell culture medium. 10 ml cell suspension were added to the cell culture dish on top of the transfection mixture. 6 hours after transfection, medium was replaced with antibiotics-free cell culture medium.

Maximum downregulation of MVP was observed around 72 hours after transfection. Around 96 hours after siRNA transfection MVP started to increase.

3.3.5 Proliferation Assay

For A549 cells treated with siRNA, assessment of the cell number by Alamar Blue assay was not feasible, because the treatment with siMVP seemed influenced the mitochondrial metabolic activity. Therefore, proliferation was assessed by cell count. The cells were seeded in 6-well plates, transfecting the cells with siRNA at the same time according to the protocol above (dividing the amount for a 10 cm dish by 5). For each condition and time point, a one well was prepared. For the assessment of the cell number with the NucleoCounter® NC-100™ (Chemometec), the cells were trypsinized, spun and resuspended in an appropriate amount of medium. The measurement was performed according to the manufacturer's specifications.

3.3.6 Clonogenic Survival Assay of MVP-Depleted Cells

For the performance of the clonogenic assay, see page 36. With regard to MVP downregulation, cells were seeded 48 hours after siRNA transfection. Irradiation was then performed at 72 hours after transfection, where MVP expression was shown to be lowest.

3.3.7 Immunofluorescence Analysis of γH2AX- and Rad51-Foci

Immunofluorescence staining was performed according to the protocol on page 37. Cells were labeled simultaneously for γH2AX and Rad51 and the DNA was counterstained with Dapi. For analysis by fluorescence microscopy, the nucleus of each cell or the nuclei of several cells at a time were captured with z-stack image sequences. Using the free LEICA software LAS AF Light, the z-series was viewed in the maximum

projection view, which merges the stack into a single image. The number of foci per cell was then counted by eye. About 75 cells were evaluated for each condition and time point.

3.3.8 Immunoprecipitation of BRCA2

1 million cells were seeded in a 10 cm cell culture dish and irradiated the following day with a dose of 5 Gy. 5 hours after irradiation, cells were washed with PBS and lysed on ice with 600 µl non-denaturing lysis buffer (20 mM Tris pH8, 137 mM NaCl, 10 % glycerol, 1 % (v/v) Nonidet P-40, 2 mM EDTA, just added before use: 50 µg/ml PMSF and aprotinin, leupeptin, pepstatin1 µg/ml each). After 10 min incubation on ice, the cells were scraped, transferred to an Eppendorf tube centrifuged in a precooled centrifuge (4°C) for 20 minutes at 20'000 g. Then the supernatant was transferred to a clean Eppendorf tube and protein concentration was determined by NanoDrop. 50 µl lysate were set aside for SDS page. 80 µl slurry of agarose-immobilized BRCA2 Ab was added and incubated overnight at 4 °C under constant agitation. Then, the tube was centrifuged tube at 2'500 g for 1 min. The supernatant was carefully removed, leaving 80 µl in the tube, not to disturb the beads. The beads are resuspended in 1000 µl lysis buffer, left on a shaker on ice for 3 min. This washing step was repeated four more times. After the last centrifugation step, the supernatant was removed as above and the remaining liquid was removed with help of a syringe. 50 µl 1x Laemmlibuffer was added to the dry beads and after vortexing they were put on a shaker for 12 min at room temperature. Then, the samples were centrifuged at 10'000 g for 5 min to pellet the beads and the supernatant was collected for Western blot analysis.

3.3.9 Synchronization of Cells by Double Thymidine Block

For synchronization of the fast proliferating A549 cells in the late G1 phase, thymidine was added to the cell culture medium to a final concentration of 2 mM and incubated for 14 h. Then the cells were washed twice with preheated PBS and then released for 10 h in fresh medium without thymidine. The second block was performed equally to the first and as well as the release.

3.3.10 Statistics

Statistical analyses were performed with Graphpad Prism Software Version 5. Error bars, depicting the standard error of mean, are only displayed for experiments performed at least twice. The number of experiments performed is indicated in the description of the graph.

3.3.11 Construction of the Expression Plasmid Coding for FLAG-tagged, siMVP-Resistant MVP

The MVP sequence was obtained from the plasmid pEW65 coding for GFP-MVP (kindly received from E. Wiemer, Rotterdam, NL) by PCR. Primers were designed using Primer-BLAST (NCBI).

Table 3.2 Primer Pairs:

N-terminal FLAG-tagged MVP:	length of PCR product: 2688 kb
Forward primer*:	5′-GGAACTGAAGAGTTCATCATCCGCATCC-3′
	- ATG sequence omitted - alanine was replaced by glycine for favorable cloning
Reverse primer*:	5′-GGATCCGGCCTACCGCAGTACAGGCACCACGT-3′
	- GGATCC (BamHI restriction site) - TAGGCC (Stop sequence)

* Underlined base pairs do not anneal.

C-terminal FLAG-tagged MVP	length of PCR product: 2694 kb
Forward primer*:	5′-GGATCCGCCGCCATGGCAACTGAAGAGTTCATCAT-3′
	- GGATCC (BamHI restriction site) - Kozak sequence before ATG (GCCGCC)
Reverse primer*:	5′- CCACCGCAGTACAGGCACCACG -3′
	- Stop sequence omitted - serine sequence (TCC) added (see manual)

* Underlined base pairs do not anneal.

The MVP PCR products were separated by gel electrophoresis and the product of the appropriate size was extracted using the QIAquick Gel Extraction Kit (Qiagen #28704).

The PCR products then were cloned into the StrataClone Expression Vectors (Agilent Technologies) according the manufacturers specifications:

- StrataClone Mammalian Expression N-Terminal FLAG Vector System #240229
- StrataClone Mammalian Expression C-Terminal FLAG Vector System #240230

StrataClone SoloPack competent cells were transformed with the ligation reactions according to the protocol and spread on LB-Agar plates containing 20 mg/ml kanamycin.

Single clones were picked and cultured for the preparation of minipreps with the QIAprep Spin Miniprep Kit (Qiagen #27104).

The plasmids were verified by restriction digest (XhoI, NEBIS or EcoRI, Life Technologies) and sequencing.

Site directed mutagenesis was performed by the QuikChange II XL Site-Directed Mutagenesis Kit (Agilent Technologies #200521) according to the manual. The PCR product was transformed into JM109 competent Escherichia coli by a standard heat shock protocol. Several clones were picked and cultured for the preparation of minipreps with the QIAprep Spin Miniprep Kit (Qiagen #27104) and the full MVP sequence containing the mutations was verified by sequencing.

Forward Primer for siMVP#2 resistant MVP*:

CATAAGAACTCAGCCCGCATCAT**CA**G**A**AC**C**GC**G**GT**G**TTTGGCTTTGAGACCTCGGAAGC

Forward Primer for siMVPmurine resistant MVP*:

CCGGAAAGGTGCGCGCTGT**A**ATTGG**CTCG**AC**G**TACATGCTGACCCAGGACG

* Underlined base pairs correspond to the siRNA sequence; bold bases were exchanged.

3.3.12 Transfection and Selection of A549 Cell Clones Expressing the Plasmid

A549 cells were transfected with Lipofectamine® 2000 according to the manufacturer's specifications. 48 h after transfection selective medium containing 800 µg/l G418 (450 µg/mg potency, Sigma) was added. 2 weeks after selection, cells were seeded in 96-wells to obtain single clones. Single clones were harvested by trypsinization; half was seeded in 12-well plates and half in 24-well plates on cover slips. The cells seeded on cover slips were stained with anti-FLAG Ab according to the immunofluorescence staining protocol on page 37 to select for clones with ectopic MVP expression.

3.4 Results

This project is a follow-up to the MVP project that has been initiated by Andreas Hollenstein during the last two years of his PhD-studies. For a brief overview to the background and our aims of the study, see section 3.2.1 and 3.2.2.

3.4.1 Knockdown of MVP Sensitizes for Ionizing Radiation

In a first step, radiosensitization in MVP-depleted cells was confirmed by means of clonogenic assays, including additional dose points. The same two siRNAs with the sequences siMVP#1 and siMVP#2 were used as in the previous experiments. Moreover, an additional siRNA targeting a third MVP sequence was tested, we will refer to as siMVP#3. This siRNA has been shown to be least toxic among other sequences tested and was very efficient in silencing MVP in HeLa cells [433]. As control siRNA, we used siLuc targeting the firefly luciferase, which is not expressed in mammalian cells. The siRNAs siMVP#1 and siMVP#2 in combination with ionizing radiation reduced clonogenic survival in A549 cells to a similar extent, in comparison to cells treated with the control siRNA siLuc. Figure 3.2 displays the data for siMVP#1. The siRNA siMVP#3 led to an even stronger radiosensitization (data not shown).

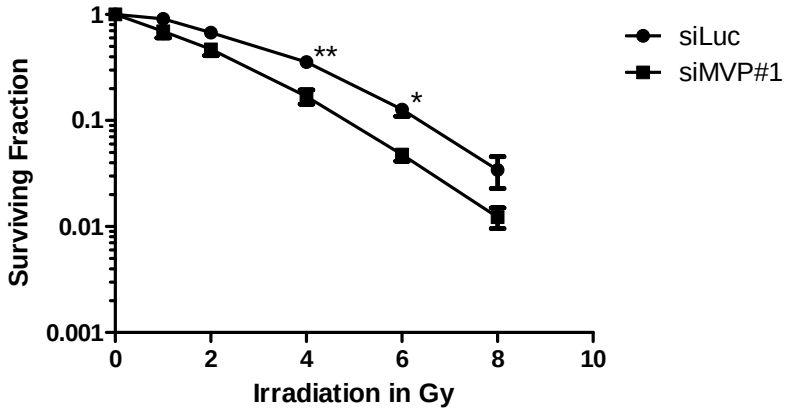

Figure 3.2 Clonogenic survival of A549 cells treated with siRNA against MVP or control siRNA against luciferase at increasing radiation doses. The diagram shows the mean of three independent experiments; the error bars represent the standard error of mean (SEM). Unpaired Student t-test, two-tailed, *p < 0.05, **p < 0.01.

3.4.2 Persistent γH2AX-Foci in MVP-Depleted A549 Cells after Treatment with Ionizing Radiation

The phosphorylated form of the histone variant H2AX, referred to as γH2AX, is used as an indirect measure for the DNA damage. At the site of DNA damage H2AX is

phosphorylated and foci of γH2AX can be detected by immunofluorescence staining. We assessed the initial DNA damage introduced by the treatment with ionizing radiation (IR) by counting the number of γH2AX-foci at an early time point and followed the repair process by the clearance of γH2AX. This analysis was previously performed, but we aimed to study the kinetics of the DNA repair process in more detail and included further time points in our study. Analysis of γH2AX-foci clearance indicated that the kinetics of DNA repair during the first 6 hours after irradiation with 2 Gy was similar for both siMVP- and siLuc-treated A549 cells (see Figure 3.3). At a later time point, 24 hours after irradiation, the level of H2AX-phosphorylation in control cells returned to the basal level of non-irradiated cells. However, the number of γH2AX-foci remained elevated in cells treated with siMVP. This result suggested that DNA damage might not be as efficiently repaired in MVP-depleted cells as in control cells.

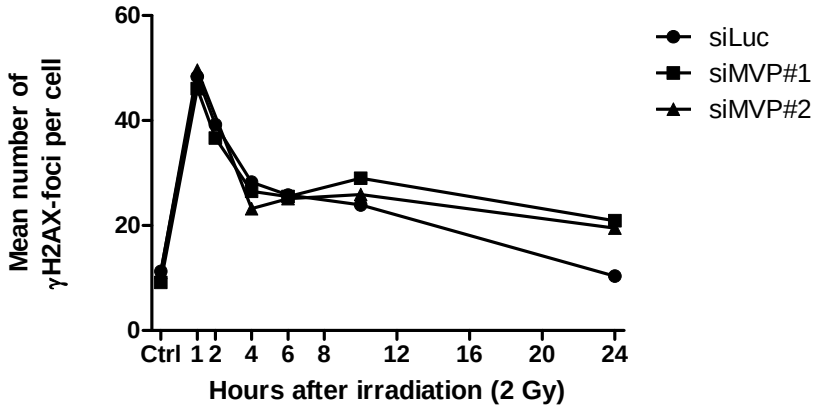

Figure 3.3 Clearance of γH2AX-foci in MVP-depleted and A549 control cells after irradiation with 2 Gy. Cells were stained with fluorescently labeled antibodies against phosphorylated H2AX. At least 75 cells were randomly chosen and analyzed by microscopy and the mean number of foci per cell is displayed in the diagram (single experiment).

3.4.3 Reduced Rad-51 Expression and Rad51-Foci Formation in A549 Cells with Knockdown of MVP

Non-homologous end joining (NHEJ) represents the fast and error prone DNA double-strand break repair pathway in mammalian systems. The kinetics of the clearance of γH2AX-foci during the first hours after IR indicates that NHEJ remained undisturbed by MVP silencing. At later time points, the remaining γH2AX-foci were removed more slowly in cells treated with siMVP than in control cells. Even though NHEJ takes place throughout the entire cell cycle, the complexity of certain DNA damage may require repair by homologous recombination (HR), the second DNA double-strand break repair mechanism. As previously shown by Andreas Hollenstein, the formation of Rad51-foci, a process essential to HR, was strongly suppressed in cells with downregulated MVP

(see Figure 3.4). Rad51-foci were assessed in a 24-hour time line, to determine whether HR was delayed or reduced for the whole period. The time line analysis revealed a general reduction of Rad51-foci formation. The quantification of the numbers of Rad51-foci per cell for the 6-hour time point, where control cells showed highest foci numbers, is depicted in Figure 3.5A. We were also interested to determine the influence of the MVP status on replication protein A (RPA) binding to the DNA. RPA covers the resected DNA strand before it is replaced by Rad51. However, for up to 6 hours, RPA-foci formation was as efficient in MVP knockdown cells as in control cells and showed even a slight increase at the 6-hour time point (see Figure 3.5B), which might be due to a reduced replacement by Rad51. From this, we concluded that HR was initiated in the siMVP-treated cells, but Rad51-foci formation was hampered.

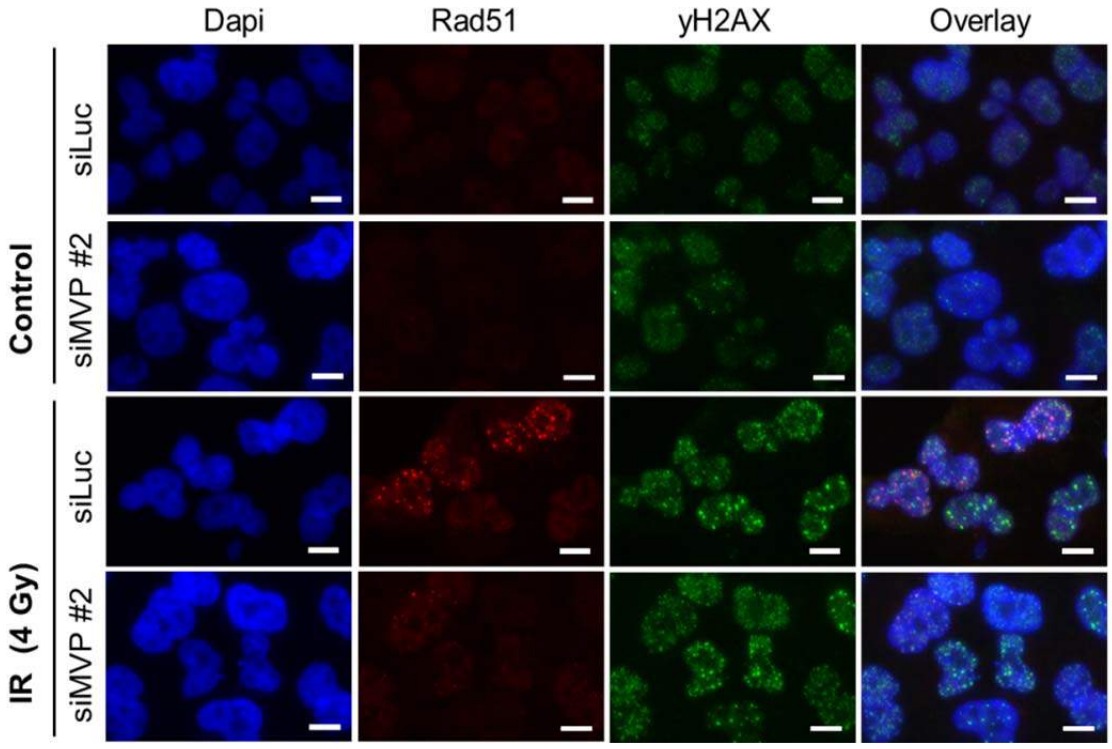

Figure 3.4 A549 cells treated with siMVP showed reduced Rad51-foci formation after treatment with IR. Cells were irradiated 72 h after siRNA-treatment with 4 Gy and assayed 6 h thereafter for Rad51 and H2AX-phosphorylation by immunofluorescent staining. Nuclear DNA was counterstained with Dapi. The scale bar represents 10 µm.

In cooperation with BRCA2, Rad51 binds to RPA-covered, single-stranded DNA and replaces RPA. Rad51 and BRCA2 are also involved in pairing the bound sequence with the intact homologous sister chromatid, which serves as template for the repair of the damaged strand [434]. The complex formation of Rad51 with BRCA2 is essential for Rad51-foci formation in response to exogenous DNA damage, but not for Rad51-foci

formation in response endogenous DNA damage, e.g. occurring due to the collapse of replication forks [435].

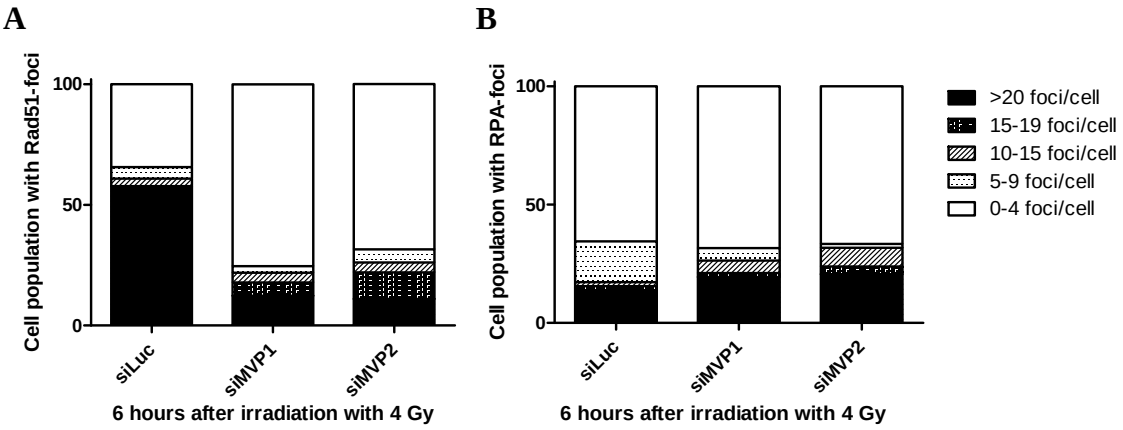

Figure 3.5 Rad51-foci formation and Rad51 protein expression was reduced in A549 cells after treatment with siRNA against MVP. 72h after treatment with the indicated siRNA, cells were irradiated with 4 Gy and fixed 6 hours thereafter, followed by immunofluorescence labeling of **(A)** Rad51 and **(B)** RPA.

Preliminary data obtained in our laboratory showed that MVP co-immunoprecipitated with BRCA2, indicating that MVP may be involved in the nuclear transport of the BRCA2/Rad51 complex [430]. Western blot analysis of Rad51-expression was performed for the time course of the MVP knockdown and revealed that Rad51 protein levels declined over time and were strongly decreased at the 70-hour time point at which irradiation for clonogenic assays and for assessment of foci was performed (see Figure 3.6). Thus, the hampered Rad51-foci formation might actually be due the reduced Rad51 expression levels. Rad51 protein levels increased when the effect of the siRNAs started to wane (data not shown).

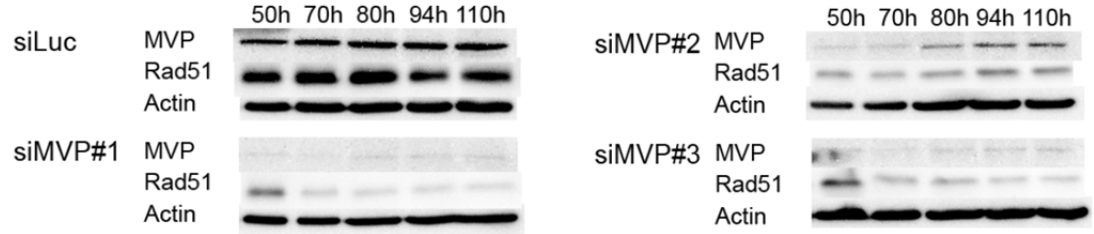

Figure 3.6 Western blot analysis of MVP and Rad51 protein levels in A549 cells treated with siLuc and siMVP#1-3 and harvested at the indicated time points after treatment.

Interestingly, the reduction of Rad51 expression level as determined by Western blot analysis, inversely correlated with the amount of siRNA applied against MVP. On the other hand, MVP-expression was already strongly downregulated at the lowest amounts of siRNA applied (see Figure 3.7A). However, we did not monitor the mRNA levels of

MVP, which might have better correlated with the Rad51 protein levels for the different siRNA conditions. Of notice, Rad51-foci formation in siMVP-treated cells was partially restored, by reducing the amount of siRNA, which also correlates with increased Rad51 protein expression (see Figure 3.7B). This indicates that the reduced Rad51 protein levels at least to some extent may be responsible for the reduced Rad51-foci formation.

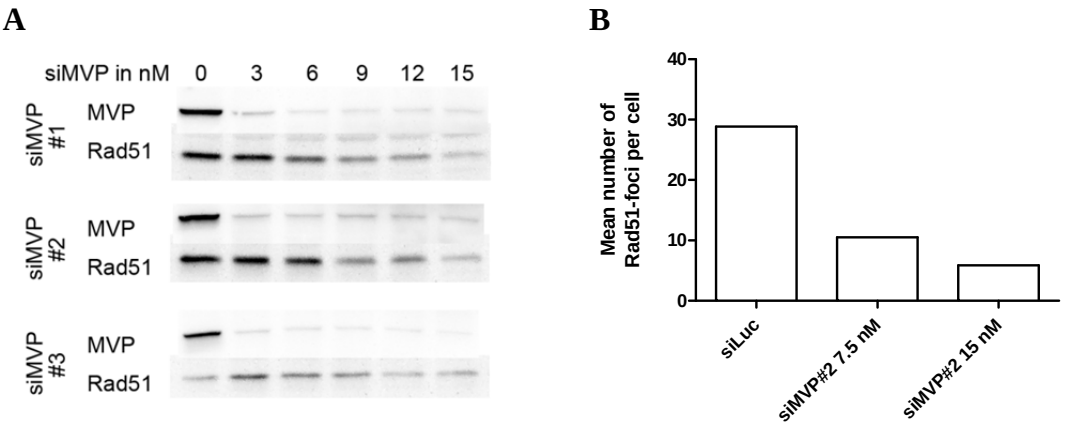

Figure 3.7 Repression of Rad51 protein level and Rad51-foci formation depends on the amount of siMVP applied. **(A)** MVP was efficiently downregulated by very low siMVP concentrations as determined by Western blot analysis, 72 h after transfection with siRNA. Concurrent downregulation of Rad51 correlated with the amount of siRNA applied. For all three siRNAs targeting MVP, the highest amount of siRNA applied led to the strongest Rad51 repression. **(B)** The mean number of Rad51-foci 6 h after radiation treatment with 4 Gy was most strongly reduced in cells treated with highest amount of siMVP#2 (single experiment).

3.4.4 BRCA2 as Interaction Partner of MVP Could Not Be Confirmed

To corroborate our previous findings that MVP may be a potential interaction partner of BRCA2, a co-immunoprecipitation (Co-IP) experiment was performed with an antibody against BRCA2. We extended the previous experiment by including CAPAN-1 cells as negative control. CAPAN-1 cells express MVP and Rad51, but only a truncated version of BRCA2. The mutation of BRCA2 is due to a deletion (6174delT) in one allele, and loss of heterozygosity led to elimination of the second wild type allele. The truncated BRCA2 is not recognized by the antibody used for IP and thus CAPAN-1 cell lysates were used to probe for non-specific binding of proteins to beads or antibody. In the previous experiment, a rabbit IgG-coupled agarose was used as an isotype control antibody. Within this experimental setup, MVP did not co-immunoprecipitate. In the control experiment, performed with CAPAN-1 cell lysates and the same polyclonal antibody used for co-immunoprecipitation in A549 cells (by A. Hollenstein [430]), MVP was pulled down as well. However, as expected, BRCA2 was not detected in the Western blot analyses of the immunoprecipitated proteins (see Figure 3.8). Thus, we could not to confirm a direct interaction between MVP and BRCA2. However, to be

able completely exclude the existence of a BRCA2/MVP interaction, additional experiments, e.g. a pull down with MVP as bait, are required.

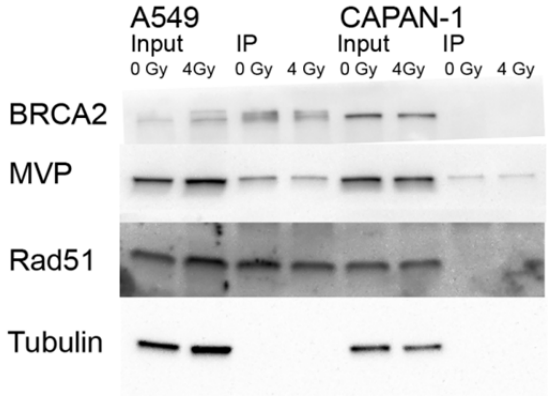

Figure 3.8 MVP was pulled down regardless of BRCA2 in the co-immunoprecipitation experiment using an antibody against BRCA2. MVP, Rad51 and BRCA2 protein levels were determined by WB. Different antibodies were used for IP and detection of BRCA2 by WB. The antibody used for the WB recognizes the truncated form of BRCA2 in CAPAN-1 cells, but BRCA2 is not recognized by the antibody used for the IP.

3.4.5 Loss of Rad51 Expression: Cause or Consequence of Cell Cycle Redistribution in A549 Cells Treated with siMVP?

As described above, Rad51-expression was strongly reduced in A549 cells 72 hours after transfection with siRNA against MVP. Previously, we determined by real-time PCR that MVP silencing resulted in a decrease of Rad51 mRNA levels in PTEN wild type HCT116 cells, whereas in the PTEN-deficient HCT116 cells, this effect was absent (see [430], p.69). A link between nuclear import of PTEN and MVP had been established earlier [339, 385]. These findings support the hypothesis that reduced MVP protein levels, upon silencing of MVP, might hamper the nuclear import of PTEN and thus lead to reduced Rad51 transcription [386].

The strong reduction of Rad51 expression that we observed upon silencing of MVP, coincided with cell cycle redistribution (see Figure 3.9A). The loss of Rad51 expression could be the cause, as well as the consequence of cell cycle redistribution. Rad51 is mainly expressed in S and G2 phase, and its expression is lost during mitosis and remains low throughout G1 phase [436]. In an osteosarcoma cell line, suppression of Rad51 by shRNA resulted in an accumulation of the cells in the G2 phase of the cell cycle [437]. Similarly, we observed a reduced S phase cell population and a G2 arrest in A549 cells upon repression of Rad51 by siRNA (see Figure 3.9B). The cell cycle distribution induced by siRad51, resembled the cell cycle distribution we observed for A549 cells treated with siMVP#1 and siMVP#2 (see Figure 3.9A). The siRNA siMVP#1 induced a strong and the siRNA siMVP#2 a mediocre G2 arrest. This difference,

however, might be due to the differential efficiencies of the two siRNAs. The phenotypes for siMVP#1 and siMVP#2 are in concert with the hypothesized MVP/PTEN/Rad51 axis. On the other hand, the sequence siMVP#3, which was very potent in MVP silencing and non-toxic to HeLa cells, resulted in a strong G1-arrest in A549 cells. A G1-arrest may explain the loss of Rad51, as Rad51 levels are low in G1 phase of the cell cycle, but does not support the hypothesis of a cell cycle redistribution following reduced Rad51 expression. If Rad51 expression was lost as a consequence of MVP silencing, A549 cells would have arrested in G2 phase (see Figure 3.9B), which we did not observed for the siRNA siMVP#3.

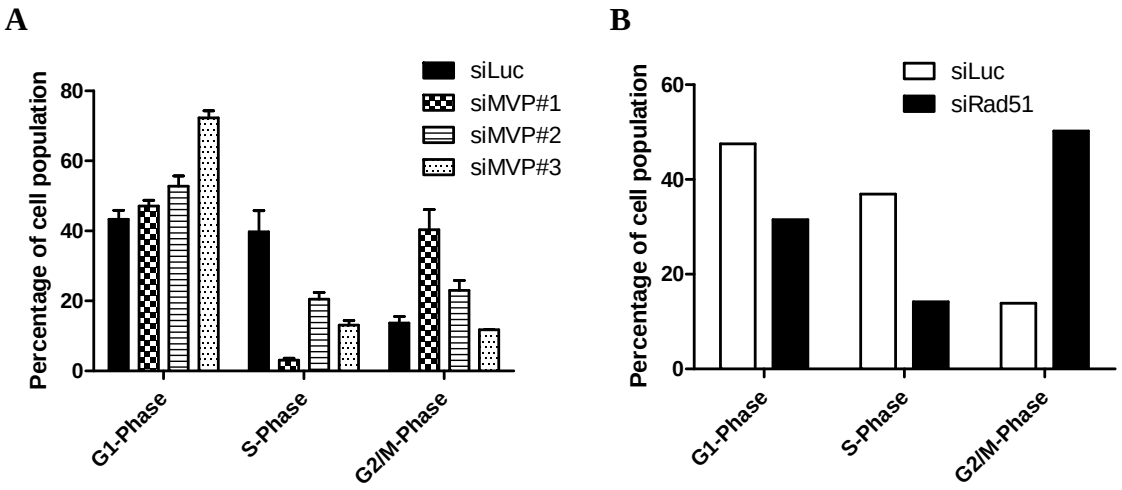

Figure 3.9 Cell cycle distribution of A549 cells 72 h after transfection with siRNA. **(A)** S phase determined by 30 min of BrdU incorporation was reduced after treatment with siMVP#1-3. The sequences siMVP#1 and siMVP#2 led to a G2 arrest while siMVP#3 shows a G1 arrest. Diagram depicts the mean of three different experiments; the error bars represent the SEM. **(B)** Downregulation of Rad51 leads to a G2 arrest 72 hours after transfection (single experiment).

As mentioned previously, MVP depletion decreased Rad51 transcription only in HCT116 PTEN-proficient cells. However on the protein level, we observed a comparable decrease of Rad51 protein levels in HCT116 PTEN-deficient and PTEN-proficient cells (see Figure 3.10A). This observation was reported previously by A. Hollenstein [430], but no explanation could be found for this discrepancy. Nonetheless, the reduction of Rad51 in HCT116 cells of either PTEN status indicates that PTEN might not be directly involved in the siMVP-dependent attenuation of Rad51 protein levels.

Silencing of MVP by siMVP#1-3 was accompanied with pronounced phenotypes of growth inhibition. Thus, we also considered the possibility that the MVP knockdown may have an effect on cell cycle progression or on the cell integrity per se, which eventually leads to reduced Rad51 expression levels. In support of this hypothesis was the fact that not all cancer cells showed a deregulated Rad51 expression level upon MVP

knockdown, such as BxPC-3 and CAPAN-1 cells. Both did also not show a growth inhibition upon treatment with siMVP#2 (see Figure 3.10B). In addition, normal cells also do not depend on MVP for Rad51 transcription, as MVP-knockout mice show a normal development. This indicates that the deregulation of Rad51 might be an indirect effect of the cell cycle arrest, rather than a direct effect of the MVP knockdown.

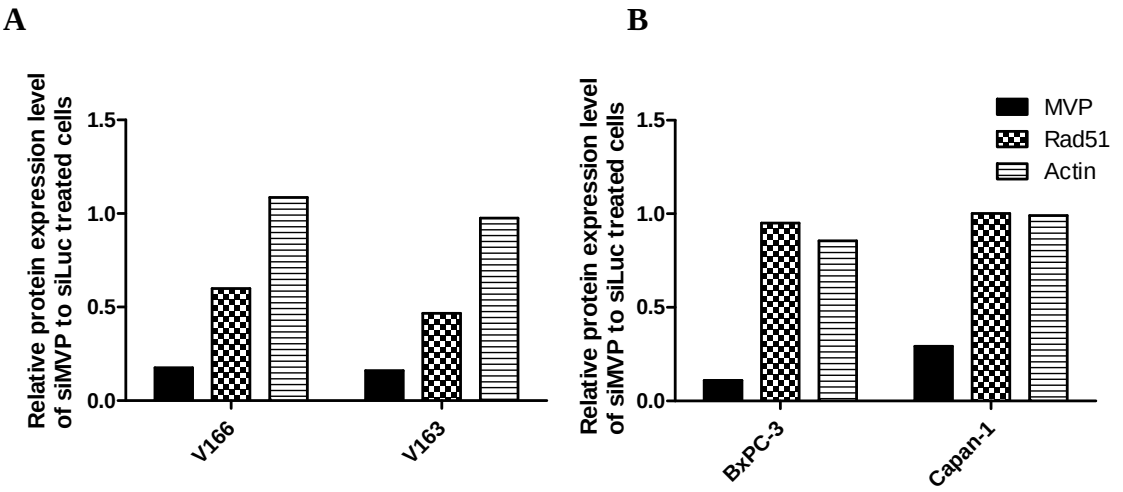

Figure 3.10 Relative expression levels of MVP and Rad51 of cells treated with siMVP#2 to cells treated with siLuc determined by WB. **(A)** Both the PTEN-proficient (HCT116 V166) and the PTEN-deficient (HCT116 V163) cells showed decreased Rad51 levels upon MVP knockdown. **(B)** The knockdown of MVP did not lead to reduced Rad51 protein levels in the pancreatic cancer cell lines BcPC-3 and CAPAN-1.

We observed that the Rad51 levels correlated well with the percentage of population in S phase of the cell cycle. For example, at 72 hours after cellular transfection with siMVP#1, the S phase cell population and the Rad51 expression level was strongly reduced in A549 cells. The same effect was already observed 48 hours after transfection, but to a less pronounced extent.

To evaluate a putative link between Rad51 repression and the reduction in S phase cell population, A549 cells were submitted to a double thymidine block right after siRNA transfection, thereby accumulating the cells in G1 phase. Then cells were released to enter S phase at around 48 hours after siRNA transfection and cell cycle distribution and protein expression were determined. Accordingly, MVP knockdown cells entering S phase under these conditions did not display reduced Rad51 protein levels, and the number of cells in S phase correlated well with the Rad51 protein level regardless of the MVP expression levels (see Figure 3.11). The extent of MVP downregulation in cells treated with the double thymidine block was equal to the knockdown in unsynchronized cells, as determined on the level of protein expression (data not shown). The 48-hour time point may be too early to determine the full consequence of the MVP knockdown. However, due to the reduced proliferation, it was technically not feasible to synchronize

the MVP-depleted cells at a later time point. Nevertheless, under the assumption of a direct link between MVP expression and Rad51 expression, it would be expected that A549 cells that enter S phase show a reduced Rad51 expression and thus eventually accumulate in G2 phase due to compromised HR and subsequent unresolved DNA damage. First, we did not detect increased γH2AX staining in the MVP knockdown cells 72 hours after transfection (see Figure 3.3) and second the correlation of the percentage of S phase cells with Rad51 expression indicates that the cells entering S phase do not display reduced Rad51 levels, which should already be visible at the 48-hour time point.

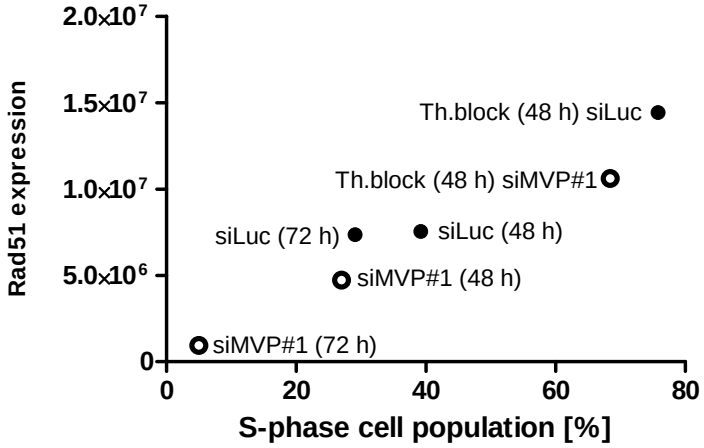

Figure 3.11 There is a correlation of Rad51 expression with the size of S phase cell cycle population. A549 cells were treated with siMVP#1 or siLuc as a control. 6 hours after transfection part of the cell dishes was submitted to a double thymidine block. These cells were released for 3 hours to enter into S phase. Finally, all samples were harvested at the indicated time point, S phase cell population (BrdU-incorporation) was determined by FACS analyses and Rad51 expression levels were determined by Western blot analysis.

In parallel to the experiments above, we also investigated Rad51 protein levels as a consequence of induction of apoptosis. Plating efficiency of cells treated with siMVP#1-#3 was significantly reduced, which is an indication for reduced cell viability. We assessed induction of apoptosis by determination of cleaved poly(ADP-ribose) polymerase (PARP) in response to treatment with siMVP#1-#3. PARP is involved in the recognition of single-strand breaks and is inactivated by caspase 3 in the early phase of programed cell death. Thus, monitoring cleaved PARP provides a mean to assess apoptosis [438]. Rad51 also is known to be a target of caspase 3 and is cleaved upon induction of apoptosis [439].

Indeed, downregulation of MVP by siRNA was accompanied by the activation of caspase 3 in a dose dependent manner with an inverse correlation to Rad51 expression levels (see Figure 3.12A). However, inhibition of caspase activity by a pan caspase

inhibitor did not restore the Rad51 protein level, indicating that induction of apoptosis is not the main cause for the reduction of the Rad51 expression level upon MVP-depletion.

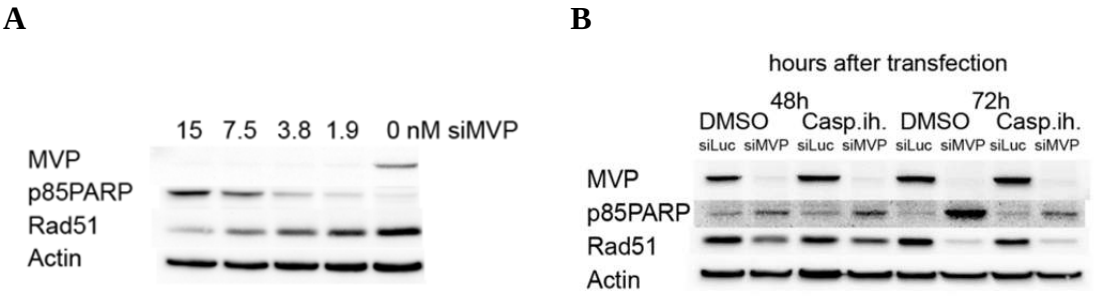

Figure 3.12 Caspase activity determined by PARP cleavage was induced in A549 cells by transfection with siMVP. **(A)** An increase of cleaved PARP was detected with increasing concentration of siMVP#2 used (72h after transfection). **(B)** The additional reduction of Rad51 between the 48- and 72-hour time points after transfection was not rescued by inhibition of caspase activity. The control was treated with the solvent DMSO only.

3.4.6 Manifestation of the MVP knockdown Phenotype Depends on p53 and p53 Is Involved in MVP Regulation

The severe phenotype we observed in A549 and HCT116 cells upon MVP-depletion raised the possibility of a putative link between MVP and resistance to oncogene-induced senescence of cancer cells (see Figure 3.13 for the phenotypes of A549 cells treated with siMVP#1-#3). Yet, MVP silencing does not result in phenotypic changes in normal cells and in various cancer cell lines. MVP-knockout mice do not display any developmental and growth defects [332]. Hervelsen et al. silenced MVP with siMVP#2 in human bladder cancer cells and did not report any adverse effect with regard to cell viability or proliferative activity [375]. Furthermore, the sequence siMVP#3 was characterized to be nontoxic in HeLa cells [433], whereas in A549 cells the siRNA with this sequence strongly impaired cell proliferation.

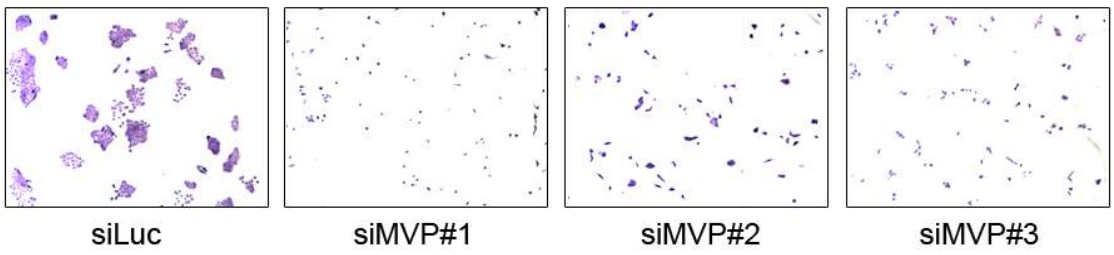

Figure 3.13 Knockdown of MVP in A549 cells leads to a severe inhibition of cell proliferation. A549 cells were transfected with 15 nM siMVP and seeded the following day at subconfluent conditions. Cells were allowed to form colonies for 72 h, were then fixed and stained with crystal violet, and documented by bright field microscopy.

To determine possible reasons for the differential response in our cell systems compared to previously documented results, we considered the genetic background of the A549 and the HCT116 cell line. Remarkably, both cell lines express wild type p53, which normally acts as a tumor suppressor and is involved in cell cycle control and apoptosis. The gene TP53 coding for p53 is among the most frequently mutated gene in cancer [440]. However, both A549 and HCT116 cells express wild type p53 and in both cells lines p53 signaling was activated upon treatment with ionizing radiation and induced the expression of the cell cycle inhibitor p21. The p53-response in HCT116 cells was delayed and p53 reached the peak of activation only 48 hours after irradiation, whereas A549 cells showed a regular activation of p53 within the first hours after irradiation (determined by Ser17-phosphorylation of p53, data not shown). This indicates that p53-signaling is at least partially intact. Furthermore, we observed that transfection with the siRNAs targeting MVP alone induced phosphorylation of p53 at Ser17 (data not shown).

Thus, we suspected that the status of the tumor suppressor p53 might play a role in the differential response to MVP silencing and decided to extend our MVP knockdown studies to additional cells lines. Various human cancer cells lines, as well as mouse embryonic fibroblasts (MEFs) were treated with siMVP#2 and siMVP#m, targeting the murine MVP sequence, respectively. Evidently, the knockdown of MVP had a stronger antiproliferative effect on cells expressing wild type p53 than on p53-deficent or p53-mutant cells. A simplified overview is presented in the table below (see Table 3.3).

Table 3.3 Schematic overview on cell lines treated with siMVP: MVP expression level, p53 status and effect of MVP-depletion on cell viability and proliferative activity

	A549	HCT116		SW480	SW620	Capan-1	BxPC-3	U2OS	SaoS-2	MEF E1A/Ras		MEF wt MEF MVP-KO	
p53 status	wt	wt	loss	mut	mut	mut	mut	wt	loss	wt	loss	wt	loss
MVP expression													
Effect of siMVP on Proliferation	↓↓	↓↓	↓	→	→	(→)	(→)	↓	→	↓↓↓	↓	→	→

p53 status: wt = wild type, mut = mutated, loss = spontaneous loss of expression, ko = knockout
MVP expression level: color intensity reflects expression level
Cell viability: ↓↓↓ = induction of apoptosis, ↓↓ and ↓ = strong and mediocre inhibition of proliferation, → no significant effect on proliferation, (→) no significant effect on proliferation, determined only by cell cycle distribution

The effect of MVP silencing was most prominent in the p53-positive E1A/Ras-transformed MEF cells, in which MVP-depletion clearly induced apoptosis. No apoptosis, but growth arrest was induced by MVP silencing in their p53-negative counterpart cells (see Figure 3.14A). Similarly, in HCT116 p53-positive cells and their p53-negative counterparts, proliferation was inhibited to a greater extent in cells expressing wild type p53 (Figure 3.14B). The same p53-dependence applied to the osteosarcoma cell lines U2OS and Saos-2, wild type and deficient in p53, respectively (Figure 3.14C). Of all three cell line pairs, the p53-deficient cell line showed notably lower doubling times to start with. Therefore, we also examined the effect of MVP silencing in the p53-mutant colon adenocarcinoma cell line SW480, which possess a comparable doubling time as observed for the p53-proficient cell lines. However, knockdown of MVP did not affect proliferation in this cell line, nor in SW620 cells, a cell line established from a metastatic tumor of the same patient (Figure 3.14D).

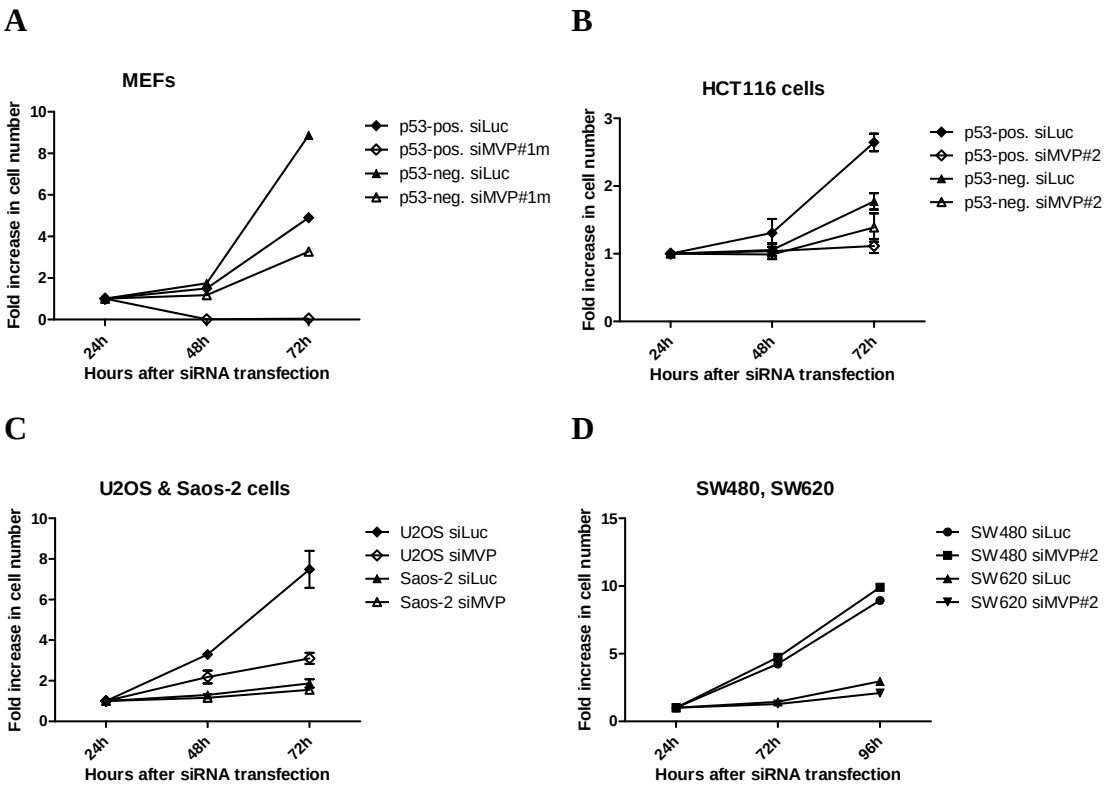

Figure 3.14A-D All cell lines, except MEFs, were treated with the siRNA sequences siLuc and siMVP#2, respectively, at a final concentration of 15 nM. MEF cells were treated with a siMVP sequence targeting the murine MVP sequence at equal concentration. 24 h after transfection, cells were reseeded in 6 well plates and the cell number was determined at the indicated time points by cell count. Diagrams A and B depict a single experiment and B and C show the result for two combined experiments (error bars stand for the SEM).

Interestingly, the 3T3 MEFs derived from MVP-knockout mice, which we kindly received from Prof. Dr. Wiemer (Rotterdam, NL), had undergone complete loss of p53

expression. The 3T3 protocol for the acquisition of immortalized fibroblasts implies a stochastic event such as loss of p53, or loss of $p19^{ARF}$ upstream of p53 [441, 442]. Thus, loss of p53 in the MVP-knockout fibroblast might provide a selective advantage related to the status of MVP or may be a mere coincidence as part of immortalization. Intriguingly, the MVP-proficient 3T3 MEFs, which express wild type p53 were also not affected by MVP-depletion. However, we did not perform further investigations with regard to this aspect. A discrepancy with regard to cell proliferation also exists between the p53-positive cancer cell lines sensitive to suppression of MVP and the MVP-knockout mouse model that is not affected by the absence of the MVP. Furthermore, no information about the effect of MVP silencing in normal human cells exists.

p53 wild type cells did not only respond in a more sensitive way to MVP silencing, but the p53 status might also correlate with increased MVP expression. For all cell lines investigated in this project, an increased MVP expression level was observed in p53 wild type cells (see Table 3.3, above). Only p53-knockdown E1A/Ras MEFs displayed a similar MVP level as their p53 wild type counterpart. Furthermore, MVP expression was reduced in p53-depleted A549 cells (see Figure 3.15), corroborating that p53 might play a role in the regulation of MVP expression. Previously, Lange et al. suggested a link between p53 and MVP based on putative p53-binding elements in the promoter region of MVP [328].

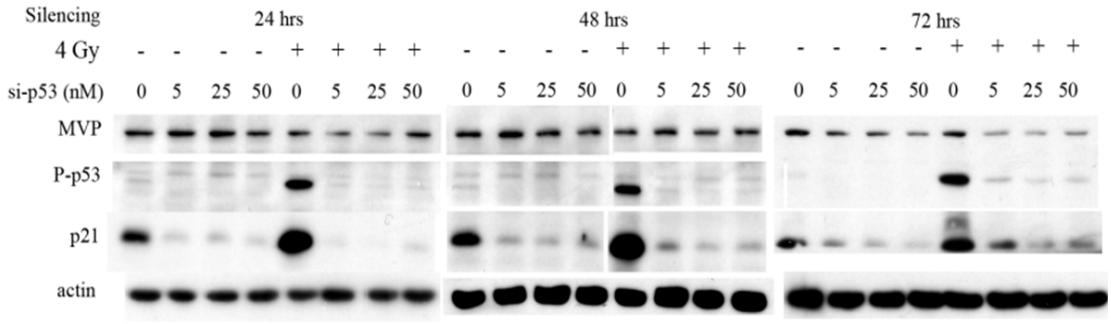

Figure 3.15 MVP expression is reduced in A549 cells upon knockdown of p53. A549 cells were treated with the indicated siRNA concentration. Cells were irradiated with 4 Gy at 24, 48, and 72 h after transfection and were harvested 6 h thereafter for Western blot analysis of MVP, p53 and p21 expression. Western blot performed by Tamara Codilupi.

3.4.7 Validation of the MVP knockdown Phenotype Could Not Be Achieved by Rescue Experiments

The discrepancy between MVP knockdown phenotype observed in the p53-positive cancer cell lines versus loss of MVP in normal cells raised unanswered questions. Furthermore, the variability of the different MVP knockdown phenotypes induced by the three siRNA sequences “remained an enigma”. All three siMVP sequences led to a

decrease in proliferation in A549 cells. However, there was a clear difference in the extent of growth inhibition and in the final cell cycle distribution. The severity of the MVP knockdown phenotype with regard to proliferation could be due to the differential efficiencies of the siRNAs, but the difference between the cell cycle distributions induced by the three siRNAs is more difficult to explain. As mentioned earlier, A549 cells arrested in G2/M phase upon application of siMVP#1 or siMVP#2, whereas treatment with siMVP#3 resulted in a strong G1 arrest (see section 3.4.5). These inconsistencies indicate that one or the other siRNA may display nonspecific effects and deregulates additional proteins and pathways.

Thus, we decided that validation of the RNAi phenotype, observed in MVP silenced p53-proficient cells, was indispensable. Validation can be performed by a rescue experiment. The target protein is reintroduced by ectopic expression of an RNAi resistant version of the target and thus the RNAi phenotype is expected to be reduced. A549 cells were transfected with a plasmid coding for a flag-tagged MVP that was resistant to siMVP#2 due to nucleotide substitutions in wobble base pairs within the siRNA-targeted MVP mRNA sequence (see Material and Methods, page 101 for further information on the construction of the expression plasmid).

For the performance of the rescue experiment, cells stably expressing the flag-tagged MVP are required. Interestingly, the expression of the flag-tagged MVP construct was suppressed in untreated control A549 cells, and was only detectable in cells treated with siMVP#2 (see Figure 3.16A). This substantially complicated the selection of clones stably expressing the MVP construct. Possibly, in A549 cells, the cellular turnover of MVP was increased by the additionally expressed MVP in presence of already high levels of endogenous MVP. Moreover, the flag-tagged MVP along with endogenous MVP most probably assembles into common vaults, which results in less pronounced staining of individual vaults; especially as the endogenous MVP level generally was higher than the ectopically expressed MVP in the selected clones. Thus, after siRNA silencing of the endogenous MVP, MVP protein levels were only partially restored by flag-tagged MVP, such as for A549 clone C2.7 (see Figure 3.16), which was one of the clones with highest expression of flag-tagged MVP.

Repeated treatment of the MVP-transfected A549 pool with siMVP#2 did not enrich cells with high flag-MVP expression (data not shown), nor did the expression of ectopic MVP increase in the clone C2.7 as determined by Western blot analysis (see Figure 3.16B). Moreover, the expression of flag-tagged MVP in clone C2.7 and other additional clones (not shown) did not release growth suppression caused by the siMVP treatment (see Figure 3.16C). Therefore, we could not confirm that the phenotype introduced by the siRNA treatment was a direct consequence of the MVP knockdown. On the other

hand, these results do not explicitly prove that the MVP knockdown phenotype we observed was due to off-target effects. This would require evidence for proper assembly and functionality of the ectopically expressed flag-tagged MVP. Immunofluorescence staining for the c-terminally flag-tagged MVP displayed the same coarse-grained appearance as for the native MVP, indicating proper assembly into vaults. Moreover, expression of c-terminally GFP-tagged MVP was performed by others, and vault assembly was validated by electron microscopy [443].

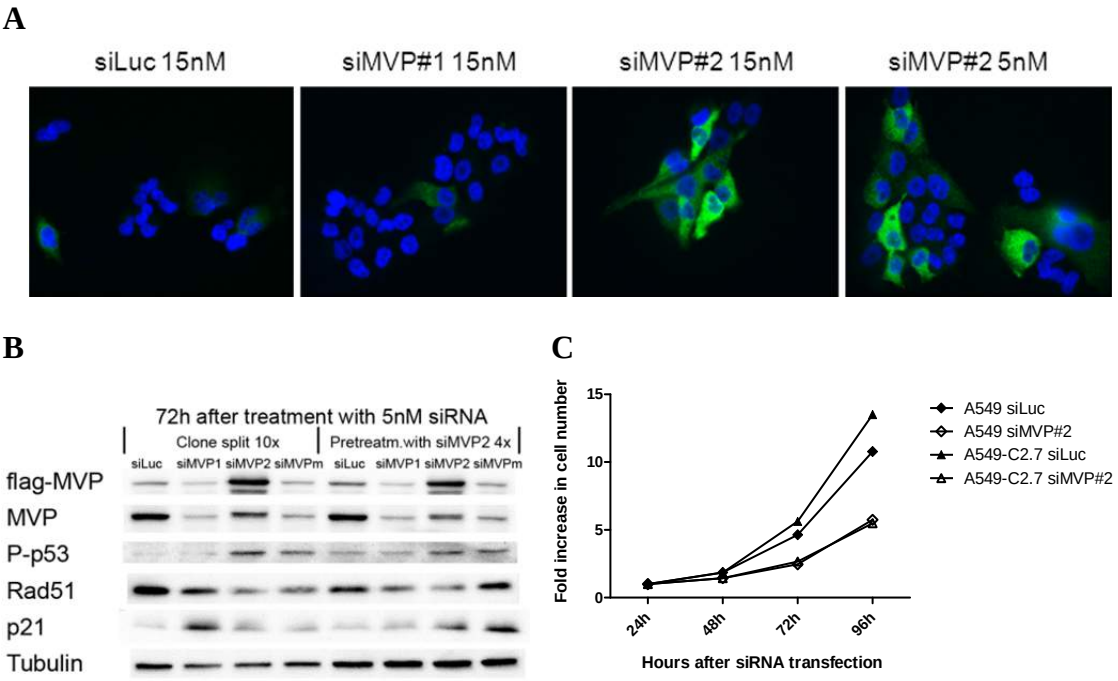

Figure 3.16 Expression of siMVP#2-resistant MVP did not rescue the proliferative activity of A549 cells. **(A)** The A549 cell clone C2.7 expressing c-terminally flag-tagged MVP was treated with the indicated siRNAs and was stained for the flag-tag 72 h after transfection. **(B)** WB of clone C2.7 after single transfection with siRNA (left) or after the fifth siRNA transfection (right). **(C)** Proliferation of original A549 cells and clone C2.7 after treatment with siLuc and siMVP#2, respectively, at a final siRNA concentration of 5 nM.

3.4.8 Combined Application of siRNA Sequences Reduced Severity of the MVP Knockdown Phenotype

Taking into consideration that the MVP knockdown phenotype might derive from the undesired knockdown of proteins other than MVP, several experiments were performed to elucidate this possibility. Off-target effects are nonspecific effects and thus the identification of the protein, or proteins affected by the siRNA, other than the target protein, is laborious, if not even impossible. Only a limited number of experiments were performed that indirectly provide further indications for possible off-target effects.

We assumed that each of the siRNA sequences targeting MVP introduces different nonspecific effects. The severity of these off-target effects might be reduced by the application of a mixture of siRNAs. The cellular response to MVP silencing by siMVP#2 alone was compared to the cellular response to a mixture of all three siMVP sequences (see Figure 3.17A). The sequence siMVP#2 manifested in the least severe MVP knockdown phenotype of all three sequences with regard to proliferation. Nonetheless, the mixture of siRNAs alleviated the phenotype, even though the same concentration of total siRNA was applied. The siRNA siMVP#2 alone strongly reduced Rad51 expression levels and induced phosphorylation of p53 at Ser17. Both effects were significantly reduced in the samples treated with the mixture of siRNAs. However, proliferative activity recovered only at very low siMVP concentrations (see Figure 3.17B). The proliferation rate of A549 cells that were treated with the siRNA mixture returned to control levels at a concentration of 0.56 nM siRNA, whereas cells treated with siMVP#2 resumed normal proliferative activity only at a the threefold lower siRNA concentration. Unfortunately, the cell proliferation assay was performed only once.

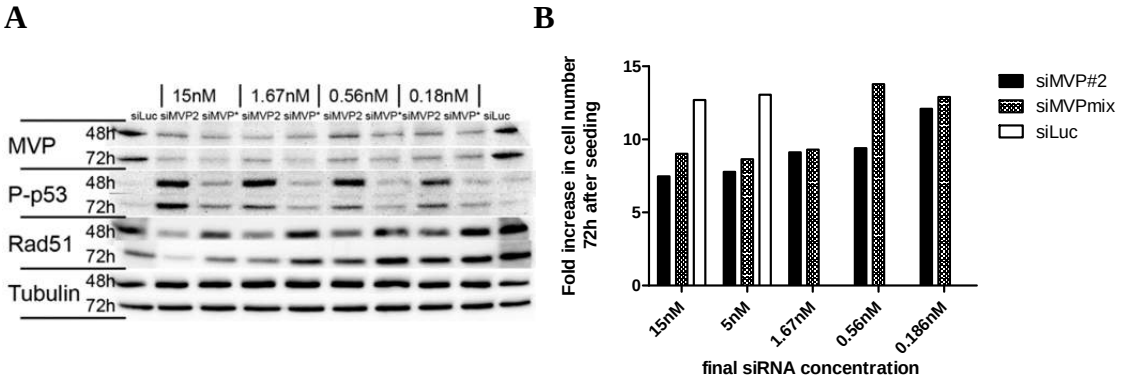

Figure 3.17 Differences in the siMVP knockdown phenotype between cells treated with siMVP#2 and a mixture of all siMVP sequences. **(A)** Determination of MVP and Rad51 expression levels, and p53-phoshorylation (Ser17) in A549 cell lysates harvested 48 and 72 h after transfection. **(B)** The fold increase in cell numbers 72 h after transfection with different concentrations of siRNA was determined by cell count.

3.4.9 Testing of Additional siRNA Sequences

Another approach to shed light on the possibility of nonspecific siRNA effects was to test siRNAs targeting different parts of the MVP mRNA than the previous siRNAs. Additional siRNA sequences were used to test and to compare their effects to those induced by the siRNAs we used so far. For the target MVP, no *in vitro* validated siRNA sequences were available. Thus, we probed three commercially available sequences (from Ambion) that had been selected for high specificity and efficiency by means of an

algorithm. These sequences will be denominated siMVP_A, siMVP_B and siMVP_C. For additional control siRNA sequences two of the obtained MVP sequences were scrambled by means of an algorithm dedicated to design non-binding siRNA sequences using the same nucleotide composition.

Astonishingly, only one of the three new siMVP sequences was capable of downregulating MVP in A549 cells; the other two sequences, especially siMVP_A rather induced MVP expression levels (see Figure 3.18A). The additional control siRNAs with the scrambled sequences_A and B did not change MVP expression levels. Additional control experiments with siLuc siRNA confirmed our previous results that transfection of siLuc induces MVP expression in A549 cells. On the level of proliferation, the siMVP_C efficiently downregulated MVP, but did not influence cell proliferation (see Figure 3.18B). These results indicate that the MVP knockdown phenotype obtained with the previously used siRNAs may indeed be due to nonspecific siRNA interactions. Of note, also the scrambled sequence_A strongly reduced proliferation, as well as the MVP-stimulating sequence siMVP_A. Our observations emphasize that nonspecific effects may be very common to the siRNA technique and that these side effects, depending on the genetic background of the cancer cell, e.g. with regard to their p53 status, may induce cell cycle arrest.

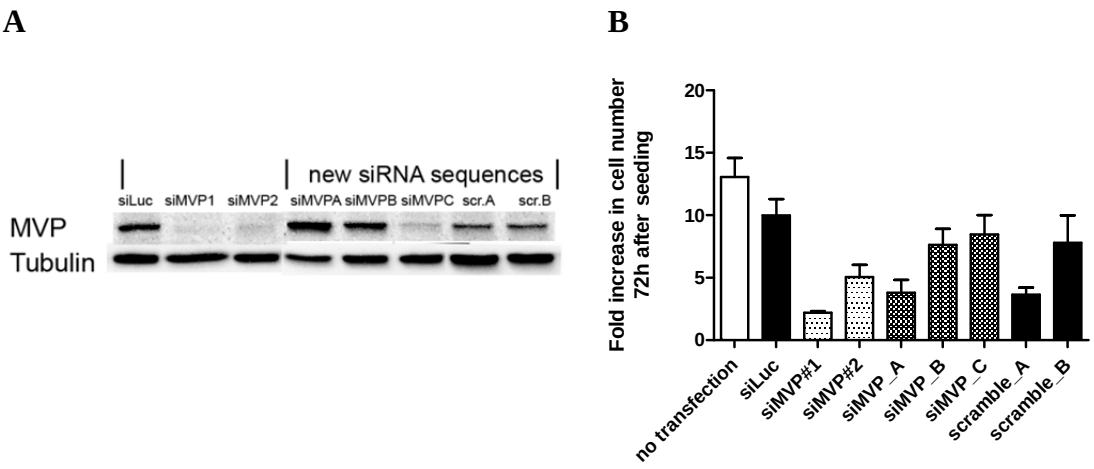

Figure 3.18 Determination of MVP knockdown by additional siRNA sequences targeting MVP and their effect on cell proliferation. **(A)** A549 cells were transfected with the siRNA sequences indicated, at a final concentration of 15 nM. Cells were harvested 72 h after transfection and MVP expression was determined by Western blotting. **(B)** The fold increase in cell number was determined at the 72-hour time point for each siRNA condition, by cell count.

3.4.10 MVP Is Induced by Ionizing Radiation and other Stress Stimuli

We could not confirm a direct link of MVP to DNA damage repair, but we observed that MVP was induced upon treatment with ionizing radiation (see **Figure 3.19**A). We did not find an increased MVP protein level as an immediate treatment response to ionizing radiation, but observed an increase at around 48 hours post irradiation in A549, HCT116, and U2OS cells. This indicated that MVP in response to IR might be involved in similar resistance mechanisms as in senescent cells. Ryu et al. observed that MVP was induced in senescent fibroblasts and in aging tissue and they suggested that vaults play a role in the resistance to apoptosis [383, 384]. 72 hours after irradiation with 10 Gray, we observed a pronounced increase of MVP in A549 cells, as well as reduced Rad51 expression (see Figure 3.19A). This indicated reduced proliferative activity, which might even be related to IR-induced senescence. Interestingly, upregulation of MVP in response to irradiation was partially mediated by secreted factors and could be counteracted by changing the medium (see Figure 3.19B).

Other cellular stress factors also upregulated MVP in the three cell lines A549, HCT116 and U2OS, like the hypoxia-mimicking agent DMOG (data not shown), supporting a putative role of MVP in stress response. Upregulation of MVP after DMOG also coincided with strongly reduced proliferation, similar as in response to high doses of IR.

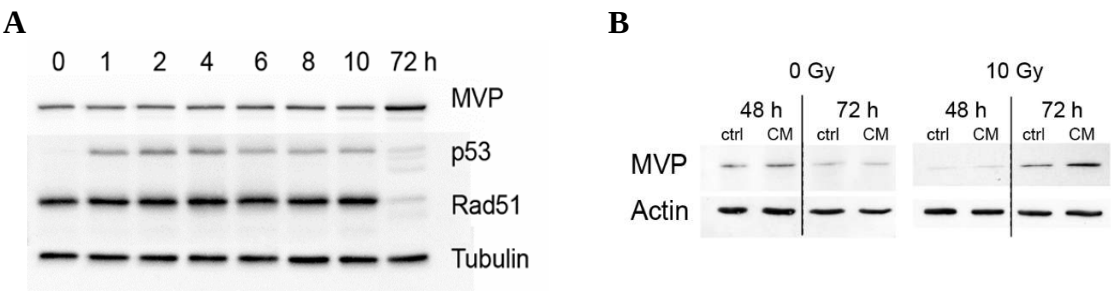

Figure 3.19 Increase of MVP upon treatment with ionizing radiation in A549 cells. **(A)** Cells were treated with IR (10 Gy) and harvested at the indicated time point after irradiation for Western blot analysis of MVP, phospho(Ser17)-p53 and Rad51 expression levels. Tubulin was used as loading control. **(B)** A549 cells were irradiated with 10 Gy or sham irradiated. Cells designated as ctrl cells were supplied with fresh medium every 24 hours. The medium of the cells designated with CM (conditioned medium) was not changed. Lysates were taken at 48 and 72 h after IR and analyzed for MVP expression. Actin was used as a loading control (WB performed by Tamara Codilupi).

For these experiments, the cells were seeded at very low density, as we previously realized that the MVP expression level substantially increased in confluent cells (Figure 3.20A). Clearly, the amount of medium added to the cultured cells, greatly influenced the process of MVP induction and confluency itself did not seem to be the major cause of MVP upregulation. This again suggested that secreted factors or other changes in the medium such as pH, lactate levels or percentage of serum might influence MVP-levels.

The increase of MVP induced by the conditioned medium proofed to be reversible. MVP expression decreased if confluent cells, with high MVP levels, were plated at subconfluent density in fresh medium (see Figure 3.20B). The reduction in MVP expression coincided with the increase in proliferative activity, which was determined by Rad51 expression levels.

Further evidence that MVP induction was not facilitated by cell density, but by the conditioned medium, was obtained by culturing subconfluent cells in conditioned medium. The MVP expression level was strongly upregulated in cells incubated in conditioned medium in comparison to cells incubated with fresh medium (Figure 3.20C). In this experiment, cells were seeded at a very low density, to assure that even at the 48-hour time point, cell density remained low. Nonetheless, in these cells MVP-expression could be induced by conditioned medium derived from plates with confluent cells. This effect was even more pronounced when confluent cells were seeded at low density and were then incubated in conditioned medium. Under these conditions MVP expression further increase, whereas in the same cells, plated in fresh medium, MVP expression returned to the basal level (see Figure 3.20D).

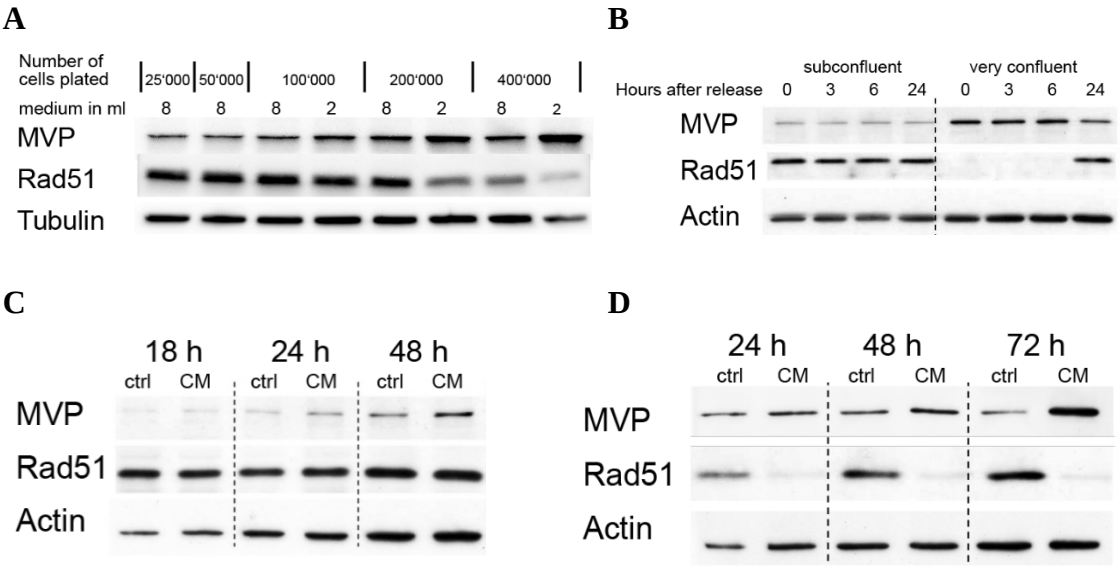

Figure 3.20 Conditioned medium facilitates upregulation of MVP in A549 cells. **(A)** A549 cells were seeded at different cell densities in 6-well plates and were incubated with 2 or 8 ml of medium. Samples were harvested 72 h after seeding and submitted to Western blotting for the analysis of MVP, Rad51 and Tubulin as loading control. **(B)** Subconfluent and very confluent A549 cells were trypsinized and reseeded in fresh medium under subconfluent conditions. Cells were harvested at different time points for the assessment of MVP expression. Subconfluent **(C)** and confluent **(D)** A549 cells were reseeded at subconfluent conditions in fresh medium or in conditioned medium from confluent cells. MVP and Rad51 protein levels were determined in lysates collected at the indicated time points. Actin was used as a loading control. WBs 19B-D were performed by Tamara Codilupi.

To assess the changes in the composition of the medium or secreted factors that were responsible for the upregulation of MVP expression, we performed additional experiments to determine the influence of obvious factors such as pH or lactate concentration on the MVP expression level. The pH of strongly conditioned medium was determined to be around 6.7 and acidification was assumed to depend on secreted lactate, which accumulates in the medium over time. However, supplementation of subconfluent cells with medium that was adjusted to a pH of 6.7 or contained 10 mM lactate, did not accelerate induction of MVP in A549 cells (Figure 3.21A).

Supposedly, conditioned medium contains a reduced amount of serum components, and the shortage of nutrients might eventually induce a stress response in cultured cells, leading to increased MVP expression. MVP indeed was shown to play a role in starvation resistance [444, 335]. Thus, to probe for the effect of nutrient deprivation on MVP expression, A549 cells were subjected to 48 hours of serum starvation (medium containing 1 % serum), followed by a release into fresh medium. 48 hours of serum starvation also had no influence on MVP expression, nor did we observe any change in MVP expression upon release from starvation (see Figure 3.21B).

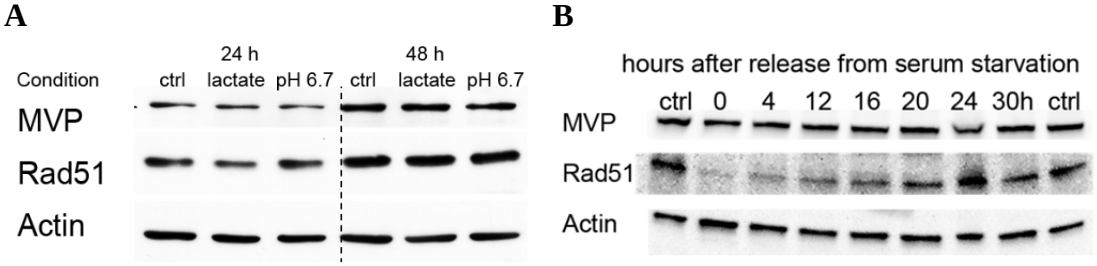

Figure 3.21 Induction of MVP in A549 cells is not mediated by low pH or the accumulation of lactate, nor by serum starvation. **(A)** A549 cells were incubated in medium of pH 6.7 or in medium containing 10 mM lactate. Lysates were collected at 24 and 48 hours for the analyses of MVP expression by WB. The experiment was performed by Tamara Codilupi. **(B)** A549 cells were starved for 48 hours and were then released into fresh medium. Sampled were taken at the indicated time points after release. Control samples show the MVP expression level of non-starved A549 cells.

Apart from changes in the medium composition, autocrine factors might be involved in upregulation of MVP. In the experiments that involved large doses of radiation (see above, Figure 3.19A), the irradiated cells do not reach confluency, due to cell cycle arrest or cell death. Thus, the composition of the medium with regard to pH and lactate might be less affected under these conditions. On the other hand, it is known that irradiation and other stress stimuli induce compensatory activation of intracellular signaling pathways such as mitogen-activated pathways involved in cell survival and repopulation [265, 445, 446]. Irradiation induces increased shedding of growth factors that are involved in epidermal growth factor receptor (EGFR) stimulation [264, 265, 447]. To

investigate an involvement of EGFR pathways in the upregulation of MVP, EGFR signaling was stimulated by epidermal growth factor (EGF). Interestingly, we observed that MVP was upregulated after EGF stimulation in a similar time frame as after irradiation (see Figure 3.22). The induction of MVP by EGFR stimulation was slightly lower in A549 cells than in the human breast carcinoma cell line MDA-MB-231. In A549 cells, upregulation of MVP over time was stronger, which might be due to a generally increased secretion of stimulatory factors.

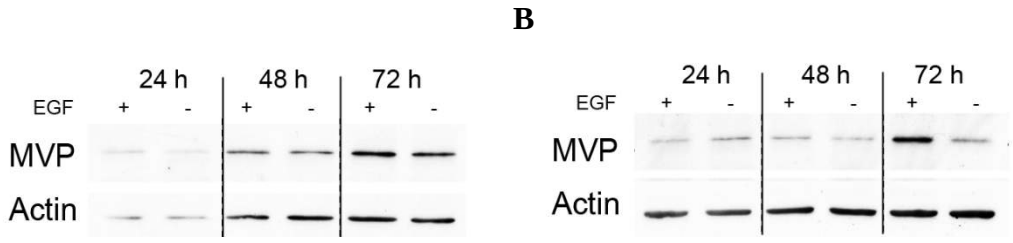

Figure 3.22 MVP expression is induced by stimulation with epidermal growth factor. A549 cells **(A)** and MDA-MB-231 **(B)** were stimulated with 100 ng/ml EGF and MVP expression was assayed at the indicated time points by Western blotting. WBs were performed by Tamara Codilupi.

Both cell lines carry an activating mutation in K-Ras downstream of EGFR [448, 449], which correlates with increased EGFR ligand production [271] and increased shedding of EGFR ligands by increased ADAM-17 activity [450]. However, we did not analyze the composition and the level of secreted growth factors to determine which specific growth factor might be responsible for the upregulation of MVP in A549 cells by the conditioned medium. Likewise, it would be interesting to test the hypothesis of a putative link between irradiation-induced growth factor shedding and the increase in MVP expression.

3.5 Discussion of the MVP Project

The promising findings of the major vault protein (MVP) as a player in the DNA repair process of homologous recombination could not be confirmed and might have been an artefact of the siRNA technique used. Thus, the first part of the discussion will be dedicated to the technique of RNAi. In the second part MVP as a player in stress response, such as in the response to ionizing radiation will be reconsidered and the regulation of MVP in response to stress factors will be discussed.

3.5.1 The Puzzling World of RNAi

At long last, we ended up with six siRNA sequences targeting the MVP, which all displayed different phenotypes in the non-small cell lung cancer cell line A549. Two of the first three siRNA sequences had been used in previous publications and the other three siRNA sequences had been designed by the company Ambion and had undergone selection by an algorithm to exclude sequences with possible nonspecific effects. Nonetheless, in our hands, the discrepancy between the effects evoked by the different sequences proofed to be a serious handicap for their use. These observations also raise the questions why in some cell systems nonspecific effects do not display, whereas in others, they do, and how these nonspecific effects could be prevented. In the following part, a brief overview on the RNAi mechanism and its scientific exploitation, will be followed by the review of “our” siRNA sequences in the context of the cell systems we worked with. Finally, the issue of off-target effects, and how they might arise will be addressed.

3.5.1.1 A Brief Overview of the Discovery of RNA Interference, of Mechanisms of RNAi and of Its Endogenous Functions

The suppression of gene expression by the ectopic introduction of nucleotide sequences has been first observed in plant science. Unexpectedly, ectopic expression of chalcone synthase (CHS) an enzyme involved in anthocyanin biosynthesis diminished endogenous CHS expression in petunia petals [451]. Similar observations were made in *Neurospora crassa* a type of red bread mold; ectopic expression of carotenoids induced an albino phenotype [452]. Even though the authors found that the introduced sequences had randomly integrated into the genome and were able to disturb endogenous expression, the effect was lost over time.

Before Andrew Fire and Craig C. Mello came across their findings that double-stranded RNA sequences were most efficient in suppression of genes [453], antisense technique

was used to downregulate protein expression in *C. elegans*. Antisense strands (single stranded RNA) were thought to bind to the messenger RNA and inhibit its translation. Curiously, Guo et al. found that not only the antisense RNA sequence, but also the sense sequence led to suppression of the target gene, the mechanism of which they were not able to explain [454]. Andrew Fire and Craig C. Mello observed similar results when the single stranded siRNA products were not purified by gel electrophoresis, but were merely treated with DNase to degrade the template. Purified RNA strands showed reduced RNAi potency. Thus, they suspected that the observed RNA interference actually came from the contamination with the template remnants when they observed that repression of gene expression by dsRNA was far more potent in *C. elegans*; only a few injected molecules were sufficient to induce the phenotype of the corresponding knockout animal. Eventually they were honored with the Nobel Prize in 2006 for their discovery of RNA interference. Fire and Mello also distinguished that the dsRNA-effect was propagated to cells distant from the injection site and was even handed down to later generations [453].

At the same time, regulation of gene expression by endogenous antisense sequences became apparent, first in plants, then in prokaryotes and bacteriophages and later also in eukaryotic cells. Some antisense sequences were found to be transcribed from the noncoding strand of the same gene locus as the regulated gene [455]. These regulatory sequences overlap with a great part of the translated region or bind to the 5’ untranslated region (5’ UTR) to inhibit translation. On the other hand, another type of regulatory RNA sequences, so-called microRNAs (miRNAs) tend to bind the 3’ UTR region and are not direct antisense transcripts.

The first miRNA named lin4 was discovered in *C. elegans* and regulates the lin14 mRNA, a transcript of a separate locus [456, 457]. However, many miRNAs are transcribed from introns of coding genes [458, 459]. The transcripts of approximately 70-80 nucleotides (nts) of length contain one to several hairpin structures, which are consequently separated by the RNAse III enzyme Drosha in the nucleus. Upon transport to the cytoplasm, the so-called pre-miRNA is further tailored by the RNAse III enzyme Dicer into a 21-25-nt long double stranded miRNA molecule, with a 2-nt overhang at each 3’ end. In the same way, endogenous siRNAs are processed by Dicer, though they derive from long sense-antisense transcripts.

Both miRNAs and siRNAs act in a similar fashion to regulate protein expression. The processed double-stranded RNAs assemble into the RNA-induced silencing complex (RISC), which contains an Argonaute 2 (Ago2) protein. Ago2 selectively binds to the guide strand, which is distinguished by the lower 5’ stability of the RNA duplex [460–462]. The second strand is then released in the presence of inherent mismatches

that are often attributed to miRNAs, or it is cleaved by the Ago2 “slicer” activity in case of a perfect match of the RNA duplex [463]. Similarly, in case of perfect match of the guide strand to the target sequence, the latter is cleaved by Ago2. MicroRNAs, other than siRNAs often imperfectly pair with their target sequence, which leads to repression, rather than to degradation of the targeted mRNA. However, some miRNAs such as miR-196, which is involved in HOX8B regulation, have been reported to match their target perfectly, leading to cleavage of the targeted transcript [464].

Initially, the RNA silencing mechanism was thought to be mainly involved in host defense against viral infection, as observed in plants [465, 466]. Further investigations indicated that some viruses might have turned the stick around, by hijacking the RNA silencing machinery to manipulate the host cell (reviewed in [467]). By now, we know that RNA-dependent mechanisms are also involved in manifold endogenous regulation processes, and RNA molecules other than miRNAs and siRNAs have been identified with different origins and mode of actions (see Table 3.4 and [468]). Also the interest in long noncoding RNAs (lncRNAs) has returned with the technical developments that allow to study whole transcriptomes; it has been suggested that about 75% of the noncoding genome is transcribed and is surmised to be involved in gene regulation [469, 470].

Table 3.4 Classes of regulatory RNAs identified in eukaryotic cells [471].

Class	Description	Biogenesis and genomic origin	Function
miRNA	MicroRNA	Processing of foldback miRNA gene transcripts by members of the Dicer and RNaseIII-like families	Post-transcriptional regulation of transcripts from a wide range of genes
Primary siRNA	Small interfering RNA	Processing of dsRNA or foldback RNA by members of the Dicer family	Binding to complementary target RNA; guide for initiation of RdRP-dependent secondary siRNA synthesis
Secondary siRNA	Small interfering RNA	RdRP activity at silenced loci (*Caenorhabditis elegans*); processing of RdRP-derived long dsRNA or long foldback RNA by members of the Dicer family (*Arabidopsis thaliana*)	Post-transcriptional regulation of transcripts; formation and maintenance of heterochromatin
tasiRNA	*Trans*-acting siRNA	miRNA-dependent cleavage and RdRP-dependent conversion of *TAS* gene transcripts to dsRNA, followed by Dicer processing	Post-transcriptional regulation of transcripts
natsiRNA	Natural antisense transcript-derived siRNA	Dicer processing of dsRNA arising from sense- and antisense-transcript pairs	Post-transcriptional regulation of genes involved in pathogen defense and stress responses in plants
piRNA	Piwi-interacting RNA	A biogenesis mechanism is emerging, which is Argonaute-dependent but Dicer-independent	Suppression of transposons and retroelements in the germ lines of flies and mammals

RdRP, RNA-dependent RNA polymerase.

3.5.1.2 RNAi a Powerful Tool in Research

In human and other mammalian cells, RNAi did not turn out to be a tool as powerful as in *C. elegans*, where siRNA molecules are amplified by RNA-dependent RNA polymerase (RdRP) enzymes [472–474] and silencing can spread among cells, and under circumstances are even transmitted to the next generation [453]. Nevertheless, RNAi has advanced to a widely used technique in scientific research to eliminate cellular proteins in order to study their function. Moreover, a lot of effort is put into

RNAi-based therapeutic approaches to treat various diseases such as cancer, viral infections and inflammatory diseases. However, the therapeutic application of RNAi and the challenges involved will not be discussed here.

In research, three RNAi methods are commonly used: transient transfection with short interfering dsRNA sequences (siRNAs), stable expression of short hairpin RNAs (shRNAs) or miRNA-adapted shRNAs (miR-shRNAs) from transient or stably transfected plasmids. The siRNA technique has the advantage that it can be easily and quickly established, and therefore is the choice of method for screen-based investigations or for short-term experiments for the assessment of potential effects. A cellular model system that can be readily transfected is a prerequisite for siRNA. A big disadvantage of the siRNA-knockdown method to the more laborious shRNA and miR-shRNA approaches is the duration of the knockdown of the target. Based on our own experience, the protein knockdown manifests around 24 to 48 hours after transfection with siRNA and starts to wear off at latest around 96 hours after transfection. Thus, during an siRNA experiment, cells may not be given enough time for recovery from the transfection procedure and the short duration of the actual knockdown may not be sufficient to investigate the scientific question. Knockdown by shRNA on the other hand can be stable over time upon integration of the vector plasmid into the host cell's genome. In case of a very severe knockdown phenotype or if required by the experimental design, shRNA expression can be regulated by means of inducible promoter elements. The coupling of naturally occurring miRNA flanking regions to shRNA drives transcription by RNA polymerase (pol) II, which also transcribes most endogenous primary miRNA transcripts [475]. The use of an endogenous promoter may prevent overexpression of shRNAs that has been associated with cellular toxicity, presumably through oversaturation of cellular microRNA/short hairpin RNA pathways [476]. Moreover, miRNA-adapted transcripts can be designed to contain several miR-shRNAs facilitating the knockdown of multiple targets at the same time [477].

3.5.1.3 Review of the siRNA Sequences siMVP#1-3 and Determination of Potential Indications for Off-Target Effects

As described, we performed the knockdown of MVP by means of siRNA. Due to the great impact of MVP knockdown in A549 cells, a stable knockdown by shRNA was not an option. However, an inducible shRNA construct was considered for future extended experiments.

The knockdown of MVP by siMVP#1 and siMVP#2 had a strong impact on cell viability and proliferation in both cell lines, the non-small cell lung carcinoma cell line A549 and the human colon cancer cell line HCT116. This observed stagnation of the

proliferative activity will be referred to as MVP knockdown phenotype. Of note, siMVP#1 was more “toxic” than siMVP#2, which was not only reflected in a reduced plating efficiency, but also in a much stronger reduction of the S phase cell population. The depletion of S phase cells had not been observed to this extent in our previous studies, since different time points for cell cycle analyses and on differential transfection protocols and transfection agents were chosen [430]. For the current studies, a reverse transfection protocol was applied, using a specific transfection reagent adapted for siRNA transfection. This may have enhanced and prolonged downregulation of MVP. Instead of the 48-hour time point, cell cycle distribution was determined 72 hours after transfection, where the siMVP knockdown phenotype became most apparent.

As mentioned above, the severity of the induced phenotype was different for the two siRNA sequences, siMVP#1 and siMVP#2, used and might have correlated with the efficiency of the MVP knockdown. To confirm the relationship we decided to use a third siRNA sequence against MVP and thus a published sequence that was declared efficient but non-toxic in HeLa cells was chosen [433]. Intriguingly, in A549 cells we were again confronted with a very strong MVP knockdown phenotype with almost completely abolished growth. To our surprise, siMVP#3-transfected A549 cells accumulated in G1 phase, whereas siMVP#1 induced a strong G2 arrest and siMVP#2 provoked a less marked G2 arrest. The difference between siMVP#3 and the other two sequences could hardly be explained by different knockdown efficiencies, and reinforced the requirement for validation of the siRNA sequences.

Indications that indeed all three siRNAs (siMVP#1-3) introduced nonspecific effects can be deduced from the following experiment. To determine the relationship between the MVP expression level and the appearance of the siMVP knockdown phenotype, the siRNAs were applied in a gradient of concentrations. As a measure for the phenotype, we probed the Rad51 expression level. Rad51 repression was assumed to indirectly reflect reduced cell cycle progression upon MVP-directed siRNA treatment, or to be a direct consequence of MVP-regulated Rad51-transcription. Previous data suggested that Rad51 transcription might be induced by MVP in a PTEN-dependent way and would therefore be reduced upon MVP-depletion, eventually leading to a G2-arrest [430]. Even though we demonstrated that Rad51-depletion indeed arrest A549 cells in the G2 phase of the cell cycle, the Rad51 expression levels in the siMVP-gradient experiments rather correlated with the amount of siRNA applied than with the MVP expression level. MVP levels were efficiently reduced even at low siRNA concentrations, whereas Rad51 levels gradually decreased with increasing siRNA concentrations for all three siMVP sequences. Thus, the MVP knockdown does not seem to be responsible for the loss of Rad51 expression. More likely, the results indicate that with rising siRNA

concentrations “toxicity” may increase, which leads to a gradual decrease in cell cycle progression and thus reduced Rad51 expression levels.

Furthermore, not in all the cell lines we tested, MVP-depletion had an effect on the Rad51 expression level. But interestingly no MVP-Rad51 interrelationship could be observed in the MVP-knockout mouse model. Thus, a cancer type-dependent addiction to MVP-facilitated Rad51 transcription might exist. However, such a pronounced dependence of Rad51-transcription on MVP, which under normal circumstances seems to be “non-essential”, may be rather unlikely. Interestingly, cell lines harboring wild type p53 were clearly more prone to Rad51 repression. Transfection with each of the three siMVP sequences led to phosphorylation of p53, which in turn might affect cell cycle progression. Although not all siMVP sequences stimulated p53 to the same extent. Interestingly, stimulation of p53 was not apparent, if a mixture of all three siRNAs was applied instead of a single siMVP siRNA. These findings suggest the presence of differential toxic effects that are “diluted” by the siRNA pool. Moreover, increased p53 activity upon MVP knockdown in cell culture or in the MVP-knockout mouse model has not been reported before, which supports the notion that nonspecific effects lead to p53 activation and may even be partially responsible for the siMVP knockdown phenotype. Possibly, a double knockout of MVP and p53 may help to understand the role of p53 in the induction of the phenotype.

With all these findings, we could not overlook the possibility that all three siMVP sequences might be accompanied by nonspecific effects that interfere with the outcome of the experimental results. Especially in the research on radiation responses, an additional though nonspecific stimulation of p53 may falsify the treatment outcome and the cellular radiosensitivity. Obviously, the loss of Rad51, if not a result of MVP-depletion, may lead to wrong conclusions with regard to homologous recombination. If deregulated cell cycle progression is the result of nonspecific effects, we are confronted with the loss of Rad51 in the G2 phase, which we observed in siMVP#1 and siMVP#2-treated cells. In the G2 phase of the cell cycle, Rad51 normally is present and facilitates homologous recombination. However, Yamamoto et al. demonstrated that mRNA levels of Rad51 were already reduced in G2-M phase and they postulated that the high stability of Rad51 that they determined by a pulse chase experiment explains its presence in G2-M phase [478]. Thus, it may be possible, that cells arrested in G2 over time show reduced Rad51 expression and lower Rad51 foci formation.

The three additional siRNA sequences siMVP_A, B and C (sequences derived from Ambion) added even more variety to our MVP knockdown phenotypes. Interestingly, two of the sequences rather induced MVP, even though they were designed based on a very advanced algorithm. Finally, the third sequence, siMVP_C, showed efficient

downregulation of MVP and surprisingly had no effect on cell proliferation, providing evidence that MVP can be downregulated without deregulation of the cell cycle. There might exist the possibility that siMVP_C, in concert with the MVP knockdown, mediates a nonspecific effect leading to increased proliferation, which then counteracted the MVP knockdown phenotype. However, the phenotype of siMVP_C best resembles the previous findings in the MVP-knockout mouse model, without additional effect on cell proliferation, indicating that this sequence should be considered for future research on MVP.

Intriguingly, nonspecific effects did not manifest in all cell lines in the same way. Some cell lines, for example the HeLa cells seemed to be “immune” to the siMVP#3-induced off-target effects and did not display any toxicity. Possibly, aggressive cancer cell lines do not react with cell cycle arrest, whereas others still do. Similarly, Fedorov et al. observed that the introduction of toxic siRNA sequences does not induce apoptosis to the same extent in all cell lines tested [479].

The siRNA technique may be a powerful tool to gain a first insight into the function of a protein. However, to our experience, nonspecific effects seem to be ubiquitously present. Thus, results obtained by siRNA technique should be considered with great care and require validation.

3.5.1.4 Mechanisms of Potential Toxicities of RNAi

With a careful design of the siRNAs, some but not all off-target effects may be avoided. As mentioned above, the guide strand is selected by the thermodynamically more instable 5’ end of the RNA duplex. Other than in miRNA processing, the passenger strand of the siRNA is cleaved once the guide strand has been recognized and is bound by Ago2 [480]. For some siRNAs, the guide strand and for others the passenger strand were shown to mediate the off-target effects. Thus, potential off-target effects could derive from an ambiguous strand selection. Moreover, Jackson et al. demonstrated that a perfect match was not necessary for gene regulation and that a sequence with only 11 complementary base pairs could induce gene silencing [481]. As mentioned above, miRNAs often incompletely match their target sequence. Specificity of miRNAs is determined by a “seed” sequence of 7 base pairs at position 2-8 that is complementary to a region in the 3’ UTR of the target mRNA [482–485]. It has been shown that miRNAs with the same “seed” sequence that are otherwise different can regulate translation of the same protein [486]. The Ago2/siRNA-complex does not differ from an Ago2/miRNA-complex and therefore may regulate genes other than the perfect matching mRNA in a miRNA-like manner, introducing unforeseen off-target effects.

In the case of siMVP_A and siMVP_B, both of which did not lead to any reduction in the target gene, the passenger strand may have been selected. Modifications of the passenger sequence can ensure the entrance of only the guide strand into the RISC complex. The sequences for siMVP_A and B were derived from Ambion. However, Ambion sells chemically modified siRNAs, whereas we ordered unmodified siRNAs. Thus, the strand selection may not have been provided.

Strand selection was considered by Brahmsen et al., to be the major determinant for the improvement of siRNA activity, as they performed a screen comparing different chemical modifications on siRNA performance [487]. In literature, numerous approaches have been investigated to enhance strand selection by the introduction of chemical modifications. As an example, 5'-phosphorylation is important for strand selection and, thus 5'-O-methylation of the passenger strand prevents phosphorylation of this strand and thus enhances specific selection of the guide strand [488]. Similarly, 5-nitroindole modification at position 15 of the siRNA passenger strand leads to reduction of off-target effects without impairing the efficiency of the siRNA [489]. Chemical modifications were also investigated to reduce miRNA-like off-target effects. Jackson et al. introduced a 2′-O-methyl modification in position 2, which lowered the thermodynamic stability of the seed region (bp 2-8). As determined by microarray analyses the modified siRNAs affected a reduced number of genes, with similar efficiency in downregulating the target mRNA [490].

Besides classic off-target effects that arise from nonspecific interactions with non-target mRNAs, some siRNA sequences evoke immune responses. However, the mechanism is not fully understood. Certain nucleic acid motifs have been associated with Toll-like receptor recognition, leading to the induction of interferons (IFNs) and inflammatory cytokines [491, 492]. This stimulation is predominantly triggered in immune cells and thus plays a role upon systemic application of RNAi. On the other hand, upregulation of the IFN-mediated pathways were also shown to take place in cell culture [493, 494]. Non-immune cells also dispose over a family of RNA sensors that recognize viral nucleic acids, including RIG-1, MDA-5 and LGP2 [495]. Whereas these sensors may recognize longer RNA duplexes and their interplay with siRNAs is not known, the dsRNA-dependent protein kinase (PKR) is stimulated by dsRNA of only 21 bps [493].

To sum up, commercially available siRNAs are usually modified to enhance the specificity of the strand selection, and analogy of the seed region of the siRNA to known seed regions are avoided. Nevertheless, many carefully selected and modified siRNAs elicit nonspecific effects and the true knockdown-related changes may be difficult to discern. Nonspecific effects may be reduced with lowered siRNA concentrations. It is therefore advised to titrate the siRNA concentration and to use the lowest concentration

necessary. On the same bases, some companies work with pools of siRNAs, targeting different sequences of the same mRNA, which allows for the application of lower concentrations for each individual siRNA. This was also shown to reduce off-target effects in our case. However, for the investigation of a gene with unknown function, it is essential to use sequences “without” off-target effects. Thus, several siRNAs should be applied individually and the phenotypes should be skeptically compared with each other. Best is the validation of an siRNA-induced phenotype by a rescue experiment, where the knockdown protein is complemented by the ectopic expression of a siRNA-resistant variant. However, as in the case of MVP, it is difficult to discern whether the ectopically expressed MVP assembles into functional vaults and thus an unsuccessful rescue may not always be proof for nonspecific effects.

3.5.2 What Did We Learn about MVP?

The precise function of MVP and vaults still has not been elucidated. Our own conclusions on the role of MVP in DNA damage repair are limited due to the technical issues related to the siRNA technique we applied. However, we observed that MVP was induced after treatment with ionizing radiation and by other stress stimuli. Upregulation of MVP by osmotic stress, hypoxia and DNA damaging agents was previously described in literature. Thus, MVP may play a role in stress response or even stress resistance. Furthermore, we observed, that the expression level of MVP was partially regulated through autocrine and/or paracrine signaling.

3.5.2.1 The Role of MVP in DNA Damage Repair

With regard to the contribution of MVP to DNA repair or more precisely to homologous recombination (HR), we are not able to draw a final conclusion. We could not confirm the hypothesis of a putative MVP/PTEN/Rad51 axis. HCT116 PTEN-knockout cells showed a similar decrease of Rad51 levels as the parental HCT116 cell line, indicating that it is not the putative MVP-PTEN interaction that is responsible for reduced Rad51 expression we observed. Furthermore, the knockdown of MVP did not lead to Rad51 repression in all cell lines, but only in those that responded with a cell cycle arrest. This suggests that cell cycle deregulation, induced by off-target effects, but not MVP-depletion determines the Rad51 expression level. As mentioned before, not all cell lines are equally sensitive to the introduction of nonspecific effects [479], which may explain the differential manifestation of the knockdown phenotype. Independent of the siRNA-induced effects, we were not able to confirm the previous finding of a direct interaction of MVP with BRCA2/Rad51 by immunoprecipitation.

Nonetheless, we observed a dose-dependent upregulation of MVP in response to ionizing radiation. However, a strong increase of the MVP levels took place only at 72 hours after irradiation, suggesting a role in stress resistance rather than a direct involvement in DNA repair. Thus, investigations with regard to this late response may reveal more information about the role of MVP in radiation response.

3.5.2.2 Is MVP a General Player in Stress Response?

We found that not only treatment with ionizing radiation, but also the hypoxia-mimicking agent DMOG, increasing cellular confluency or even transfection with certain siRNA sequences led to an increase in MVP expression. Several studies reported that MVP expression was upregulated in response to stress factors such as DNA-damaging agents and ultraviolet rays [378], hyperosmotic stress [496], hyperthermia [497] and hypoxia [498]. MVP was also shown to be induced in virus-infected cell systems [499, 351] or in peripheral blood mononuclear cells (PBMCs) and in liver cells of hepatitis C virus (HCV) patients [500]. Steiner et al. showed that specifically interferon gamma (IFNγ), which is mainly released by T-cells and natural killer (NK) cells upon viral infections, stimulated MVP expression on a transcriptional and translational level [330]. However, Guo et al. performed his experiments in Hep2 cells that do not produce IFNγ, indicating that there are different ways how viral infections induce MVP expression. Similar to viral genomes, siRNAs can trigger cellular responses to the foreign dsRNA, which may rely on specific RNA motifs. We observed did not investigate the responsible mechanism leading to the induction of MVP expression in response to certain siRNA sequences, may it be similar to the viral infection of Hep2 cells or other mechanisms. Among the sequences that induced MVP were the “non-toxic” control siRNA, targeting luciferase, and the sequences siMVP_A and siMVP_C, which resulted in upregulation instead of a downregulation of MVP. Other control siRNAs, such as scramble_A and scramble_B did not induce MVP expression. Therefore, the transfection process alone cannot be the sole cause of MVP induction, nor the mere presence of double-stranded RNA. Thus, sequence-specific recognition by dsRNA sensors or nonspecific effects introduced by the siRNAs may be possible causes of the siRNA-dependent upregulation of MVP.

In response to ionizing radiation (IR), we found that MVP was substantially upregulated at around 72 hours after irradiation. The knockdown of p53 by siRNA reduced radiation-dependent induction of MVP, as had been demonstrated before in human diploid fibroblasts (HDFs) with regard to the senescence-induced increase of MVP [501]. Interestingly, also the basal MVP level was reduced upon p53-depletion, indicating that p53 might play a general role in the regulation of MVP expression. Most of the cancers

cells, for which we determined high MVP expression levels, harbored wild type p53. In senescent cells, phosphorylation of p53 is often increased [502], which may result in enhanced p53-transcriptional activity. However, this was not the case for the cancer cell lines we worked with. Eventually, a more sensitive and more comprehensive assay may be required to precisely determine the activity status of p53 in cancer cells.

Of note, the MVP expression level was difficult to follow, since with increasing cell confluency MVP expression levels increased as well. This upregulation of MVP could be counteracted by replacing the medium with fresh medium or performing the experiments at low cell densities. We learnt that it is the number of cells and conditioning of the supernatant and not the confluency itself that affected MVP expression. Thus, unknown factors released by the cells might induce MVP expression in an autocrine manner, which could explain that increasing the amount of medium, or replacing the medium, reduced the inductive stimuli. Moreover, cellular irradiation seemed to increase secretion of such stimulatory factors. MVP levels increased after irradiation with 10 Gy, even though the cell number remained low and 24-hour medium changes reduced the induction of MVP to a large extent. Furthermore, medium that was conditioned for 48 hours by irradiated cells led to stronger induction of MVP in untreated cells, than conditioned medium from unirradiated cells. Though, again, to find the right control condition was difficult, because non-irradiated cells proliferate faster and the cell number critically influences the amount of factors released. Importantly, we could exclude that low pH and increasing lactate concentrations contribute to the induction of MVP expression.

Stimulation of the EGFR receptor by EGF led to an increase in MVP expression in A549 cells. This cell line expresses aberrant, constitutively active Ras, which has been linked to increased release of EGFR ligands upon irradiation [269, 270]. Furthermore, ADAM metallopeptidase domain 17 (ADAM17), which is involved in the shedding of EGFR ligands, displayed increased activity in response to ionizing radiation (preliminary results obtained by Ashish Sharma, in our group). Thus, EGFR signaling may contribute to radiation-induced MVP expression. Further investigations are required to evaluate the importance of the EGFR in upregulation of MVP upon IR and to elucidate the precise mechanism leading to increased MVP expression.

3.5.2.3 Conclusion

Elucidation of the pathways involved in MVP upregulation by the different stimuli could be a next step. Our observations imply that secreted factors play a crucial role in the regulation of MVP expression. It would be interesting to know if and how the numerous stimuli that lead to the induction of MVP, converge on the signaling level.

Interferon γ has been proposed to act through the JAK/STAT pathway on MVP transcription, even though the main increase in the MVP protein level upon stimulation with IFNγ has been designated to an increased translation rate [330]. IFNγ, according to literature, is not released by solid cancer cells, though respective murine *in vivo* models could shed more light on the putative role of paracrine stimulation of MVP expression in cancer cells by IFNγ.

We found that EGFR-stimulation resulted in an increased MVP expression and Johnson et al. showed that the MVP protein levels were significantly elevated in glioblastoma tumor xenografts expressing the constitutively active EGFRvIII compared to xenografts with wild type EGFR [503]. The exact mechanism by which EGFR leads to MVP upregulation is not known, but EGFR is also known to activate STAT proteins. Interestingly, combined activation of the JAK/STAT and EGFR signaling has been demonstrated to contribute to carcinogenesis [504] and both pathways were found to be constitutively active across most human hepatocellular carcinomas [505]. That MVP is not merely a silent passenger, upregulated by these two pathways, is indicated by two recent publications. Loetsch et al. determined a link between MVP and PI3K-signaling in a glioblastoma cell line. Their data suggest that MVP might interact with EGFR or a binding partner of EGFR, thus enhancing receptor stability or altering receptor recycling [506]. And Losert et al. reported a link between MVP and resistance to the EGFR inhibitor gefitinib. They observed that in hepatocellular carcinoma cells, expression of MVP increased EGFR-independent phosphorylation of Akt, which might explain the increased resistance to EGFR-inhibitors in presence of MVP expression [507]. Probably, MVP not only confers apoptotic resistance to senescent human diploid fibroblast but also to cancers cells, essentially to those harboring wild type p53 and thus may contribute to early carcinogenesis.

References

1. Ferlay J, Steliarova-Foucher E, Lortet-Tieulent J et al. (2013) Cancer incidence and mortality patterns in Europe: estimates for 40 countries in 2012. Eur J Cancer 49(6): pp. 1374–1403
2. Ashley DJ (1969) Colonic cancer arising in polyposis coli. J Med Genet 6(4): pp. 376–378
3. Knudson AG, JR (1971) Mutation and cancer: statistical study of retinoblastoma. Proc Natl Acad Sci U S A 68(4): pp. 820–823
4. Ashley DJ (1969) The two "hit" and multiple "hit" theories of carcinogenesis. Br J Cancer 23(2): pp. 313–328
5. Manchester KL (1995) Theodor Boveri and the origin of malignant tumours. Trends in Cell Biology 5(10): pp. 384–387
6. Hanahan D, Weinberg RA (2011) Hallmarks of Cancer: The Next Generation. Cell 144(5): pp. 646–674
7. Grivennikov SI, Greten FR, Karin M (2010) Immunity, inflammation, and cancer. Cell 140(6): pp. 883–899
8. Peto R, Darby S, Deo H et al. (2000) Smoking, smoking cessation, and lung cancer in the UK since 1950: combination of national statistics with two case-control studies. BMJ 321(7257): pp. 323–329
9. Pirie K, Peto R, Reeves GK et al. (2013) The 21st century hazards of smoking and benefits of stopping: a prospective study of one million women in the UK. Lancet 381(9861): pp. 133–141
10. Turati F, Garavello W, Tramacere I et al. (2013) A meta-analysis of alcohol drinking and oral and pharyngeal cancers: results from subgroup analyses. Alcohol 48(1): pp. 107–118
11. Hashibe M, Brennan P, Chuang S et al. (2009) Interaction between tobacco and alcohol use and the risk of head and neck cancer: pooled analysis in the International Head and Neck Cancer Epidemiology Consortium. Cancer Epidemiol Biomarkers Prev 18(2): pp. 541–550
12. Scheffner M, Werness BA, Huibregtse JM et al. (1990) The E6 oncoprotein encoded by human papillomavirus types 16 and 18 promotes the degradation of p53. Cell 63(6): pp. 1129–1136
13. Ganguly N, Parihar SP (2009) Human papillomavirus E6 and E7 oncoproteins as risk factors for tumorigenesis. J Biosci 34(1): pp. 113–123
14. Matsuzaki K, Murata M, Yoshida K et al. (2007) Chronic inflammation associated with hepatitis C virus infection perturbs hepatic transforming growth factor beta signaling, promoting cirrhosis and hepatocellular carcinoma. Hepatology 46(1): pp. 48–57
15. Hanahan D, Weinberg RA (2000) The hallmarks of cancer. Cell 100(1): pp. 57–70

16. Hollander MC, Blumenthal GM, Dennis PA (2011) PTEN loss in the continuum of common cancers, rare syndromes and mouse models.
Nat Rev Cancer 11(4): pp. 289–301

17. Phatak P, Burger AM (2007) Telomerase and its potential for therapeutic intervention. Br J Pharmacol 152(7): pp. 1003–1011

18. Warburg O, Posener K., Negelein E. (1924) Ueber den Stoffwechsel der Tumoren. Biochemische Zeitschrift(152): pp. 319–344

19. Zhao Y, Butler EB, Tan M (2013) Targeting cellular metabolism to improve cancer therapeutics. Cell Death Dis 4: pp. e532

20. Bergers G, Benjamin LE (2003) Tumorigenesis and the angiogenic switch.
Nat Rev Cancer 3(6): pp. 401–410

21. Mantovani A, Allavena P, Sica A et al. (2008) Cancer-related inflammation.
Nature 454(7203): pp. 436–444

22. Sparmann A, Bar-Sagi D (2004) Ras-induced interleukin-8 expression plays a critical role in tumor growth and angiogenesis. Cancer Cell 6(5): pp. 447–458

23. Soucek L, Lawlor ER, Soto D et al. (2007) Mast cells are required for angiogenesis and macroscopic expansion of Myc-induced pancreatic islet tumors.
Nat Med 13(10): pp. 1211–1218

24. Wu M, Frieboes HB, McDougall SR et al. (2013) The effect of interstitial pressure on tumor growth: coupling with the blood and lymphatic vascular systems.
J Theor Biol 320: pp. 131–151

25. Bristow RG, Hill RP (2008) Hypoxia and metabolism. Hypoxia, DNA repair and genetic instability. Nat Rev Cancer 8(3): pp. 180–192

26. Cairns RA, Kalliomaki T, Hill RP (2001) Acute (Cyclic) Hypoxia Enhances Spontaneous Metastasis of KHT Murine Tumors.
Cancer Research 61(24): pp. 8903–8908

27. Cairns RA, Hill RP (2004) Acute Hypoxia Enhances Spontaneous Lymph Node Metastasis in an Orthotopic Murine Model of Human Cervical Carcinoma.
Cancer Res 64(6): pp. 2054–2061

28. Rofstad EK, Galappathi K, Mathiesen B et al. (2007) Fluctuating and diffusion-limited hypoxia in hypoxia-induced metastasis.
Clin Cancer Res 13(7): pp. 1971–1978

29. Mani SA, Guo W, Liao M et al. (2008) The epithelial-mesenchymal transition generates cells with properties of stem cells. Cell 133(4): pp. 704–715

30. Pardali K, Moustakas A (2007) Actions of TGF-beta as tumor suppressor and pro-metastatic factor in human cancer. Biochim Biophys Acta 1775(1): pp. 21–62

31. Lester RD, Jo M, Montel V et al. (2007) uPAR induces epithelial-mesenchymal transition in hypoxic breast cancer cells. J Cell Biol 178(3): pp. 425–436

32. Cheng Z, Sun B, Wang S et al. (2011) Nuclear factor-kappaB-dependent epithelial to mesenchymal transition induced by HIF-1alpha activation in pancreatic cancer cells under hypoxic conditions. PLoS One 6(8): pp. e23752

33. Zhu G, Huang C, Feng Z et al. (2013) Hypoxia-Induced Snail Expression Through Transcriptional Regulation by HIF-1alpha in Pancreatic Cancer Cells. Dig Dis Sci

34. Thompson EW, Newgreen DF, Tarin D (2005) Carcinoma invasion and metastasis: a role for epithelial-mesenchymal transition?
Cancer Res 65(14): pp. 5991-5; discussion 5995

35. Tarin D, Thompson EW, Newgreen DF (2005) The fallacy of epithelial mesenchymal transition in neoplasia.
Cancer Res 65(14): pp. 5996-6000; discussion 6000-1

36. Trimboli AJ, Fukino K, Bruin A de et al. (2008) Direct Evidence for Epithelial-Mesenchymal Transitions in Breast Cancer. Cancer Res 68(3): pp. 937–945

37. Pollard JW (2004) Tumour-educated macrophages promote tumour progression and metastasis. Nat Rev Cancer 4(1): pp. 71–78

38. Hiratsuka S, Nakamura K, Iwai S et al. (2002) MMP9 induction by vascular endothelial growth factor receptor-1 is involved in lung-specific metastasis.
Cancer Cell 2(4): pp. 289–300

39. Bergers G, Brekken R, McMahon G et al. (2000) Matrix metalloproteinase-9 triggers the angiogenic switch during carcinogenesis. Nat Cell Biol 2(10): pp. 737–744

40. Allavena P, Sica A, Garlanda C et al. (2008) The Yin-Yang of tumor-associated macrophages in neoplastic progression and immune surveillance.
Immunol Rev 222(1): pp. 155–161

41. Meacham CE, Morrison SJ (2013) Tumour heterogeneity and cancer cell plasticity. Nature 501(7467): pp. 328–337

42. Delaney G, Jacob S, Featherstone C et al. (2005) The role of radiotherapy in cancer treatment: estimating optimal utilization from a review of evidence-based clinical guidelines. Cancer 104(6): pp. 1129–1137

43. Levy RP, Schulte RWM (2012) Stereotactic radiosurgery with charged-particle beams: technique and clinical experience. Transl Cancer Res 1(3): pp. 159–172

44. Azzam EI, Jay-Gerin J, Pain D (2012) Ionizing radiation-induced metabolic oxidative stress and prolonged cell injury. Cancer Lett 327(1): pp. 48–60

45. Bertout JA, Patel SA, Simon MC (2008) The impact of O2 availability on human cancer. Nat Rev Cancer 8(12): pp. 967–975

46. Brown JM, Wilson WR (2004) Exploiting tumour hypoxia in cancer treatment. Nat Rev Cancer 4(6): pp. 437–447

47. Terasima T, Tolmach LJ (1963) Variations in several responses of HeLa cells to x-irradiation during the division cycle. Biophys J 3: pp. 11–33

48. Vogelstein B, Lane D, Levine AJ (2000) Surfing the p53 network.
Nature 408(6810): pp. 307–310

49. Chamberlain WE, Young BR (1937) Should the Method of Coutard be Applied in All Cases of Cancer Treated by Roentgen Rays? Radiology 29(2): pp. 186–189

50. (2013) International Association for the Study of Lung Cancer (2013, September 4). Accelerated radiotherapy more efficient than current practice, study suggests. ScienceDaily

51. Guckenberger M, Andratschke N, Alheit H et al. (2013) Definition of stereotactic body radiotherapy: Principles and practice for the treatment of stage I non-small cell lung cancer (Definition der stereotaktischen Strahlentherapie : Behandlung des nichtkleinzelligen Bronchialkarzinoms (NSCLC) Grad I).
Strahlenther Onkol (Article not assigned to an issue)

52. Berman AT, Rengan R (2008) New approaches to radiotherapy as definitive treatment for inoperable lung cancer.
Semin Thorac Cardiovasc Surg 20(3): pp. 188–197

53. Lanni TB, JR, Grills IS, Kestin LL et al. (2011) Stereotactic radiotherapy reduces treatment cost while improving overall survival and local control over standard fractionated radiation therapy for medically inoperable non-small-cell lung cancer.
Am J Clin Oncol 34(5): pp. 494–498

54. Pearce AG, Segura TM, Rintala AC et al. (2001) The Generation and Characterization of a Radiation-Resistant Model System to Study Radioresistance in Human Breast Cancer Cells. Radiation Research 156(6): pp. 739–750

55. Mihatsch J, Toulany M, Bareiss PM et al. (2011) Selection of radioresistant tumor cells and presence of ALDH1 activity in vitro.
Radiotherapy and Oncology 99(3): pp. 300–306

56. Weichselbaum RR, Dahlberg W, Beckett M et al. (1986) Radiation-resistant and repair-proficient human tumor cells may be associated with radiotherapy failure in head- and neck-cancer patients. Proc Natl Acad Sci U S A 83(8): pp. 2684–2688

57. Tyrsina EG, Slanina SV, Kakpakova ES et al. (2005) Isolation and Characterization of Highly Radioresistant Malignant Hamster Fibroblasts that Survive Acute γ Irradiation with 20 Gy. Radiation Research 164(6): pp. 745–754

58. Brown DC, Trott KR (1994) Clonal heterogeneity in the progeny of HeLa cells which survive X-irradiation. Int J Radiat Biol 66(2): pp. 151–155

59. Tarnawski R, Kummermehr J, Trott KR (1998) The radiosensitivity of recurrent clones of an irradiated murine squamous cell carcinoma in the in vitro megacolony system. Radiother Oncol 46(2): pp. 209–214

60. Bao S, Wu Q, McLendon RE et al. (2006) Glioma stem cells promote radioresistance by preferential activation of the DNA damage response.
Nature 444(7120): pp. 756–760

61. Zafarana G, Bristow R (2010) Tumor senescence and radioresistant tumor-initiating cells (TICs): let sleeping dogs lie! Breast Cancer Research 12(4): 111

62. Wang W, Wu S, Liu J et al. (2013) MYC regulation of CHK1 and CHK2 promotes radioresistance in a stem cell-like population of nasopharyngeal carcinoma cells. Cancer Res 73(3): pp. 1219–1231

63. Longley DB, Harkin DP, Johnston PG (2003) 5-fluorouracil: mechanisms of action and clinical strategies. Nat Rev Cancer 3(5): pp. 330–338

64. Ewald B, Sampath D, Plunkett W (2007) H2AX phosphorylation marks gemcitabine-induced stalled replication forks and their collapse upon S-phase checkpoint abrogation. Mol Cancer Ther 6(4): pp. 1239–1248

65. Lawrence TS, Blackstock AW, McGinn C (2003) The mechanism of action of radiosensitization of conventional chemotherapeutic agents. Semin Radiat Oncol 13(1): pp. 13–21

66. Jordan P, Carmo-Fonseca M (2000) Molecular mechanisms involved in cisplatin cytotoxicity. Cell Mol Life Sci 57(8-9): pp. 1229–1235

67. Florea A, Büsselberg D (2011) Cisplatin as an Anti-Tumor Drug: Cellular Mechanisms of Activity, Drug Resistance and Induced Side Effects. Cancers 3(1): pp. 1351–1371

68. Montecucco A, Biamonti G (2007) Cellular response to etoposide treatment. Cancer Lett 252(1): pp. 9–18

69. Paccagnella A, Ghi MG, Loreggian L et al. (2010) Concomitant chemoradiotherapy versus induction docetaxel, cisplatin and 5 fluorouracil (TPF) followed by concomitant chemoradiotherapy in locally advanced head and neck cancer: a phase II randomized study. Ann Oncol 21(7): pp. 1515–1522

70. Lorch JH, Goloubeva O, Haddad RI et al. (2011) Induction chemotherapy with cisplatin and fluorouracil alone or in combination with docetaxel in locally advanced squamous-cell cancer of the head and neck: long-term results of the TAX 324 randomised phase 3 trial. Lancet Oncol 12(2): pp. 153–159

71. Ralph SJ, Rodriguez-Enriquez S, Neuzil J et al. (2010) Bioenergetic pathways in tumor mitochondria as targets for cancer therapy and the importance of the ROS-induced apoptotic trigger. Mol Aspects Med 31(1): pp. 29–59

72. Bokemeyer C, van Cutsem E, Rougier P et al. (2012) Addition of cetuximab to chemotherapy as first-line treatment for KRAS wild-type metastatic colorectal cancer: Pooled analysis of the CRYSTAL and OPUS randomised clinical trials. Eur J Cancer 48(10): pp. 1466–1475

73. Presta LG, Chen H, O'Connor SJ et al. (1997) Humanization of an anti-vascular endothelial growth factor monoclonal antibody for the therapy of solid tumors and other disorders. Cancer Res 57(20): pp. 4593–4599

74. Winkler F, Kozin SV, Tong RT et al. (2004) Kinetics of vascular normalization by VEGFR2 blockade governs brain tumor response to radiation: role of oxygenation, angiopoietin-1, and matrix metalloproteinases. Cancer Cell 6(6): pp. 553–563

75. Hoang T, Huang S, Armstrong E et al. (2012) Enhancement of radiation response with bevacizumab. J Exp Clin Cancer Res 31(37)

76. Mangoni M, Vozenin M, Biti G et al. (2012) Normal tissues toxicities triggered by combined anti-angiogenic and radiation therapies: hurdles might be ahead. Br J Cancer 107(2): pp. 308–314

77. Fokas E, Im JH, Hill S et al. (2012) Dual inhibition of the PI3K/mTOR pathway increases tumor radiosensitivity by normalizing tumor vasculature. Cancer Res 72(1): pp. 239–248

78. Liu P, Cheng H, Roberts TM et al. (2009) Targeting the phosphoinositide 3-kinase pathway in cancer. Nat Rev Drug Discov 8(8): pp. 627–644

79. Fokas E, Yoshimura M, Prevo R et al. (2012) NVP-BEZ235 and NVP-BGT226, dual phosphatidylinositol 3-kinase/mammalian target of rapamycin inhibitors, enhance tumor and endothelial cell radiosensitivity. Radiat Oncol 7(48)

80. Mukherjee B, Tomimatsu N, Amancherla K et al. (2012) The dual PI3K/mTOR inhibitor NVP-BEZ235 is a potent inhibitor of ATM- and DNA-PKCs-mediated DNA damage responses. Neoplasia 14(1): pp. 34–43

81. Ismail IH, Martensson S, Moshinsky D et al. (2004) SU11752 inhibits the DNA-dependent protein kinase and DNA double-strand break repair resulting in ionizing radiation sensitization. Oncogene 23(4): pp. 873–882

82. Zhao Y, Thomas HD, Batey MA et al. (2006) Preclinical evaluation of a potent novel DNA-dependent protein kinase inhibitor NU7441.
Cancer Res 66(10): pp. 5354–5362

83. Shaheen FS, Znojek P, Fisher A et al. (2011) Targeting the DNA Double Strand Break Repair Machinery in Prostate Cancer. PLoS One 6(5): pp. e20311

84. Chalmers AJ, Lakshman M, Chan N et al. (2010) Poly(ADP-ribose) polymerase inhibition as a model for synthetic lethality in developing radiation oncology targets. Semin Radiat Oncol 20(4): pp. 274–281

85. Yap TA, Sandhu SK, Carden CP et al. (2011) Poly(ADP-ribose) polymerase (PARP) inhibitors: Exploiting a synthetic lethal strategy in the clinic.
CA Cancer J Clin 61(1): pp. 31–49

86. Dungey FA, Löser DA, Chalmers AJ (2008) Replication-Dependent Radiosensitization of Human Glioma Cells by Inhibition of Poly(ADP-Ribose) Polymerase: Mechanisms and Therapeutic Potential.
Int J Radiat Oncol Biol Phys 72(4): pp. 1188–1197

87. Löser DA, Shibata A, Shibata AK et al. (2010) Sensitization to Radiation and Alkylating Agents by Inhibitors of Poly(ADP-ribose) Polymerase Is Enhanced in Cells Deficient in DNA Double-Strand Break Repair.
Mol Cancer Ther 9(6): pp. 1775–1787

88. Powell C, Mikropoulos C, Kaye SB et al. (2010) Preclinical and clinical evaluation of PARP inhibitors as tumour-specific radiosensitisers.
Cancer Treat Rev 36(7): pp. 566–575

89. Bucher N, Britten CD (2008) G2 checkpoint abrogation and checkpoint kinase-1 targeting in the treatment of cancer. Br J Cancer 98(3): pp. 523–528

90. Chen T, Stephens PA, Middleton FK et al. (2012) Targeting the S and G2 checkpoint to treat cancer.
Special Issue on Cancer Dev 17(5–6): pp. 194–202

91. Graves PR, Yu L, Schwarz JK et al. (2000) The Chk1 protein kinase and the Cdc25C regulatory pathways are targets of the anticancer agent UCN-01.
J Biol Chem 275(8): pp. 5600–5605

92. Mitchell JB, Choudhuri R, Fabre K et al. (2010) In vitro and in vivo radiation sensitization of human tumor cells by a novel checkpoint kinase inhibitor, AZD7762.
Clin Cancer Res 16(7): pp. 2076–2084

93. Ma CX, Cai S, Li S et al. (2012) Targeting Chk1 in p53-deficient triple-negative breast cancer is therapeutically beneficial in human-in-mouse tumor models. J Clin Invest 122(4): pp. 1541–1552

94. Ma CX, Janetka JW, Piwnica-Worms H (2011) Death by releasing the breaks: CHK1 inhibitors as cancer therapeutics. Trends Mol Med 17(2): pp. 88–96

95. Mitchell C, Park M, Eulitt P et al. (2010) Poly(ADP-ribose) polymerase 1 modulates the lethality of CHK1 inhibitors in carcinoma cells. Mol Pharmacol 78(5): pp. 909–917

96. Tang Y, Hamed HA, Poklepovic A et al. (2012) Poly(ADP-ribose) polymerase 1 modulates the lethality of CHK1 inhibitors in mammary tumors. Mol Pharmacol 82(2): pp. 322–332

97. Thompson R, Eastman A (2013) The cancer therapeutic potential of Chk1 inhibitors: how mechanistic studies impact on clinical trial design. Br J Clin Pharmacol 76(3): pp. 358–369

98. Jorissen RN, Walker F, Pouliot N et al. (2003) Epidermal growth factor receptor: mechanisms of activation and signalling. Exp Cell Res 284(1): pp. 31–53

99. Olayioye MA, Graus-Porta D, Beerli RR et al. (1998) ErbB-1 and ErbB-2 acquire distinct signaling properties dependent upon their dimerization partner. Mol Cell Biol 18(9): pp. 5042–5051

100. Higashiyama S, Iwabuki H, Morimoto C et al. (2008) Membrane-anchored growth factors, the epidermal growth factor family: beyond receptor ligands. Cancer Sci 99(2): pp. 214–220

101. Jura N, Endres NF, Engel K et al. (2009) Mechanism for activation of the EGF receptor catalytic domain by the juxtamembrane segment. Cell 137(7): pp. 1293–1307

102. Coskun Ü, Simons K (2011) Cell Membranes: The Lipid Perspective. Structure 19(11): pp. 1543–1548

103. Arkhipov A, Shan Y, Das R et al. (2013) Architecture and Membrane Interactions of the EGF Receptor. Cell 152(3): pp. 557–569

104. Huang F, Khvorova A, Marshall W et al. (2004) Analysis of clathrin-mediated endocytosis of epidermal growth factor receptor by RNA interference. J Biol Chem 279(16): pp. 16657–16661

105. Goh LK, Huang F, Kim W et al. (2010) Multiple mechanisms collectively regulate clathrin-mediated endocytosis of the epidermal growth factor receptor. J Cell Biol 189(5): pp. 871–883

106. Danglot L, Chaineau M, Dahan M et al. (2010) Role of TI-VAMP and CD82 in EGFR cell-surface dynamics and signaling. J Cell Sci 123(Pt 5): pp. 723–735

107. Walz HA, Shi X, Chouinard M et al. (2010) Isoform-specific regulation of Akt signaling by the endosomal protein WDFY2. J Biol Chem 285(19): pp. 14101–14108

108. Hyatt DC, Ceresa BP (2008) Cellular localization of the activated EGFR determines its effect on cell growth in MDA-MB-468 cells. Exp Cell Res 314(18): pp. 3415–3425

109. Lin SY, Makino K, Xia W et al. (2001) Nuclear localization of EGF receptor and its potential new role as a transcription factor. Nat Cell Biol 3(9): pp. 802–808

110. Huo L, Wang Y, Xia W et al. (2010) RNA helicase A is a DNA-binding partner for EGFR-mediated transcriptional activation in the nucleus. Proc Natl Acad Sci U S A 107(37): pp. 16125–16130

111. Lo H, Hsu S, Ali-Seyed M et al. (2005) Nuclear interaction of EGFR and STAT3 in the activation of the iNOS/NO pathway. Cancer Cell 7(6): pp. 575–589

112. Mills IG (2012) Nuclear translocation and functions of growth factor receptors. Seminars in Cell & Developmental Biology 23(2): pp. 165–171

113. Toulany M, Schickfluss T, Fattah KR et al. (2011) Function of erbB receptors and DNA-PKcs on phosphorylation of cytoplasmic and nuclear Akt at S473 induced by erbB1 ligand and ionizing radiation. Radiother Oncol 101(1): pp. 140–146

114. Roepstorff K, Grandal MV, Henriksen L et al. (2009) Differential effects of EGFR ligands on endocytic sorting of the receptor. Traffic 10(8): pp. 1115–1127

115. Longva KE, Blystad FD, Stang E et al. (2002) Ubiquitination and proteasomal activity is required for transport of the EGF receptor to inner membranes of multivesicular bodies. J Cell Biol 156(5): pp. 843–854

116. Zaczek A, Brandt B, Bielawski KP (2005) The diverse signaling network of EGFR, HER2, HER3 and HER4 tyrosine kinase receptors and the consequences for therapeutic approaches. Histol Histopathol 20(3): pp. 1005–1015

117. Ang KK, Berkey BA, Tu X et al. (2002) Impact of epidermal growth factor receptor expression on survival and pattern of relapse in patients with advanced head and neck carcinoma. Cancer Res 62(24): pp. 7350–7356

118. Suzuki S, Dobashi Y, Sakurai H et al. (2005) Protein overexpression and gene amplification of epidermal growth factor receptor in nonsmall cell lung carcinomas. An immunohistochemical and fluorescence in situ hybridization study. Cancer 103(6): pp. 1265–1273

119. Hanawa M, Suzuki S, Dobashi Y et al. (2006) EGFR protein overexpression and gene amplification in squamous cell carcinomas of the esophagus. Int J Cancer 118(5): pp. 1173–1180

120. Temam S, Kawaguchi H, El-Naggar AK et al. (2007) Epidermal growth factor receptor copy number alterations correlate with poor clinical outcome in patients with head and neck squamous cancer. J Clin Oncol 25(16): pp. 2164–2170

121. Selvaggi G, Novello S, Torri V et al. (2004) Epidermal growth factor receptor overexpression correlates with a poor prognosis in completely resected non-small-cell lung cancer. Annals of Oncology 15(1): pp. 28–32

122. Rokita M, Stec R, Bodnar L et al. (2013) Overexpression of epidermal growth factor receptor as a prognostic factor in colorectal cancer on the basis of the Allred scoring system. Onco Targets Ther 6: pp. 967–976

123. Schiff BA, McMurphy AB, Jasser SA et al. (2004) Epidermal growth factor receptor (EGFR) is overexpressed in anaplastic thyroid cancer, and the EGFR inhibitor gefitinib inhibits the growth of anaplastic thyroid cancer. Clin Cancer Res 10(24): pp. 8594–8602

124. Vogt U, Bielawski K, Schlotter CM et al. (1998) Amplification of erbB-4 oncogene occurs less frequently than that of erbB-2 in primary human breast cancer. Gene 223(1-2): pp. 375–380

125. Gilmour LM, Macleod KG, McCaig A et al. (2001) Expression of erbB-4/HER-4 growth factor receptor isoforms in ovarian cancer. Cancer Res 61(5): pp. 2169–2176

126. Lee JC, Wang S, Chow N et al. (2002) Investigation of the prognostic value of coexpressed erbB family members for the survival of colorectal cancer patients after curative surgery. Eur J Cancer 38(8): pp. 1065–1071

127. Normanno N, Luca A de, Bianco C et al. (2006) Epidermal growth factor receptor (EGFR) signaling in cancer. Gene 366(1): pp. 2–16

128. Zhang K, Sun J, Liu N et al. (1996) Transformation of NIH 3T3 Cells by HER3 or HER4 Receptors Requires the Presence of HER1 or HER2. J Biol Chem 271(7): pp. 3884–3890

129. Campiglio M, Locatelli A, Olgiati C et al. (2004) Inhibition of proliferation and induction of apoptosis in breast cancer cells by the epidermal growth factor receptor (EGFR) tyrosine kinase inhibitor ZD1839 ('Iressa') is independent of EGFR expression level. J Cell Physiol 198(2): pp. 259–268

130. Normanno N, Campiglio M, De LA et al. (2002) Cooperative inhibitory effect of ZD1839 (Iressa) in combination with trastuzumab (Herceptin) on human breast cancer cell growth. Ann Oncol 13(1): pp. 65–72

131. Luca A de, Arra C, D'Antonio A et al. (2000) Simultaneous blockage of different EGF-like growth factors results in efficient growth inhibition of human colon carcinoma xenografts. Oncogene 19(51): pp. 5863–5871

132. Andl CD, Mizushima T, Nakagawa H et al. (2003) Epidermal growth factor receptor mediates increased cell proliferation, migration, and aggregation in esophageal keratinocytes in vitro and in vivo. J Biol Chem 278(3): pp. 1824–1830

133. Tsutsui S, Ohno S, Murakami S et al. (2002) Prognostic value of c-erbB2 expression in breast cancer. J Surg Oncol 79(4): pp. 216–223

134. Piccart M, Lohrisch C, Di Leo A et al. (2001) The predictive value of HER2 in breast cancer. Oncology 61(Suppl 2): pp. 73–82

135. Xia W, Lau YK, Zhang HZ et al. (1999) Combination of EGFR, HER-2/neu, and HER-3 is a stronger predictor for the outcome of oral squamous cell carcinoma than any individual family members. Clin Cancer Res 5(12): pp. 4164–4174

136. Abd El-Rehim DM, Pinder SE, Paish CE et al. (2004) Expression and co-expression of the members of the epidermal growth factor receptor (EGFR) family in invasive breast carcinoma. Br J Cancer 91(8): pp. 1532–1542

137. Bonner JA, Harari PM, Giralt J et al. (2006) Radiotherapy plus cetuximab for squamous-cell carcinoma of the head and neck. N Engl J Med 354(6): pp. 567–578

138. Bonner JA, Harari PM, Giralt J et al. (2010) Radiotherapy plus cetuximab for locoregionally advanced head and neck cancer: 5-year survival data from a phase 3 randomised trial, and relation between cetuximab-induced rash and survival. Lancet Oncol 11(1): pp. 21–28

139. Allegra CJ, Jessup JM, Somerfield MR et al. (2009) American Society of Clinical Oncology provisional clinical opinion: testing for KRAS gene mutations in patients with metastatic colorectal carcinoma to predict response to anti-epidermal growth factor receptor monoclonal antibody therapy. J Clin Oncol 27(12): pp. 2091–2096

140. Kim R (2009) Cetuximab and panitumumab: are they interchangeable? Lancet Oncol 10(12): 1140–1141

141. Resch G, Schaberl-Moser R, Kier P et al. (2011) Infusion reactions to the chimeric EGFR inhibitor cetuximab--change to the fully human anti-EGFR monoclonal antibody panitumumab is safe. Ann Oncol 22(2): 486–487

142. Saif MW, Kaley K, Chu E et al. (2010) Safety and efficacy of panitumumab therapy after progression with cetuximab: experience at two institutions. Clin Colorectal Cancer 9(5): pp. 315–318

143. Garred P, Michaelsen TE, Aase A (1989) The IgG subclass pattern of complement activation depends on epitope density and antibody and complement concentration. Scand J Immunol 30(3): pp. 379–382

144. Bindon CI, Hale G, Bruggemann M et al. (1988) Human monoclonal IgG isotypes differ in complement activating function at the level of C4 as well as C1q. J Exp Med 168(1): pp. 127–142

145. Tao MH, Smith RI, Morrison SL (1993) Structural features of human immunoglobulin G that determine isotype-specific differences in complement activation. J Exp Med 178(2): pp. 661–667

146. Schneider-Merck T, van Lammerts Bueren JJ, Berger S et al. (2010) Human IgG2 Antibodies against Epidermal Growth Factor Receptor Effectively Trigger Antibody-Dependent Cellular Cytotoxicity but, in Contrast to IgG1, Only by Cells of Myeloid Lineage. The Journal of Immunology 184(1): pp. 512–520

147. Montagut C, Dalmases A, Bellosillo B et al. (2012) Identification of a mutation in the extracellular domain of the Epidermal Growth Factor Receptor conferring cetuximab resistance in colorectal cancer. Nat Med 18(2): pp. 221–223

148. Bardelli A, Siena S (2010) Molecular mechanisms of resistance to cetuximab and panitumumab in colorectal cancer. J Clin Oncol 28(7): pp. 1254–1261

149. Di Nicolantonio F, Martini M, Molinari F et al. (2008) Wild-type BRAF is required for response to panitumumab or cetuximab in metastatic colorectal cancer. J Clin Oncol 26(35): pp. 5705–5712

150. Giampieri R, Scartozzi M, Del Prete M et al. (2013) Molecular biomarkers of resistance to anti-EGFR treatment in metastatic colorectal cancer, from classical to innovation. Critical Reviews in Oncology/Hematology 88(2): pp. 272–283

151. Jun HJ, Bronson RT, Charest A (2013) Inhibition of EGFR induces a c-MET driven stem cell population in Glioblastoma. Stem Cells (Ahead of print)

152. Bardelli A, Corso S, Bertotti A et al. (2013) Amplification of the MET receptor drives resistance to anti-EGFR therapies in colorectal cancer. Cancer Discov 3(6): pp. 658–673

153. Lynch TJ, Bell DW, Sordella R et al. (2004) Activating Mutations in the Epidermal Growth Factor Receptor Underlying Responsiveness of Non–Small-Cell Lung Cancer to Gefitinib. N Engl J Med 350(21): pp. 2129–2139

154. Mitsudomi T, Yatabe Y (2007) Mutations of the epidermal growth factor receptor gene and related genes as determinants of epidermal growth factor receptor tyrosine kinase inhibitors sensitivity in lung cancer. Cancer Sci 98(12): pp. 1817–1824

155. Laurie SA, Goss GD (2013) Role of Epidermal Growth Factor Receptor Inhibitors in Epidermal Growth Factor Receptor Wild-Type Non–Small-Cell Lung Cancer. J Clin Oncol 31(8): pp. 1061–1069

156. Shepherd FA, Rodrigues Pereira J, Ciuleanu T et al. (2005) Erlotinib in previously treated non-small-cell lung cancer. N Engl J Med 353(2): pp. 123–132

157. Zhu C, da Cunha Santos G, Ding K et al. (2008) Role of KRAS and EGFR as biomarkers of response to erlotinib in National Cancer Institute of Canada Clinical Trials Group Study BR.21. J Clin Oncol 26(26): pp. 4268–4275

158. Gelsomino F, Agustoni F, Niger M et al. (2013) Epidermal Growth Factor Receptor Tyrosine Kinase Inhibitor Treatment in Patients With EGFR Wild-Type Non–Small-Cell Lung Cancer: The Never-Ending Story. J Clin Oncol 31(26): pp. 3291–3293

159. Geyer CE, Forster J, Lindquist D et al. (2006) Lapatinib plus capecitabine for HER2-positive advanced breast cancer. N Engl J Med 355(26): pp. 2733–2743

160. Cameron D, Casey M, Press M et al. (2008) A phase III randomized comparison of lapatinib plus capecitabine versus capecitabine alone in women with advanced breast cancer that has progressed on trastuzumab: updated efficacy and biomarker analyses. Breast Cancer Res Treat 112(3): pp. 533–543

161. Blivet-Van Eggelpoël M, Chettouh H, Fartoux L et al. (2012) Epidermal growth factor receptor and HER-3 restrict cell response to sorafenib in hepatocellular carcinoma cells. Journal of Hepatology 57(1): pp. 108–115

162. Ezzoukhry Z, Louandre C, Trecherel E et al. (2012) EGFR activation is a potential determinant of primary resistance of hepatocellular carcinoma cells to sorafenib. Int J Cancer 131(12): pp. 2961–2969

163. Polli JW, Humphreys JE, Harmon KA et al. (2008) The Role of Efflux and Uptake Transporters in N-{3-Chloro-4-[(3-fluorobenzyl)oxy]phenyl}-6-[5-({[2-(methylsulfonyl)ethyl]amino}methyl)-2-furyl]-4-quinazolinamine (GW572016, Lapatinib) Disposition and Drug Interactions. Drug Metab Dispos 36(4): pp. 695–701

164. Galetti M, Alfieri RR, Cavazzoni A et al. (2010) Functional characterization of gefitinib uptake in non-small cell lung cancer cell lines. Biochem Pharmacol 80(2): pp. 179–187

165. Kohler G, Milstein C (1975) Continuous cultures of fused cells secreting antibody of predefined specificity. Nature 256(5517): pp. 495–497

166. Smith GP (1985) Filamentous fusion phage: novel expression vectors that display cloned antigens on the virion surface. Science 228(4705): pp. 1315–1317

167. McCafferty J, Griffiths AD, Winter G et al. (1990) Phage antibodies: filamentous phage displaying antibody variable domains. Nature 348(6301): pp. 552–554

168. Lahlou A, Blanchet B, Carvalho M et al. (2009) Mechanically-induced aggregation of the monoclonal antibody cetuximab. Ann Pharm Fr 67(5): pp. 340–352

169. Nelson AL (2010) Antibody fragments: hope and hype. MAbs 2(1): pp. 77–83

170. Ward ES, Martinez C, Vaccaro C et al. (2005) From sorting endosomes to exocytosis: association of Rab4 and Rab11 GTPases with the Fc receptor, FcRn, during recycling. Mol Biol Cell 16(4): pp. 2028–2038

171. Yokota T, Milenic DE, Whitlow M et al. (1992) Rapid tumor penetration of a single-chain Fv and comparison with other immunoglobulin forms. Cancer Res 52(12): pp. 3402–3408

172. Skerra A (2007) Alternative non-antibody scaffolds for molecular recognition. Curr Opin Biotechnol 18(4): pp. 295–304

173. Gebauer M, Skerra A (2009) Engineered protein scaffolds as next-generation antibody therapeutics. Curr Opin Chem Biol 13(3): pp. 245–255

174. Weidle UH, Auer J, Brinkmann U et al. (2013) The Emerging Role of New Protein Scaffold-based Agents for Treatment of Cancer. Cancer Genomics Proteomics 10(4): pp. 155–168

175. Moore SJ, Leung CL, Cochran JR (2012) Knottins: disulfide-bonded therapeutic and diagnostic peptides. Drug Discovery Today: Technologies 9(1): pp. e3–11

176. Lipovsek D (2011) Adnectins: engineered target-binding protein therapeutics. Protein Eng Des Sel 24(1-2): pp. 3–9

177. Gebauer M, Skerra A (2012) Anticalins small engineered binding proteins based on the lipocalin scaffold. Methods Enzymol 503: pp. 157–188

178. Ranasinghe S, McManus DP (2013) Structure and function of invertebrate Kunitz serine protease inhibitors. Dev Comp Immunol 39(3): pp. 219–227

179. Silverman J, Liu Q, Bakker A et al. (2005) Multivalent avimer proteins evolved by exon shuffling of a family of human receptor domains. Nat Biotechnol 23(12): pp. 1556–1561

180. Grabulovski D, Kaspar M, Neri D (2007) A Novel, Non-immunogenic Fyn SH3-derived Binding Protein with Tumor Vascular Targeting Properties. Journal of Biological Chemistry 282(5): pp. 3196–3204

181. Schlatter D, Brack S, Banner DW et al. (2012) Generation, characterization and structural data of chymase binding proteins based on the human Fyn kinase SH3 domain. MAbs 4(4): pp. 497–508

182. Allen JE, Ferrini R, Dicker DT et al. (2012) Targeting TRAIL death receptor 4 with trivalent DR4 Atrimer complexes. Mol Cancer Ther 11(10): pp. 2087–2095

183. Feldwisch J, Tolmachev V (2012) Engineering of affibody molecules for therapy and diagnostics. Methods Mol Biol 899: pp. 103–126

184. Tamaskovic R, Simon M, Stefan N et al. (2012) Designed ankyrin repeat proteins (DARPins) from research to therapy. Meth. Enzymol. 503: pp. 101–134

185. Ebersbach H, Fiedler E, Scheuermann T et al. (2007) Affilin-novel binding molecules based on human gamma-B-crystallin, an all beta-sheet protein. J Mol Biol 372(1): pp. 172–185

186. Mirecka EA, Hey T, Fiedler U et al. (2009) Affilin molecules selected against the human papillomavirus E7 protein inhibit the proliferation of target cells. J Mol Biol 390(4): pp. 710–721

187. Parmeggiani F, Pellarin R, Larsen AP et al. (2008) Designed armadillo repeat proteins as general peptide-binding scaffolds: consensus design and computational optimization of the hydrophobic core. J Mol Biol 376(5): pp. 1282–1304

188. Varadamsetty G, Tremmel D, Hansen S et al. (2012) Designed Armadillo repeat proteins: library generation, characterization and selection of peptide binders with high specificity. J Mol Biol 424(1-2): pp. 68–87

189. Mosavi LK, Cammett TJ, Desrosiers DC et al. (2004) The ankyrin repeat as molecular architecture for protein recognition. Protein Sci 13(6): pp. 1435–1448

190. Stumpp MT, Binz HK, Amstutz P (2008) DARPins: a new generation of protein therapeutics. Drug Discov Today 13(15-16): pp. 695–701

191. Breeden L, Nasmyth K (1987) Similarity between cell-cycle genes of budding yeast and fission yeast and the Notch gene of Drosophila. Nature 329(6140): pp. 651–654

192. Zweifel ME, Leahy DJ, Hughson FM et al. (2003) Structure and stability of the ankyrin domain of the Drosophila Notch receptor. Protein Sci 12(11): pp. 2622–2632

193. Binz HK, Stumpp MT, Forrer P et al. (2003) Designing repeat proteins: well-expressed, soluble and stable proteins from combinatorial libraries of consensus ankyrin repeat proteins. J Mol Biol 332(2): pp. 489–503

194. Mosavi LK, Peng Z (2003) Structure-based substitutions for increased solubility of a designed protein. Protein Eng 16(10): pp. 739–745

195. Wetzel SK, Settanni G, Kenig M et al. (2008) Folding and unfolding mechanism of highly stable full-consensus ankyrin repeat proteins. J Mol Biol 376(1): pp. 241–257

196. Simon M, Zangemeister-Wittke U, Plückthun A (2012) Facile double-functionalization of designed ankyrin repeat proteins using click and thiol chemistries. Bioconjug Chem 23(2): pp. 279–286

197. Dreier B, Plückthun A (2011) Ribosome display: a technology for selecting and evolving proteins from large libraries. Methods Mol Biol 687: pp. 283–306

198. Steiner D, Forrer P, Plückthun A (2008) Efficient selection of DARPins with sub-nanomolar affinities using SRP phage display. J Mol Biol 382(5): pp. 1211–1227

199. Campochiaro PA, Channa R, Berger BB et al. (2013) Treatment of diabetic macular edema with a designed ankyrin repeat protein that binds vascular endothelial growth factor: a phase I/II study. Am J Ophthalmol 155(4): pp. 697-704, 704.e1-2

200. Stahl A, Stumpp MT, Schlegel A et al. (2013) Highly potent VEGF-A-antagonistic DARPins as anti-angiogenic agents for topical and intravitreal applications. Angiogenesis 16(1): pp. 101–111

201. Zahnd C, Pecorari F, Straumann N et al. (2006) Selection and characterization of Her2 binding-designed ankyrin repeat proteins. J Biol Chem 281(46): pp. 35167–35175

202. Boersma YL, Chao G, Steiner D et al. (2011) Bispecific designed ankyrin repeat proteins (DARPins) targeting epidermal growth factor receptor inhibit A431 cell proliferation and receptor recycling. J Biol Chem 286(48): pp. 41273–41285

203. Stefan N, Martin-Killias P, Wyss-Stoeckle S et al. (2011) DARPins recognizing the tumor-associated antigen EpCAM selected by phage and ribosome display and engineered for multivalency. J Mol Biol 413(4): pp. 826–843

204. Zahnd C, Kawe M, Stumpp MT et al. (2010) Efficient tumor targeting with high-affinity designed ankyrin repeat proteins: effects of affinity and molecular size. Cancer Res. 70(4): pp. 1595–1605

205. Martin-Killias P, Patricia M, Stefan N et al. (2011) A novel fusion toxin derived from an EpCAM-specific designed ankyrin repeat protein has potent antitumor activity. Clin Cancer Res 17(1): pp. 100–110

206. Winkler J, Martin-Killias P, Pluckthun A et al. (2009) EpCAM-targeted delivery of nanocomplexed siRNA to tumor cells with designed ankyrin repeat proteins. Mol Cancer Ther 8(9): pp. 2674–2683

207. Jost C, Schilling J, Tamaskovic R et al. (2013) Structural Basis for Eliciting a Cytotoxic Effect in HER2-Overexpressing Cancer Cells via Binding to the Extracellular Domain of HER2. Structure 21(11): pp. 1979–1991

208. Seely JE, Richey CW (2001) Use of ion-exchange chromatography and hydrophobic interaction chromatography in the preparation and recovery of polyethylene glycol-linked proteins. J Chromatogr A 908(1-2): pp. 235–241

209. MacLeod CL, Luk A, Castagnola J et al. (1986) EGF induces cell cycle arrest of A431 human epidermoid carcinoma cells. J Cell Physiol 127(1): pp. 175–182

210. Konger RL, Chan TC (1993) Epidermal growth factor induces terminal differentiation in human epidermoid carcinoma cells. J. Cell. Physiol. 156(3): pp. 515–521

211. Rosdy M, Bernard BA, Schmidt R et al. (1986) Incomplete epidermal differentiation of A431 epidermoid carcinoma cells. In Vitro Cell Dev Biol 22(5): pp. 295–300

212. Rosdy M (1988) Opposite effects of EGF on involucrin accumulation of A431 keratinocytes and a variant which is not growth-arrested by EGF. In Vitro Cell Dev Bio 24(11): pp. 1127–1132

213. Ramana CV, Chatterjee-Kishore M, Nguyen H et al. (2000) Complex roles of Stat1 in regulating gene expression. Oncogene 19(21): pp. 2619–2627

214. Eke I, Schneider L, Förster C et al. (2013) EGFR/JIP-4/JNK2 signaling attenuates cetuximab-mediated radiosensitization of squamous cell carcinoma cells. Cancer Res 73(1): pp. 297–306

215. Dittmann K, Mayer C, Rodemann H (2005) Inhibition of radiation-induced EGFR nuclear import by C225 (Cetuximab) suppresses DNA-PK activity. Radiother Oncol 76(2): pp. 157–161

216. Mukohara T, Engelman JA, Hanna NH et al. (2005) Differential effects of gefitinib and cetuximab on non-small-cell lung cancers bearing epidermal growth factor receptor mutations. J Natl Cancer Inst 97(16): pp. 1185–1194

217. Wild R, Fager K, Flefleh C et al. (2006) Cetuximab preclinical antitumor activity (monotherapy and combination based) is not predicted by relative total or activated epidermal growth factor receptor tumor expression levels. Mol Cancer Ther 5(1): pp. 104–113

218. Luo FR, Yang Z, Dong H et al. (2005) Correlation of pharmacokinetics with the antitumor activity of Cetuximab in nude mice bearing the GEO human colon carcinoma xenograft. Cancer Chemother. Pharmacol. 56(5): pp. 455–464

219. Lan W, Hao G, Wang J et al. (2010) Duplexed On-Microbead Binding Assay for Competitive Inhibitor of Epidermal Growth Factor Receptor by Quantitative Flow Cytometry. Basic & Clinical Pharmacology & Toxicology 107(1): pp. 560–564

220. Berger C, Krengel U, Stang E et al. (2011) Nimotuzumab and cetuximab block ligand-independent EGF receptor signaling efficiently at different concentrations. J Immunother 34(7): pp. 550–555

221. Avraham R, Yarden Y (2011) Feedback regulation of EGFR signalling: decision making by early and delayed loops. Nat Rev Mol Cell Biol 12(2): pp. 104–117

222. Segatto O, Anastasi S, Alemà S (2011) Regulation of epidermal growth factor receptor signalling by inducible feedback inhibitors. J Cell Sci 124(11): pp. 1785–1793

223. Li X, Huang Y, Jiang J et al. (2008) ERK-dependent threonine phosphorylation of EGF receptor modulates receptor downregulation and signaling. Cell Signal 20(11): pp. 2145–2155

224. Schoeberl B, Eichler-Jonsson C, Gilles ED et al. (2002) Computational modeling of the dynamics of the MAP kinase cascade activated by surface and internalized EGF receptors. Nat Biotechnol 20(4): pp. 370–375

225. Mirzoeva OK, Das D, Heiser LM et al. (2009) Basal subtype and MAPK/ERK kinase (MEK)-phosphoinositide 3-kinase feedback signaling determine susceptibility of breast cancer cells to MEK inhibition. Cancer Res 69(2): pp. 565–572

226. Gan Y, Shi C, Inge L et al. (2010) Differential roles of ERK and Akt pathways in regulation of EGFR-mediated signaling and motility in prostate cancer cells. Oncogene 29(35): pp. 4947–4958

227. Turke AB, Song Y, Costa C et al. (2012) MEK inhibition leads to PI3K/AKT activation by relieving a negative feedback on ERBB receptors. Cancer Res 72(13): pp. 3228–3237

228. Kimura H, Sakai K, Arao T et al. (2007) Antibody-dependent cellular cytotoxicity of cetuximab against tumor cells with wild-type or mutant epidermal growth factor receptor. Cancer Sci 98(8): pp. 1275–1280

229. Brown WR, Newcomb RW, Ishizaka K (1970) Proteolytic degradation of exocrine and serum immunoglobulins. J Clin Invest 49(7): pp. 1374–1380

230. Wang Q, Villeneuve G, Wang Z (2005) Control of epidermal growth factor receptor endocytosis by receptor dimerization, rather than receptor kinase activation. EMBO Rep 6(10): pp. 942–948

231. Mandic R, Rodgarkia-Dara CJ, Zhu L et al. (2006) Treatment of HNSCC cell lines with the EGFR-specific inhibitor cetuximab (Erbitux) results in paradox phosphorylation of tyrosine 1173 in the receptor. FEBS Lett. 580(20): pp. 4793–4800

232. Li C, Iida M, Dunn EF et al. (2010) Dasatinib blocks cetuximab- and radiation-induced nuclear translocation of the epidermal growth factor receptor in head and neck squamous cell carcinoma. Radiother Oncol 97(2): pp. 330–337

233. Gaumann A, Tews DS, Mentzel T et al. (2003) Expression of drug resistance related proteins in sarcomas of the pulmonary artery and poorly differentiated leiomyosarcomas of other origin. Virchows Arch. 442(6): pp. 529–537

234. Chapman AP (2002) PEGylated antibodies and antibody fragments for improved therapy: a review. Adv Drug Deliv Rev 54(4): pp. 531–545

235. Tan AR, Moore DF, Hidalgo M et al. (2006) Pharmacokinetics of Cetuximab After Administration of Escalating Single Dosing and Weekly Fixed Dosing in Patients with Solid Tumors. Clin Cancer Res 12(21): pp. 6517–6522

236. Dirks NL, Meibohm B (2010) Population pharmacokinetics of therapeutic monoclonal antibodies. Clin Pharmacokinet 49(10): pp. 633–659

237. Ghetie V, Ward ES (1997) FcRn: the MHC class I-related receptor that is more than an IgG transporter. Immunol Today 18(12): pp. 592–598

238. Claypool SM, Dickinson BL, Wagner JS et al. (2004) Bidirectional transepithelial IgG transport by a strongly polarized basolateral membrane Fcgamma-receptor. Mol Biol Cell 15(4): pp. 1746–1759

239. Tabrizi MA, Tseng CL, Roskos LK (2006) Elimination mechanisms of therapeutic monoclonal antibodies. Drug Discov Today 11(1-2): pp. 81–88

240. Lee C, Tannock I (2010) The distribution of the therapeutic monoclonal antibodies cetuximab and trastuzumab within solid tumors. BMC Cancer 10(1): 255

241. Milas L, Mason K, Hunter N et al. (2000) In vivo enhancement of tumor radioresponse by C225 antiepidermal growth factor receptor antibody. Clin Cancer Res 6(2): pp. 701–708

242. Saleh MN, Raisch KP, Stackhouse MA et al. (1999) Combined Modality Treatment of A431 Human Epidermoid Cancer Using Anti-EGFr Antibody C225. Cancer Biother Radiopharm 14(6): pp. 451–463

243. Fan Z, Baselga J, Masui H et al. (1993) Antitumor effect of anti-epidermal growth factor receptor monoclonal antibodies plus cis-diamminedichloroplatinum on well established A431 cell xenografts. Cancer Res 53(19): pp. 4637–4642

244. Goldstein NI, Prewett M, Zuklys K et al. (1995) Biological efficacy of a chimeric antibody to the epidermal growth factor receptor in a human tumor xenograft model. Clin Cancer Res 1(11): pp. 1311–1318

245. Croy BA, Di Santo JP, Manz M et al. Chapter 13 - Mouse Models of Immunodeficiency. In: In: James GF, Muriel TD, Fred WQ et al. (eds) The Mouse in Biomedical Research (Second Edition). Academic Press, Burlington, Volume IV: Immunology, *pp* 275–289

246. Barok M, Isola J, Palyi-Krekk Z et al. (2007) Trastuzumab causes antibody-dependent cellular cytotoxicity-mediated growth inhibition of submacroscopic JIMT-1 breast cancer xenografts despite intrinsic drug resistance. Mol Cancer Ther 6(7): pp. 2065–2072

247. Collins DM, O'Donovan N, McGowan PM et al. (2012) Trastuzumab induces antibody-dependent cell-mediated cytotoxicity (ADCC) in HER-2-non-amplified breast cancer cell lines. Ann Oncol 23(7): pp. 1788–1795

248. Glennie MJ, French RR, Cragg MS et al. (2007) Mechanisms of killing by anti-CD20 monoclonal antibodies. Mol Immunol 44(16): pp. 3823–3837

249. Masui H, Moroyama T, Mendelsohn J (1986) Mechanism of antitumor activity in mice for anti-epidermal growth factor receptor monoclonal antibodies with different isotypes. Cancer Res 46(11): pp. 5592–5598

250. Mendelsohn J (1989) Anti-EGF receptor monoclonal antibodies: biological studies and potential clinical applications. Trans Am Clin Climatol Assoc.; 100: 100: pp. 31–38

251. Kawaguchi Y, Kono K, Mimura K et al. (2007) Cetuximab induce antibody-dependent cellular cytotoxicity against EGFR-expressing esophageal squamous cell carcinoma. Int J Cancer 120(4): pp. 781–787

252. Arnoletti JP, Buchsbaum DJ, Huang Z et al. (2004) Mechanisms of resistance to Erbitux (anti-epidermal growth factor receptor) combination therapy in pancreatic adenocarcinoma cells. J Gastrointest Surg 8(8): pp. 960-9; discussion 969-70

253. Quesnelle KM, Grandis JR (2011) Dual kinase inhibition of EGFR and HER2 overcomes resistance to cetuximab in a novel in vivo model of acquired cetuximab resistance. Clin Cancer Res 17(18): pp. 5935–5944

254. Yonesaka K, Zejnullahu K, Okamoto I et al. (2011) Activation of ERBB2 signaling causes resistance to the EGFR-directed therapeutic antibody cetuximab. Sci Transl Med 3(99): pp. 99ra86

255. Saki M, Toulany M, Rodemann HP (2013) Acquired resistance to cetuximab is associated with the overexpression of Ras family members and the loss of radiosensitization in head and neck cancer cells. Radiother Oncol 108(3): pp. 473–478

256. Huang SM, Harari PM (2000) Modulation of radiation response after epidermal growth factor receptor blockade in squamous cell carcinomas: inhibition of damage repair, cell cycle kinetics, and tumor angiogenesis. Clin Cancer Res 6(6): pp. 2166–2174

257. Nasu S, Ang KK, Fan Z et al. (2001) C225 antiepidermal growth factor receptor antibody enhances tumor radiocurability. Int J Radiat Oncol Biol Phys 51(2): pp. 474–477

258. Raben D, Helfrich B, Chan DC et al. (2005) The effects of cetuximab alone and in combination with radiation and/or chemotherapy in lung cancer. Clin Cancer Res 11: pp. 795–805

259. Barker FG, Simmons ML, Chang SM et al. (2001) EGFR overexpression and radiation response in glioblastoma multiforme.
Int J Radiat Oncol Biol Phys 51(2): pp. 410–418

260. Liang K, Ang KK, Milas L et al. (2003) The epidermal growth factor receptor mediates radioresistance. Int J Radiat Oncol Biol Phys 57(1): pp. 246–254

261. Schmidt-Ullrich RK, Mikkelsen RB, Dent P et al. (1997) Radiation-induced proliferation of the human A431 squamous carcinoma cells is dependent on EGFR tyrosine phosphorylation. Oncogene 15(10): pp. 1191–1197

262. Akimoto T, Hunter NR, Buchmiller L et al. (1999) Inverse relationship between epidermal growth factor receptor expression and radiocurability of murine carcinomas. Clin Cancer Res 5(10): pp. 2884–2890

263. Pueyo G, Mesia R, Figueras A et al. (2010) Cetuximab may inhibit tumor growth and angiogenesis induced by ionizing radiation: a preclinical rationale for maintenance treatment after radiotherapy. Oncologist 15(9): pp. 976–986

264. Goldkorn T, Balaban N, Shannon M et al. (1997) EGF receptor phosphorylation is affected by ionizing radiation. Biochim Biophys Acta 1358(3): pp. 289–299

265. Dent P, Reardon DB, Park JS et al. (1999) Radiation-induced release of transforming growth factor alpha activates the epidermal growth factor receptor and mitogen-activated protein kinase pathway in carcinoma cells, leading to increased proliferation and protection from radiation-induced cell death.
Mol Biol Cell 10(8): pp. 2493–2506

266. Bonner JA, Raisch KP, Trummell HQ et al. (2000) Enhanced apoptosis with combination C225/radiation treatment serves as the impetus for clinical investigation in head and neck cancers. J Clin Oncol 18(21 Suppl): pp. 47S-53S

267. Kim I, Bae S, Fernandes A et al. (2005) Selective inhibition of Ras, phosphoinositide 3 kinase, and Akt isoforms increases the radiosensitivity of human carcinoma cell lines. Cancer Res 65(17): pp. 7902–7910

268. Minjgee M, Toulany M, Kehlbach R et al. (2011) K-RAS(V12) induces autocrine production of EGFR ligands and mediates radioresistance through EGFR-dependent Akt signaling and activation of DNA-PKcs.
Int J Radiat Oncol Biol Phys 81(5): pp. 1506–1514

269. Toulany M, Dittmann K, Baumann M et al. (2005) Radiosensitization of Ras-mutated human tumor cells in vitro by the specific EGF receptor antagonist BIBX1382BS. Radiother Oncol 74(2): pp. 117–129

270. Toulany M, Dittmann K, Krüger M et al. (2005) Radioresistance of K-Ras mutated human tumor cells is mediated through EGFR-dependent activation of PI3K-AKT pathway. Radiother Oncol 76(2): pp. 143–150

271. Toulany M, Baumann M, Rodemann HP (2007) Stimulated PI3K-AKT signaling mediated through ligand or radiation-induced EGFR depends indirectly, but not directly, on constitutive K-Ras activity. Mol Cancer Res 5(8): pp. 863–872

272. Di Fiore F, Blanchard F, Charbonnier F et al. (2007) Clinical relevance of KRAS mutation detection in metastatic colorectal cancer treated by Cetuximab plus chemotherapy. Br J Cancer 96(8): pp. 1166–1169

273. Karapetis CS, Khambata-Ford S, Jonker DJ et al. (2008) K-ras mutations and benefit from cetuximab in advanced colorectal cancer.
N Engl J Med 359(17): pp. 1757–1765

274. Lièvre A, Bachet J, Boige V et al. (2008) KRAS Mutations As an Independent Prognostic Factor in Patients With Advanced Colorectal Cancer Treated With Cetuximab. J Clin Oncol 26(3): pp. 374–379

275. Yen L, Uen Y, Wu D et al. (2010) Activating KRAS mutations and overexpression of epidermal growth factor receptor as independent predictors in metastatic colorectal cancer patients treated with cetuximab. Ann Surg 251(2): pp. 254–260

276. Grimminger PP, Danenberg P, Dellas K et al. (2011) Biomarkers for cetuximab-based neoadjuvant radiochemotherapy in locally advanced rectal cancer.
Clin Cancer Res 17(10): pp. 3469–3477

277. Bengala C, Bettelli S, Bertolini F et al. (2009) Epidermal growth factor receptor gene copy number, K-ras mutation and pathological response to preoperative cetuximab, 5-FU and radiation therapy in locally advanced rectal cancer.
Ann Oncol 20(3): pp. 469–474

278. Debucquoy A, Haustermans K, Daemen A et al. (2009) Molecular Response to Cetuximab and Efficacy of Preoperative Cetuximab-Based Chemoradiation in Rectal Cancer. J Clin Oncol 27(17): pp. 2751–2757

279. Erben P, Ströbel P, Horisberger K et al. (2011) KRAS and BRAF Mutations and PTEN Expression Do Not Predict Efficacy of Cetuximab-Based Chemoradiotherapy in Locally Advanced Rectal Cancer.
Int J Radiat Oncol Biol Phys 81(4): pp. 1032–1038

280. Kim SY, Hong YS, Kim DY et al. (2011) Preoperative Chemoradiation With Cetuximab, Irinotecan, and Capecitabine in Patients With Locally Advanced Resectable Rectal Cancer: A Multicenter Phase II Study.
Int J Radiat Oncol Biol Phys 81(3): pp. 677–683

281. Caron RW, Yacoub A, Zhu X et al. (2005) H-RAS V12-induced radioresistance in HCT116 colon carcinoma cells is heregulin dependent.
Mol Cancer Ther 4(2): pp. 243–255

282. Choi EJ, Ryu YK, Kim SY et al. (2010) Targeting epidermal growth factor receptor-associated signaling pathways in non-small cell lung cancer cells: implication in radiation response. Mol Cancer Res 8(7): pp. 1027–1036

283. Shin HK, Kim M, Lee JK et al. (2010) Combination effect of cetuximab with radiation in colorectal cancer cells. Tumori 96(5): pp. 713–720

284. Bussink J, van der Kogel AJ, Kaanders JH (2008) Activation of the PI3-K/AKT pathway and implications for radioresistance mechanisms in head and neck cancer.
Lancet Oncol 9(3): pp. 288–296

285. Jackson SP, Jeggo PA (1995) DNA double-strand break repair and V(D)J recombination: involvement of DNA-PK. Trends Biochem Sci 20(10): pp. 412–415

286. Mladenov E, Iliakis G (2011) Induction and repair of DNA double strand breaks: the increasing spectrum of non-homologous end joining pathways.
Mutat Res 711(1-2): pp. 61–72

287. Friedmann BJ, Caplin M, Savic B et al. (2006) Interaction of the epidermal growth factor receptor and the DNA-dependent protein kinase pathway following gefitinib treatment. Mol Cancer Ther 5(2): pp. 209–218

288. Ferrara N, Davis-Smyth T (1997) The biology of vascular endothelial growth factor. Endocr Rev 18(1): pp. 4–25

289. Becker A, Stadler P, Krause U et al. (2001) Association between elevated serum VEGF and polarographically measured tumor hypoxia in head and neck carcinomas (Assoziation zwischen erhohten Serum-VEGF-Werten und polarographisch gemessener Tumorhypoxie bei Patienten mit Kopf-Hals-Karzinomen). Strahlenther Onkol 177(4): pp. 182–188

290. Ellis LM (2004) Epidermal growth factor receptor in tumor angiogenesis. Hematol Oncol Clin North Am 18(5): pp. 1007-21, viii

291. Kim KJ, Li B, Winer J et al. (1993) Inhibition of vascular endothelial growth factor-induced angiogenesis suppresses tumour growth in vivo. Nature 362(6423): pp. 841–844

292. Perrotte P, Matsumoto T, Inoue K et al. (1999) Anti-epidermal growth factor receptor antibody C225 inhibits angiogenesis in human transitional cell carcinoma growing orthotopically in nude mice. Clin Cancer Res 5(2): pp. 257–265

293. Petit AM, Rak J, Hung MC et al. (1997) Neutralizing antibodies against epidermal growth factor and ErbB-2/neu receptor tyrosine kinases down-regulate vascular endothelial growth factor production by tumor cells in vitro and in vivo: angiogenic implications for signal transduction therapy of solid tumors. Am J Pathol 151(6): pp. 1523–1530

294. Gorski DH, Beckett MA, Jaskowiak NT et al. (1999) Blockage of the vascular endothelial growth factor stress response increases the antitumor effects of ionizing radiation. Cancer Res 59(14): pp. 3374–3378

295. Hovinga KE, Stalpers LJA, van Bree C et al. (2005) Radiation-enhanced vascular endothelial growth factor (VEGF) secretion in glioblastoma multiforme cell lines--a clue to radioresistance? J Neurooncol 74(2): pp. 99–103

296. Garcia-Barros M, Paris F, Cordon-Cardo C et al. (2003) Tumor response to radiotherapy regulated by endothelial cell apoptosis. Science 300(5622): pp. 1155–1159

297. Lee CG, Heijn M, Di Tomaso E et al. (2000) Anti-Vascular endothelial growth factor treatment augments tumor radiation response under normoxic or hypoxic conditions. Cancer Res 60(19): pp. 5565–5570

298. Jain RK (2005) Normalization of Tumor Vasculature: An Emerging Concept in Antiangiogenic Therapy. Science 307(5706): pp. 58–62

299. Horsman MR, Siemann DW (2006) Pathophysiologic Effects of Vascular-Targeting Agents and the Implications for Combination with Conventional Therapies. Cancer Res 66(24): pp. 11520–11539

300. Schwarz G. (1909) Uber Desensibilisierung gegen Rontgen- und Radiumstrahlen. MMW Munch Med Wochenschr 56: 1217–1218

301. Gray LH, Conger AD, Ebert M et al. (1953) The concentration of oxygen dissolved in tissues at the time of irradiation as a factor in radiotherapy. Br J Radiol 26(312): pp. 638–648

302. Fowler JF (1983) The second Klaas Breur memorial lecture. La Ronde--radiation sciences and medical radiology. Radiother Oncol 1(1): pp. 1–22

303. Murray D, Mirzayans R, Scott AL et al. (2003) Influence of oxygen on the radiosensitivity of human glioma cell lines. Am J Clin Oncol 26(5): pp. e169-77

304. Overgaard J (2007) Hypoxic radiosensitization: adored and ignored. J Clin Oncol 25(26): pp. 4066–4074

305. Stadler P, Becker A, Feldmann HJ et al. (1999) Influence of the hypoxic subvolume on the survival of patients with head and neck cancer. Int J Radiat Oncol Biol Phys 44(4): pp. 749–754

306. Nordsmark M, Bentzen SM, Rudat V et al. (2005) Prognostic value of tumor oxygenation in 397 head and neck tumors after primary radiation therapy. An international multi-center study. Radiother Oncol 77(1): pp. 18–24

307. Kedersha NL, Heuser JE, Chugani DC et al. (1991) Vaults. III. Vault ribonucleoprotein particles open into flower-like structures with octagonal symmetry. J Cell Biol 112(2): pp. 225–235

308. Kedersha NL, Miquel MC, Bittner D et al. (1990) Vaults. II. Ribonucleoprotein structures are highly conserved among higher and lower eukaryotes. J Cell Biol 110(4): pp. 895–901

309. Scheffer GL, Wijngaard PL, Flens MJ et al. (1995) The drug resistance-related protein LRP is the human major vault protein. Nat Med 1(6): pp. 578–582

310. Kickhoefer VA, Siva AC, Kedersha NL et al. (1999) The 193-kD vault protein, VPARP, is a novel poly(ADP-ribose) polymerase. J Cell Biol 146(5): pp. 917–928

311. Kickhoefer VA, Stephen AG, Harrington L et al. (1999) Vaults and Telomerase Share a Common Subunit, TEP1. J Biol Chem 274(46): pp. 32712–32717

312. Tanaka H, Kato K, Yamashita E et al. (2009) The structure of rat liver vault at 3.5 angstrom resolution. Science 323(5912): pp. 384–388

313. Anderson DH, Kickhoefer VA, Sievers SA et al. (2007) Draft crystal structure of the vault shell at 9-A resolution. PLoS Biol. 5(11): pp. e318

314. Goldsmith LE, Yu M, Rome LH et al. (2007) Vault nanocapsule dissociation into halves triggered at low pH. Biochemistry 46(10): pp. 2865–2875

315. Xia Y, Ramgopal Y, Li H et al. (2010) Immobilization of recombinant vault nanoparticles on solid substrates. ACS Nano 4(3): pp. 1417–1424

316. Yang J, Kickhoefer VA, Ng BC et al. (2010) Vaults are dynamically unconstrained cytoplasmic nanoparticles capable of half vault exchange. ACS Nano 4(12): pp. 7229–7240

317. Poderycki MJ, Kickhoefer VA, Kaddis CS et al. (2006) The vault exterior shell is a dynamic structure that allows incorporation of vault-associated proteins into its interior. Biochem 45(39): pp. 12184–12193

318. Mikyas Y, Makabi M, Raval-Fernandes S et al. (2004) Cryoelectron microscopy imaging of recombinant and tissue derived vaults: localization of the MVP N termini and VPARP. J Mol Biol 344(1): pp. 91–105

319. Liu Y, Snow BE, Kickhoefer VA et al. (2004) Vault poly(ADP-ribose) polymerase is associated with mammalian telomerase and is dispensable for telomerase function and vault structure in vivo. Mol Cell Biol 24(12): pp. 5314–5323

320. Kickhoefer VA, Liu Y, Kong LB et al. (2001) The Telomerase/vault-associated protein TEP1 is required for vault RNA stability and its association with the vault particle. J Cell Biol 152(1): pp. 157–164

321. Kong LB, Siva AC, Kickhoefer VA et al. (2000) RNA location and modeling of a WD40 repeat domain within the vault. RNA 6(6): pp. 890–900

322. Scheper RJ, Broxterman HJ, Scheffer GL et al. (1993) Overexpression of a Mr 110,000 Vesicular Protein in Non-P-Glycoprotein-mediated Multidrug Resistance. Cancer Res 53(7): pp. 1475–1479

323. Izquierdo MA, Scheffer GL, Flens MJ et al. (1996) Broad distribution of the multidrug resistance-related vault lung resistance protein in normal human tissues and tumors. Am J Pathol 148(3): pp. 877–887

324. Kedersha NL, Rome LH (1990) Vaults: large cytoplasmic RNP's that associate with cytoskeletal elements. Mol Biol Rep 14(2-3): 121–122

325. Chugani DC, Rome LH, Kedersha NL (1993) Evidence that vault ribonucleoprotein particles localize to the nuclear pore complex. J Cell Sci 106 (Pt 1): pp. 23–29

326. Slovak ML, Ho JP, Cole SP et al. (1995) The LRP gene encoding a major vault protein associated with drug resistance maps proximal to MRP on chromosome 16: evidence that chromosome breakage plays a key role in MRP or LRP gene amplification. Cancer Res 55(19): pp. 4214–4219

327. Izquierdo MA, van der Zee AG, Vermorken JB et al. (1995) Drug resistance-associated marker Lrp for prediction of response to chemotherapy and prognoses in advanced ovarian carcinoma. J Natl Cancer Inst 87(16): pp. 1230–1237

328. Lange C, Walther W, Schwabe H et al. (2000) Cloning and initial analysis of the human multidrug resistance-related MVP/LRP gene promoter. Biochem Biophys Res Commun 278(1): pp. 125–133

329. Schroder K, Hertzog PJ, Ravasi T et al. (2004) Interferon-gamma: an overview of signals, mechanisms and functions. J Leukoc Biol 75(2): pp. 163–189

330. Steiner E, Holzmann K, Pirker C et al. (2006) The major vault protein is responsive to and interferes with interferon-gamma-mediated STAT1 signals. J Cell Sci 119(Pt 3): pp. 459–469

331. Mossink M, van Zon A, Fränzel-Luiten E et al. (2002) The genomic sequence of the murine major vault protein and its promoter. Gene 294(1-2): pp. 225–232

332. Mossink MH, van Zon A, Fränzel-Luiten E et al. (2002) Disruption of the murine major vault protein (MVP/LRP) gene does not induce hypersensitivity to cytostatics. Cancer Res 62(24): pp. 7298–7304

333. Herrmann C, Kellner R, Volknandt W (1998) Major vault protein of electric ray is a phosphoprotein. Neurochem. Res 23(1): pp. 39–46

334. Ehrnsperger C, Volknandt W (2001) Major vault protein is a substrate of endogenous protein kinases in CHO and PC12 cells. Biol Chem 382(10): pp. 1463–1471

335. Kolli S, Zito CI, Mossink MH et al. (2004) The major vault protein is a novel substrate for the tyrosine phosphatase SHP-2 and scaffold protein in epidermal growth factor signaling. J Biol Chem 279(28): pp. 29374–29385

336. Shi Z, Yu D, Park M et al. (2000) Molecular Mechanism for the Shp-2 Tyrosine Phosphatase Function in Promoting Growth Factor Stimulation of Erk Activity. Mol Cell Biol 20(5): pp. 1526–1536

337. Kim E, Lee S, Mian MF et al. (2006) Crosstalk between Src and major vault protein in epidermal growth factor-dependent cell signalling. FEBS J. 273(4): pp. 793–804

338. Yu Z, Fotouhi-Ardakani N, Wu L et al. (2002) PTEN associates with the vault particles in HeLa cells. J Biol Chem 277(43): pp. 40247–40252

339. Chung J, Ginn-Pease ME, Eng C (2005) Phosphatase and tensin homologue deleted on chromosome 10 (PTEN) has nuclear localization signal-like sequences for nuclear import mediated by major vault protein. Cancer Res 65(10): pp. 4108–4116

340. Yi C, Li S, Chen X et al. (2005) Major vault protein, in concert with constitutively photomorphogenic 1, negatively regulates c-Jun-mediated activator protein 1 transcription in mammalian cells. Cancer Res 65(13): pp. 5835–5840

341. Hess J, Angel P, Schorpp-Kistner M (2004) AP-1 subunits: quarrel and harmony among siblings. J Cell Sci 117(Pt 25): pp. 5965–5973

342. Iwashita K, Ikeda R, Takeda Y et al. (2010) Major vault protein forms complexes with hypoxia-inducible factor (HIF)-1alpha and reduces HIF-1alpha level in ACHN human renal adenocarcinoma cells. Cancer Sci. 101(4): pp. 920–926

343. Kowalski MP, Dubouix-Bourandy A, Bajmoczi M et al. (2007) Host resistance to lung infection mediated by major vault protein in epithelial cells. Science 317(5834): pp. 130–132

344. Dortet L, Mostowy S, Samba-Louaka A et al. (2011) Recruitment of the major vault protein by InlK: a Listeria monocytogenes strategy to avoid autophagy. PLoS Pathog7(8): pp. e1002168

345. Ben J, Zhang Y, Zhou R et al. (2013) Major Vault Protein Regulates Class A Scavenger Receptor-mediated Tumor Necrosis Factor-α Synthesis and Apoptosis in Macrophages. J Biol Chem 288(27): pp. 20076–20084

346. Balkwill F (2009) Tumour necrosis factor and cancer. Nat Rev Cancer 9(5): pp. 361–371

347. Berger W, Steiner E, Grusch M et al. (2009) Vaults and the major vault protein: novel roles in signal pathway regulation and immunity. Cell Mol Life Sci 66(1): pp. 43–61

348. Schroeijers AB, Reurs AW, Scheffer GL et al. (2002) Up-regulation of drug resistance-related vaults during dendritic cell development. J Immuno l168(4): pp. 1572–1578

349. Mossink MH, Groot J de, van Zon A et al. (2003) Unimpaired dendritic cell functions in MVP/LRP knockout mice. Immunology 110(1): pp. 58–65

350. Motsch N, Pfuhl T, Mrazek J et al. (2007) Epstein-Barr virus-encoded latent membrane protein 1 (LMP1) induces the expression of the cellular microRNA miR-146a. RNA Biol 4(3): pp. 131–137

351. Mrázek J, Kreutmayer SB, Grässer FA et al. (2007) Subtractive hybridization identifies novel differentially expressed ncRNA species in EBV-infected human B cells. Nucleic Acids Res 35(10): pp. e73

352. Kickhoefer VA, Vasu SK, Rome LH (1996) Vaults are the answer, what is the question? Trends Cell Biol. 6(5): pp. 174–178

353. Steiner E, Holzmann K, Elbling L et al. (2006) Cellular functions of vaults and their involvement in multidrug resistance. Curr Drug Targets 7(8): pp. 923–934

354. Suprenant KA (2002) Vault ribonucleoprotein particles: sarcophagi, gondolas, or safety deposit boxes? Biochemistry 41(49): pp. 14447–14454

355. Hall MD, Handley MD, Gottesman MM (2009) Is resistance useless? Multidrug resistance and collateral sensitivity. Trends Pharmacol Sci 30(10): pp. 546–556

356. Scheffer GL, Schroeijers AB, Izquierdo MA et al. (2000) Lung resistance-related protein/major vault protein and vaults in multidrug-resistant cancer. Curr Opin Oncol 12(6): pp. 550–556

357. Izquierdo MA, Shoemaker RH, Flens MJ et al. (1996) Overlapping phenotypes of multidrug resistance among panels of human cancer-cell lines. Int J Cancer 65(2): pp. 230–237

358. Laurençot CM, Scheffer GL, Scheper RJ et al. (1997) Increased LRP mRNA expression is associated with the MDR phenotype in intrinsically resistant human cancer cell lines. Int J Cancer 72(6): pp. 1021–1026

359. Berger W, Elbling L, Micksche M (2000) Expression of the major vault protein LRP in human non-small-cell lung cancer cells: activation by short-term exposure to antineoplastic drugs. Int J Cancer 88(2): pp. 293–300

360. Berger W, Spiegl-Kreinecker S, Buchroithner J et al. (2001) Overexpression of the human major vault protein in astrocytic brain tumor cells. Int J Cancer 94(3): pp. 377–382

361. Kickhoefer VA, Rajavel KS, Scheffer GL et al. (1998) Vaults are up-regulated in multidrug-resistant cancer cell lines. J Biol Chem 273(15): pp. 8971–8974

362. Moran E, Cleary I, Larkin AM et al. (1997) Co-expression of MDR-associated markers, including P-170, MRP and LRP and cytoskeletal proteins, in three resistant variants of the human ovarian carcinoma cell line, OAW42. Eur J Cancer 33(4): pp. 652–660

363. Combs SE, Schulz-Ertner D, Roth W et al. (2007) In vitro responsiveness of glioma cell lines to multimodality treatment with radiotherapy, temozolomide, and epidermal growth factor receptor inhibition with cetuximab. Int J Radiat Oncol Biol Phys 68(3): pp. 873–882

364. Kitazono M, Sumizawa T, Takebayashi Y et al. (1999) Multidrug resistance and the lung resistance-related protein in human colon carcinoma SW-620 cells. J Natl Cancer Inst 91(19): pp. 1647–1653

365. Alfarano P, Varadamsetty G, Ewald C et al. (2012) Optimization of designed armadillo repeat proteins by molecular dynamics simulations and NMR spectroscopy. Protein Science 21(9): pp. 1298–1314

366. Verovski VN, van den Berge DL, Delvaeye MM et al. (1996) Low-level doxorubicin resistance in P-glycoprotein-negative human pancreatic tumour PSN1/ADR cells implicates a brefeldin A-sensitive mechanism of drug extrusion. Br J Cancer 73(5): pp. 596–602

367. Versantvoort CH, Withoff S, Broxterman HJ et al. (1995) Resistance-associated factors in human small-cell lung-carcinoma GLC4 sub-lines with increasing adriamycin resistance. Int J Cancer 61(3): pp. 375–380

368. Wyler B, Shao Y, Schneider E et al. (1997) Intermittent exposure to doxorubicin in vitro selects for multifactorial non-P-glycoprotein-associated multidrug resistance in RPMI 8226 human myeloma cells. Br J Haematol 97(1): pp. 65–75

369. Ikuta K, Takemura K, Sasaki K et al. (2005) Expression of multidrug resistance proteins and accumulation of cisplatin in human non-small cell lung cancer cells. Biol Pharm Bull 28(4): pp. 707–712

370. Siva AC, Raval-Fernandes S, Stephen AG et al. (2001) Up-regulation of vaults may be necessary but not sufficient for multidrug resistance. Int J Cancer 92(2): pp. 195–202

371. Hu H, Ye F, Zhang D et al. (2010) iTRAQ quantitative analysis of multidrug resistance mechanisms in human gastric cancer cells. J Biomed Biotechnol 2010: 571343

372. Kitazono M, Okumura H, Ikeda R et al. (2001) Reversal of LRP-associated drug resistance in colon carcinoma SW-620 cells. Int J Cancer 91(1): pp. 126–131

373. Schuurhuis GJ, Broxterman HJ, Lange JH de et al. (1991) Early multidrug resistance, defined by changes in intracellular doxorubicin distribution, independent of P-glycoprotein. Br J Cancer 64(5): pp. 857–861

374. Dietel M, Arps H, Lage H et al. (1990) Membrane vesicle formation due to acquired mitoxantrone resistance in human gastric carcinoma cell line EPG85-257. Cancer Res 50(18): pp. 6100–6106

375. Herlevsen M, Oxford G, Owens CR et al. (2007) Depletion of major vault protein increases doxorubicin sensitivity and nuclear accumulation and disrupts its sequestration in lysosomes. Mol Cancer Ther 6(6): pp. 1804–1813

376. Persson H, Kvist A, Vallon-Christersson J et al. (2009) The non-coding RNA of the multidrug resistance-linked vault particle encodes multiple regulatory small RNAs. Nat Cell Biol 11(10): pp. 1268–1271

377. Mitra R, Guo Z, Milani M et al. (2011) CYP3A4 mediates growth of estrogen receptor-positive breast cancer cells in part by inducing nuclear translocation of phospho-Stat3 through biosynthesis of (+/-)-14,15-epoxyeicosatrienoic acid (EET). J Biol Chem 286(20): pp. 17543–17559

378. Shimamoto Y, Sumizawa T, Haraguchi M et al. (2006) Direct activation of the human major vault protein gene by DNA-damaging agents.
Oncol Rep 15(3): pp. 645–652

379. Raval-Fernandes S, Kickhoefer VA, Kitchen C et al. (2005) Increased susceptibility of vault poly(ADP-ribose) polymerase-deficient mice to carcinogen-induced tumorigenesis. Cancer Res 65(19): pp. 8846–8852

380. Lloret M, Lara PC, Bordón E et al. (2009) Major vault protein may affect nonhomologous end-joining repair and apoptosis through Ku70/80 and bax downregulation in cervical carcinoma tumors. Int J Radiat Oncol Biol Phys 73(4): pp. 976–979

381. Amsel AD, Rathaus M, Kronman N et al. (2008) Regulation of the proapoptotic factor Bax by Ku70-dependent deubiquitylation.
Proc Natl Acad Sci U S A 105(13): pp. 5117–5122

382. Wang Q, Gao F, May WS et al. (2008) Bcl2 negatively regulates DNA double-strand-break repair through a nonhomologous end-joining pathway.
Mol Cell 29(4): pp. 488–498

383. Ryu SJ, An HJ, Oh YS et al. (2008) On the role of major vault protein in the resistance of senescent human diploid fibroblasts to apoptosis.
Cell Death Differ 15(11): pp. 1673–1680

384. Ryu SJ, Park SC (2009) Targeting major vault protein in senescence-associated apoptosis resistance. Expert Opin. Ther. Targets 13(4): pp. 479–484

385. Minaguchi T, Waite KA, Eng C (2006) Nuclear localization of PTEN is regulated by Ca(2+) through a tyrosil phosphorylation-independent conformational modification in major vault protein. Cancer Res 66(24): pp. 11677–11682

386. Shen WH, Balajee AS, Wang J et al. (2007) Essential Role for Nuclear PTEN in Maintaining Chromosomal Integrity. Cell 128(1): pp. 157–170

387. Puc J, Keniry M, Li HS et al. (2005) Lack of PTEN sequesters CHK1 and initiates genetic instability. Cancer Cell 7(2): pp. 193–204

388. Dedes KJ, Wetterskog D, Mendes-Pereira AM et al. (2010) PTEN deficiency in endometrioid endometrial adenocarcinomas predicts sensitivity to PARP inhibitors. Sci Transl Med 2(53): pp. 53ra75

389. Mendes-Pereira AM, Martin SA, Brough R et al. (2009) Synthetic lethal targeting of PTEN mutant cells with PARP inhibitors. EMBO Mol Med 1(6-7): pp. 315–322

390. Bottke D, Koychev D, Busse A et al. (2008) Fractionated irradiation can induce functionally relevant multidrug resistance gene and protein expression in human tumor cell lines. Radiat Res 170(1): pp. 41–48

391. Mitchell JB, Russo A, Cook JA et al. (1989) Tumor cell drug and radiation resistance: does an interrelationship exist? Cancer Treat Res 48: pp. 189–203

392. Filipits M, Pohl G, Stranzl T et al. (1998) Expression of the lung resistance protein predicts poor outcome in de novo acute myeloid leukemia.
Blood 91(5): pp. 1508–1513

393. Filipits M, Jaeger U, Simonitsch I et al. (2000) Clinical relevance of the lung resistance protein in diffuse large B-cell lymphomas.
Clin Cancer Res 6(9): pp. 3417–3423

394. Pirker R, Pohl G, Stranzl T et al. (1999) The lung resistance protein (LRP) predicts poor outcome in acute myeloid leukemia. Adv. Exp. Med. Biol. 457: pp. 133–139

395. Xu D, Areström I, Virtala R et al. (1999) High levels of lung resistance related protein mRNA in leukaemic cells from patients with acute myelogenous leukaemia are associated with inferior response to chemotherapy and prior treatment with mitoxantrone. Br J Haematol 106(3): pp. 627–633

396. Oh E, Kahng J, Kim Y et al. (2003) Expression of functional markers in acute lymphoblastic leukemia. Leuk Res 27(10): pp. 903–908

397. Valera ET, Scrideli CA, Queiroz RGP de et al. (2004) Multiple drug resistance protein (MDR-1), multidrug resistance-related protein (MRP) and lung resistance protein (LRP) gene expression in childhood acute lymphoblastic leukemia. Sao Paulo Med J 122(4): pp. 166–171

398. Volm M, Mattern J, Koomägi R (1997) Expression of lung resistance-related protein (LRP) in non-small cell lung carcinomas of smokers and non-smokers and its predictive value for doxorubicin resistance. Anticancer Drugs 8(10): pp. 931–936

399. Ohno N, Tani A, Uozumi K et al. (2001) Expression of functional lung resistance--related protein predicts poor outcome in adult T-cell leukemia. Blood 98(4): pp. 1160–1165

400. Sakaki Y, Terashi K, Yamaguchi A et al. (2002) Human T-cell lymphotropic virus type I Tax activates lung resistance-related protein expression in leukemic clones established from an adult T-cell leukemia patient. Exp Hematol 30(4): pp. 340–345

401. Rimsza LM, Campbell K, Dalton WS et al. (1999) The major vault protein (MVP), a new multidrug resistance associated protein, is frequently expressed in multiple myeloma. Leuk Lymphoma 34(3-4): pp. 315–324

402. Schwarzenbach H (2002) Expression of MDR1/P-glycoprotein, the multidrug resistance protein MRP, and the lung-resistance protein LRP in multiple myeloma. Med Oncol 19(2): pp. 87–104

403. Brinkhuis M, Izquierdo MA, Baak JPA et al. (2002) Expression of multidrug resistance-associated markers, their relation to quantitative pathologic tumour characteristics and prognosis in advanced ovarian cancer. Anal Cell Pathol 24(1): pp. 17–23

404. Wang H, Chen X, Qiu F (2004) Correlation of expression of multidrug resistance protein and messenger RNA with 99mTc-methoxyisobutyl isonitrile (MIBI) imaging in patients with hepatocellular carcinoma. World J Gastroenterol 10(9): pp. 1281–1285

405. Arts HJ, Katsaros D, Vries EG de et al. (1999) Drug resistance-associated markers P-glycoprotein, multidrug resistance-associated protein 1, multidrug resistance-associated protein 2, and lung resistance protein as prognostic factors in ovarian carcinoma. Clin Cancer Res 5(10): pp. 2798–2805

406. Mayr D, Pannekamp U, Baretton GB et al. (2000) Immunohistochemical analysis of drug resistance-associated proteins in ovarian carcinomas. Pathol Res Pract 196(7): pp. 469–475

407. Burger H, Foekens JA, Look MP et al. (2003) RNA expression of breast cancer resistance protein, lung resistance-related protein, multidrug resistance-associated proteins 1 and 2, and multidrug resistance gene 1 in breast cancer: correlation with chemotherapeutic response. Clin Cancer Res 9(2): pp. 827–836

408. Schneider J, Gonzalez-Roces S, Pollán M et al. (2001) Expression of LRP and MDR1 in locally advanced breast cancer predicts axillary node invasion at the time of rescue mastectomy after induction chemotherapy.
Breast Cancer Res 3(3): pp. 183–191

409. Berger W, Setinek U, Hollaus P et al. (2005) Multidrug resistance markers P-glycoprotein, multidrug resistance protein 1, and lung resistance protein in non-small cell lung cancer: prognostic implications.
J Cancer Res Clin Oncol 131(6): pp. 355–363

410. Chiou JF, Liang JA, Hsu WH et al. (2003) Comparing the relationship of Taxol-based chemotherapy response with P-glycoprotein and lung resistance-related protein expression in non-small cell lung cancer. Lung 181(5): pp. 267–273

411. Komdeur R, Klunder J, van der Graaf WTA et al. (2003) Multidrug resistance proteins in rhabdomyosarcomas: comparison between children and adults.
Cancer 97(8): pp. 1999–2005

412. Komdeur R, Plaat BEC, van der Graaf WTA et al. (2003) Expression of multidrug resistance proteins, P-gp, MRP1 and LRP, in soft tissue sarcomas analysed according to their histological type and grade. Eur. J. Cancer 39(7): pp. 909–916

413. Diestra JE, Condom E, Del Muro XG et al. (2003) Expression of multidrug resistance proteins P-glycoprotein, multidrug resistance protein 1, breast cancer resistance protein and lung resistance related protein in locally advanced bladder cancer treated with neoadjuvant chemotherapy: biological and clinical implications.
J Urol 170(4 Pt 1): pp. 1383–1387

414. Schadendorf D, Makki A, Stahr C et al. (1995) Membrane transport proteins associated with drug resistance expressed in human melanoma.
Am J Pathol 147(6): pp. 1545–1552

415. Mándoky L, Géczi L, Doleschall Z et al. (2004) Expression and prognostic value of the lung resistance-related protein (LRP) in germ cell testicular tumors.
Anticancer Res 24(2C): pp. 1097–1104

416. Tews DS, Nissen A, Külgen C et al. (2000) Drug resistance-associated factors in primary and secondary glioblastomas and their precursor tumors.
J Neurooncol 50(3): pp. 227–237

417. Silva P, West CM, Slevin N et al. (2007) Tumor expression of major vault protein is an adverse prognostic factor for radiotherapy outcome in oropharyngeal carcinoma. Int J Radiat Oncol Biol Phys 69(1): pp. 133–140

418. Ramani P, Dewchand H (1995) Expression of mdr1/P-glycoprotein and p110 in neuroblastoma. J Pathol 175(1): pp. 13–22

419. Dingemans AM, van Ark-Otte J, van der Valk P et al. (1996) Expression of the human major vault protein LRP in human lung cancer samples and normal lung tissues. Ann. Oncol. 7(6): pp. 625–630

420. Linn SC, Pinedo HM, van Ark-Otte J et al. (1997) Expression of drug resistance proteins in breast cancer, in relation to chemotherapy. Int J Cancer 71(5): pp. 787–795

421. Uozaki H, Horiuchi H, Ishida T et al. (1997) Overexpression of resistance-related proteins (metallothioneins, glutathione-S-transferase pi, heat shock protein 27, and lung resistance-related protein) in osteosarcoma. Relationship with poor prognosis. Cancer 79(12): pp. 2336–2344

422. Pohl G, Filipits M, Suchomel RW et al. (1999) Expression of the lung resistance protein (LRP) in primary breast cancer. Anticancer Res. 19(6B): pp. 5051–5055

423. Volm M, Rittgen W (2000) Cellular predictive factors for the drug response of lung cancer. Anticancer Res 20(5B): pp. 3449–3458

424. Goff BA, Paley PJ, Greer BE et al. (2001) Evaluation of chemoresistance markers in women with epithelial ovarian carcinoma. Gynecol Oncol 81(1): pp. 18–24

425. Pohl G, Suchomel RW, Stranzl T et al. (2001) Expression of the lung resistance protein in primary colorectal carcinomas. Anticancer Res. 21(1A): pp. 201–204

426. Harada T, Ogura S, Yamazaki K et al. (2003) Predictive value of expression of P53, Bcl-2 and lung resistance-related protein for response to chemotherapy in non-small cell lung cancers. Cancer Sci 94(4): pp. 394–399

427. Lloret M, Lara PC, Bordón E et al. (2008) MVP expression is related to IGF1-R in cervical carcinoma patients treated by radiochemotherapy. Gynecol Oncol 110(3): pp. 304–307

428. Lloret M, Lara PC, Bordón E et al. (2007) IGF-1R expression in localized cervical carcinoma patients treated by radiochemotherapy. Gynecol Oncol 106(1): pp. 8–11

429. Henriquez-Hernandez LA, Moreno M, Rey A et al. (2012) MVP expression in the prediction of clinical outcome of locally advanced oral squamous cell carcinoma patients treated with radiotherapy. Radiat Oncol 7: 147

430. Hollenstein A (2009) New functions for the major vault protein in the ionizing radiation induced stress response and DNA repair. Diss., Eidgenössische Technische Hochschule ETH Zürich, Nr. 18695, 2009. ETH, Zürich

431. Puget N, Knowlton M, Scully R (2005) Molecular analysis of sister chromatid recombination in mammalian cells. DNA Repair (Amst) 4(2): pp. 149–161

432. Lowe SW, Ruley HE, Jacks T et al. (1993) p53-dependent apoptosis modulates the cytotoxicity of anticancer agents. Cell 74(6): pp. 957–967

433. Li Z, Fortin Y, Shen S (2009) Forward and robust selection of the most potent and noncellular toxic siRNAs from RNAi libraries. Nucleic Acids Res. 37(1): pp. e8

434. Jensen RB, Carreira A, Kowalczykowski SC (2010) Purified human BRCA2 stimulates RAD51-mediated recombination. Nature 467(7316): pp. 678–683

435. Tarsounas M, Davies D, West SC (2003) BRCA2-dependent and independent formation of RAD51 nuclear foci. Oncogene 22(8): pp. 1115–1123

436. Chen F, Nastasi A, Shen Z et al. (1997) Cell cycle-dependent protein expression of mammalian homologs of yeast DNA double-strand break repair genes Rad51 and Rad52. Mutat Res 384(3): pp. 205–211

437. Du L, Wang Y, Wang H et al. (2011) Knockdown of Rad51 expression induces radiation- and chemo-sensitivity in osteosarcoma cells.
Med Oncol 28(4): pp. 1481–1487

438. Mullen P (2004) PARP Cleavage as a Means of Assessing Apoptosis. In: Langdon S (ed) Cancer Cell Culture, vol 88. Humana Press, *pp* 171-181

439. Flygare J, Hellgren D, Wennborg A (2000) Caspase-3 mediated cleavage of HsRad51 at an unconventional site. Eur J Biochem 267(19): pp. 5977–5982

440. Olivier M, Hollstein M, Hainaut P (2010) TP53 mutations in human cancers: origins, consequences, and clinical use.
Cold Spring Harb Perspect Biol 2(1): pp. a001008

441. Kamijo T, Zindy F, Roussel MF et al. (1997) Tumor suppression at the mouse INK4a locus mediated by the alternative reading frame product p19ARF.
Cell 91(5): pp. 649–659

442. Sharpless NE (2006) Chapter 28 - Preparation and Immortalization of Primary Murine Cells. In: Julio E. Celis (ed) Cell Biology (Third Edition).
Academic Press, Burlington, *pp* 223–228

443. Slesina M, Inman EM, Rome LH et al. (2005) Nuclear localization of the major vault protein in U373 cells. Cell Tissue Res. 321(1): pp. 97–104

444. Vasu SK, Rome LH (1995) Dictyostelium vaults: disruption of the major proteins reveals growth and morphological defects and uncovers a new associated protein. J Biol Chem 270(28): pp. 16588–16594

445. Dent P, Yacoub A, Contessa J et al. (2003) Stress and radiation-induced activation of multiple intracellular signaling pathways. Radiat Res 159(3): pp. 283–300

446. Dent P, Yacoub A, Fisher PB et al. (2003) MAPK pathways in radiation responses. Oncogene 22(37): pp. 5885–5896

447. Baba I, Shirasawa S, Iwamoto R et al. (2000) Involvement of deregulated epiregulin expression in tumorigenesis in vivo through activated Ki-Ras signaling pathway in human colon cancer cells. Cancer Res 60(24): pp. 6886–6889

448. Eckert LB, Repasky GA, Ulku AS et al. (2004) Involvement of Ras activation in human breast cancer cell signaling, invasion, and anoikis.
Cancer Res 64(13): pp. 4585–4592

449. Wu Y, Feng Z, Gao S et al. (2012) Interplay between menin and K-Ras in regulating lung adenocarcinoma. J Biol Chem 287(47): pp. 40003–40011

450. van Schaeybroeck S, Kyula JN, Fenton A et al. (2011) Oncogenic Kras promotes chemotherapy-induced growth factor shedding via ADAM17.
Cancer Res 71(3): pp. 1071–1080

451. Napoli C, Lemieux C, Jorgensen R (1990) Introduction of a Chimeric Chalcone Synthase Gene into Petunia Results in Reversible Co-Suppression of Homologous Genes in trans. The Plant Cell Online 2(4): pp. 279–289

452. Romano N, Macino G (1992) Quelling: transient inactivation of gene expression in Neurospora crassa by transformation with homologous sequences.
Mol Microbiol 6(22): pp. 3343–3353

453. Fire A, Xu S, Montgomery MK et al. (1998) Potent and specific genetic interference by double-stranded RNA in Caenorhabditis elegans. Nature 391(6669): pp. 806–811

454. Guo S, Kemphues KJ (1995) par-1, a gene required for establishing polarity in C. elegans embryos, encodes a putative Ser/Thr kinase that is asymmetrically distributed. Cell 81(4): pp. 611–620

455. Hildebrandt M, Nellen W (1992) Differential antisense transcription from the Dictyostelium EB4 gene locus: implications on antisense-mediated regulation of mRNA stability. Cell 69(1): pp. 197–204

456. Lee RC, Feinbaum RL, Ambros V (1993) The C. elegans heterochronic gene lin-4 encodes small RNAs with antisense complementarity to lin-14. Cell 75(5): pp. 843–854

457. Wightman B, Ha I, Ruvkun G (1993) Posttranscriptional regulation of the heterochronic gene lin-14 by lin-4 mediates temporal pattern formation in C. elegans. Cell 75(5): pp. 855–862

458. Mattick JS, Makunin IV (2005) Small regulatory RNAs in mammals. Hum Mol Genet 14(suppl 1): pp. R121

459. Hoeppner MP, White S, Jeffares DC et al. (2009) Evolutionarily Stable Association of Intronic snoRNAs and microRNAs with Their Host Genes. Genome Biol Evol (Genome Biology and Evolution) 1: pp. 420–428

460. Schwarz DS, Hutvágner G, Du T et al. (2003) Asymmetry in the Assembly of the RNAi Enzyme Complex. Cell 115(2): pp. 199–208

461. Khvorova A, Reynolds A, Jayasena SD (2003) Functional siRNAs and miRNAs Exhibit Strand Bias. Cell 115(2): pp. 209–216

462. Preall JB, He Z, Gorra JM et al. (2006) Short interfering RNA strand selection is independent of dsRNA processing polarity during RNAi in Drosophila. Curr Biol 16(5): pp. 530–535

463. Siomi H, Siomi MC (2009) On the road to reading the RNA-interference code. Nature 457(7228): pp. 396–404

464. Yekta S, Shih I, Bartel DP (2004) MicroRNA-directed cleavage of HOXB8 mRNA. Science 304(5670): pp. 594–596

465. Ratcliff F, Harrison BD, Baulcombe DC (1997) A similarity between viral defense and gene silencing in plants. Science 276(5318): pp. 1558–1560

466. Ratcliff, MacFarlane, Baulcombe (1999) Gene silencing without DNA. rna-mediated cross-protection between viruses. Plant Cell 11(7): pp. 1207–1216

467. Dunoyer P, Voinnet O (2005) The complex interplay between plant viruses and host RNA-silencing pathways. Curr Opin Plant Biol 8(4): pp. 415–423

468. Zamore PD, Haley B (2005) Ribo-gnome: The Big World of Small RNAs. Science 309(5740): pp. 1519–1524

469. Derrien T, Johnson R, Bussotti G et al. (2012) The GENCODE v7 catalog of human long noncoding RNAs: analysis of their gene structure, evolution, and expression. Genome Res 22(9): pp. 1775–1789

470. Huarte M (2013) LncRNAs have a say in protein translation.
Cell Res 23(4): pp. 449–451

471. Chapman EJ, Carrington JC (2007) Specialization and evolution of endogenous small RNA pathways. Nat Rev Genet 8(11): pp. 884–896

472. Baulcombe DC (2007) Molecular biology. Amplified silencing.
Science 315(5809): 199–200

473. Pak J, Fire A (2007) Distinct populations of primary and secondary effectors during RNAi in C. elegans. Science 315(5809): pp. 241–244

474. Sijen T, Steiner FA, Thijssen KL et al. (2007) Secondary siRNAs result from unprimed RNA synthesis and form a distinct class.
Science 315(5809): pp. 244–247

475. Lee Y, Kim M, Han J et al. (2004) MicroRNA genes are transcribed by RNA polymerase II. EMBO J 23(20): pp. 4051–4060

476. Grimm D, Streetz KL, Jopling CL et al. (2006) Fatality in mice due to oversaturation of cellular microRNA/short hairpin RNA pathways.
Nature 441(7092): pp. 537–541

477. Zhu X, Santat LA, Chang MS et al. (2007) A versatile approach to multiple gene RNA interference using microRNA-based short hairpin RNAs.
BMC Mol Biol 8: 98

478. Yamamoto A, Taki T, Yagi H et al. (1996) Cell cycle-dependent expression of the mouse Rad51 gene in proliferating cells. Mol Gen Genet 251(1): pp. 1–12

479. Fedorov Y, Anderson EM, Birmingham A et al. (2006) Off-target effects by siRNA can induce toxic phenotype. RNA 12(7): pp. 1188–1196

480. Leuschner PJF, Ameres SL, Kueng S et al. (2006) Cleavage of the siRNA passenger strand during RISC assembly in human cells. EMBO Rep 7(3): pp. 314–320

481. Jackson AL, Bartz SR, Schelter J et al. (2003) Expression profiling reveals off-target gene regulation by RNAi. Nat Biotech 21(6): pp. 635–637

482. Lai EC (2002) Micro RNAs are complementary to 3' UTR sequence motifs that mediate negative post-transcriptional regulation. Nat Genet 30(4): 363–364

483. Doench JG, Sharp PA (2004) Specificity of microRNA target selection in translational repression. Genes Dev 18(5): pp. 504–511

484. Brennecke J, Stark A, Russell RB et al. (2005) Principles of microRNA-target recognition. PLoS Biol 3(3): pp. e85

485. Jackson AL, Burchard J, Schelter J et al. (2006) Widespread siRNA "off-target" transcript silencing mediated by seed region sequence complementarity.
RNA 12(7): pp. 1179–1187

486. Lai EC, Tam B, Rubin GM (2005) Pervasive regulation of Drosophila Notch target genes by GY-box-, Brd-box-, and K-box-class microRNAs.
Genes Dev 19(9): pp. 1067–1080

487. Bramsen JB, Laursen MB, Nielsen AF et al. (2009) A large-scale chemical modification screen identifies design rules to generate siRNAs with high activity, high stability and low toxicity. Nucleic Acids Res 37(9): pp. 2867–2881

488. Chen PY, Weinmann L, Gaidatzis D et al. (2008) Strand-specific 5'-O-methylation of siRNA duplexes controls guide strand selection and targeting specificity. RNA 14(2): pp. 263–274

489. Zhang J, Zheng J, Lu C et al. (2012) Modification of the siRNA Passenger Strand by 5-Nitroindole Dramatically Reduces its Off-Target Effects. ChemBioChem 13(13): pp. 1940–1945

490. Jackson AL, Burchard J, Leake D et al. (2006) Position-specific chemical modification of siRNAs reduces "off-target" transcript silencing. RNA 12(7): pp. 1197–1205

491. Hornung V, Guenthner-Biller M, Bourquin C et al. (2005) Sequence-specific potent induction of IFN-alpha by short interfering RNA in plasmacytoid dendritic cells through TLR7. Nat Med 11(3): pp. 263–270

492. Judge AD, Sood V, Shaw JR et al. (2005) Sequence-dependent stimulation of the mammalian innate immune response by synthetic siRNA. Nat Biotechnol 23(4): pp. 457–462

493. Sledz CA, Holko M, Veer MJ de et al. (2003) Activation of the interferon system by short-interfering RNAs. Nat Cell Biol 5(9): pp. 834–839

494. Reynolds A, Anderson EM, Vermeulen A et al. (2006) Induction of the interferon response by siRNA is cell type- and duplex length-dependent. RNA 12(6): pp. 988–993

495. Barral PM, Sarkar D, Su Z et al. (2009) Functions of the cytoplasmic RNA sensors RIG-I and MDA-5: key regulators of innate immunity. Pharmacol Ther 124(2): pp. 219–234

496. Ikeda R, Iwashita K, Sumizawa T et al. (2008) Hyperosmotic stress up-regulates the expression of major vault protein in SW620 human colon cancer cells. Exp. Cell Res. 314(16): pp. 3017–3026

497. Stein U, Jürchott K, Schläfke M et al. (2002) Expression of multidrug resistance genes MVP, MDR1, and MRP1 determined sequentially before, during, and after hyperthermic isolated limb perfusion of soft tissue sarcoma and melanoma patients. J Clin Onco. 20(15): pp. 3282–3292

498. Lara PC, Lloret M, Clavo B et al. (2009) Severe hypoxia induces chemo-resistance in clinical cervical tumors through MVP over-expression. Radiat Oncol 4: 29

499. Guo Y, Guo H, Zhang L et al. (2005) Genomic analysis of anti-hepatitis B virus (HBV) activity by small interfering RNA and lamivudine in stable HBV-producing cells. J Virol 79(22): pp. 14392–14403

500. Liu S, Hao Q, Peng N et al. (2012) Major vault protein: A virus-induced host factor against viral replication through the induction of type-I interferon. Hepatology (Baltimore, Md.) 56(1): pp. 57–66

501. An H, Ryu S, Kim S et al. (2009) Age associated high level of major vault protein is p53 dependent. Cell Biochem. Funct. 27(5): pp. 289–295

502. Kuilman T, Michaloglou C, Mooi WJ et al. (2010) The essence of senescence. Genes Dev 24(22): pp. 2463–2479

503. Johnson H, Del Rosario AM, Bryson BD et al. (2012) Molecular characterization of EGFR and EGFRvIII signaling networks in human glioblastoma tumor xenografts. Mol Cell Proteomics 11(12): pp. 1724–1740

504. Hombría JC, Serras F (2013) Why should we care about fly tumors?: The case of JAK-STAT and EGFR cooperation in oncogenesis.
JAK-STAT 2(2): pp. e23203

505. Calvisi DF, Ladu S, Gorden A et al. (2006) Ubiquitous activation of Ras and Jak/Stat pathways in human HCC. Gastroenterology 130(4): pp. 1117–1128

506. Loetsch D, Steiner E, Holzmann K et al. (2013) Major vault protein supports glioblastoma survival and migration by upregulating the EGFR/PI3K signalling axis. Oncotarget; Vol 4: Advance Online Publications 4(11): pp. 1904–1918

507. Losert A, Lötsch D, Lackner A et al. (2012) The major vault protein mediates resistance to epidermal growth factor receptor inhibition in human hepatoma cells. Cancer Lett. 319(2): pp. 164–172

Curriculum Vitae

Surname	ZIMMERMANN
Name	MARTINA
Date of Birth	May 29, 1977
Nationality	Swiss, Visperterminen VS

Education

1994-2000	Diploma in Education (Primary School), Teachers Training College Kreuzlingen
1995	Exchange Students in the USA (Ramsey High School NJ)
2004-2009	Universität Zürich, Biologiestudium, Master in Humanbiologie
	Masterarbeit: Bioluminescence Imaging of Radiation Responses Xenograft Tumors in Nude Mice
2009-present	PhD Student at the Faculty of Science at University of Zurich Participant of the Cancer Biology Program, Cancer Network Zurich

Publications

Orlowski K, Rohrer Bley C, Zimmermann M et al. (2012) Dynamics of tumor hypoxia in response to patupilone and ionizing radiation. PLoS One 7(12): pp. e51476

Lara PC, Pruschy M, Zimmermann M et al. (2011) MVP and vaults: a role in the radiation response. Radiat Oncol 6: 148

Oral Presentations

Kolloquium in angewandter Krebsforschung USZ 2010
Zimmermann M, Pruschy M
Imaging of radiation responses in xenograft tumors in nude mice

Kolloquium in angewandter Krebsforschung USZ 2011
Zimmermann M, Pruschy M
Major Vault Protein and Ionizing Irradiation

Kolloquium in angewandter Krebsforschung USZ 2013
Zimmermann M, Pruschy M
Combined treatment modality of ionizing radiation with inhibition of epidermal growth factor signaling by ankyrin repeat proteins

Poster Presentations

Student Retreat 2010
Zimmermann M, Pruschy M
Major Vault Protein and Ionizing Irradiation

12th Wolfsberg Meeting on Molecular Radiation Biology/Oncology
Zimmermann M, Pruschy M
Major Vault Protein and Ionizing Irradiation

ICTR 2012 International Conference on Translational Research in Radiation Oncology
February 27 - March 2, 2012
Zimmermann M, Pruschy M
Major Vault Protein and Ionizing Irradiation

Acknowledgements

I would like to express my gratitude to Prof. Dr. Martin Pruschy for awaking my interest in cancer research and for accepting me as a PhD student. I greatly appreciated the opportunity to increase my knowledge in the field of radiation and tumor biology.

I would also like to thank Martin Pruschy for his support and the enthusiasm he brought towards my projects. I greatly appreciate his efforts to correct my thesis.

A special thanks also to my PhD committee, Prof. Dr. Martin Pruschy, Prof. Dr. Alex Sartori and PD Dr. Manuel Stucki for their helpful input and support.

I would also like to acknowledge the Cancer Network Zurich for accepting me in the Cancer Biology Ph.D. Program. I also would like to thank Dr. Eveline Bergmüller for her administrative help and for her supportive words. I enjoyed the get to know other students and to exchange ideas at the student retreats and appreciated the courses that were offered by the program.

Furthermore, I would like to thank all the present and former group members Katrin Orlowski, Nadia Sanchez, Van Vuong, Nicole Grosse, Polina Furmanova-Hollenstein, Andreas Hollenstein, Carla Rohrer-Bley, Angela Broggini, Colette Shen, Andrea Fontana, Daniel Hug, Matthias Eggel, Tamara Codilupi, Marc Augsburger, Katarzyna Nytko-Karouzakis, Sabine Bender for sharing their thoughts and for making life in the lab a good time. A special thanks to the F-Lab members for keeping me good company and their kind support helped me to stay motivated!

I would also like to thanks to Van Vuong for his great support with the animal experiments, I could profit from his wide experience in mouse handling and could count on his help. A special thanks also to Carla Rohrer for introducing me to working with animals. Her calm and confident manner in handling the mice were exemplary to me. I also would like to acknowledge Mirzet Delic for his support with special techniques and for willingly giving advice.

A special thanks to Tamara Codilupi, who joined our lab and my project for her Master Thesis. I would like to thank her for her commitment and her positive attitude.

I would also like to acknowledge the physicists and MTRAs for their technical support in the irradiation facility.

I also would like to acknowledge Prof. Dr. Andreas Plückthun (University Zurich) for his collaboration, for taking the time to discuss the EGFR project and results. A special thanks to Dr. Manuel Simon, Hannes Merten, Nikolas Steffen, Gabriel Nagy-Davidescu, Dr. Birgit Dreier and Dr. Hüsnü Topal for the supply of DARPins, for their helpful advice with regard to the handling of DARPins and especially with regard to the ELISA protocol for the detection of DARPins in blood serum.

Thanks also to Dr. Katja Storch (Dresden) for taking the time to introduce me be to the 3D cell culture.

I especially would like to thank Dr. Elias August for his great support and especially for the proofreading of my thesis.

A special thanks also to my parents who supported me in my wish to study biology, it is to them that I was able to pursue this studies. A special thanks also to my sister Judith and my parents for always lending me an ear and for believing in my abilities.

Finally, I would like to express my biggest thanks to my partner Chris for his continuous support and his great spirit. It meant a lot to me that he showed interest in my work. Chris also contributed a great deal to my work-life balance; during our visits to the mountains, I could recharge energy and motivation.